

Scalable and safe synthetic organic electroreduction inspired by Li-ion battery chemistry

Byron K. Peters¹, Kevin X. Rodriguez¹, Solomon H. Reisberg¹, Sebastian B. Beil¹, David P. Hickey⁴, Yu Kawamata¹, Michael Collins², Jeremy Starr,² Longrui Chen³, Sagar Udyavara⁵, Kevin Klunder⁴, Tim Gorey⁴, Scott L. Anderson⁴, Matthew Neurock^{5*}, Shelley D. Minteer^{4*}, Phil S. Baran^{1*}.

¹Department of Chemistry, The Scripps Research Institute (TSRI), 10550 North Torrey Pines Road, La Jolla, California, 92037, USA.

²Discovery Sciences, Medicine Design, Pfizer Global Research and Development, 445 Eastern Point Road, Groton, Connecticut 06340, United States

³Asymchem Life Science (Tianjin), Tianjin Economic-Technological Development Zone, Tianjin 300457, China

⁴Department of Chemistry, University of Utah, Salt Lake City, UT 84112

⁵Department of Chemical Engineering and Material Science, University of Minnesota, Minneapolis, MN 55455

*pbaran@scripps.edu, minteer@chem.utah.edu, mneurock@umn.edu

Supplementary Materials

Table of Contents

A Survey of Other (<i>Selected</i>) Electrochemical Birch Reductions	10
General Experimental	11
General Procedure: Electroreduction of Organic Compounds	12
General Procedure A	12
General Procedure B	12
Experimental Procedure for a 10g Scale EC-Birch reaction of Compound 12	15
Experimental Procedure for a 100g Scale EC-Birch reaction of Compound 12	22
Price cost analysis of Compound 12	24
General Procedure: Mechanistic Studies and Surface Analysis	27
Experimental: Electrochemistry for mechanistic studies	27
Experimental: X-ray Photoelectron spectroscopy (XPS)	31
SEM Analysis	33
Computational Study	34
Graphical Guides	47
Graphical Supporting Information for drying LiBr (optional)	47
Graphical Supporting Information for drying DMU	50
Graphical Supporting Information for electrode assembly	52
Graphical Supporting Information for setting up a room temperature Electroreduction reaction (representative EC Birch example)	54
Graphical Supporting Information for setting up a -78 °C Electroreduction reaction (representative EC Birch example)	56
Graphical Supporting Information for setting up the ElectraSyn device for an Electroreduction reaction	57

Graphical Supporting Information for Working-Up the Electroreduction reactions	59
Graphical Supporting Information for cleaning the electrode assembly after a reaction	61
Graphical Supporting Information for a 10g Scale-Up of Compound 12	63
Graphical Supporting Information for a 100g Scale-Up of Compound 12 in flow	66
Electrochemical Birch Reduction	71
Optimization	71
Comparison with other ammonia-free variants – SiGNa and Na-dispersion/15-crown-5. ..	76
NMR Comparisons on Phenylethanol	78
Kinetic Study and Diffusion Experiments of Compound 4	80
Troubleshooting: Frequently Asked Questions	82
Experimental Procedures and Characterization Data	87
Compound SI-4	87
Compound SI-6	87
Compound SI-7	87
Compound SI-8	88
Compound SI-9	88
Compound SI-10	89
Compound SI-11	89
Compound SI-12	90
Compound SI-13	90
Compound SI-14	91
Compound SI-15	91
Compound SI-16	92
Compound SI-17	92
Compound SI-18	93

Compound SI-19.....	93
Compound SI-20.....	94
Compound SI-21.....	94
Compound SI-22.....	95
Compound SI-23.....	95
Compound SI-24.....	96
Compound SI-25.....	96
Compound SI-26.....	97
Compound SI-27.....	97
Compound SI-28.....	98
Compound SI-29.....	98
Compound SI-30.....	99
Compound SI-31.....	99
Compound SI-32.....	100
Compound SI-33.....	100
Compound SI-34.....	101
Compound SI-35.....	101
Compound SI-36.....	102
Compound SI-38.....	103
Compound SI-39.....	103
Compound SI-40.....	104
Compound SI-42.....	104
Compound SI-44.....	105
Compound SI-46.....	105
Compound SI-1.....	106

Compound PNU-95666E (Sumanirole, 2).....	106
Compound SI-47.....	107
Compound SI-48.....	108
Compound SI-49.....	108
Compound SI-50.....	108
Compound SI-51.....	109
Compound SI-52.....	110
References.....	110
NMR Spectra.....	117
Compound SI-4 ¹ H NMR.....	117
Compound SI-4 ¹³ C NMR.....	118
Compound SI-6 ¹ H NMR.....	119
Compound SI-6 ¹³ C NMR.....	120
Compound SI-7 ¹ H NMR.....	121
Compound SI-7 ¹³ C NMR.....	122
Compound SI-8 ¹ H NMR.....	123
Compound SI-8 ¹³ C NMR.....	124
Compound SI-9 ¹ H NMR.....	125
Compound SI-9 ¹³ C NMR.....	126
Compound SI-10 ¹ H NMR.....	127
Compound SI-10 ¹³ C NMR.....	128
Compound SI-11 ¹ H NMR.....	129
Compound SI-11 ¹³ C NMR.....	130
Compound SI-12 ¹ H NMR.....	131
Compound SI-12 ¹³ C NMR.....	132

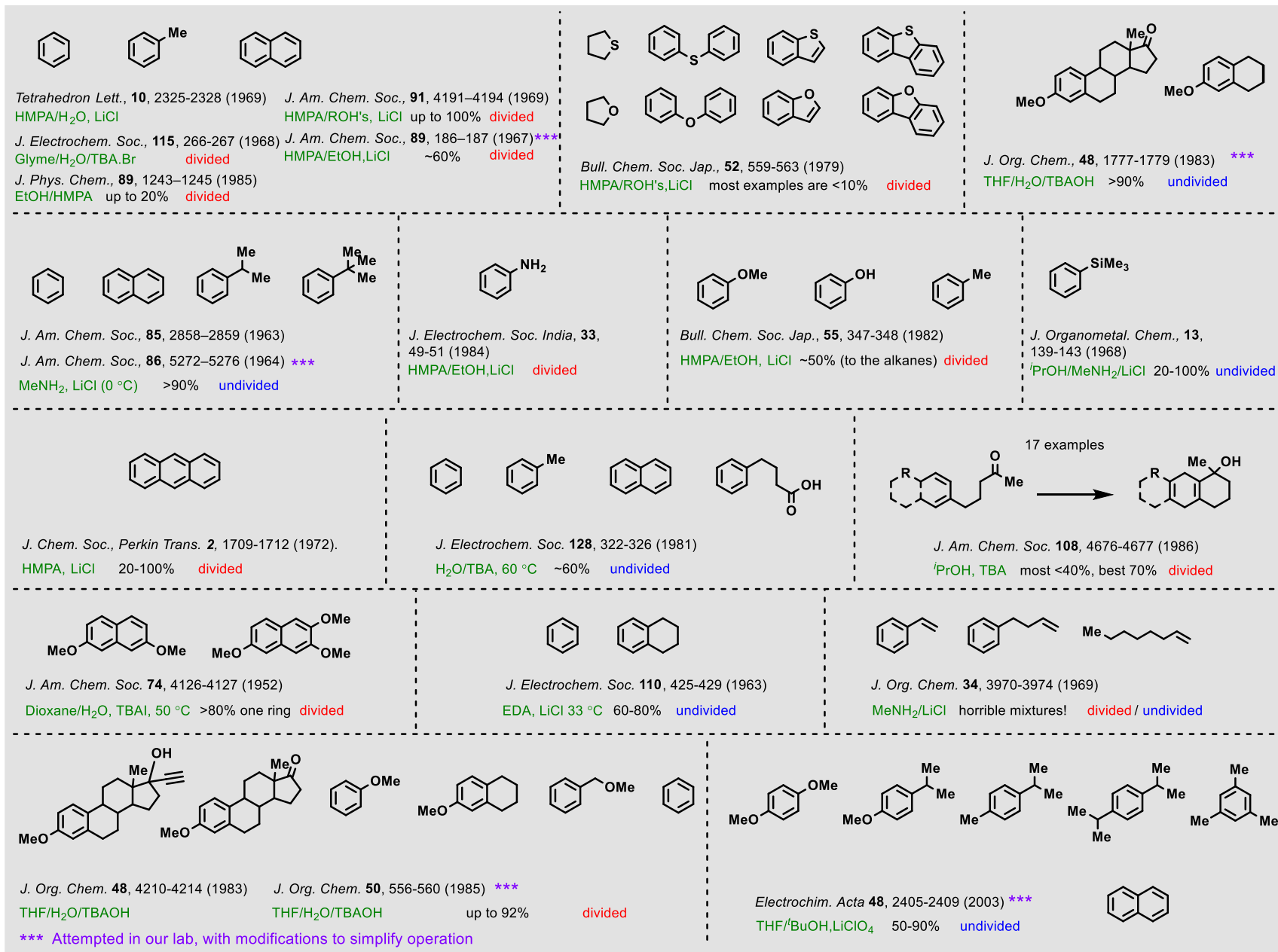
Compound SI-13 ^1H NMR.....	133
Compound SI-13 ^{13}C NMR	134
Compound SI-14 ^1H NMR.....	135
Compound SI-14 ^{13}C NMR	136
Compound SI-15 ^1H NMR.....	137
Compound SI-15 ^{13}C NMR	138
Compound SI-16 ^1H NMR.....	139
Compound SI-16 ^{13}C NMR	140
Compound SI-17 ^1H NMR.....	141
Compound SI-17 ^{13}C NMR	142
Compound SI-18 ^1H NMR.....	143
Compound SI-18 ^{13}C NMR	144
Compound SI-19 ^1H NMR.....	145
Compound SI-19 ^{13}C NMR	146
Compound SI-20 ^1H NMR.....	147
Compound SI-20 ^{13}C NMR	148
Compound SI-21 ^1H NMR.....	149
Compound SI-21 ^{13}C NMR	150
Compound SI-22 ^1H NMR.....	151
Compound SI-22 ^{13}C NMR	152
Compound SI-23 ^1H NMR.....	153
Compound SI-23 ^{13}C NMR	154
Compound SI-24 ^1H NMR.....	155
Compound SI-24 ^{13}C NMR	156
Compound SI-25 ^1H NMR.....	157

Compound SI-25 ¹³ C NMR	158
Compound SI-26 ¹ H NMR.....	159
Compound SI-26 ¹³ C NMR	160
Compound SI-27 ¹ H NMR.....	161
Compound SI-27 ¹³ C NMR	162
Compound SI-28 ¹ H NMR.....	163
Compound SI-28 ¹³ C NMR	164
Compound SI-28, carbazole overlay ¹ H NMR	165
Compound SI-28, carbazole overlay ¹³ C NMR	166
Compound SI-29 ¹ H NMR.....	167
Compound SI-29 ¹³ C NMR	168
Compound SI-30 ¹ H NMR.....	169
Compound SI-30 ¹³ C NMR	170
Compound SI-31 ¹ H NMR.....	171
Compound SI-31 ¹³ C NMR	172
Compound SI-32 ¹ H NMR.....	173
Compound SI-32 ¹³ C NMR	174
Compound SI-33 ¹ H NMR.....	175
Compound SI-33 ¹³ C NMR	176
Compound SI-34 ¹ H NMR.....	177
Compound SI-34 ¹³ C NMR	178
Compound SI-35 ¹ H NMR.....	179
Compound SI-35 ¹³ C NMR	180
Compound SI-36 ¹ H NMR.....	181
Compound SI-36 ¹³ C NMR	182

Compound SI-38 ¹ H NMR.....	183
Compound SI-38 ¹³ C NMR	184
Compound SI-39 ¹ H NMR.....	185
Compound SI-39 ¹³ C NMR	186
Compound SI-40 ¹ H NMR.....	187
Compound SI-40 ¹³ C NMR	188
Compound SI-42 ¹ H NMR.....	189
Compound SI-42 ¹³ C NMR	190
Compound SI-44 ¹ H NMR.....	191
Compound SI-44 ¹³ C NMR	192
Compound SI-46 ¹ H NMR.....	193
Compound SI-46 ¹³ C NMR	194
Compound SI-1 ¹ H NMR.....	195
Compound SI-1 ¹³ C NMR	196
PNU95666E (2) ¹ H NMR.....	197
PNU95666E (2) ¹³ C NMR.....	198
Compound SI-47 ¹ H NMR.....	199
Compound SI-47 ¹³ C NMR	200
Compound SI-48 ¹ H NMR.....	201
Compound SI-48 ¹³ C NMR	202
Compound SI-49 ¹ H NMR.....	203
Compound SI-49 ¹³ C NMR	204
Compound SI-50 ¹ H NMR.....	205
Compound SI-50 ¹³ C NMR	206
Compound SI-51 ¹ H NMR.....	207

Compound SI-51 ^{13}C NMR	208
Compound SI-51 ^1H NMR.....	209
Compound SI-52 ^{13}C NMR	210

A Survey of Other (*Selected*) Electrochemical Birch Reductions



General Experimental

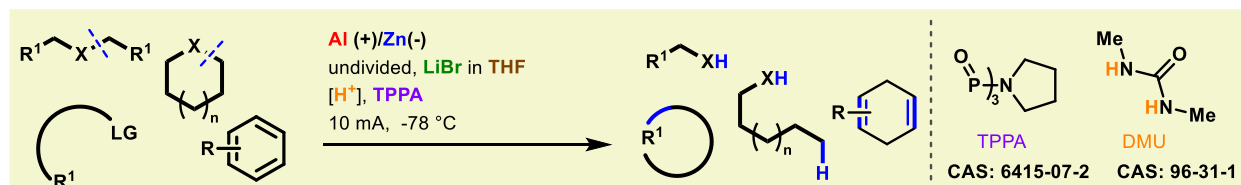
Lithium bromide was purchased from either Combi-blocks or Oakwood chemicals and dried after receiving (*vide infra*). Dimethylurea (DMU) was purchased from Acros chemicals and dried after receiving (*vide infra*). Tetrahydrofuran (THF), acetonitrile (CH₃CN), and dichloromethane (CH₂Cl₂) were obtained by passing the previously degassed solvents through an activated alumina column(1). TPPA (anhydrous, 99.5%) was purchased from Combi-blocks and used without further purification. All substrates that were purchased (from cheapest supplier), were used without further purification. Yields refer to chromatographically and spectroscopically (¹H NMR) homogeneous material, unless otherwise stated. Reactions were monitored by GC/MS, LC/MS, and thin layer chromatography (TLC). TLC was performed using 0.25 mm E. Merck silica plates (60F-254), using short-wave UV light as the visualizing agent, and phosphomolybdic acid and Ce(SO₄)₂, acidic ethanolic anisaldehyde, KMnO₄, or iodine absorbed on silica gel was used, and heat as developing agents (not for iodine staining). NMR spectra were recorded on Bruker DRX-600, DRX-500, and AMX-400 instruments and are referenced using residual undeuterated solvent (CHCl₃ at 7.26 ppm ¹H NMR, 77.16 ppm ¹³C NMR; acetone at 2.05 ppm ¹H NMR, 29.84 ppm ¹³C NMR; CH₃OH at 3.31 ppm ¹H NMR, 49.0 ppm ¹³C NMR; C₆H₆ at 7.16 ppm ¹H NMR, 128.06 ppm ¹³C NMR)(2). The following abbreviations were used to explain multiplicities: s = singlet, d = doublet, t = triplet, q = quartet, m = multiplet, br = broad. Column chromatography was performed using E. Merck silica (60, particle size 0.043–0.063 mm), and pTLC was performed on Merck silica plates (60F-254). High-resolution mass spectra (HRMS) were recorded on an Agilent LC/MSD TOF mass spectrometer by electrospray ionization time of flight reflectron experiments. Gas chromatography-mass spectrometry (GCMS) were recorded on an Agilent 5975 MSD Series spectrometer.

General Procedure: Electroreduction of Organic Compounds

- **A:** Low temperature reaction using an **Al** anode and **Zn** cathode
- **B:** Room temperature reaction using a **Mg** anode and **Galvanized steel wire** cathode

See drying procedures for LiBr and DMU (*vide infra*)

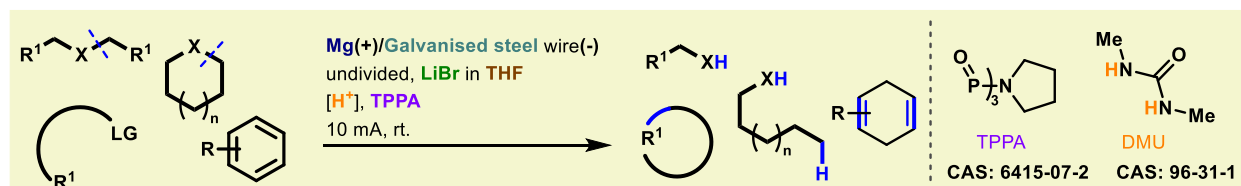
General Procedure A



Setup (see graphical guide):

IKA **Al** (anode) and **Zn** (cathode) plate electrodes were connected accordingly to an ElectraSyn vial cap. To either an oven or flame-dried ElectraSyn vial was added substrate (0.1 mmol, 1.0 eq.), 1,3-dimethylurea (**DMU**, 0.3 mmol, 3.0 eq) and tri(pyrrolidin-1-yl)phosphine oxide (**TPPA**, 10 eq.), followed by 500 μ L's of a 1.5 M **THF** solution of **LiBr** (0.75 mmol, 7.5 eq.). Next, 3 mL of dry **THF** (30 mL/mmol substrate) was added and the reaction headspace was purged with argon and the solution thoroughly degassed by argon sparge (optional). The reaction mixture was then cooled to -78 °C using a dry ice/acetone bath mix. The ElectraSyn was setup as follows: *New exp.* > *Constant current* > *10 mA* > *No ref. electrode* > *Total charge* > *0.1 mmol, F/mol* (see individual compounds) > *No alternating polarity* > *start*. The temperature was maintained at -78 °C throughout the duration of the reaction, keeping it shielded from air and moisture (Figure 1). The reaction in some cases could be monitored by TLC, following the disappearance of a UV signal and generation of a new UV signal (e.g. SI-24 to SI-31) or generation with a higher sensitivity to an iodine stain (e.g. SI-6 to SI-23).

General Procedure B



Setup (see graphical guide):

An IKA **Mg** (anode) plate and **Galvanized steel wire** (cathode – see graphical guide for assembly) electrodes were connected accordingly to an ElectraSyn vial cap. To either an oven or

flame-dried ElectraSyn vial was added substrate (0.1 mmol, 1.0 eq.), 1,3-dimethylurea (**DMU**, 0.3 mmol, 3.0 eq) and tri(pyrrolidin-1-yl)phosphine oxide (**TPPA**, 10 eq.), followed by 500 μL 's of a 1.5 M **THF** solution of **LiBr** (0.75 mmol, 7.5 eq.). Next, 3 mL of dry **THF** (30 mL/mmol substrate) was added and the reaction headspace was purged with argon and the solution thoroughly degassed by argon sparge (optional). The ElectraSyn was setup as follows: *New exp.* > *Constant current* > *10 mA* > *No ref. electrode* > *Total charge* > *0.1 mmol* > *F/mol* (see individual compounds) > *No alternating polarity* > *start*. The reaction in some cases could be monitored by TLC, following the disappearance a UV signal and a higher sensitivity to an iodine stain.

Workup (see respective graphical guide):

The contents of the vial were transferred to a RBF and the vial and electrodes washed with Et_2O . The volatiles were then removed on the rotavap (>120 mbar, 40 °C bath). A solution of Rochelles' salt was then added to the crude followed by Et_2O and the turbid biphasic mixture was then stirred until two clear layers formed. The organic layer was separated, and the aqueous layer was extracted twice with Et_2O . The combined organic layers were dried over anhydrous MgSO_4 and the volatile organics removed on the rotavap. Most of the **TPPA** could be removed via a plug of silica and eluting with 100% EtOAc .

Optional: *Drying the LiBr* (consult the graphical guide)

While successful reductions were carried out by simply weighing out freshly purchased **LiBr** into the reaction vial, **LiBr** is very hygroscopic (especially over extended shelf life), and it was found to be much more effective to prepare a stock solution as follows:

Commercial, reagent grade **LiBr** (~1.5 g) was weighed out into a 20 mL culture tube. The cap and septa were fastened and **LiBr** placed under high vacuum (~1 mbar), by piercing the septa with a 16 guage needle connected to syringe tube and vacuum line. The tube was uniformly heated using a flame torch (propane:butane) until the **LiBr** just starts to melt. Water droplets can be observed condensing on the tube running from the vacuum line. After about a minute of heating the tube and contents are left to cool under vacuum until cool enough for addition of **THF**. Approximately 10% (150 mg) of the mass of the initially weighed **LiBr** has been lost as water vapour. Once cool, the tube is purged with argon and then left under an atmosphere of argon. **THF** (10 mL) is then added to the tube via a syringe, and the **LiBr** is dissolved via shaking

and sonication. After the solution is homogenous, the cap is reinforced by melting layers of parafilm over the septa and cap using a heatgun.

This stock solution was typically good for 5 days but would turn yellow if not shielded from light. Therefore, aluminium foil was used to cover the tube.

Alternatively, another successful procedure suitable for drying the LiBr – which avoids the use of an open flame – is conventional heating using an oil-bath at 110 °C for 2 hours under high vacuum and use as described.

Drying Dimethylurea (DMU)

This is optional and was carried out as a precaution that DMU might hold a significant amount of water. DMU (~5 g) was weighed into an RBF and then MeOH (5 mL) was added to the RBF, and the DMU dissolved by swirling the flask. Benzene (5 mL) was then added, and the solvents removed under vacuum on a rotavap. Afterwards a flakey, dry solid is obtained, which unlike before, was readily soluble in benzene. Benzene (5 mL) is added, and the DMU dissolved. The volatiles were again removed on the rotavap. This was repeated one more time, and then the flakey DMU solid was placed under high vacuum (~1 mbar) for 6 hours before use. ¹H NMR is used to confirm that not benzene is present.

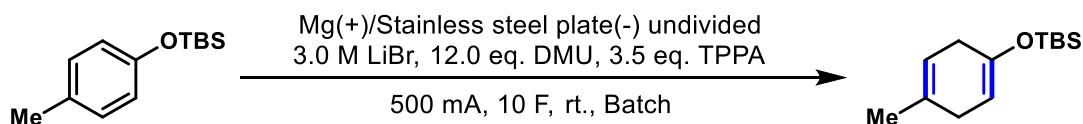
Experimental Procedure for a 10g Scale EC-Birch reaction of Compound 12

Optimization

Entry/Scale (g)	Con. of SM (mmol/mL)	Anode(+)/Cathode(-)	Electrolyte (in THF)	TPPA (eq./M)	DMU (eq.)	Temperature (°C)	F/mol	Current (mA) /Voltage (V)	CD (mA/cm ²)	HPLC	
										SM	TP
2455/1.0 (4.5mmol)	0.14	Al plate(+)/S.S. plate(-)	3.0M LiBr	3.5eq/0.5M	3.0	30	6F/8h	100/25-32	11.90	2.67%	95.30%
2456/1.0 (4.5mmol)	0.14	Zn plate(+)/S.S. plate(-)	3.0M LiBr	3.5eq/0.5M	3.0	30	6F/8h	100/25-32	11.90	93.10%	5.88%
2451/2.0 (9.0mmol)	0.14	Mg plate(+)/S.S. plate(-)	3.0M LiBr	3.5eq/0.5M	3.0	30	6F/15h	100/25-32	18.18	0.00%	100.00%
2452/3.0 (13.5mmol)	0.42	Mg plate(+)/S.S. plate(-)	3.0M LiBr	1.2eq/0.5M	3.0	30	2F/7h	100/26-32	11.90	53.50%	46.45%
						30	3F/10.5h	100/26-32	11.90	42.12%	57.82%
						30	4F/14h	100/28-32	11.90	13.20%	85.45%
						30	5F/17.5h	100/32	11.90	0.00%	100.00%
2454/4.0 (18.0mmol)	0.14	Mg plate(+)/S.S. plate(-)	3.0M LiBr	3.5eq/0.5M	3.0	45	4F/9.5h	200/23-32	3.63	50.92%	48.77%
						55	6F/14.5h	200/25-32	3.63	4.43%	95.16%
						55	8F/19h	200/25-32	3.63	2.09%	97.10%
2445/2.0 (9.0mmol)	0.28	Mg plate(+)/S.S. plate(-)	3.0M LiBr	1.4eq/0.4M	3.0	30	6F/14h	100/25-32	11.90	0.00%	100.00%
2446/2.0 (9.0mmol)	0.28	Mg plate(+)/S.S. plate(-)	3.0M LiBr	1.0eq/0.3M	3.0	30	6F/14h	100/25-32	11.90	0.00%	100.00%
2449/0.5 (2.25mmol)	0.07	Mg plate(+)/S.S. plate(-)	3.0M LiBr	0/0	3.0	30	6F/3.5h	100/27-32	11.90	54.75%	45.23%
2450/0.5 (2.25mmol)	0.07	Mg plate(+)/S.S. plate(-)	3.0M LiBr	0/0	8.0	30	6F/3.5h	100/23-28	11.90	7.19%	83.39%

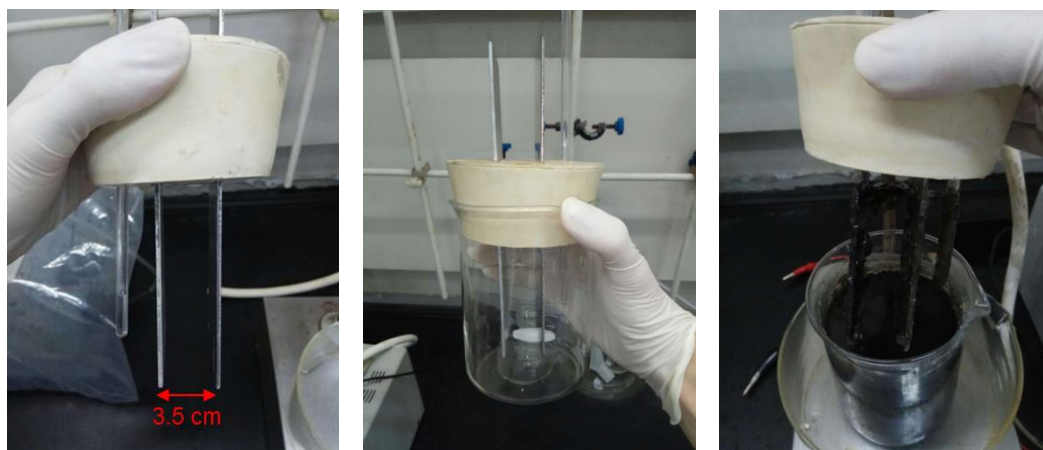
On scale-up we observed that the reaction can successfully proceed in the absence of TPPA by replacement with excess DMU. It was ultimately determined that excess DMU gave reduced overall voltage and delivered higher current to give the desired product as high as 80% conversion.

10g scale-up (in batch)

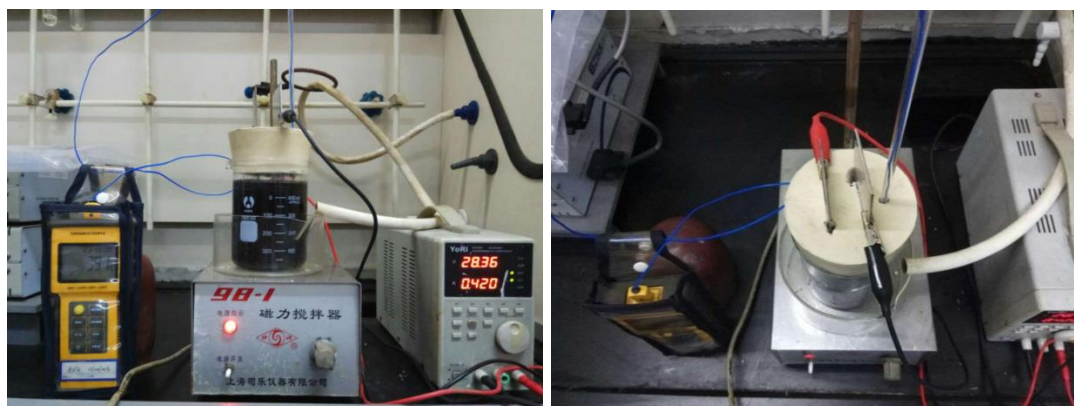


Preparation of LiBr solution in THF (3.0 M): A capped 500 mL round bottom flask was charged with LiBr (83.4 g, 1.0 mol) and then flame-dried under reduced pressure until the complete disappearance of water deposit. Upon cooling to ambient temperature, the round bottom was backfilled with a nitrogen balloon, after which THF (320 mL) was added via a syringe under stirring. The resulting mixture was stirred vigorously until a homogeneous solution was obtained.

Experimental procedure: A clean and dry 500 mL beaker with a stir bar was charged with *tert*-butyldimethyl(*p*-tolylxy)silane (10.0 g, 45.0 mmol), 1,3-dimethylurea (DMU, 47.5 g, 540.0 mmol), tris(pyrrolidinophosphine) oxide (TPPA, 40.5 g, 157.5 mmol) and LiBr solution (320 mL). The anode (Mg plate) and cathode (Stainless steel plate), embedded a rubber cap with a distance of 3.5 cm between them, were inserted into the reaction mixture. The submerged surface area of each electrode was adjusted to 4.0 cm×10.0 cm. The reaction mixture was deoxygenated with nitrogen for 20 min, and then electrolyzed under a constant current of 500 mA from DC power for 25 h until the complete consumption of TBS-cresol as judged by HPLC or GC/MS. After reaction, the electrodes were taken out and rinsed with *tert*-butyl methyl ether (MTBE). The mixture was transferred to a 1.0 L round bottom and volatiles were then removed on the rotavap (>120 mbar, 40 °C water bath). 1.5 L of MTBE was then added, and the residue transferred to a 2.0 L flask, followed by the addition of water (200 mL) with stirring (15 min) to help precipitate the solid and form a liquid-solid bilayer. The upper layer solvent was then poured into a 3.0 L separatory funnel followed by washing with water three times (1.0 L × 3). The organic layer was dried over anhydrous magnesium sulfate, filtered and concentrated *in vacuo*. The crude material (yellow oil) obtained was purified by column chromatography (eluting with *n*-Hexane) and basic alumina (300 g, 13 cm length) to afford 7.1 g (70%) of **Compound 12** as a colorless oil.

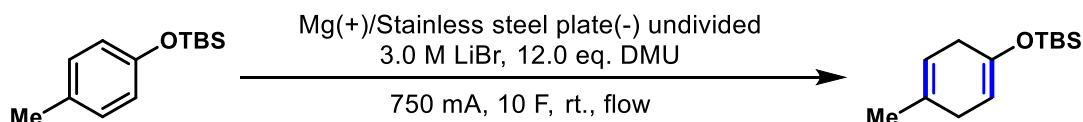


(*Left*) Magnesium anode and stainless-steel cathode. (*Middle*) electrodes set up. (*Right*) After reaction.



(Left) Electrolysis set up. (Right) Top view of electrolysis set up.

10g scale-up in flow

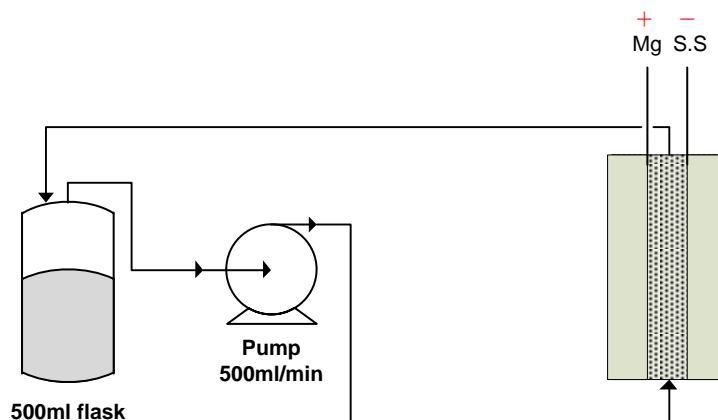


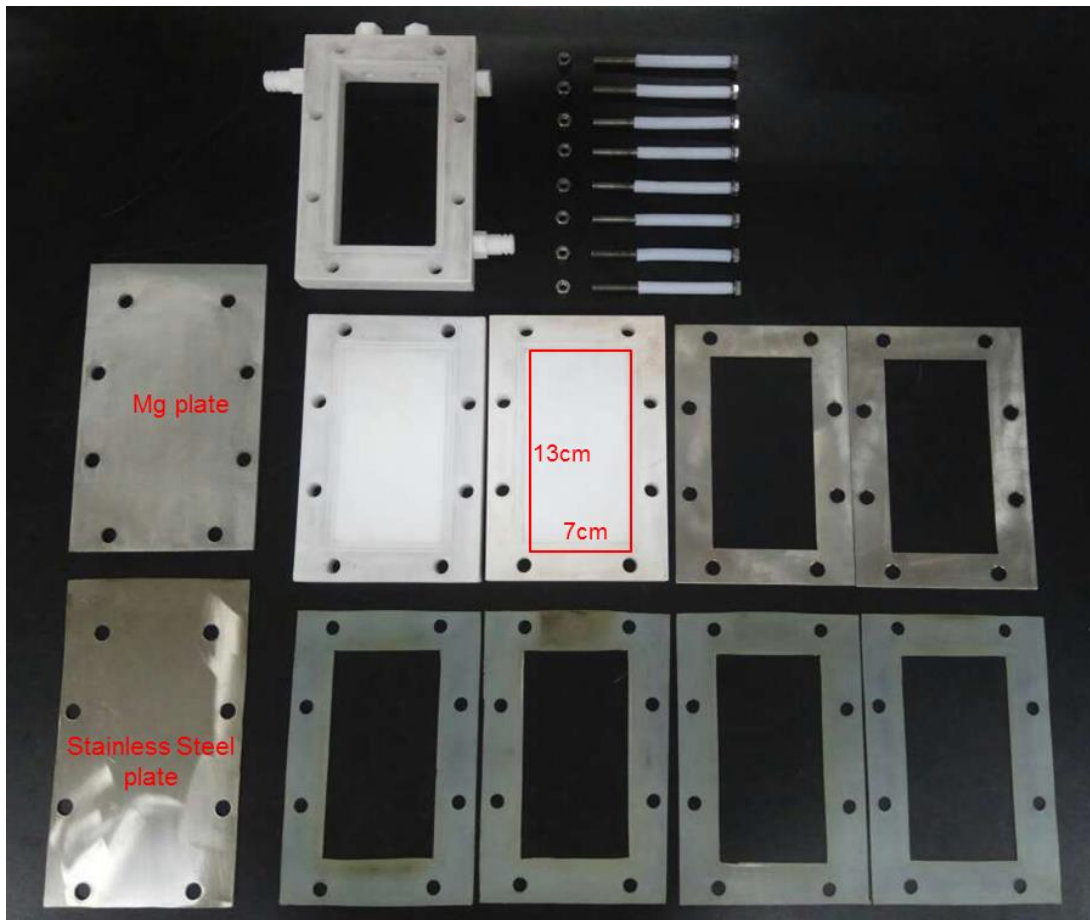
Preparation of LiBr solution in THF (3.0 M): A capped 500 mL round bottom flask was charged with LiBr (83.4 g, 1.0 mol) and then flame-dried under reduced pressure until the complete disappearance of water deposit. Upon cooling to ambient temperature, the round bottom was backfilled with a nitrogen balloon, after which THF (320 mL) was added via a syringe under stirring. The resulting mixture was stirred vigorously until a homogeneous solution was obtained.

Experimental procedure: A dry 500 ml 4-neck round-bottom flask with a stir bar was charged with *tert*-butyldimethyl(*p*-tolylxy)silane (10.0 g, 45.0 mmol), 1,3-dimethylurea (DMU, 47.5 g, 539.1 mmol) and LiBr solution (320 mL). The anode (Mg plate) and cathode (Stainless steel plate) were equipped in frame cell (with a distance of 2.0 cm) and connected to DC power. The immersion surface area of each electrode was 7.0 cm x 13.0 cm. The external round bottom was then connected to a frame cell (rubber tube 6 mm in diameter and Teflon tube 6 mm in diameter). After deoxygenated the reaction mixture (bubbling with nitrogen for 20 minutes), the reaction mixture was pumped into the frame cell with a speed of 500 mL/min as a loop driven by a peristaltic pump. The electrolysis was conducted under a constant current of 750 mA from DC

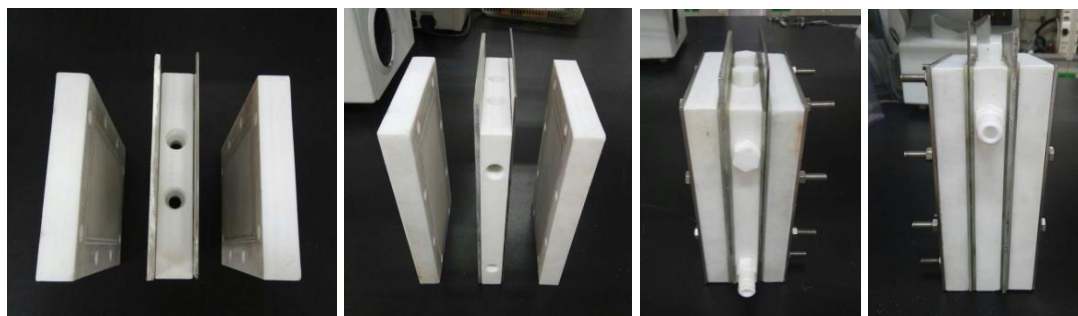
power for 16 h until the complete consumption of the starting material as judged by HPLC or GC/MS. Upon completion, the reaction contents were transferred into a 1.0 L flask from frame cell and external round bottom by peristaltic pump after which MTBE (600 mL) was circulated for 5 min to wash both the frame cell and connecting tubes (300 mL x 2). The volatiles were removed under reduced pressure (>120 mbar, 40 °C water bath). MTBE (1.5 L) was then added, and the residue transferred to a 2.0 L flask, followed by the addition of water (200 mL) with stirring (15 min) to help precipitate the solid and form a liquid-solid bilayer. The upper layer solvent was then poured into a 3.0 L separatory funnel followed by washing with water three times (1.0 L \times 3). The organic layer was dried over anhydrous magnesium sulfate, filtered and concentrated *in vacuo*. The crude material (yellow oil) obtained was purified by column chromatography (eluting with *n*-Hexane) and basic alumina (300 g, 13 cm length) to afford 7.5 g (74%) of **Compound 9** as a colorless oil.

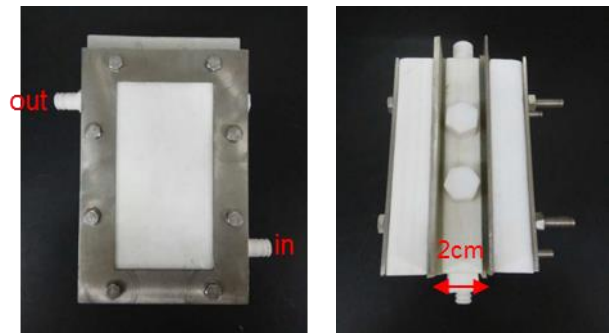
10g scale up flow diagram:



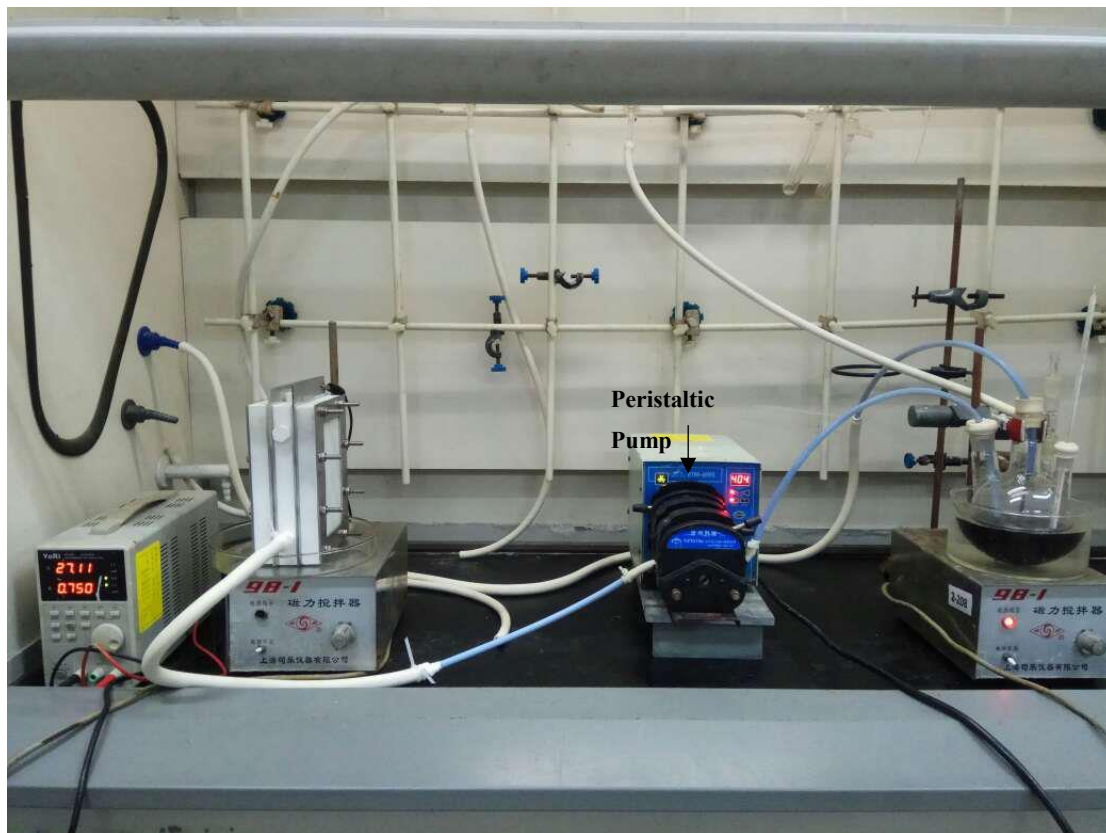


Components of frame cell

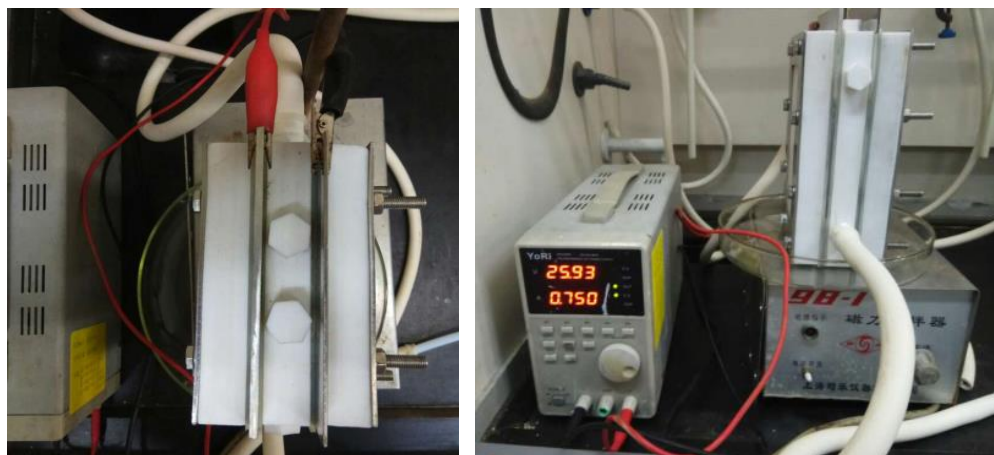




Frame cell set up

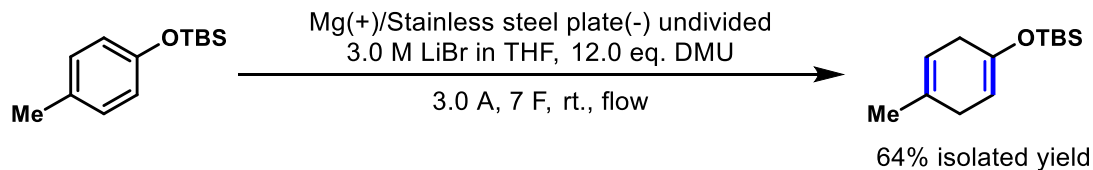


Electrolysis set up in flow



(Left) Top view of cell during electrolysis. *(Right)* DC power and frame cell.

Experimental Procedure for a 100g Scale EC-Birch reaction of Compound 12



Preparation of LiBr solution in THF (3.0 M): A capped 3.0 L round bottom was charged with LiBr (651.0 g, 7.5 mol). The round bottom was then flame-dried under reduced pressure until the complete disappearance of water deposit. Upon cooling to ambient temperature, the round bottom was backfilled with a nitrogen balloon, whereupon THF (2.5 L) was added via a syringe under stirring. The resulting mixture was stirred vigorously with ultrasound until a homogeneous solution was obtained.

Frame Cell Setup: Six Teflon frame block (length: 18.0 cm, width: 12.0 cm, thickness: 2.0 cm) were packed in a row, 4 Stainless steel plates (length: 20.5 cm, width: 12.0 cm, thickness: 2.0 mm) as cathode and 3 magnesium plates (length: 20.5 cm, width: 12.0 cm, thickness: 3.0 mm) as anode which have two silica pads (length: 18.0 cm, width: 12.0 cm, thickness: 2.0 mm) attached on their both sides were inserted between each frame. The two ends of frame cell were attached by two Teflon plates (length: 18.0 cm, width: 12.0 cm, thickness: 2.0 cm) and all components were then threaded through 8 stainless steel screws (length: 25.0 cm, diameter: 5.0 mm) and locked by nuts above stainless steel gasket. The side of each frame was screwed a Teflon joint with which connected rubber tube (6 mm in diameter) (Figure 2). The immersion surface area of each electrode in frame cell was 7.0 cm×13.0 cm.

Experimental procedure: A clean and dry 3.0 L 4-necked round bottom with a stir bar as external container was charged with TBS-cresol (0.45 mol, 100.0 g, 1.0 equiv.), 1,3-dimethylurea (DMU, 5.39 mol, 475.4 g, 12.0 equiv.) and LiBr solution (3.0 M, 2.5 L). A peristaltic pump was connected with frame cell and external round bottom by rubber tubes (diameter: 6.0 mm) and Teflon tubes (diameter: 6.0 mm) respectively to form a circulatory system. The loop system was then purged by nitrogen for 10 minutes followed by bubbling the reaction mixture with nitrogen for 20 minutes; the mixture was then pumped into frame cell with a speed of 400 rpm in the loop by peristaltic pump. The frame cell with a distance of 2.0 cm between each electrode was then

conducted electrolysis (Figure 1) under a constant current of 3.0 A from DC power for 62 h until the complete consumption of TBS-cresol judged by HPLC. After reaction, all mixture was drove into a 5.0 L flask from frame cell and external round bottom by peristaltic pump. 2.0 L MTBE was added and circulated for 5 min to wash frame cell and connecting tube twice (1.0 L \times 2). The volatiles were removed on the rotavap (>120 mbar, 40 °C water bath). A solution of 10% Roschelles' salt 1.5 L was then added and transferred mixture to a 5.0 L flask, followed by adding 1.0 L MTBE stir 30 min to help precipitate solid and form a liquid-solid diphasic system. The upper layer solvent was then poured into a 3.0 L separatory funnel followed by washing with water three times (1.5 L \times 3). The organic layer was dried over anhydrous magnesium sulfate and concentrated in vacuo. The crude material obtained as yellow oil (79.0 g) and was purified by column chromatography (n-Hexane) with basic alumina (500.0 g, 25.0 cm length) to afford desired product 64.5 g as colorless oil with 64 % isolated yield.

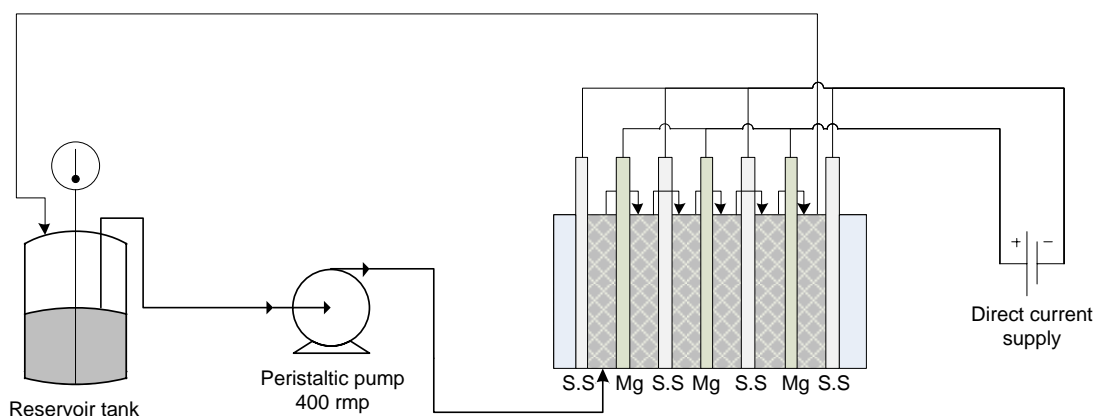
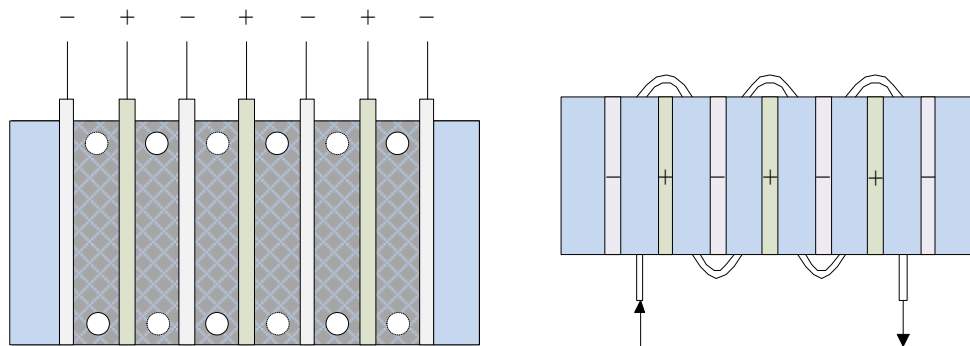


Figure 1. 100.0 g scale up flow diagram



(*Left*) Cross-section perspective of frame cell. (*Right*) Top perspective of frame cell

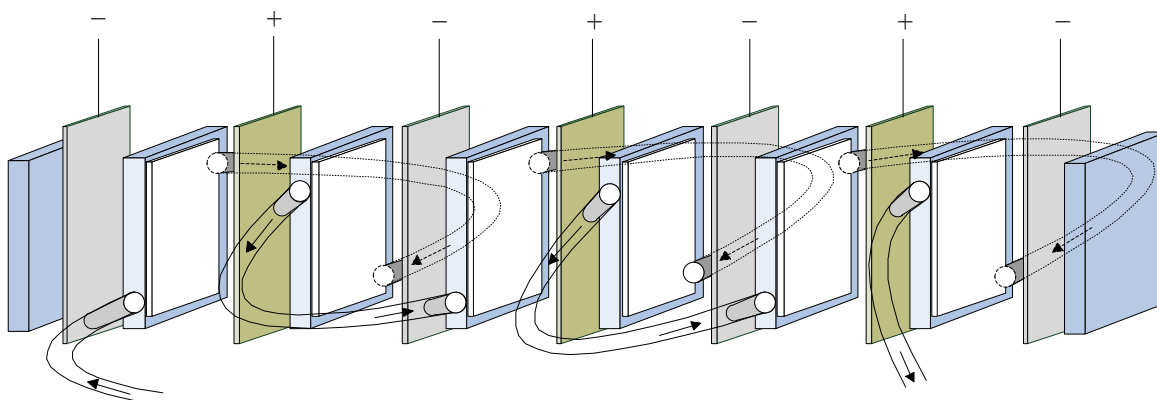


Figure 2. Disassemble figure of continuous flow in frame cell

Price cost analysis of Compound 12

Cost list:

Item	Name	Unit price	Quantity	Cost
Starting material synthesis	p-Cresol	\$43/Kg	55.5 g	\$2.4
	Imidazole	\$50/Kg	70.0 g	\$3.5
	TBSCl	\$146/Kg	77.5 g	\$11.3
	Acetonitrile	\$2/Kg	0.5 L	\$1.1
EC-Birch reagent	TBS-cresol (87.5% isolated yield)	--	100.0 g	--
	1,3-dimethylurea (DMU)	\$45/Kg	475.4 g	\$21.6
	LiBr	\$57/Kg	651.0 g	\$37.1
	THF	\$2.5/Kg	2.5 L	\$6.3
Workup	Roschelles' salt	\$6/Kg	150.0 g	\$0.9
	MTBE	\$2/Kg	2.0 L	\$4.0
	Water	--	6.0 L	--
	Magnesium anhydride	\$1.5/Kg	50.0 g	\$0.1
Washing flow	MTBE	\$2/Kg	2.0 L	\$4.0
Equipment	Teflon Frame with dent	\$30/piece	6 pieces	\$180.0

(length: 18.0 cm, width: 12.0 cm, thickness: 2.0 cm)	(customized price)		
Teflon Plate with dent (length: 18.0 cm, width: 12.0 cm, thickness: 2.0 cm)	\$30/piece (customized price)	2 pieces	\$60.0
Magnesium plate (anode) (length: 20.5 cm, width: 12.0 cm, thickness: 3.0 mm)	\$20/Kg	3 pieces Total: 420.0 g	\$8.4
Stainless steel plate (cathode) (length: 20.5 cm, width: 12.0 cm, thickness: 2.0 mm)	\$2/Kg	4 pieces Total: 1.44 Kg	\$2.9
Rubber tube (total length: 2.5 m, diameter: 6.0 mm)	--	7 pieces	--
Teflon tube (total length: 1.5 m, diameter: 6.0 mm)	--	2 pieces	--
Fluororubber tube (for peristaltic pump) (length: 20.0 cm, diameter: 6.0 mm, thickness: 1.6 mm)	\$10/meter	1 piece Length: 0.2 m	\$2.0
Peristaltic pump (flow rate range: 1.7-1740 ml/min)	--	1 piece	--
DC power supply (32V/5A/160W)	--	1 piece	--
Silicone pad (length: 18.0 cm, width: 12.0 cm, thickness: 2.0 mm)	\$5/m ²	14 pieces Total: 0.3 m ²	\$1.5

	12.0 cm, thickness: 2.0 mm)			
	Stainless steel gasket (length: 18.0 cm, width: 12.0 cm, thickness: 2.0 mm)	--	2 pieces	--
	Stainless steel screw (length: 25.0 cm, diameter: 5.0 mm)	\$5/meter	8 pieces Total: 2m	\$10
	Stainless steel nut	--	16 pieces	--
Total				\$357.1

General Procedure: Mechanistic Studies and Surface Analysis

Experimental: Electrochemistry for mechanistic studies

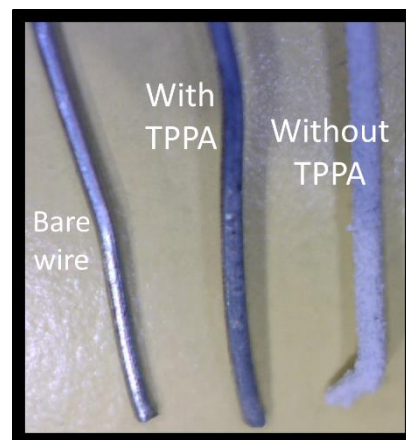
Mechanistic studies using cyclic voltammetry were performed with a Biologic (Model SP-150) with a silver nitrate reference electrode (BAS porous CoralPor™ tip), the reference electrode solution contained the same electrolyte and solvent as the working solution. Platinum gauze was used as the counter with a BAS glassy carbon 0.0708 cm² working electrode. All reagents were purified analogous to the electrolysis experiments to reach anhydrous conditions. Concentrations were 1 mM naphthalene and/or phenethyl alcohol, 3 mM LiBr, and 3.5 mM DMU unless specified otherwise. All square wave voltammetry experiments were performed in a drybox under argon with sub –ppm levels of oxygen and water.

Square Wave Voltammetry Analysis

Variable frequency square wave voltammetry (SWV) was performed on solutions containing 1 mM naphthalene (**5**) in the presence or absence of 3 mM LiBr and 3.5 mM DMU, at a pulse height of 5 mV, step height of 5 mV, and frequencies of 10, 20, and 40 Hz, using a solution of 100 mM NBu₄BF₄ in THF at 25 °C. As described in the main text, SWVs of **5** in the presence of LiBr and DMU exhibit a single broad peak at low frequencies that correspond to the electrochemical reduction of naphthalene. However, a separate peak is resolved at faster frequencies that suggests an ECE mechanism, where the final chemical step (protonation of a species resulting from the second electrochemical reduction) would result in an overall ECEC mechanism.

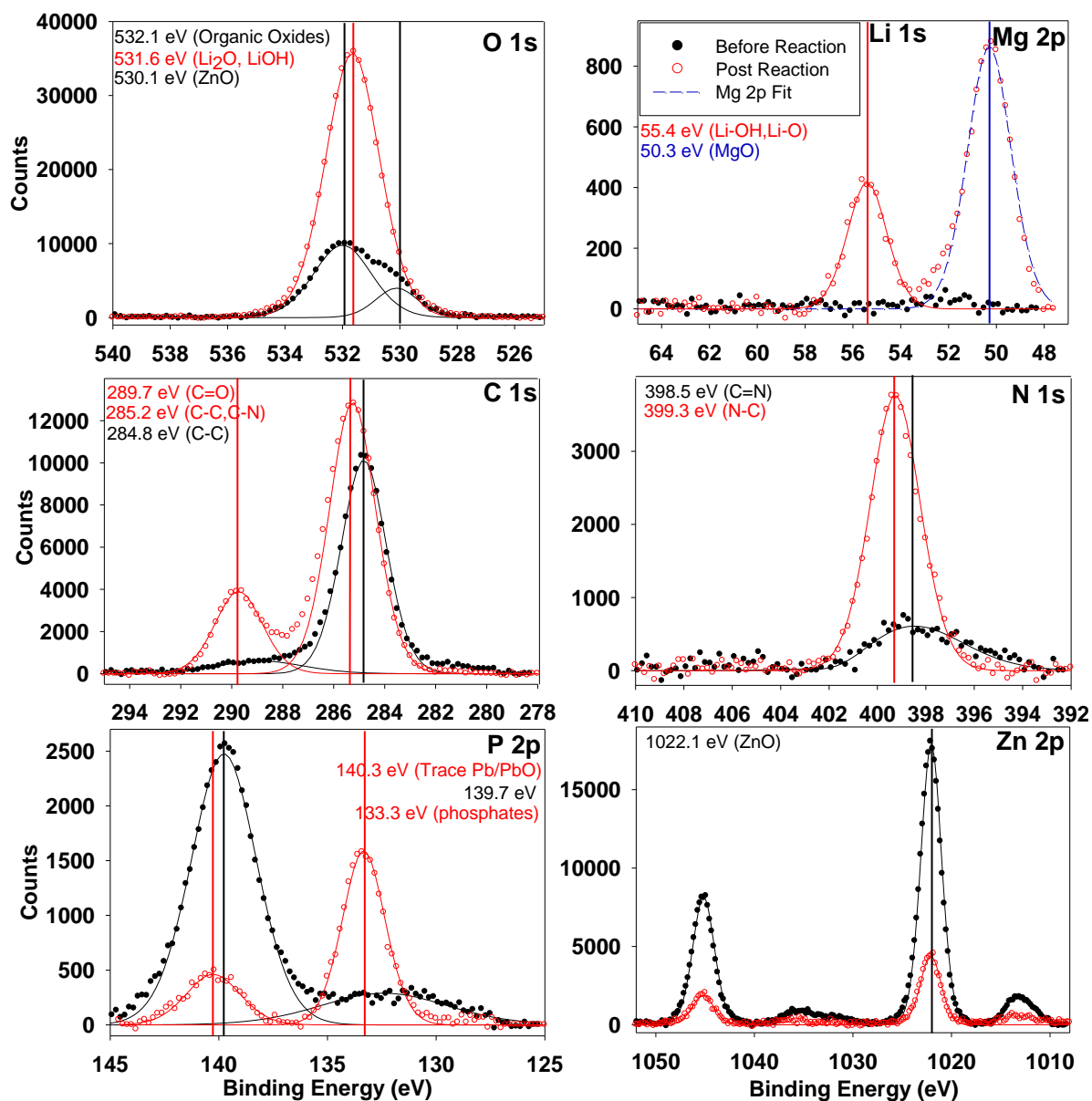
Role of TPPA and Electrode Passivation

Experiments to measure conductivity changes on the electrode surface after electrolysis were conducted with a magnesium counter and a galvanized wire working electrode. Substrate and additive concentrations were the same as the main text, with a current density of ~45 mA cm⁻². Electrolysis was performed for one hour using an IKA ElectraSyn 2.0. Conductivity measurements were performed with a CH-Instruments 611E potentiostat using the built-in IR

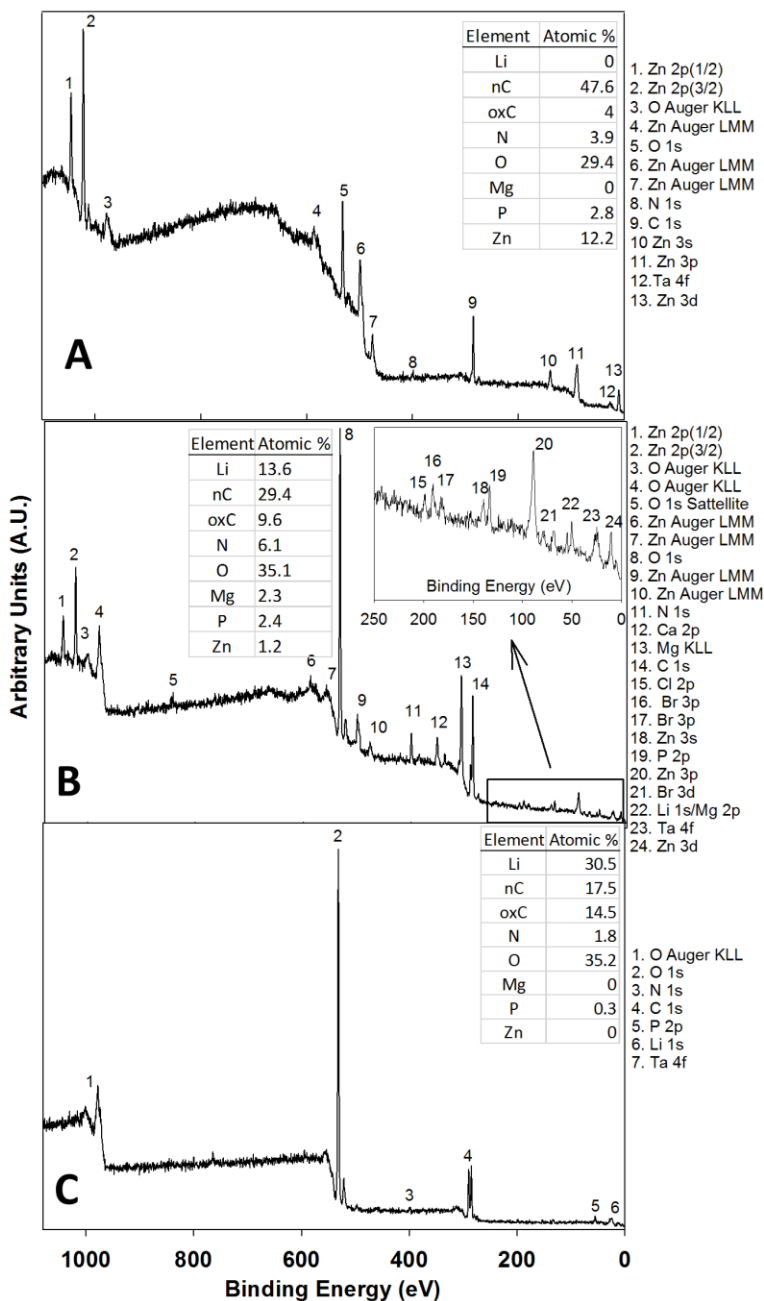


compensation technique. Conditions used were 0 volts applied with a 0.02 V step amplitude, in a two-electrode configuration using a magnesium counter/reference and galvanized wire as the working electrode. Electrodes were held at a distance of ~0.6 cm apart during the resistivity measurements. As can be observed in the photograph, TPPA is necessary to prevent too thick of a SEI layer from forming and completely passivating the electrode. The cell resistance measurements below confirm this data.

Condition	Cell Resistance (Ω)
LiBr/DMU	8000 \pm 2000
LiBr/DMU/naphalene	10000 \pm 200
LiBr/DMU/TPPA/naphalene	1200 \pm 600



High resolution XPS spectra of zinc oxide (galvanized) steel wire before and post reaction. Inset values designate binding energies for specific chemical environments.



(A) Survey scan XPS spectra of zinc oxide (galvanized) steel wire before the electrochemical reaction and (B) post reaction. (C) Survey scan XPS of a zinc electrode post reaction that was run with wet THF stored in ambient conditions. The peaks are numbered and their corresponding identity is located to the right of the spectra. The inset shows atomic percent at the surface of the electrode. The percentages labeled nC and oxC refer to non-highly electron withdrawing groups attached to carbon (alkanes and alkenes) and highly oxidized carbons respectively.

Experimental: X-ray Photoelectron spectroscopy (XPS)

Samples for XPS were generated using an IKA ElectraSyn 2.0 the optimized reaction conditions of a galvanized wire and magnesium anode were used. The substrate was naphalene (0.1 mmol) with the inclusion of TPPA (10 eq), DMU (3 eq) and LiBr (3.5 eq). The reaction was run for 3 hours at a constant current of 10 mA which realized nearly full conversion of the substrate determined via TLC. The post reaction electrodes were rinsed with THF and then placed under high vacuum in the XPS within a few hours after the electrochemical synthesis.

XPS was performed using a Physical Electronics Mg and Al $K\alpha$ X-ray source and energy spectrometer. The electrode was attached to a tantalum backing plate and analyzed in 1×10^{-10} torr ultra high vacuum. Survey and region scans were collected using Al $K\alpha$ and Mg $K\alpha$ radiation respectively. Al $K\alpha$ was used for the surveys to allow observation of the full energy range, and Mg $K\alpha$ was used for the region scans to increase the photoemission cross section for Li 1s. The energy scale was corrected for sample charging by reference to the reported binding energy for Zn $2p_{3/2}$ in ZnO, as reported in the NIST XPS database.⁽³⁾ The shifts were 1.95 eV for a new, unreacted electrode, and 2.65 eV for the electrode analyzed after reaction.

High resolution region scans were integrated to estimate approximate atomic percentages. Intensities were corrected for their corresponding sensitivity factors, and concentrations were calculated as follows, where “I” is each emitting element present; “N” is corrected XPS intensity; “S” is the PHI atomic sensitivity factor; and “C” is concentration.

$$N_x = \frac{I_x}{S_x} \rightarrow C_x = \frac{N_x}{\sum_i N_i}$$

Note that this estimation method assumes that the sample is uniform over the sampling depth of XPS, i.e., roughly 2.5 – 5 nm depending on element.

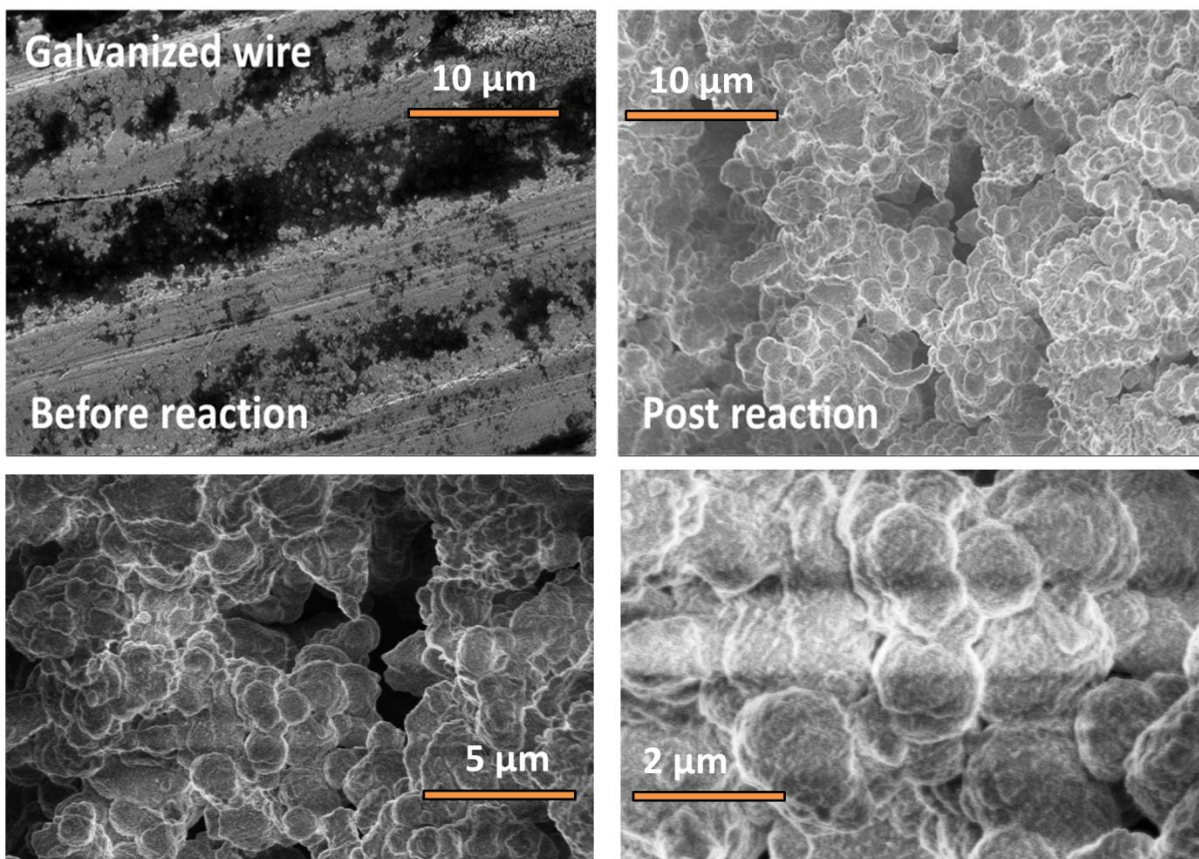
Interpretation of XPS

The spectra from the unreacted electrode is quite different from that of the post-reaction electrode. A major change is the shift of the carbon peak to higher binding energies. The main carbon peak around 285 eV is shifted slightly to higher binding energies, indicating a greater number of C-O bonds. There is also a new carbon peak at a higher binding energy of ~ 290 eV (labeled oxC), that accounts for 9.6 % of the atomic percent in the sample. After electrolysis the

oxC intensity doubles, relative to the intensity from adventitious carbon on the unreacted electrode. The source of the new carbon species is potentially from decomposition of the solvent, TPPA, or DMU which all contain C=O bond, thus supporting the idea that DMU and TPPA are involved at the electrode surface. The substantial increase in peaks for P (2.4%) and N (6.1%) in the post-reaction spectra also give evidence for the additives being present during electrolysis.

As expected, lithium is present in relatively large quantities for the post-electrolysis electrodes. The lithium is most likely originating from solvent decomposition which can form lithium alkoxide, as well as lithium oxide species commonly found within the SEI layer of lithium ion batteries. The presence of magnesium in the post electrolysis electrode is logical as it could be acting as an electrolyte, especially at longer electrolysis times. The survey scan of a film generated with non-anhydrous conditions was drastically different than that with anhydrous conditions. The surface of the hydrous condition was composed almost entirely of Li, O, and C, indicating that surface chemistry is radically different if there is a readily available, labile proton source. The hydrous electrode also appeared to form a thicker film than the anhydrous electrode, as shown by the complete attenuation of Zn signal from the supporting electrode. In addition, the hydrous electrode also failed to achieve full electrolysis of the substrate. The hydrous electrode surface is completely devoid of N, P, and Mg, indicating that water is dominating the surface chemistry and the formation of the SEI layer.

SEM Analysis



(Left) SEM image of a bare galvanized wire at 10,000X magnification. (Right) SEM image of a galvanized wire after 3 hours of electrochemical reduction at constant current of 10 mA. The bottom images (left) are at 20,000X and (right) 50,000X magnification of the post reaction electrode. SEM was performed with a Helios NanoLab 650, operating at an accelerating voltage of 5 kV and 2 kV for the pre and post reaction electrodes respectively.

Computational Study

Ab initio density functional theory calculations were used herein to simulate the Birch reduction of different substrates via: 1) Li(0) atoms in the solution phase using density functional theory (DFT) calculations with a continuum model to simulate the solvent and 2) Zn electroctode at the THF/Zn interface using explicit solvent potential-dependent DFT surface simulations.

1) Gaussian calculations

1A) Gaussian parameters

Solution phase quantum chemical calculations reported in the paper were carried out using the Gaussian 09 program(4). The B3LYP functional(5-7) was used along with a 6-31+G(d) basis set(8-10) to carry out all geometry optimizations and transition state searches. Frequency calculations were carried out on the optimized structures to ensure that the geometry optimizations converged to stable structures with no imaginary frequencies and transition state structures which have a single imaginary frequency along the reaction coordinate of interest. Entropic and zero-point energy corrections were employed to convert the electronic energies to free energies at 1 atm and 298.15 K. The gas phase optimized structures were then used to run single point energy calculations using the SMD solvation model(7) with tetrahydrofuran (THF) as the solvent to examine solvation effects. The free energy in solvent phase was then computed as,

$$G_{\text{sol}} = G_{\text{gas}} + (E_{\text{sol}} - E_{\text{gas}})$$

where, G_{sol} is the solvent phase Gibbs free energy, G_{gas} is the gas phase Gibbs free energy, E_{sol} is the solvent phase electronic energies, E_{gas} is the gas phase electronic energies.

1B) Calculation of the free energy barrier for electron transfer reactions

The free energy barrier for electron transfer reaction carried out by Li(0) in solution was determined using Marcus theory(11) as,

$$\Delta G_{\text{act}} = \frac{(\Delta G_{\text{rxn}} + \lambda)^2}{4\lambda}$$

wherein ΔG_{rxn} is the free energy of reaction of the electron transfer step and λ is the reorganization energy which is defined as the sum of the inner sphere reorganization energy (λ_i) and the outer sphere reorganization energy (λ_o) as follows:

$$\lambda = \lambda_o + \lambda_i$$

The inner sphere reorganization energy (λ_i) for homogeneous reactions was estimated as,

$$\lambda_i = [E(D^*) - E(D^+)] + [E(A^*) - E(A^-)]$$

wherein, $E(D^*)$ is the electronic energy of the donor species (solvated lithium in this case) in its cationic state with neutral geometry, $E(D^+)$ is the energy of the cationic state of the donor species in its optimized cationic geometry, $E(A^*)$ is the energy of the acceptor species (the aromatic substrate) in its anionic state with neutral geometry and, $E(A^-)$ is the energy of the anionic state of the acceptor species in its optimized anionic geometry.

The outer sphere reorganization energy (λ_o) for homogeneous electron transfer reactions is given as(10),

$$\lambda_o = \frac{e^2}{4\pi\epsilon_0} \left(\frac{1}{2a_1} + \frac{1}{2a_2} - \frac{1}{(a_1 + a_2)} \right) \left(\frac{1}{\epsilon_{\text{op}}} - \frac{1}{\epsilon_s} \right)$$

wherein the dielectric constants (static dielectric constant (ϵ_s) and optical dielectric constant (ϵ_{op})) for the solution is assumed to be that of THF and the radii of the donor and acceptor species (a_1 and a_2) involved in the electron transfer is approximated to be the distance between the two farthest atoms within the molecule.

1C) Computation of reduction potentials:

The reduction potentials of the individual species vs NHE (E_{red}^0) were calculated using the computed solvent phase free energy values of the neutral species and the anionic (reduced) species as follows, wherein the Gibbs Free energies (G_{sol}) are given in J/mol.

$$E_{\text{red}}^0 = \frac{[(G_{\text{sol}})_{\text{reduced species}} - (G_{\text{sol}})_{\text{neutral species}}]}{(-96500)} - 4.28$$

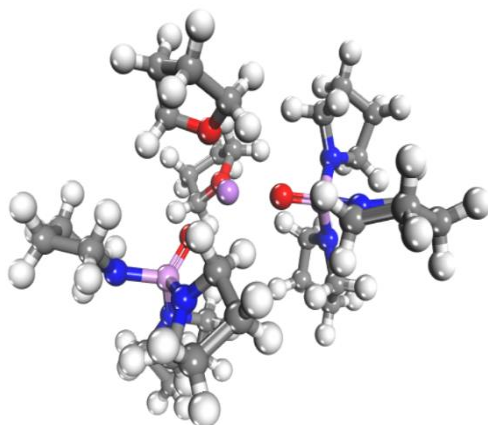


Fig. S11. Solvated lithium atom model (Li^0) used to consider solvation by THF and TPPA. The carbon, hydrogen, oxygen, nitrogen and Li atoms are shown as grey, white, red, blue and purple spheres

1D) Solvated lithium modeling:

Li metal in solution is typically solvated by the solvent molecules as seen in the case of ammonia(12, 13). The first solvation shell of lithium consists of four solvent molecules usually bound in a tetrahedral configuration. Hence, it is likely that Li in THF as well exists in a tetrahedral configuration which is also confirmed by crystallographic identification of various Li salts in THF solvent(14-17). In addition, when TPPA is added as a polar additive, it is likely that TPPA replaces THF in the first solvation shell of lithium which is similar to the observations reported by Reich et al(18). upon the addition of HMPA (another similar polar additive) to LiBr in THF. Therefore, in order to consider the additional solvation effects by TPPA, 2 THF molecules were replaced by 2 TPPA molecules in the first solvation shell (Fig. S11) since 2-3 equivalents of TPPA are used per mole of LiBr.

2) VASP calculations

2A) VASP parameters:

Periodic density functional theory calculations were carried out to simulate reactions at the electrode surface using the Vienna Ab initio Simulation Program (VASP)(19-21). The Perdew-Burke-Ernzerhof (PBE) functional (22) was used within the generalized gradient approximation (GGA) to calculate the exchange and correlation energies. The interactions between the core and the valence electrons were considered by using PAW pseudopotentials to describe the core electrons in the system(23, 24). D3-type dispersion corrections(25) were used to calculate dispersion interactions between naphthalene/phenylethylalcohol (PEA) molecules and the metal surface for the gas phase calculations and, in addition, the interactions of THF and DMU molecules for the solution phase simulations. The transition states for different reactions were calculated using the nudged-elastic band (NEB) method(26, 27) to establish reliable initial transition state structures which were subsequently used as input to the dimer method to isolate the transition states(28). Plane waves were constructed using an energy cutoff of 450 eV. Numerical integrations were performed using a k-point mesh of 2x2x1. A tolerance limit of 10^{-6} eV for the electronic energy and 0.05 eV/Å for the force were considered as the convergence criteria for geometry optimizations. The changes in free energy were calculated as a function of potential using the double reference method developed by Filhol and Neurock(29, 30). The geometries and electronic structures in the double reference method were converged using a force convergence criterion of 0.3 eV/Å and energy convergence criteria of 10^{-4} eV was used.

2B) Surface modeling:

In order to simulate the adsorption, electron transfer and protonation reactions that occur at the zinc electrode surface, we carried out periodic DFT calculations using the most stable Zn (001) surface of hexagonally close packed (HCP) bulk Zn structure to construct a 5x5 supercell. A slab model with three layers of metal and a vacuum space of 15 Å was used for the calculations, keeping the bottom layer frozen to the bulk parameters. To model the effect of LiBr on the naphthalene/phenylethyl alcohol (PEA) adsorption/electron transfer rates, two molecules of LiBr were adsorbed onto the Zn surface. The simulations discussed below in section 3 and 4A systematically examine the adsorption of naphthalene and phenylethyl alcohol, respectively on the ideal Zn(001) surface in the absence of solvent and explore the influence of LiBr. This allows for the direct calculation of the PEA adsorption strength as well as the degree of electron transfer

as a function of potential. Subsequent calculations reported in section 4B and 4C below include the explicit THF solvent as well as DMU proton sources to extend the results to more faithful interfacial models.

3) Adsorption of Naphthalene on Zn Surface

Naphthalene adsorbs on the Zn(001) surface via strong π -bonding interaction between the planar aromatic rings of naphthalene and the Zn substrate. The adsorption energy in the absence of a potential is -78 kJ/mol. Its adsorption energy weakens to \sim -35 kJ/mol as the charge is increased out to -8 electrons. The negative charge is a surrogate for the negative potentials which are calculated when the solution phase is included.

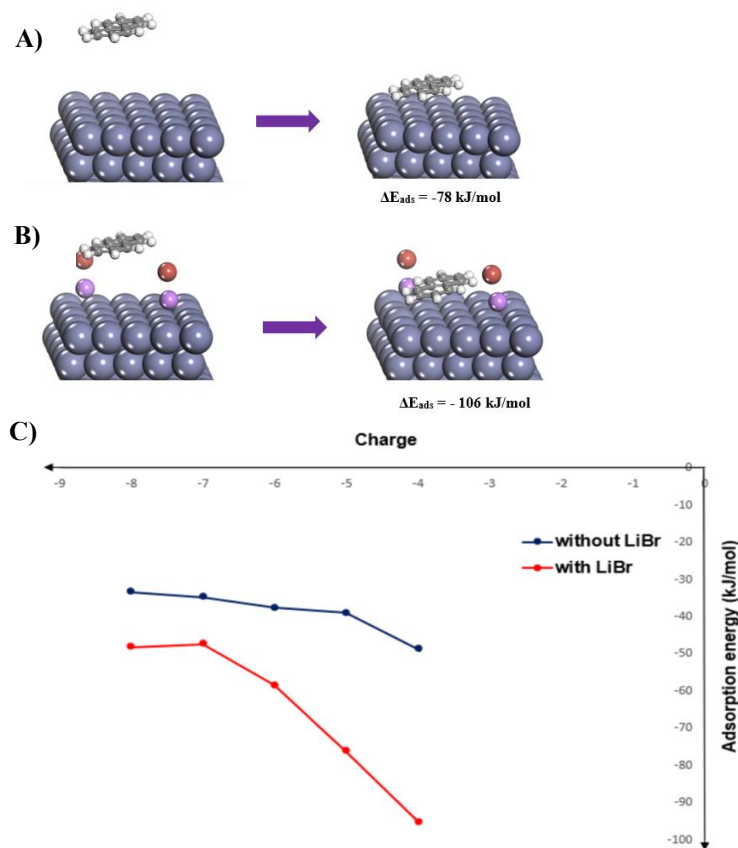


Fig. SI2. The adsorption of naphthalene onto A) the bare Zn(001) surface onto B) LiBr promoted Zn(001) surface C) The change in the adsorption energy of naphthalene on pristine Zn(001) surface (blue) and LiBr covered Zn(001) (red) as a function of negative charge (potential).

Electron transfer typically proceeds upon the adsorption of the substrate to the electrode surface as was shown previously in the electrocatalytic adsorption and reduction of CO₂(31, 32). Bader charge analyses(33) carried out herein indicate that 0.3 electrons transfer from the Zn to the naphthalene substrate upon adsorption in the absence of an applied potential. Increasing the negative charge (i.e. decreasing the potential) to higher potentials (of ~ -5 electrons) results in a full electron transfer to bound naphthalene.

Similar calculations were carried out over the Zn surface in the presence of bound LiBr to explore the influence of the electrolyte on the naphthalene adsorption (shown in red in Fig. SI2). The results shows that the naphthalene adsorption of naphthalene increases from -78 kJ/mol on the bare Zn(001) surface to -106 kJ/mol on the LiBr promoted Zn(001) surface in the absence of potential. LiBr helps to promote the adsorption of naphthalene to the electrode surface as well as electron transfer from the metal to adsorbed naphthalene. This is in good agreement with the increased current obtained in CV's when LiBr is added into the reaction mixture. This is likely the result of the stabilization of the negatively charged reduced naphthalene substrate by the positively charged cationic-like state of Li in LiBr. Similar cationic effects have also been observed in the electroreduction of CO₂ wherein the adsorbed CO₂ species is shown to be stabilized by imidazolium(32) and potassium cations on the surface(31). Thus, LiBr plays a role in promoting the electron transfer step which ultimately leads to the faster formation of the products which in turn is consistent with the irreversibility seen in the cyclic voltammeteries (CV's).

4) Computational study of the electrode mediated kinetics of phenylethyl alcohol (PEA)

4A) Adsorption/electron transfer of PEA

Similar calculations were also carried out to examine the adsorption and electron transfer to PEA and the influence of the LiBr electrolyte. The adsorption studies indicate that PEA binds to the Zn surface with an energy of -51 kJ/mol at 0 V NHE where 0.3 electrons are transferred from the Zn to the PEA. The binding of PEA is ~ 0.27 eV weaker than that of naphthalene. Further, NEB calculations indicate that the process is barrierless.

Similar to the naphthalene results, the addition of LiBr was found to promote electron transfer as

well as the adsorption of PEA to the metal surface where the binding of PEA increases to -83 kJ/mol. The adsorption of PEA and electron transfer to form the PEA radical anion is therefore assumed to be facile and as such the electrode surface is likely covered by the reduced aromatic species which would result in the measured zero-order kinetics

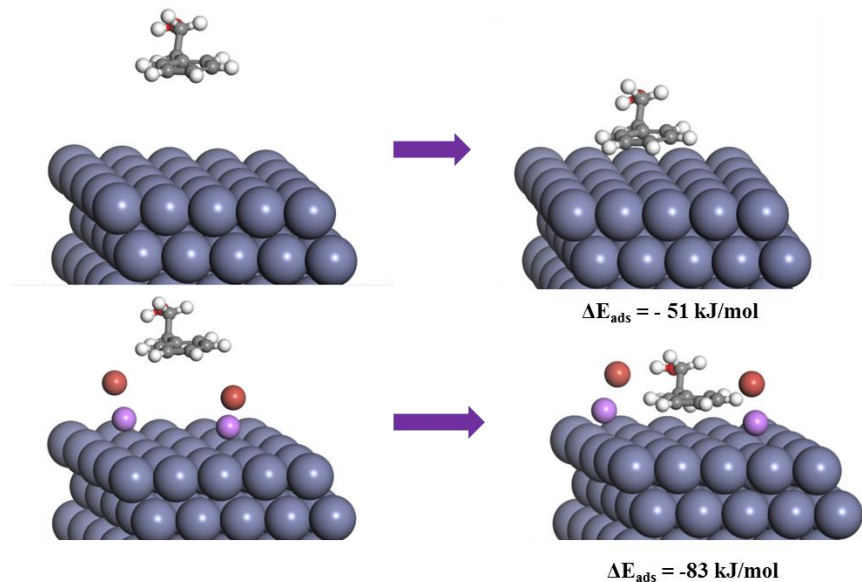


Fig. SI3. The adsorption of phenethyl alcohol onto A) the bare Zn(001) surface onto B) LiBr promoted Zn(001) surface.

4B) Modeling of the electrode mediated kinetics of PEA

As discussed in the previous section, the adsorption of PEA onto the Zn electrode and the electron transfer from the Zn to the PEA are coupled in a facile step thus resulting in a surface that is likely covered by the PEA substrate. The rate appears to be subsequently controlled by proton transfer to the bound PEA substrate in the rate-determining step. In order to effectively probe proton transfer, we carried out more rigorous calculations that explicitly include the THF solvent, DMU proton source as well as the potential in order to calculate the potential dependent reaction energies for all of the elementary steps including adsorption, electron transfer, protonation and desorption steps.

In order to simulate the liquid/solid interface, the vacuum space for the model system discussed above was filled with the explicit THF solvent molecules to match the density of THF. Two dimethyl urea (DMU) were added as proton source molecules. One of the DMU molecules is

used to replace the bound THF molecule on the surface whereas the second replaces a THF molecule in the solution. In addition to the solvent and proton source, two molecules of the LiBr were added to the Zn surface via the Li cations and sit vicinal to adsorbed phenylethyl alcohol (PEA) as shown in Fig. SI4A.

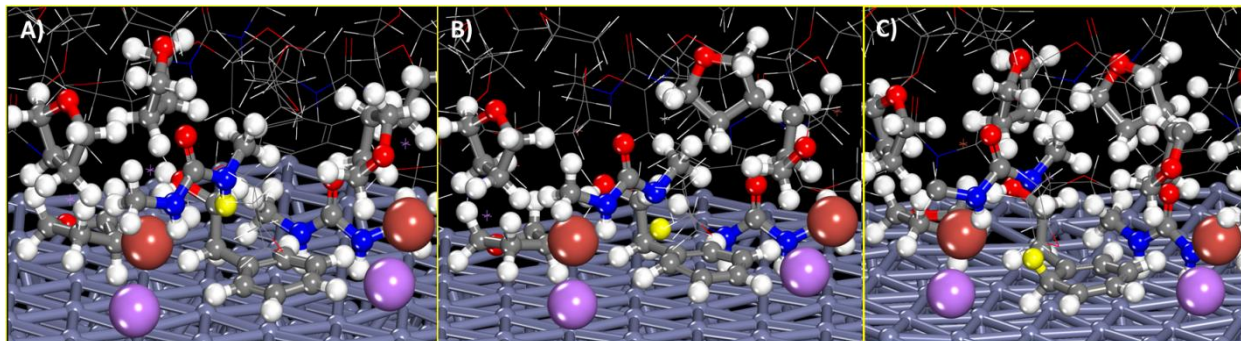


Fig. SI4. The lowest energy reactant, transition and product states in the protonation of bound phenylethyl alcohol (PEA) on the Zn(001) surface in the presence of the solution phase THF solvent and DMU protonation source and surface LiBr promoters. The configurations from ab initio molecular dynamics simulation for the: A) reactant, B) transition state and C) product state in the protonation of the adsorbed PEA from the DMU in the THF solution at the THF/LiBr/Zn(001) interface. The reactive proton is highlighted in yellow. The light blue, purple, red, blue, grey and white spheres refer to the Zn surface atoms, the Li cation, oxygen, carbon and hydrogen atoms.

Ab initio potential-dependent MD simulations were carried out to establish a reliable low energy configuration of the THF solvent, DMU, PEA and LiBr at the Zn surface at different electrode potentials that were subsequently used to carry out reaction energy calculations. The ab initio molecular dynamics simulations were run in an NVT ensemble for 3 picoseconds with a time step of 1 femtosecond. Simulated annealing simulations were subsequently carried out to establish the low energy system configurations. In the first 1500 steps, the system was annealed from 500 K to 300 K and the same was done for the next 1500 steps. The lowest energy configurations obtained from the MD simulations were then sampled and each of the lowest energy structures was optimized. The minimum energy structures obtained from the MD samples were then used in subsequent calculations.

The potential dependence of the various intermediates formed via electron transfer and proton transfer to the substrate (PEA^{*-} (**3a***), PEA-H^{*} (**3c***), PEA-2H^{*} (**4***)) was calculated using the

double reference method by Neurock and Filhol. In this method, the system is charged by either adding or subtracting excess electron density (-q) into the metal. This is counterbalanced by a homogeneous charge of the same magnitude (+q) distributed over the background in order to keep the overall system neutral. In the presence of solution, the charges create a double layer with a potential and an electric field that reliably represent those established by explicit electrolyte.

The optimizations and the transition state calculations were run at these differently charged systems. The potentials at different charges for a given intermediate structure were subsequently determined comparing with two reference potentials. The first reference relates the potential at the metal/solution interface for the uncharged system to the vacuum reference. This is done by inserting a 20 Å vacuum slab in the middle of solvent layer. The second reference is the potential at the middle of the solvent layer which is referred to the vacuum referenced metal surface potential at zero charge. Thus, the potential at the middle solvent layer for different charged systems was calculated by referencing it to the middle solvent layer of the uncharged system which is in turn calculated via reference to the vacuum reference metal surface potential. This allows one to determine the potential of the charge system which is subsequently referenced to NHE by adding -4.8 V to the calculated potential. The total energy of the system at each potential was then determined by correcting the VASP calculated energies for the excess charge and the interaction with the background charge. The energies for the various intermediates are then plotted as a function of potential to determine the energy of each state as a function of potential which is shown below and used to determine the reaction energy differences as well as the activation energies at specific potentials.

4C) Results and discussion

The simulations reported herein explore the potential dependence for the following intermediates: free PEA in THF/DMU solution, adsorbed PEA which occurs with electron transfer to form the bound radical anion PEA^{*-} (**3a***) (Fig. SI4A), the protonated PEA intermediate (PEA-H (**3c***)) (Fig. SI4C), the subsequent electron and proton transfer to form the bound reduced PEA-2H (**4***) (Fig. SI5B) intermediate, and the desorbed PEA-2H (**4**).

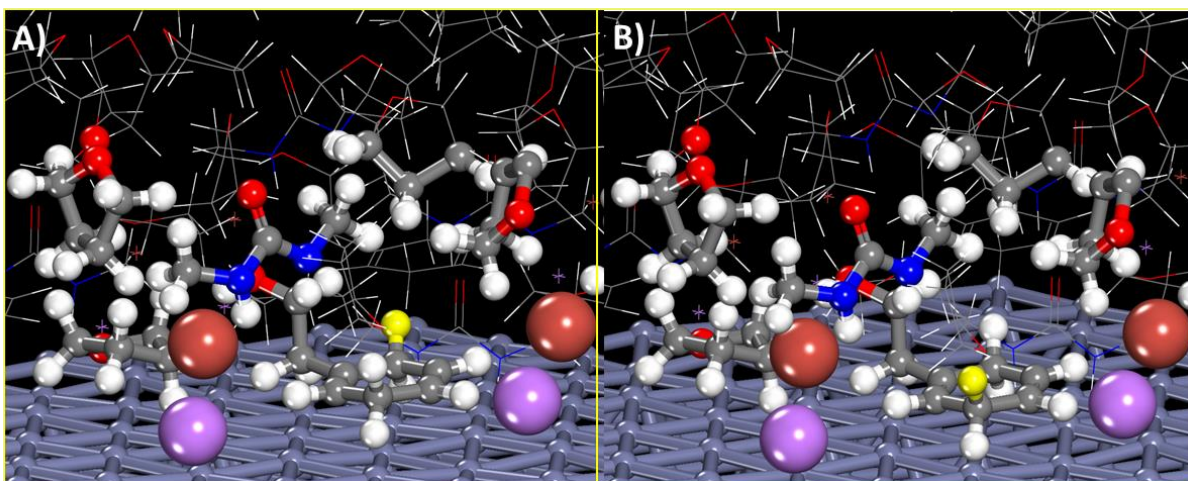


Fig. SI5. The lowest energy reactant, and product states in the second protonation of the bound PEA-H radical anion intermediate on the Zn(001) surface in the presence of the solution phase THF solvent and DMU protonation source and surface LiBr promoters. A) The adsorbed PEA-H radical anion reaction intermediate at the THF/DMU/LiBr/Zn(001) interface and B) the final reduced PEA-H₂ product onto the Zn(001) surface. The yellow sphere refers to the hydrogen atom that transfers from DMU to the substrate. The light blue, purple, red, blue, grey and white spheres refer to the Zn surface atoms, the Li cation, oxygen, carbon and hydrogen atoms.

The resulting energies as a function of potential for each state is shown in Fig. SI6 below.

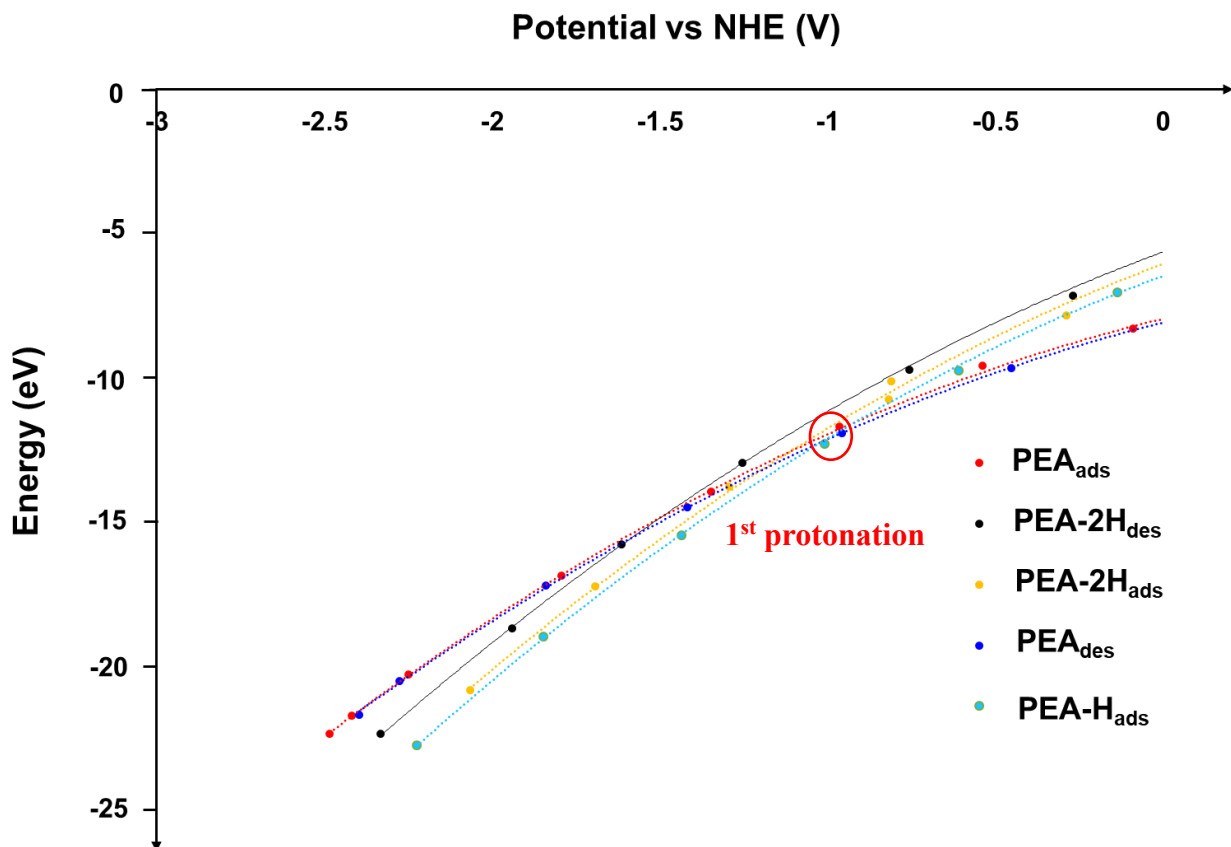


Fig. SI6. A comparison of the energies as a function of potential for the PEA in solution (PEA_{des} blue) (3), the adsorbed PEA radical anion (PEA_{ads} red) ($3\mathbf{a}^*$), the adsorbed protonated PEA ($\text{PEA-H}_{\text{ads}}$ light blue) ($3\mathbf{c}^*$), the 2nd protonated adsorbed PEA ($\text{PEA-2H}_{\text{ads}}$ yellow) (4^*) and the final reduced PEA in solution ($\text{PEA-2}_{\text{des}}$ black) (4).

The results shown in Fig. SI6 above indicate that the adsorbed PEA is more favorable over the full range of potentials examined. This is consistent with the simpler gas phase calculations reported above. The results indicate that the PEA likely covers the surface which agrees with kinetic results and the kinetic models discussed later. A charge analysis indicates that electron transfers upon adsorption. This is consistent with the experimental results which indicate that the proton transfer is rate limiting. It is difficult though to quantify the kinetics for electron transfer using unconstrained electronic structure calculations. We instead explore the energetics for the first and second proton transfer reactions in the results presented in Fig. SI7 and SI8, respectively.

The adsorbed state for each of the protonation steps corresponds to its reduced form which is validated by Bader charge analysis. The first protonation appears to occur at a potential of -1.0 V NHE whereas the second proton transfer does not occur until potentials of less than -2.9 V NHE which is consistent with the experimental results that find that the second proton transfer controls the rate. The transition state for the first proton transfer was calculated as a function of potential and is plotted together with the initial adsorbed PEA radical anion as well as the protonated product in Fig. SI7. The activation barrier decreases quadratically from 145 kJ/mol at -1 V NHE to 0 at -2.5 V NHE. The results indicate that overall reaction will not proceed until less than -2 V NHE and that the second proton transfer step appears to control the rate.

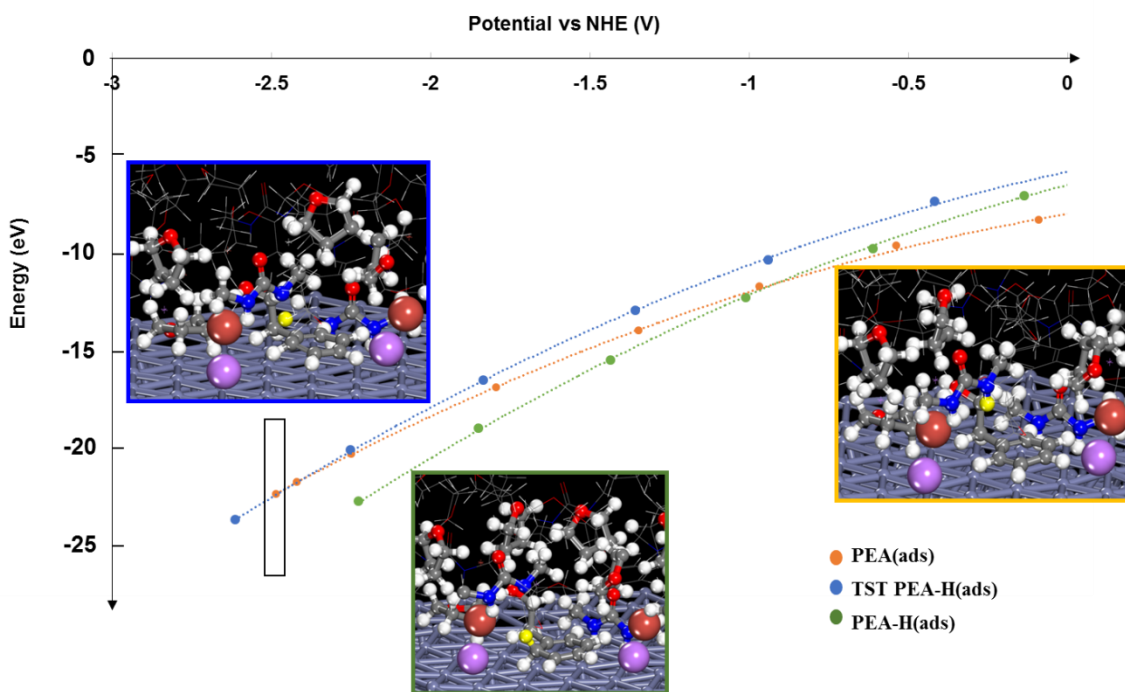


Fig. SI7. Potential dependent energies for the reactant (PEA*⁻ + DMU-H) (orange), product (PEA-H*⁻--DMU(-)) and transition state (PEA*⁻--H⁺--DMU(-)) involved in the first protonation step (PEA*⁻ + H⁺ → PEAH*) of phenylethyl alcohol (PEA) which is fitted to a parabolic curve

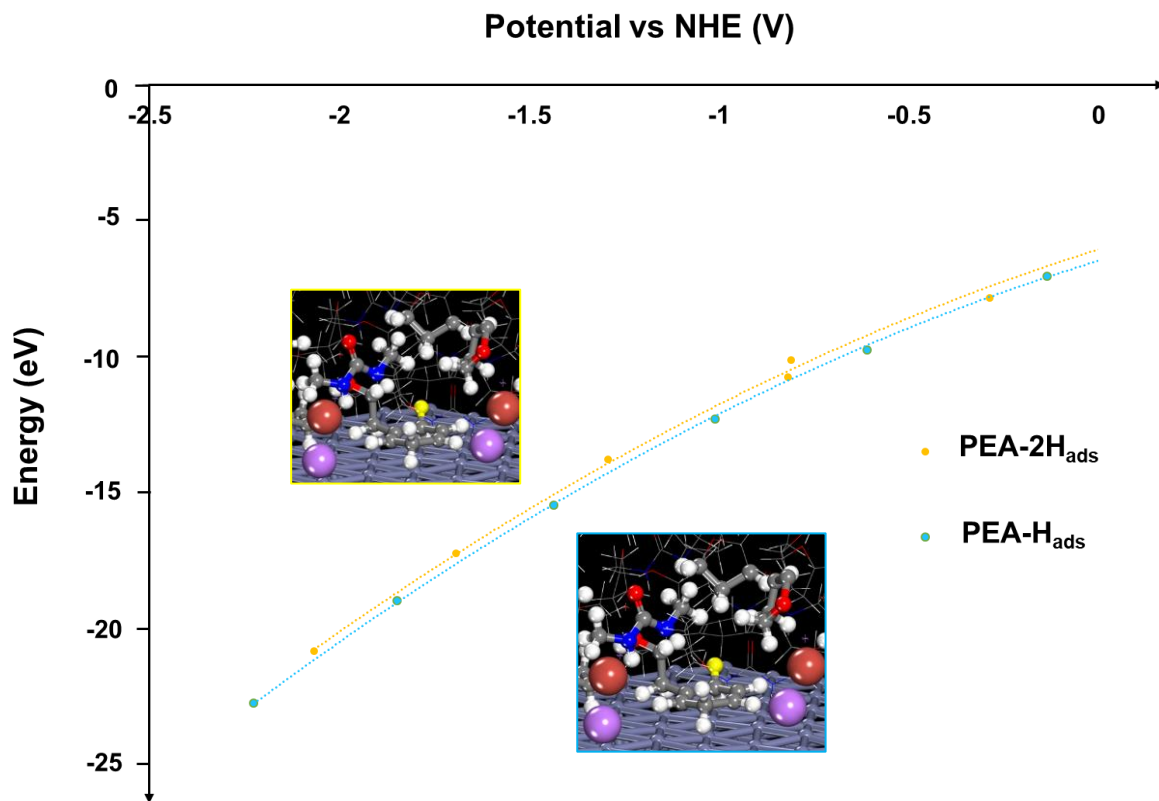


Fig. S18. Potential dependent energies for the reactant (PEAH*⁻ + DMU-H) (orange) and product (PEA2H*⁻-DMU(-)) (blue) involved in the second protonation step (PEAH*⁻ + H⁺ → PEA2H*) of phenylethyl alcohol (PEA) which is fitted to a parabolic curve

Graphical Guides

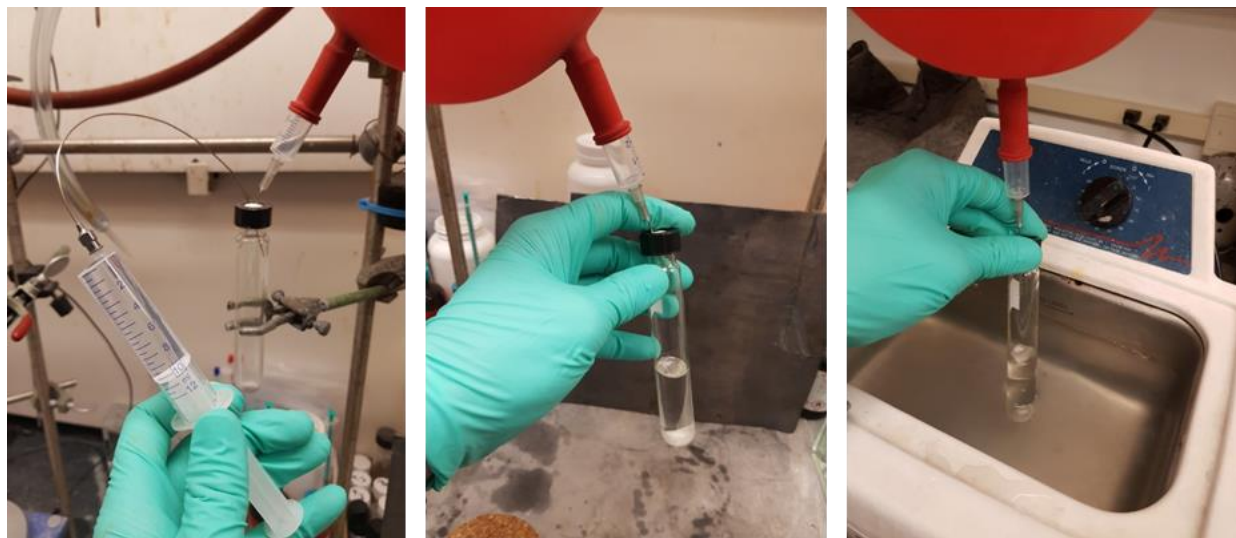
Graphical Supporting Information for drying LiBr (optional)



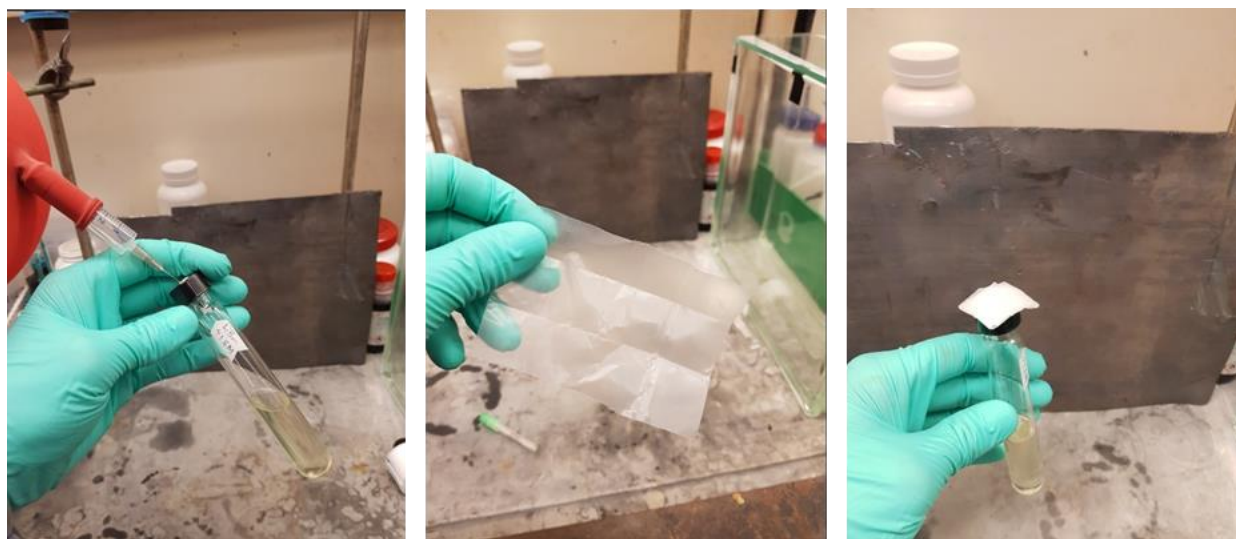
(Left) LiBr is weighed out on a piece of weighing paper. **(Center)** The LiBr is then transferred into a culture tube, which is then capped. **(Right)** The weighing paper used, two minutes after transferring the LiBr (demonstrates hygroscopic nature of the salt).



(Left) The LiBr is then placed under vacuum by piercing the septa with a 16-gauge needle (any big needle will do), which is connected to a vacuum line. The LiBr is then heat under vacuum using a propane/butane torch. **(Center)** After heating for a few seconds, liberation of H₂O is clear (typically, it was found that H₂O constituted 10%/W, even from a new, anhydrous bottle of LiBr). **(Right)** After heating until no more H₂O could be seen on the walls of the tube (typically 1-2 min) the dried LiBr was allowed to cool under vacuum.



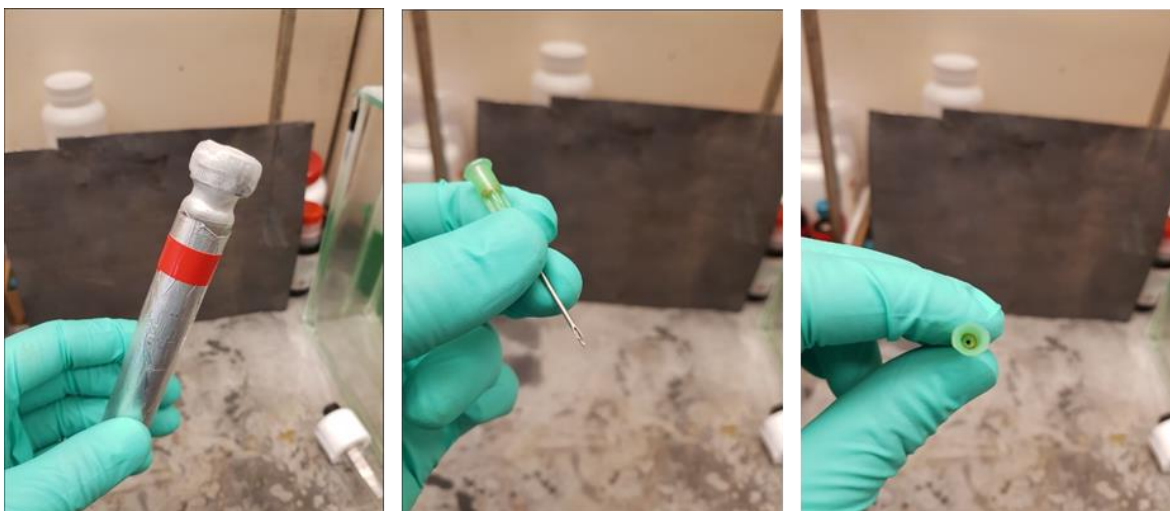
(Left) THF is then added to the cool, dry LiBr, **(Center)** which is resistant to dissolving in the THF. **(Right)** Sonication is necessary, and often shaking for some time to dissolve all the LiBr.



(Left) After dissolving, the solution will become transparent. **(Center)** Since these solutions were used for screening over several days, a useful technique that preserves the seal involves cutting a piece of Parafilm® as shown. **(Right)** Parafilm® is folded to rest over the cap as shown.



(Left) The Parafilm® is heated gently using a heat gun to soften/melt it. **(Center)** Using a spatula, the Parafilm® can be shaped easily of the cap of the culture tube. **(Right)** After the Parafilm® has cooled, it acts as a good back up seal to the cap. More Parafilm® can be applied over the cap after needle holes have been made, and again heated to make a seal. After enough Parafilm® is been applied over time, the excess can simply be heated to softness and the needle holes covered by pressing over them with a spatula.



(Left) LiBr solutions would often turn yellow standing in the fume hood. While no effect on the electroreduction was observed due to this, the yellow color could be suppressed by protection of the LiBr stock solution from light using Al-foil. **(Center)** and **(Right)** Occasionally the LiBr stock solution would be yellow from the start. This was observed to be due to contamination by the needle used for vacuum that generates this colour on heating. However, this was not observed to have an impact on any electroreduction reactions.

Graphical Supporting Information for drying DMU



(Left) DMU from the bottle compared to the same batch which has been dried. **(Center)** In addition to having a fish like odor (amine type), the bottle grade also leaves a moist residue compared to after being dried. **(Right)** Transfer the bottle grade DMU to a RBF.

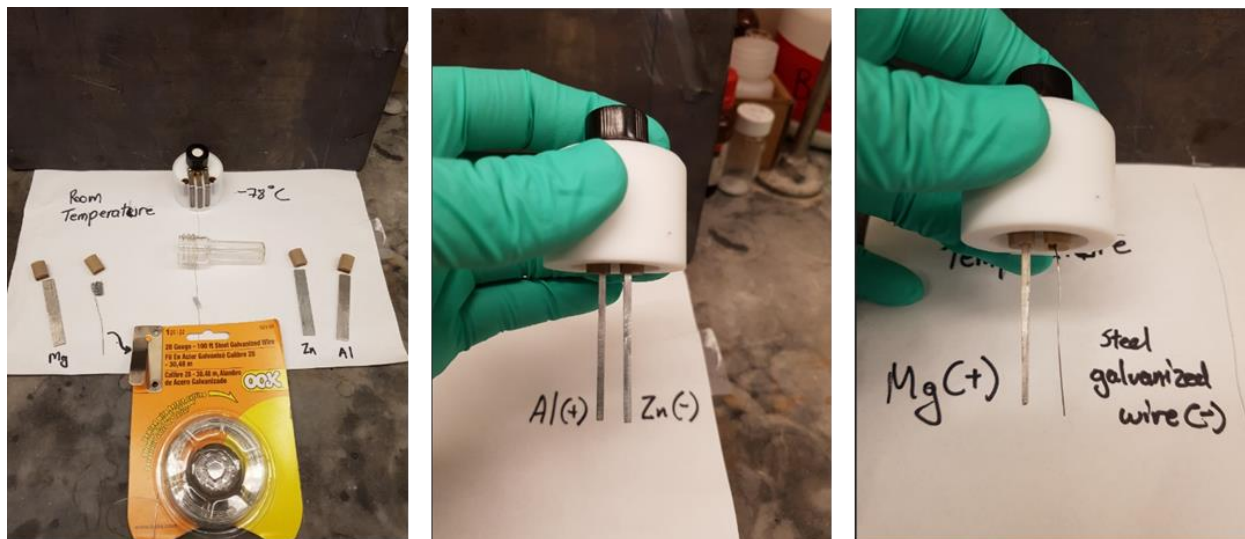


(Left) The bottle grade DMU has poor solubility, but does dissolve in MeOH, then benzene or toluene can be added. And the solvents removed on the rotavap. After the first drying the DMU is readily soluble in benzene. Benzene or toluene coevaporations are repeated two more times. **(Center)** After drying on the rotavap finer white solid is obtained. **(Right)** This solid is dried for two hours under high vacuum.



(Left) The dry solid can be easily scrapped from the RBF to produce a free-flowing flakey powder, which has considerably higher solubility in the reaction solvent than the DMU directly from the bottle. **(Right)** The dried DMU can be stored in any vial, and no additional precautions need be taken to ensure that it is protected from the atmosphere.

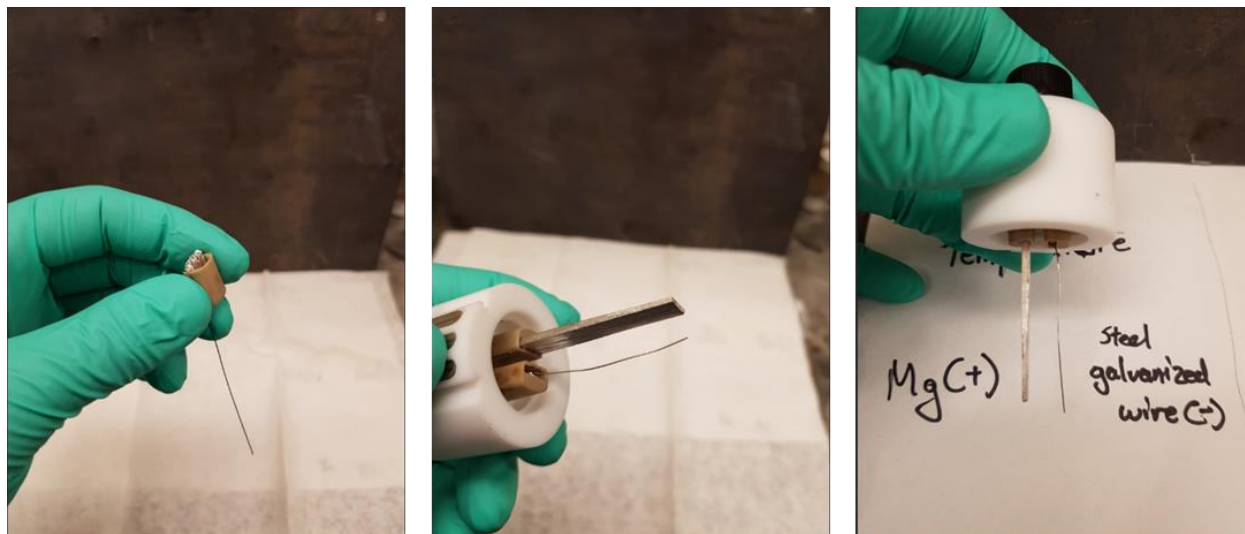
Graphical Supporting Information for electrode assembly



(Left) Electrodes and parts needed. **(Center)** Assembly for a $-78\text{ }^{\circ}\text{C}$ reaction. **(Right)** Assembly for a room temperature reaction.



(Left) Al foil, piece of cardboard and galvanized steel wire needed for the cathode for a room temperature reaction. **(Center)** Wrap the foil over the piece of cardboard. **(Right)** Wind the wire over this piece several times.



(Left) Insert the now into the holder for the IKA electrodes. **(Center)** Connect to the ElecraSyn cap. **(Right)** Completed assembly for a room temperature electroreduction reaction.

Graphical Supporting Information for setting up a room temperature Electroreduction reaction (representative EC Birch example)



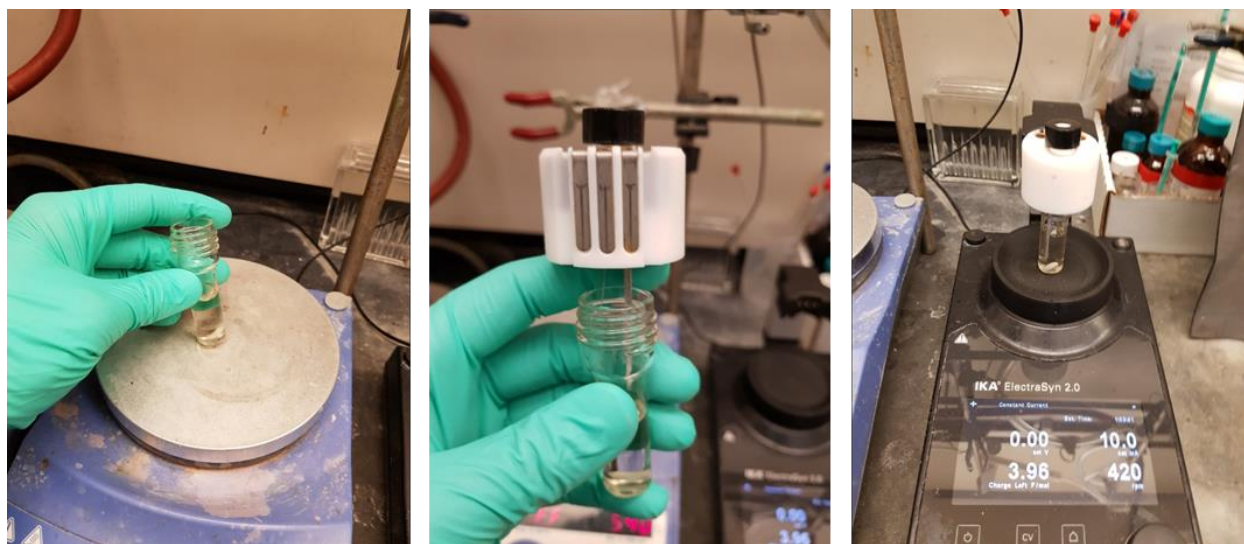
(Left) Reagents needed. **(Center)** Solids (DMU and substrate (if solid)) weighed out, open to the air, no precautions taken. **(Right)** Solids dispensed first into a clean ElectraSyn vial with magnetic stirrer bar.



(Left) TPPA (pale yellow) taken up by syringe. **(Center)** TPPA is added to the solids in the ElectraSyn vial (no precautions needed). **(Right)** The necessary amount of LiBr is drawn from a 1.5 M stock (preparation demonstrated above – see *Graphical Guide for the Preparation of LiBr Solution*).



(Left) Addition of the LiBr solution to the TPPA/DMU/Substrate mixture (because excessive moisture is problematic, a septum is used to protect the reaction while collecting THF) **(Center)** THF is drawn from a solvent purification system (no BHT, ~ 15 ppm H₂O by Karl-Fischer). **(Right)** THF is quickly added to the ElectraSyn reaction vial with the rest of the reactants/reagents.

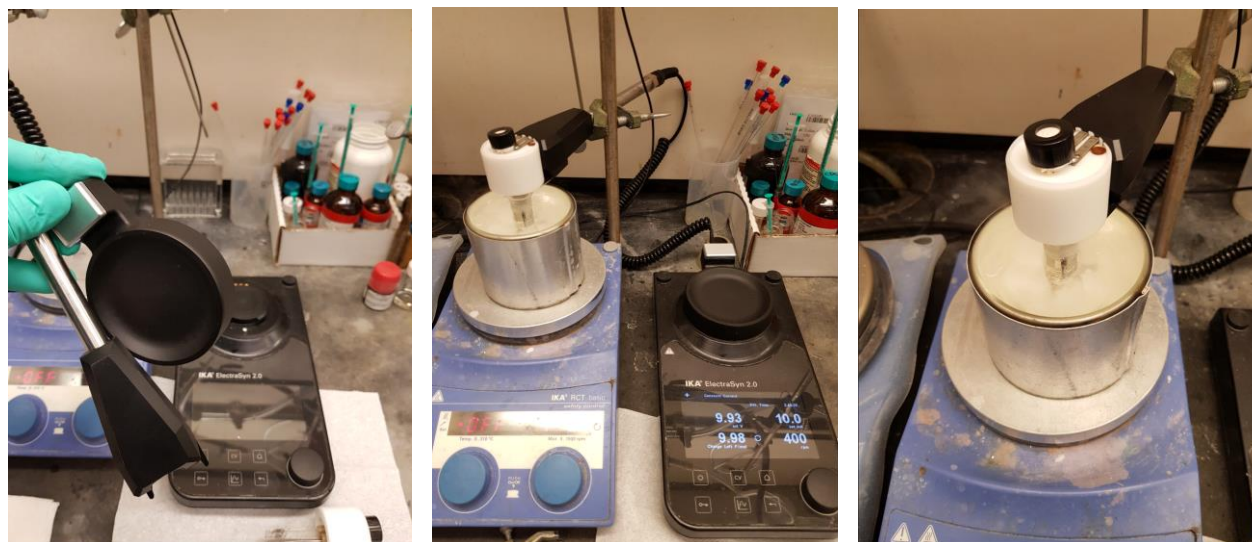


(Left) The contents are briefly mixed by stirring to ensure homogeneity. **(Center)** The ElectraSyn cap is fastened to the vial. **(Right)** The vial is connected to the ElectraSyn and the reaction is started (See ElectraSyn setup graphical guide).

Graphical Supporting Information for setting up a -78 °C Electroreduction reaction (representative EC Birch example)

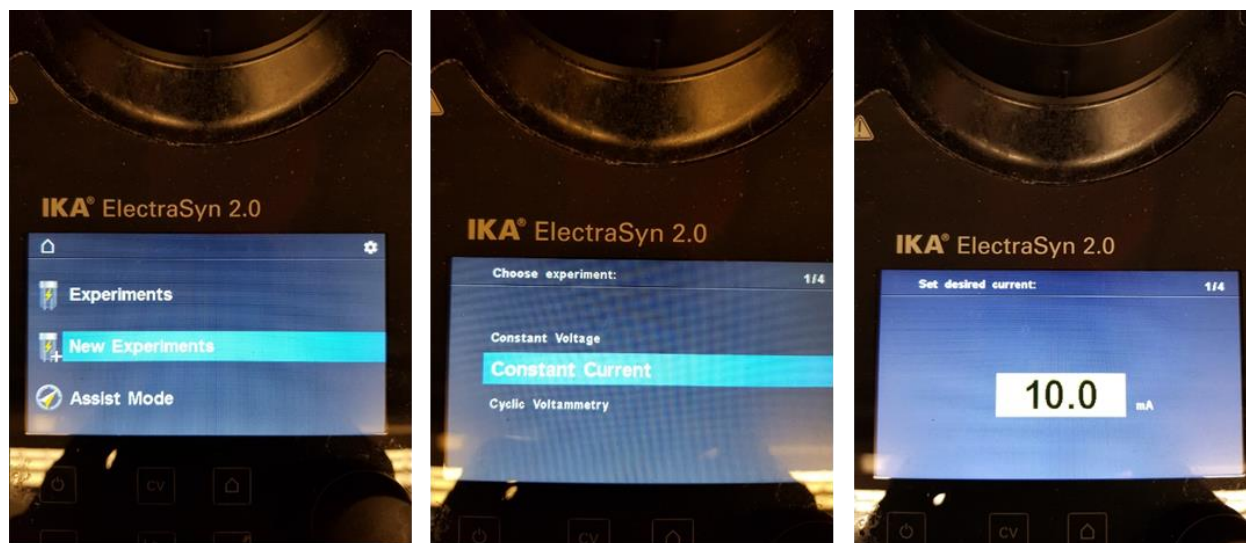


(Left) A small bowl is filled with dry ice and then acetone or *i*-PrOH and then placed onto the ElectroSyn. **(Right)** The reaction vial is then immersed and connected. Approximately 1 minute is allowed for cooling prior to starting the electrolysis (See ElectroSyn setup graphical guide).

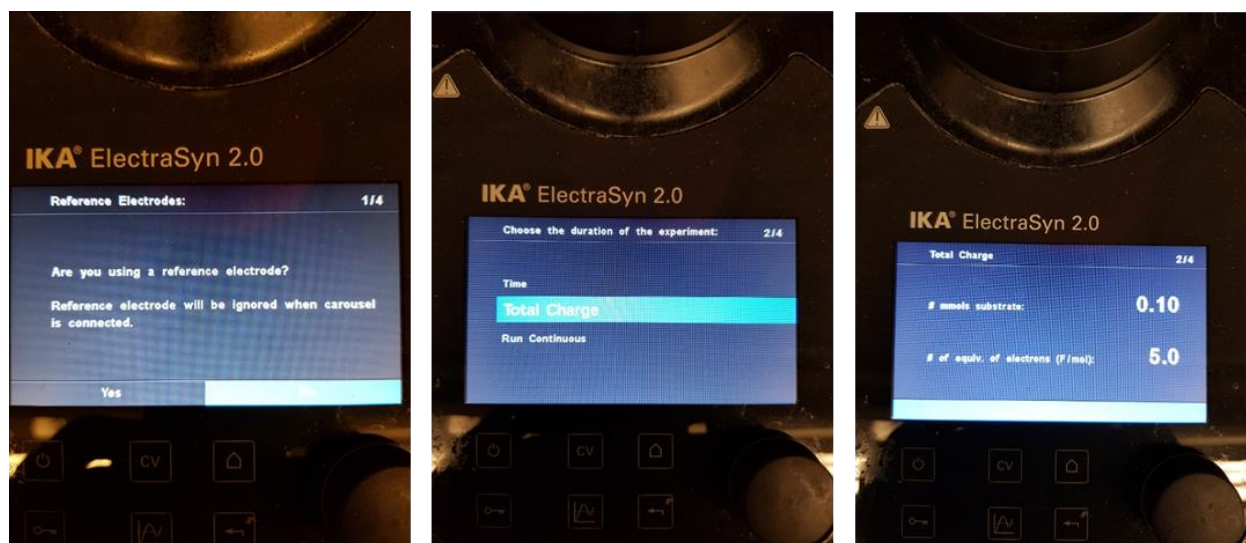


(Left) Alternatively, the IKA extension can be used if longer reaction times are needed and a Dewar flask is preferred. **(Center)** and **(Right)** Assembled extension and reaction carried out a -78 °C.

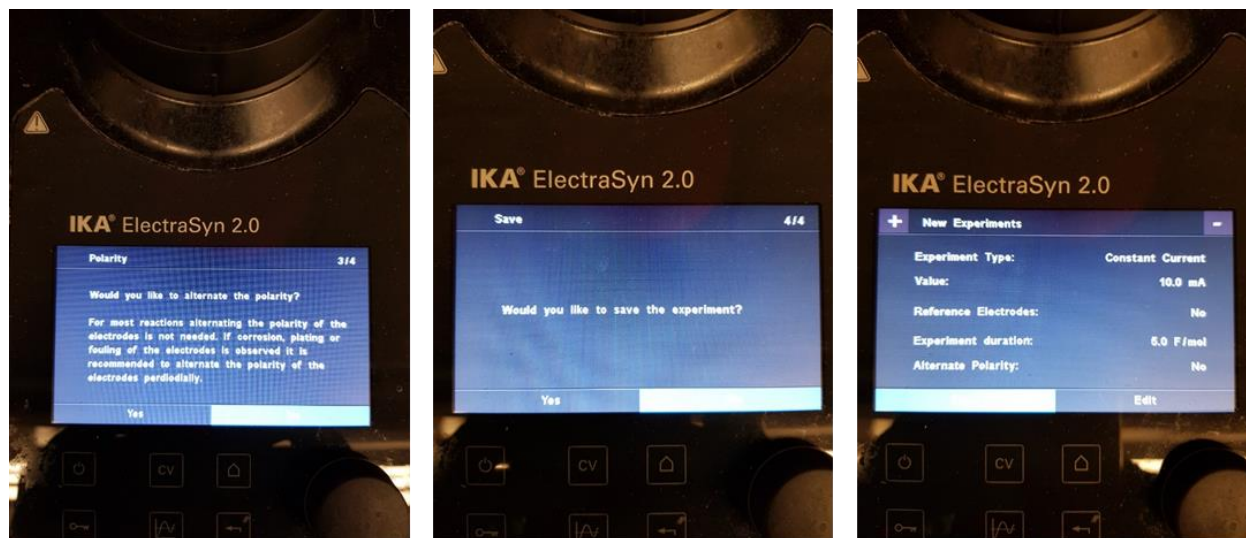
Graphical Supporting Information for setting up the ElectraSyn device for an Electroreduction reaction



(Left) Selecting a new experiment. **(Center)** Select constant current. **(Right)** Set the current to 10 mA (for a 0.1 mmol scale).



(Left) No need to use a reference electrode, so select *No*. **(Center)** Reactions are run based on how much charge they need. **(Right)** Typically reactions were run on a 0.1 mmol scale and typically current efficiencies are around 50 %, so select double/triple what is needed. NOTE: ALL REACTIONS WERE MONITORED AND STOPPED ACCORDING TO TLC ANALYSIS (consumption of starting material), MORE OR LESS CHARGE MAY BE REQUIRED FOR EACH INDIVIDUAL CASE!



(Left) No need to alternate the polarity, if fact, that will result in NO REACTION. **(Center)** This is up to the individual, but there is really no need to save the experiment. **(Right)** Start when ready!



(Left) Typical readbacks for a room temperature reaction, however, it is very substrate dependent, so a potential of 15-20 V is not uncommon. **(Right)** Balloon isn't crucial, but the reactions do proceed slightly faster by keeping oxygen out.

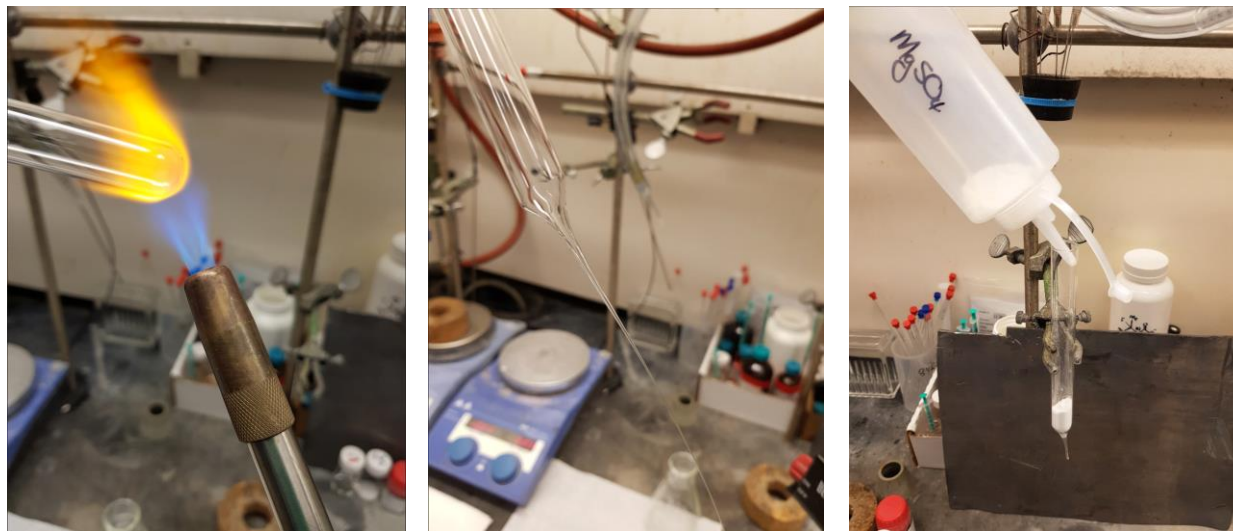
Graphical Supporting Information for Working-Up the Electroreduction reactions



(Left) Typical appearance after a low temperature reaction (can also be turbid and much darker, depending on the substrate). **(Center)** Turbid appearance of the room temperature reaction (again, not always and can also be darker). **(Right)** Simply dump the reaction into a separatory funnel.



(Left) Add deionized water. **(Center)** Then add EtOAc, and shake. **(Right)** Separate layers (most of the TPPA and all the DMU will be in the aqueous phase and the product will be in the EtOAc layer).



(Left) As filters, culture tubes were fashioned into columns using a propane/butane flame. **(Center)** Using a pair of forceps, whilst hot they can be pulled into the shape, and the ends snapped off to form the column structure desired. **(Right)** Plugging the end with either cotton or ChemWipes paper, MgSO_4 can be added to the column (1.5 cm).



The EtOAc layer can be passed through the plug of MgSO_4 and the volatiles removed on the rotavap to provide the crude material, which was purified using prep-TLC.

Graphical Supporting Information for cleaning the electrode assembly after a reaction



(Left) After the room temperature reaction, the Mg-anode (even the wire cathode) are typically dirty. **(Center)** This dark junk can be scraped off with a blade (applies to all electrodes, even the Al and Zn for the $-78\text{ }^{\circ}\text{C}$ reaction). **(Right)** The shiny appearance of the electrode is returned upon scraping (this does erode the electrode, but >30 EC Birch reactions can be run before the Mg electrode – or other – becomes too worn to use. It is advised not to scrape excessively.



(Left) After scraping the electrodes are rinsed with deionized water. **(Center)** and **(Right)** After a water rinse the electrodes and the reaction vial are washed with acetone.

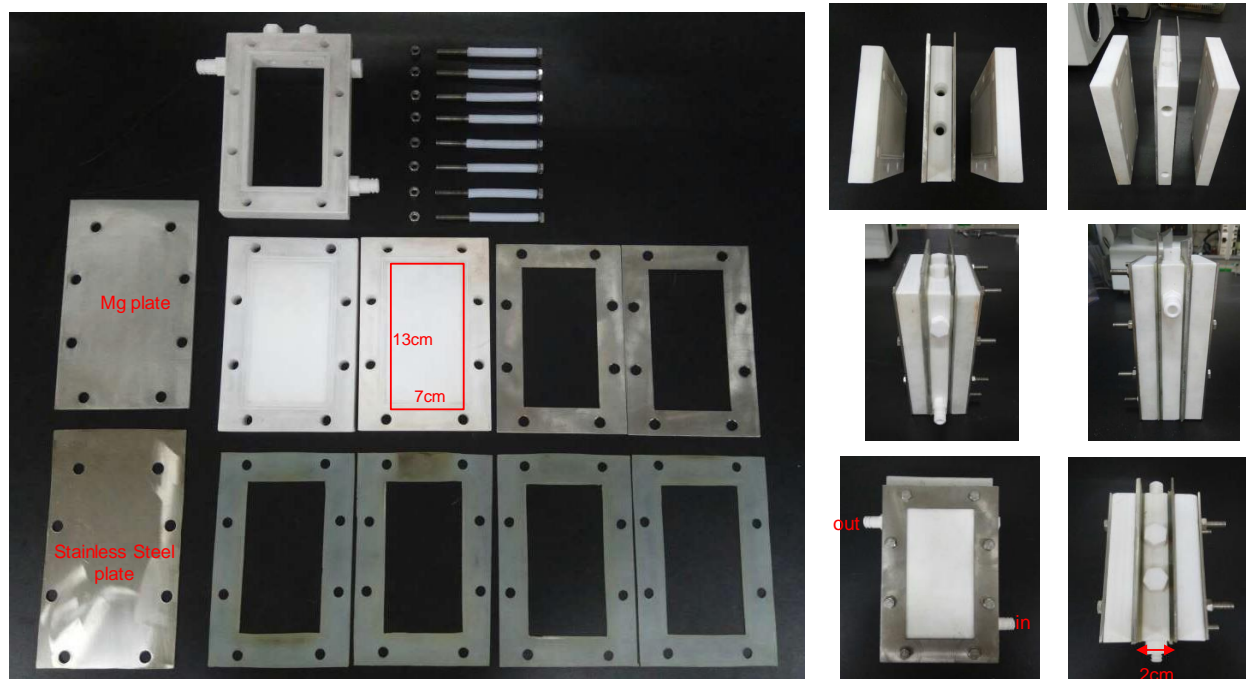


To properly clean the vial, fill with 1 M HCl, and allow to stir for one minute. Afterwards, rinse again with acetone and allow to dry before setting up the next EC Birch.

Graphical Supporting Information for a 10g Scale-Up of Compound 12

In flow:

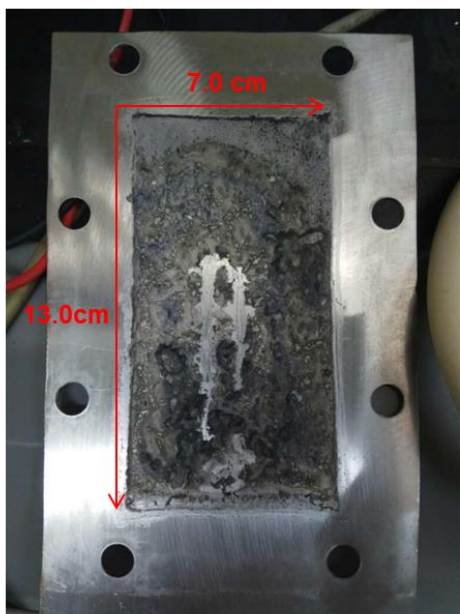
Components for flow apparatus (left) and assembly (right)



Reaction in progress, with progress after one hour (top right)



After 16h reaction:



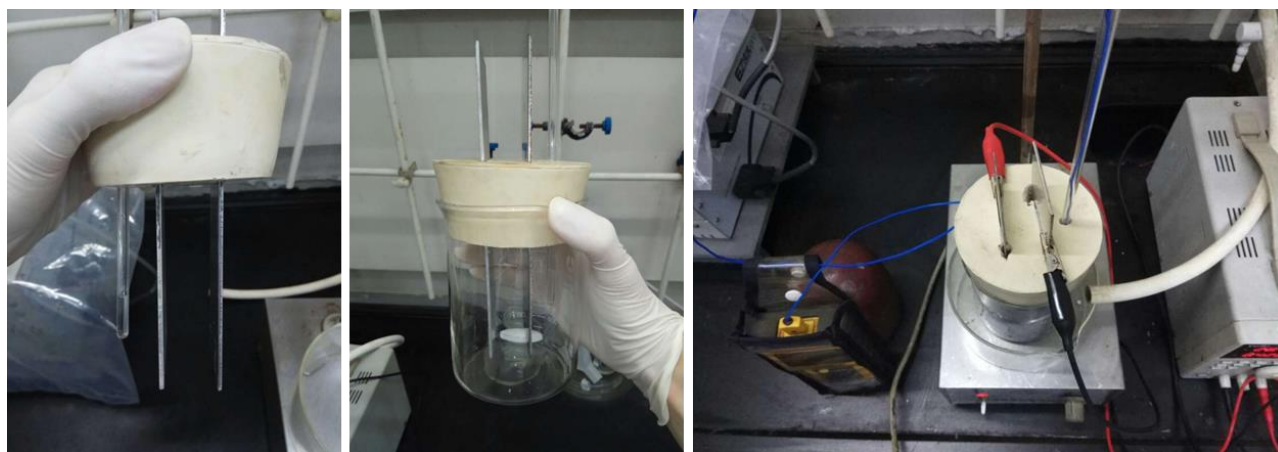
Stainless Steel Cathode
(Coated with a thick solid)



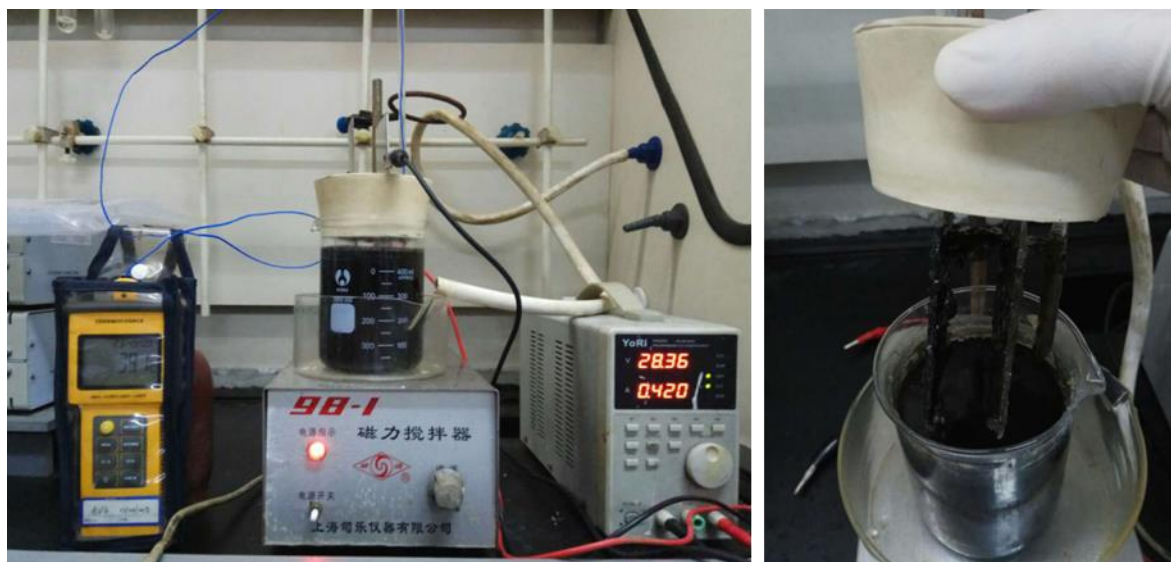
Magnesium Anode

In Batch:

Batch reaction assembly



Batch reaction in progress (left). Completed reaction (right)



Separation of layers (left). Combined product (23 g) after three scale-up reaction (right).



Graphical Supporting Information for a 100g Scale-Up of Compound 12 in flow

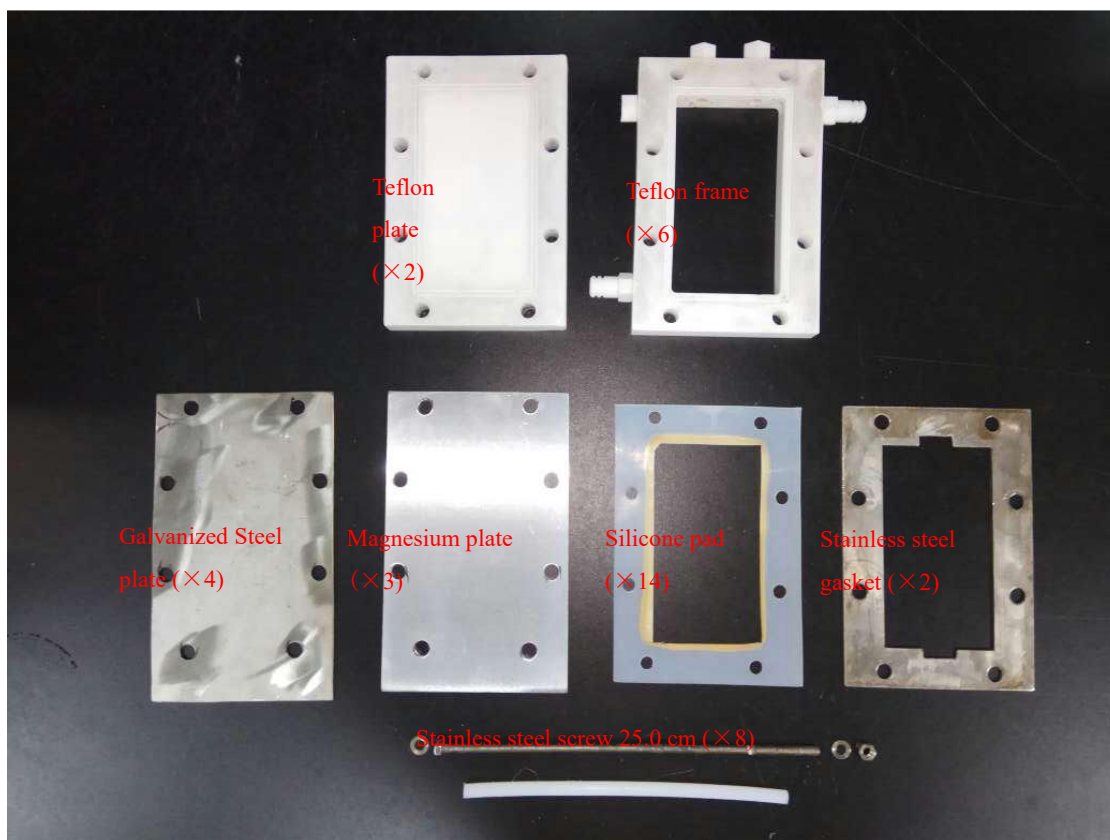


Figure 3. Components of Frame Cell

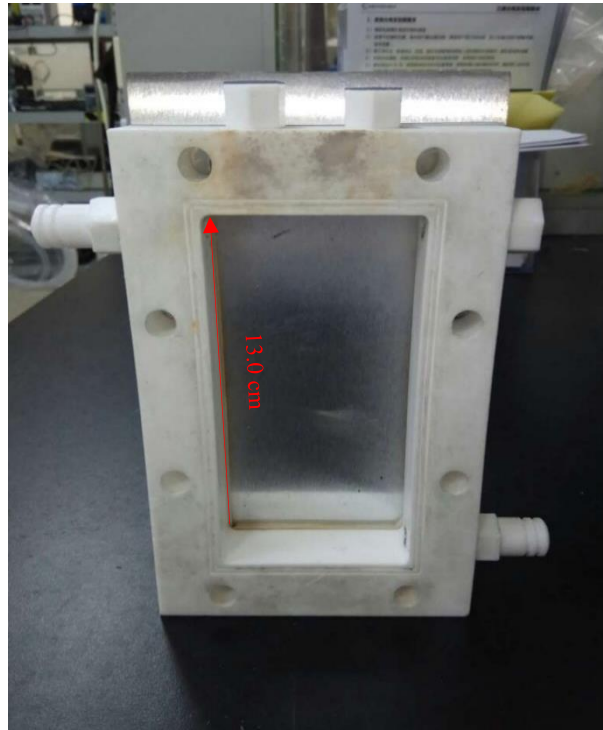
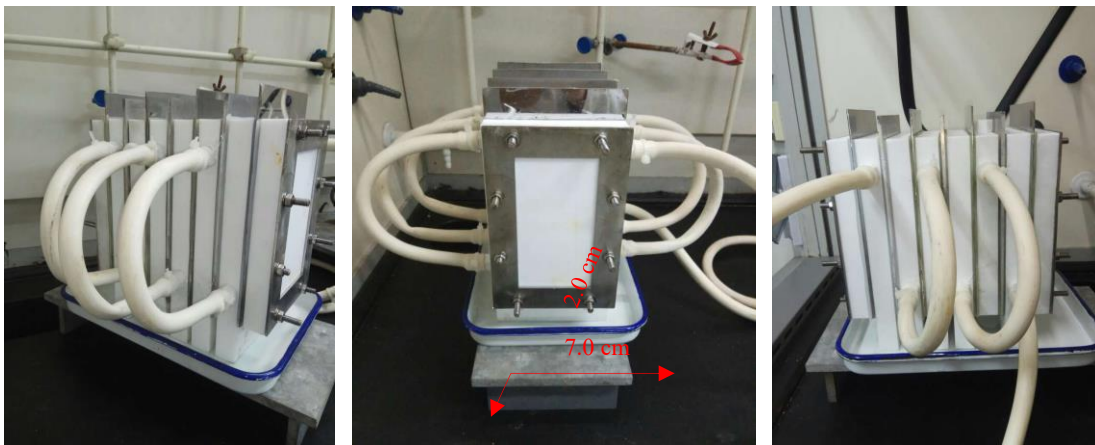
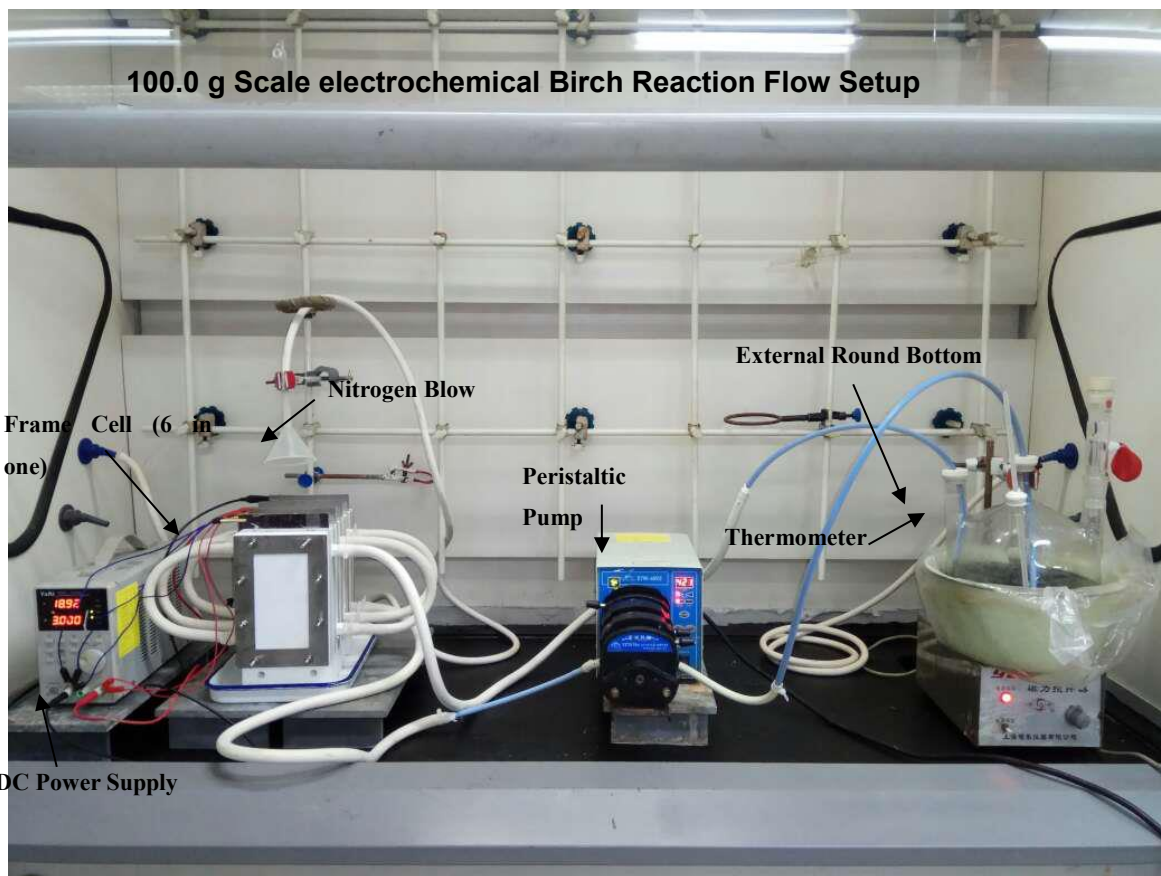


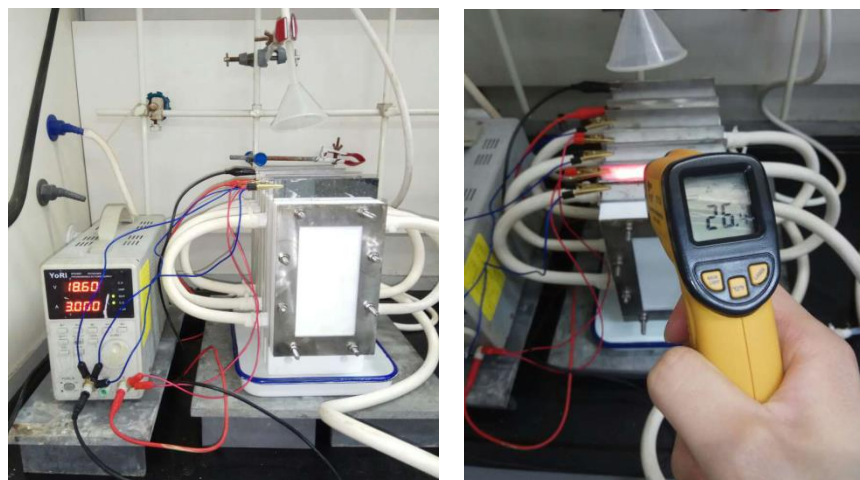
Figure 4. One single cell



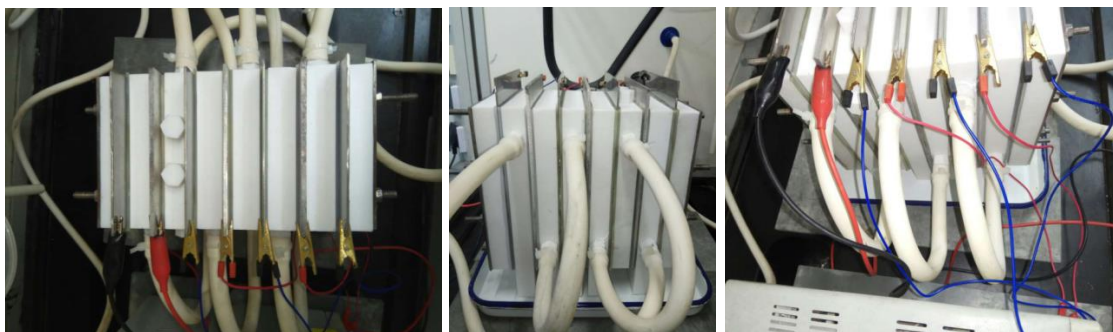
Frame Cell set up: left, front, right views.



Electrolysis set up in flow



(Left) Frame cell and DC power during electrolysis. (Right) Temperature monitor of frame cell.



(Left) Top view of frame cell in electrolysis. **(Middle)** Right side view of frame cell in electrolysis. **(Right)** Left side view of frame cell in electrolysis.



(Left) Peristaltic pump and fluororubber tube. **(Right)** External round bottom in flow.



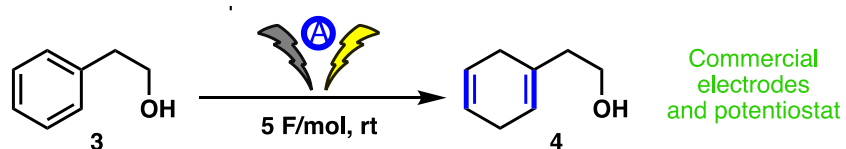
(Left) Reaction mixture washes with 10% Roschelles' salt solution. *(Right)* Reaction mixture washes with water.



Left to right: crude product, basic alumina chromatography, pure product (bottom and product)

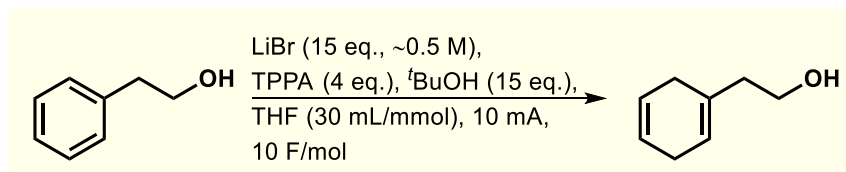
Electrochemical Birch Reduction

Optimization



Entry	Ref	Electrodes	Conditions	Yield	By-prod.
1	42, 44	Pt(+)/Pt(-)	MeNH ₂ , LiCl	<5%	-
2	54	SS(+)/Hg(-)	THF/H ₂ O, TBA.OH	<5%	-
3	55, 56	C(+)/Al(-)	HMPA/EtOH, LiCl, divided cell	<5%	-
4	62	Mg(+)/Mg(-)	THF/ ^t BuOH, LiClO ₄ , sonication	<5%	-
5	-	Al(+)/Zn(-)	THF, ^t BuOH, LiBr	<5%	-
6	-	Al(+)/Zn(-)	THF, ^t BuOH, LiBr, TPPA	50%	30%
7	-	Al(+)/Zn(-)	THF, DMU, LiBr, TPPA	65%	14%
8	-	Al(+)/Zn(-)	THF, DMU, LiBr, TPPA, -78 °C	74%	<5%
9	-	Mg(+)/GSW(-)	THF, DMU, LiBr, TPPA	70%	<5%

Survey of electrolyte, temperature, voltage and additives



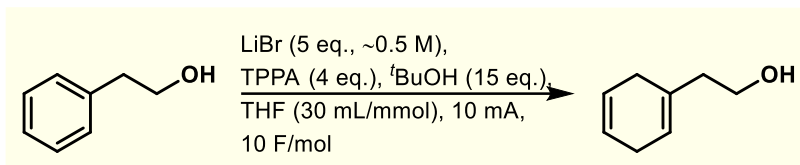
	entry	anode	cathode	other change	% prod.	% aliphatics	% isomers	% SM
conditions	1	Al	Zn	LiBr (45 eq.)	15	43	15	28
	2	Al	Zn	EtOH (15 eq.)	19	46	18	18
	3	Al	Zn	TPPA (45 eq.)	12	46	21	21
	4	Al	Zn	30 F/mol	29	31	21	19
	5	Al	Zn	-78 to -20 °C	37	33	21	10
	6	Al	Zn	LiBr (3.5 eq.) - 0.2 M	60	16	15	9
	7	Al	Zn	5 mA	32	22	17	29
	8	Al	Zn	20 mA	4	10	7	78
	9	Al	Zn	TBA.BF ₄ + LiBr	Messy			

entry	anode	cathode	other change	% prod.	% aliphatics	% isomers	% SM	
conditions	1	Al	Zn	LiBr (45 eq.)	15	43	15	28
	2	Al	Zn	EtOH (15 eq.)	19	46	18	18
	3	Al	Zn	TPPA (45 eq.)	12	46	21	21
	4	Al	Zn	30 F/mol	29	31	21	19
	5	Al	Zn	-78 to -20 °C	37	33	21	10
	6	Al	Zn	LiBr (3.5 eq.) - 0.2 M	38	29	23	9
	7	Al	Zn	5 mA	32	22	17	29
	8	Al	Zn	20 mA	4	10	7	78
	9	Al	Zn	TBA.BF ₄ + LiBr	Messy			

entry	anode	cathode	other change	% prod.	% aliphatics	% isomers	% SM	
additives	1	Al	Zn	NaO ^t Bu (15 eq.), TBA.BF ₄	} conductivity poor, no rxn			
	2	Al	Zn	LiOMe (15 eq.), TBA.BF ₄				
	3	Al	Zn	LiO ^t Bu	43	21	0	37
	4	Al	Zn	LiHMDS	-	-	-	100
	5	Al	Zn	LiN(Tf) ₂	39	18	13	31
	6	Al	Zn	LiPF ₆	-	-	-	100
	7	Al	Zn	LiBF ₄	-	-	-	100
	8	Al	Zn	LiClO ₄	9	7	4	80
	9	Al	Zn	LiTFA	-	-	-	100
	10	Al	Zn	LiOTf	-	-	-	100
	11	Al	Zn	NaI	-	-	-	100
	12	Al	Zn	NaBr	} Solubility issues			
	13	Al	Zn	KBr				
	14	Al	Zn	LiI	5	20	49	25
	15	Al	Zn	LiOAc	-	-	-	100
	16	Al	Zn	TMEDA (3.5 eq.)	33	20	19	28
	17	Al	Zn	LiO ^t Bu at 2 mA, 10 F/mol	9	7	4	80
	18	Al	Zn	PVP	38	20	3	39
	19	Al	Zn	K ₂ CO ₃	30	8	10	52

In optimization tables, values represent % contribution by ¹H NMR

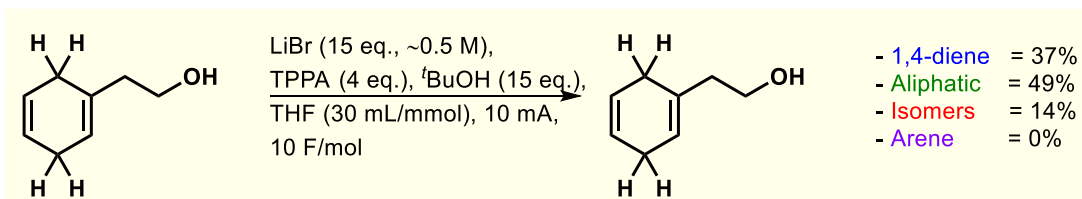
Survey of electrodes:



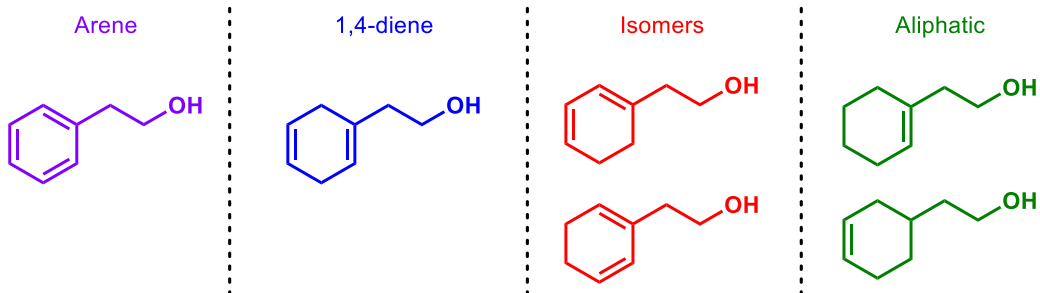
entry	anode	cathode	other change	% prod.	% aliphatics	% isomers	% SM	
anodes	1	Al	Zn		28	44	0	29
	2	Mg	Zn		18	33	21	28
	3	Cu	Zn		0	0	0	100
	4	Zn	Zn		10	30	4	56
	5	C	Zn	Pyrrole	-	-	-	-
	6	C	Zn	Hydrazine (dry)	-	-	-	-
	7	C	BDD	Li-formate, MeOH	-	-	-	-
cathodes	8	Al	Cu		27	29	18	27
	9	Al	Fe		28	27	18	27
	10	Al	GC		30	22	17	31
	11	Mg	Mg	AP = 10 min	10	30	4	56
	12	Al	RVC		26	54	14	6
	13	Al	Al	AP = 10 min	-	-	-	100
	14	Al	Zn	-78 °C, DMU, TPPA (10 eq.)	74%	-	-	-
	15	Mg	GSW	rt., DMU, TPPA (10 eq.)	72%	-	-	-

AP = Alternating polarity

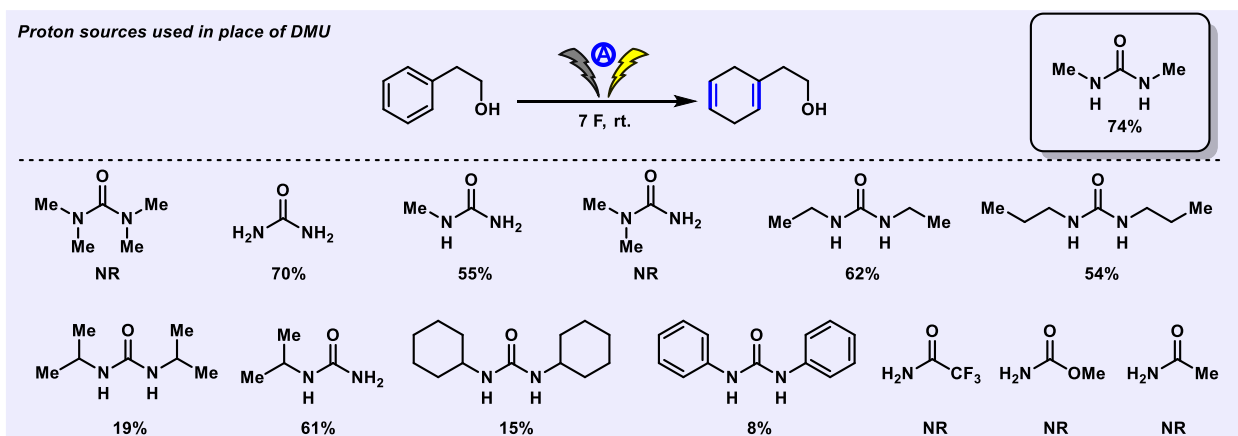
Product stability experiment:



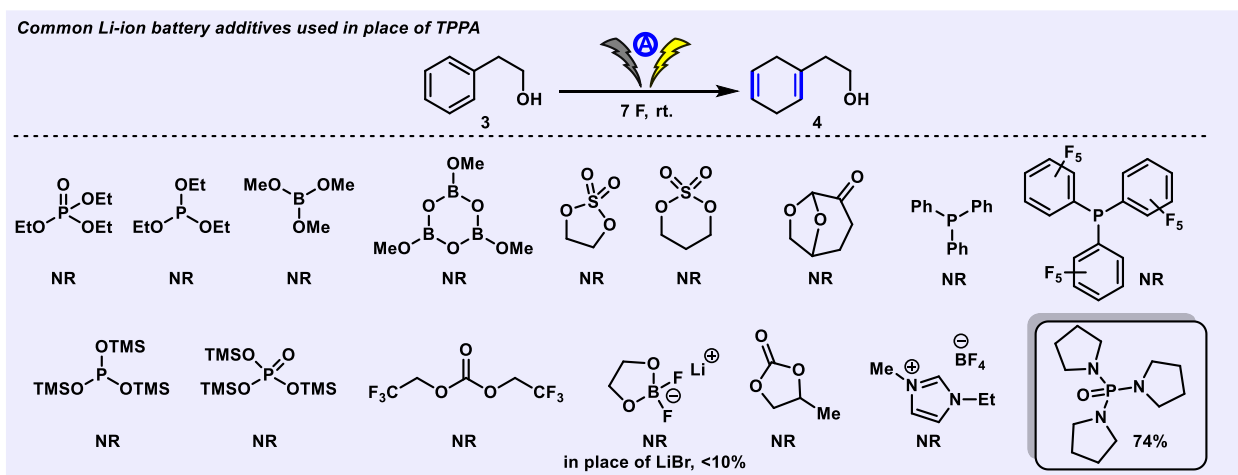
- 1,4-diene = 37%
- Aliphatic = 49%
- Isomers = 14%
- Arene = 0%



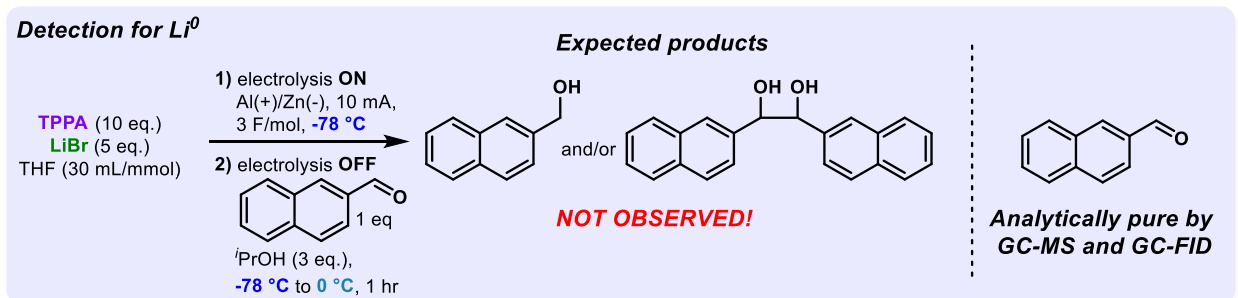
Proton source study:



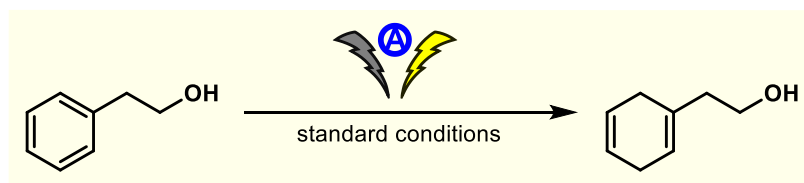
Study of common additives found in Li-ion batteries:



Li⁰-detection experiment

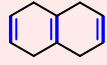
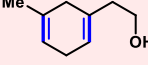
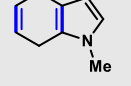
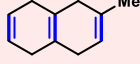
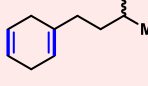
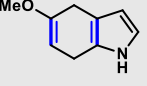
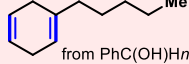
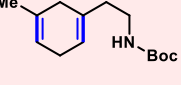
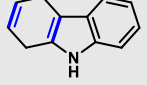
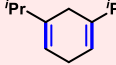
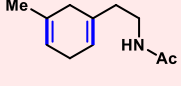
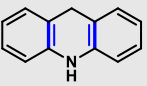
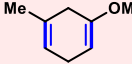
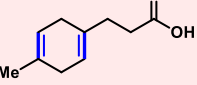
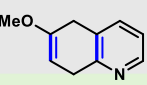
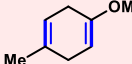
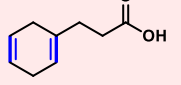
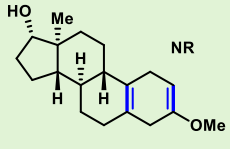
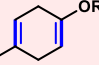
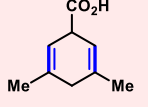
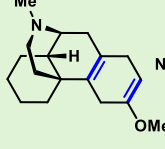
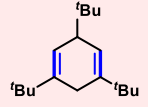
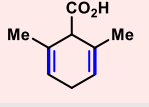
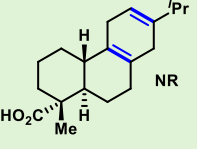
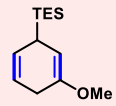
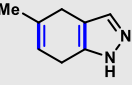
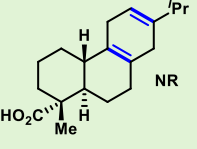
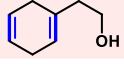
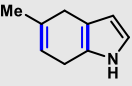
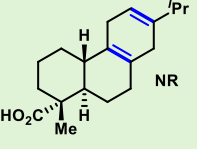


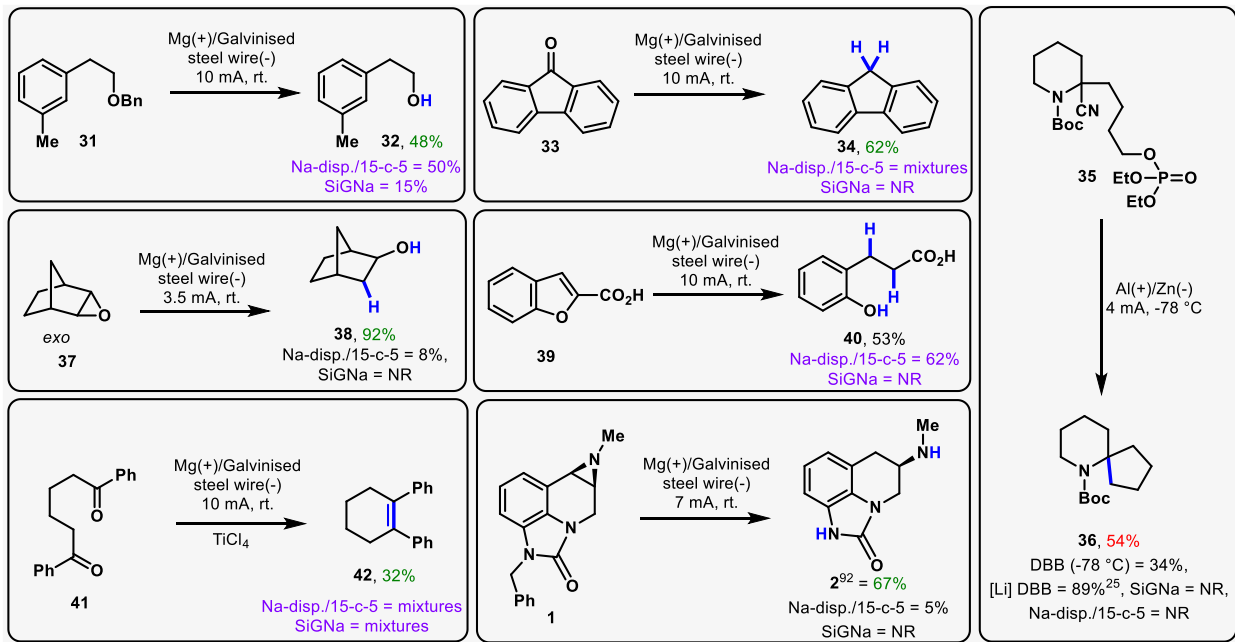
MgBr₂ Additive Experiment



entry	anode	cathode	other change	% prod.
1	Mg	GSW	rt., DMU, TPPA (10 eq.)	72%
MgBr ₂ 2	Mg	GSW	1 equiv. MgBr ₂	30%
3	Mg	GSW	4 equiv. MgBr ₂	15%
4	Mg	GSW	8 equiv. MgBr ₂	16%

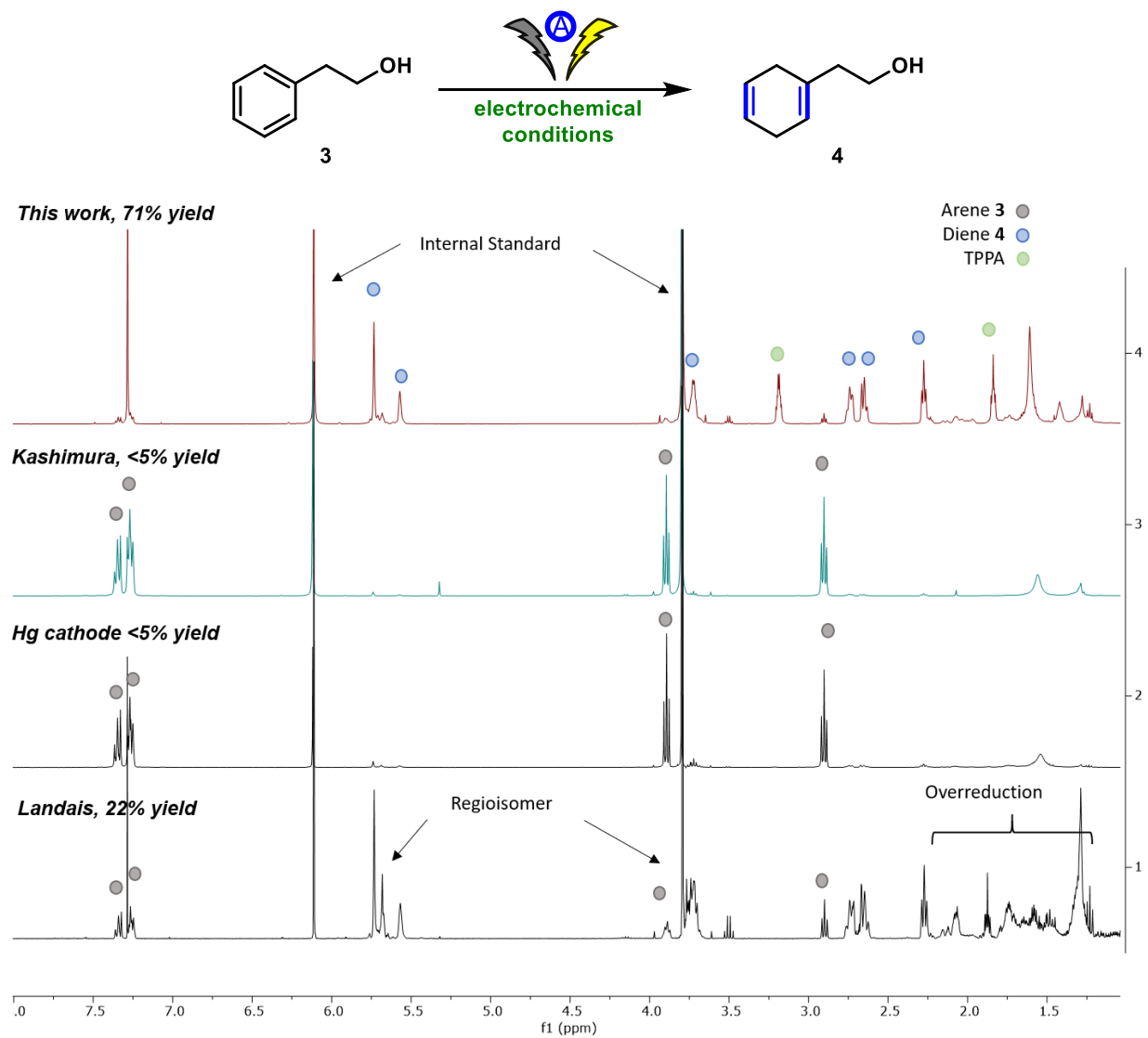
Comparison with other ammonia-free variants – SiGNa and Na-dispersion/15-crown-5.

Entry	Product	SiGNa	Na-disp/ 15-c-5	This work	Product	SiGNa	Na-disp/ 15-c-5	This work	Product	SiGNa	Na-disp/ 15-c-5	This work		
1		mono-ene 50%	6%	71%		NR	76%	76%		NR	opp. regio. chem.	53%		
2		isomers	isomers	68%		NR	<5%	70%		NR	28%	48%		
3	 from PhC(OH)HrBu	NR	NR	58%		NR	26%	69%		NR	<5%	39%		
4		NR	NR	85%		NR	51%	43%		NR	99% ¹⁴	45%		
5		NR	6%	60%		NR	<5%	50%		<5%	NR	40%		
6		NR	15%	64%		NR	14%	68%		NR	99% ¹⁴	65%		
7	 R = TBS = TES	NR NR	7% <5%	72% 70%		NR	6%	50%		NR	NR	59%		
8		NR	NR	65%		NR	NR	55%		NR	NR	60%		
9		NR	NR	65%		NR	NR	39%		NR	NR	60%		
10		NR	10%	50%		NR	NR	76%		NR	NR	60%		
				A					B					C

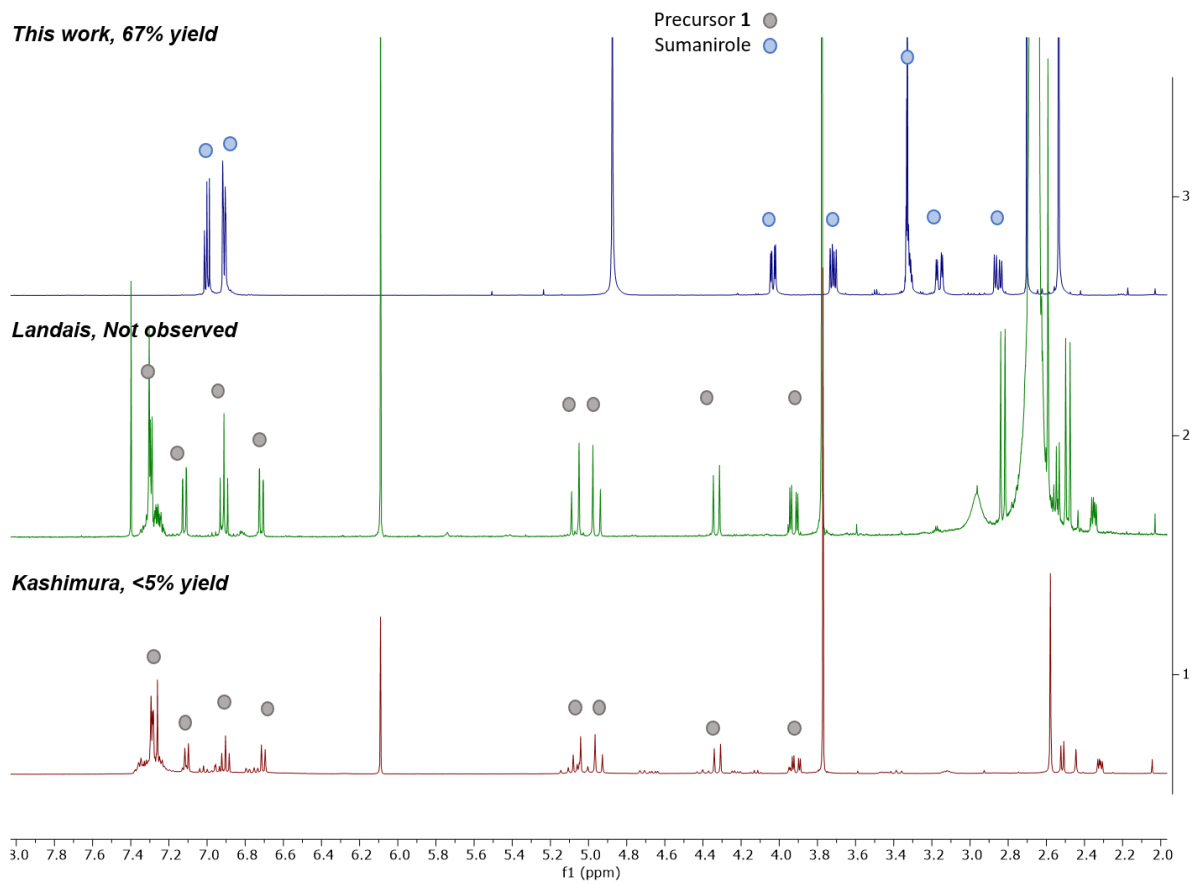
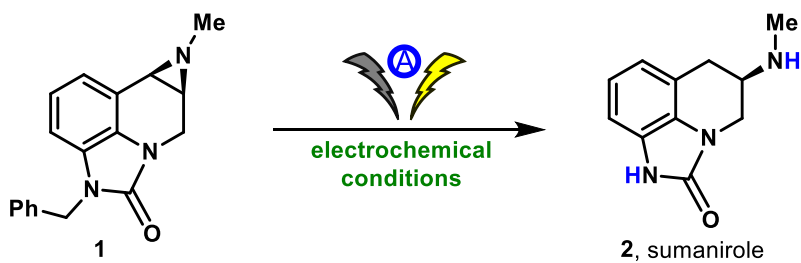


NMR Comparisons on Phenylethanol

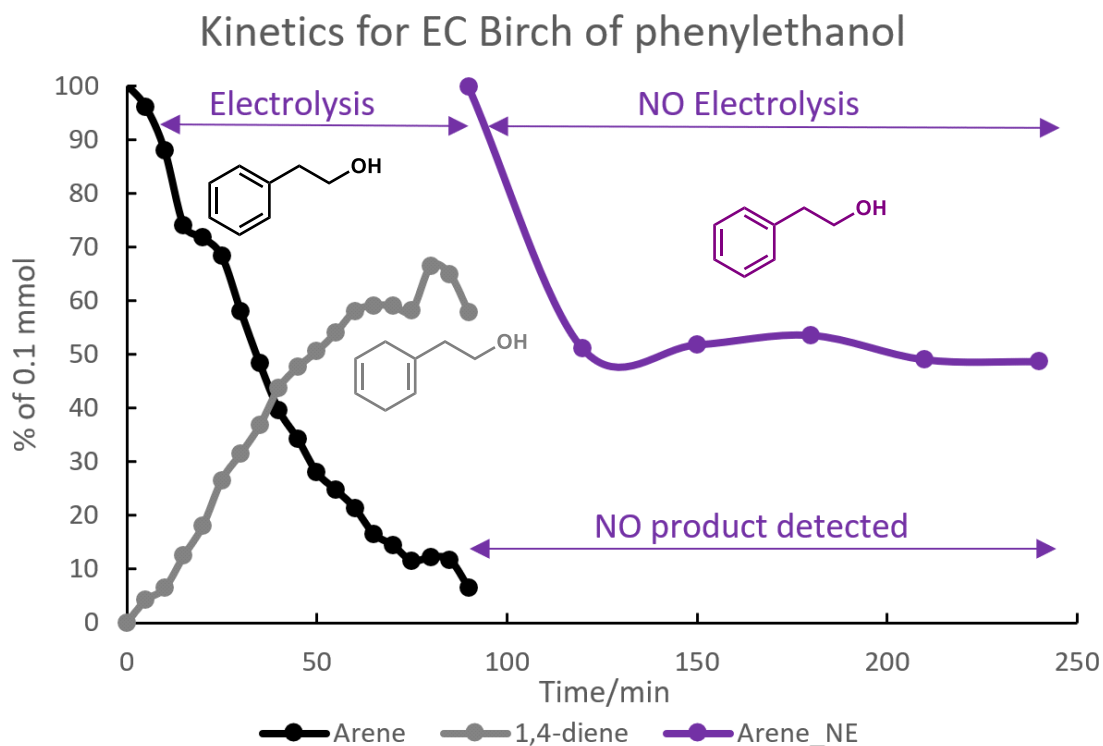
Crude NMR comparisons with known electrochemical methods on phenylethanol:



Sumanirole Comparison vs. known electrochemical methods:



Kinetic Study and Diffusion Experiments of Compound 4



Reactions were setup on a 0.1 mmol substrate scale as detailed for the representative Electroreduction procedure (*vide infra/supra*), however rigorous drying and degassing were carried out. Dodecane was added as an internal standard. 100 μ L aliquots were drawn from the reaction every 5 min and passed through a 1 cm plug of silica gel, eluting with EtOAc. The samples were analysed on a GC-FID-MS instrument. Signals were identified by comparison with authentic samples and by their parent ion MS signal. Areas of the starting material and products were calibrated about the dodecane internal standard. The no electrolysis experiment was set up the same way, however the substrate was omitted and later added after 90 min. Before adding substrate, the electrolysis was stopped, and a strict atmosphere of argon was maintained throughout the study.

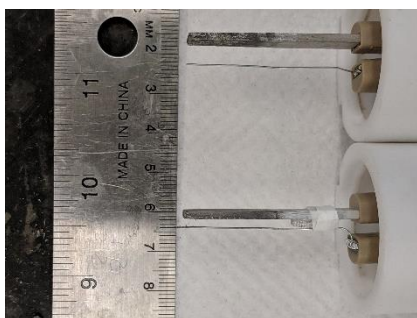
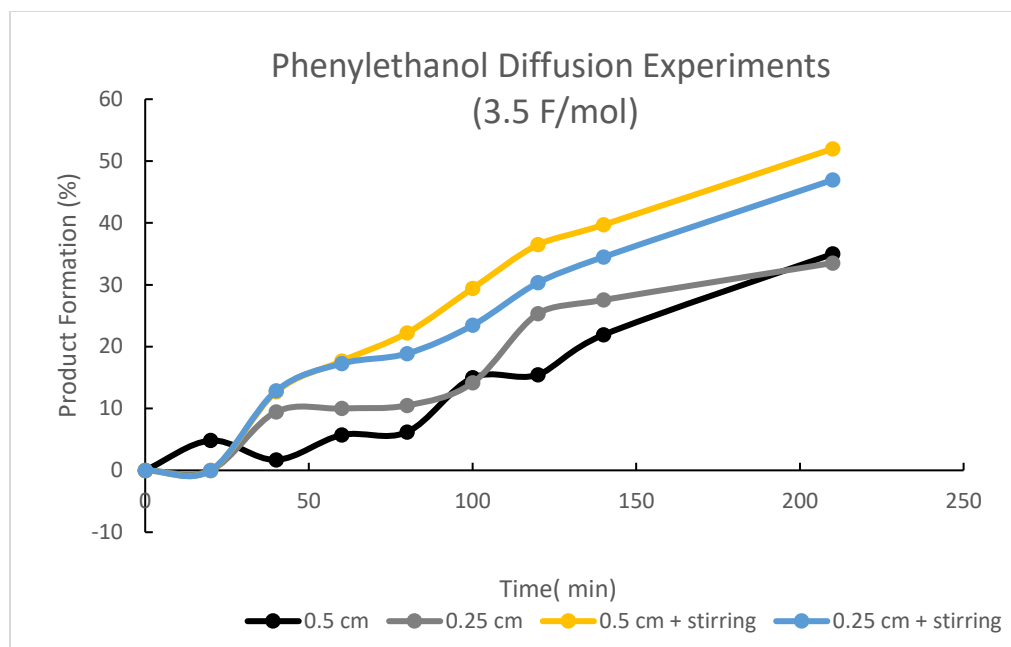


Figure 1. Electrode Distance Setup



Figure 2. After reaction (with no stirring)

Reactions were setup on a 0.4 mmol substrate scale as detailed for the representative Electroreduction procedure (*vide infra/supra*), however rigorous drying and degassing were carried out at $t_{1/2}$ (3.5 F/mol). Dodecane was added as an internal standard. 100 μ L aliquots were drawn from the reaction mixture every 20 min and passed through a 1 cm plug of silica gel, eluting with EtOAc. The samples were analysed on a GC-FID-MS instrument. Signals were identified by comparison with authentic samples and by their parent ion MS signal. Areas of the starting material and products were calibrated about the dodecane internal standard.

Troubleshooting: Frequently Asked Questions

Question 1:

How do I monitor the reaction?

Answer:

We use TLC analysis with UV visualization (254 nm) to see the starting material (SM). Staining with iodine (absorbed on silica gel) brings about a strong deep red spot for the product. The SM is much less responsive to the iodine stain, likewise the product has essentially no absorption at 254 nm. Therefore, even though in many cases the SM and the product coelute, the disappearance of a UV signal (254 nm) and an increasing sensitivity to iodine staining is a positive sign for the progress of the reaction. In addition, ^1H NMR aliquot analysis could also be used to monitor reaction progress.

Question 2:

Can you separate a mixture of product and SM coming from an EC Birch reduction?

Answer:

At least with the substrates we have chosen to demonstrate it is possible to do so, but in many cases, it is very challenging, and prep-TLC is the best way we have found. The most convenient solution is simply to allow the reaction to go to completion. If this is a problem you encounter using the room temperature protocol, it is worth trying the reaction at $-78\text{ }^\circ\text{C}$ *vide supra*.

Question 3:

How much can the reaction be scaled up on the ElectraSyn? Does it take longer if you scale up?

Answer:

We have gone as much as 0.4 mmols of substrate using the IKA 20 mL ElectraSyn vials (still using 10 mA). This does mean that the reaction takes longer to run (4x as long for 0.4 mmols as it does for 0.1 mmols). In principle, increasing the current would speed up the reaction (as was done by AsymmChem who scaled up the EC Birch reaction – see paper), however, at some point one reaches the 30 V, or 100 mA capacity of the ElectraSyn, and would require the use of a more powerful DC power supply.

NOTE: It's worth knowing that you can try to run the reaction more concentrated, and we have had intermittent success with that, but eventually we settled for the conditions which provided us with the most reproducible results.

Question 4:

Is there another reagent beside TPPA that can be used? Alternatively, is there an easier way to remove TPPA?

Answer:

HMPA was found to be as effective as TPPA, however there are health risks associated with the use of that reagent (we recommend that you avoid using it). The morpholine version of TPPA/HMPA was also investigated but was found to have poor solubility and did not provide the desired effects as TPPA or HMPA did. Other phosphoramides were not investigated. We have several methods to remove the TPPA, but they are largely substrate specific (TPPA is very polar, $R_f = 0.2$ in $\text{CH}_2\text{Cl}_2/\text{MeOH}$ 10:0.5, and partially back extractable in aqueous acid). The most useful ones are:

1. Absorb the reaction directly onto silica gel and pour the absorbed crude onto a short plug of silica gel and wash with several "column" volumes of EtOAc. *Good for relatively non-polar – non-volatile – products.*
2. Dilute the reaction with *n*-pentane/hexane (diethyl ether can be used too, but more TPPA comes over into it) and wash with water (or ideally 1M $\text{HCl}_{(\text{aq})}$ if the compound is stable to acid). Dry over MgSO_4 and evaporate (gently if necessary). *This protocol is good for VERY non-polar and volatile products.*
3. Essentially the same as the 1st protocol, but replace the silica gel for basic alumina, and elute with 1:1 diethyl ether/Hexane. *Good for acid sensitive, relatively non-polar – non-volatile – compounds.*

Question 5:

How moisture sensitive is the reaction? Is it worth while just operating under Schlenk-type conditions to be sure? Are there any signs that moisture has been is a problem?

Answer:

Provided the LiBr and the DMU has been dried as shown in the respective graphical guides, it is not necessary to be so careful. Of course, leaving the reaction exposed to the atmosphere for an extended period is not advised either. Another possibility is to flame dry the ElectroSyn vial, if you are uncertain or are having trouble to get the reaction to work well (see image).



One minute of flame drying as shown is enough. Sometimes, before discovering the amount of water the LiBr was absorbing whilst weighing out the LiBr was the problem for reaction reproducibility, we often noticed that large quantities of grey solid (looked like an LAH reaction) would be generated in the reaction. However, not always! It is better not to assume just based on appearance that the reaction has not worked or has!

Question 6:

Is there another way to dry the LiBr besides flame drying?

Answer:

Yes! We have also used a method from the Armarego's Purification of Laboratory Reagents book, which says to dry the LiBr under vacuum at 120 °C (we used an oil bath for this) for two hours. This procedure also works, but as you can imagine flame drying is faster, hence we used it.

Question 7:

The procedure says that the reaction is degassed, and the headspace cleared prior to starting electrolysis. However, it is mentioned after stating this, that the degassing is not so crucial! Which is it?

Answer:

Depending how much oxygen is in solution, it will be reduced to peroxide (and ultimately water) prior to the substrate, which will result in a longer induction time for the desired reaction to occur. However, the down-stream fate of oxygen reduction does not seem affect the overall reaction-product distribution. Nevertheless, it just seemed faster to remove the oxygen via degassing with argon (+/- 5 min) than to electrochemically remove it.

Question 8:

Did you try to use other Alkali and Alkaline earth metals salts such as Na, K, Mg, Ca salts etc.?

Answer:


We did, however, aside from most of them being insoluble in THF /TPPA, the ones that were and served as reasonable electrolytes (NaI, KI), did not afford Birch reduction products.

Question 9:

The resistance of the reaction is very high and ElectraSyn can't deliver the set charge, or just registers that the resistance is too high and will not carry out the electrolysis, what could be wrong?

Answer:

Several things could be wrong, so let's go through them step by step:

- The electrode surfaces might be contaminated. Wiping with a cloth vigorously is advised. Sonication can also help.
- The electrode connections to the terminals of the cap might be poor. Make sure the contact is good, otherwise wipe both surfaces with some sand paper until shiny.
- The solution is not mixed well prior to electrolysis. Ensure the TPPA has mixed with the THF, by stirring or sonication.
- The upper Voltage limit on the ElectraSyn might be set too low. To adjust, on the home screen, select the  (top right corner) > Voltage limit > set to 30V

A useful trick is to remove the vial and replace it with a short vial or bowl containing brine. Brine is an excellent conductor, so there are still conductivity issues using brine, it is very likely a connection issue that is occurring either between the electrodes and the cap, or the cap and the ElectraSyn (turning off and unplugging the devices helps occasionally). This also occurs for

some substrates at $-78\text{ }^{\circ}\text{C}$, where the resistance will spike after a while (this occurs at room temperature too, by usually the reaction is complete before this point). This is normal, and the reaction is still proceeding, even though a lower current is being passed through the solution. Continue to monitor by TLC.

Question 10:

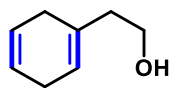
The reaction becomes extremely turbid when I leave the reaction to stand for a few hours or overnight, is this bad and how do you work the reaction up?

Answer:

What has happened is the THF has probably polymerized forming this jelly. If you remove the cap (scrapping the contents off the electrodes into the reaction flask), afterwards add EtOAc to the reaction mixture and mechanically mix them until the media becomes sufficiently fluid enough to transfer. A normal aqueous workup can be conducted as described in the general procedures.

Experimental Procedures and Characterization Data

Compound SI-4



2-(cyclohexa-1,4-dien-1-yl)ethan-1-ol (SI-2).(34, 35)

Following **General Procedure A** or **B** on 0.1 mmol scale (6-7 F/mol) with phenylethanol. Purification by prep-TLC (3:1 hexanes:EtOAc) afforded 8.9 mg (72%, Faradic yield: 33%) of the title compound **SI-4**.

Physical State: colorless oil.

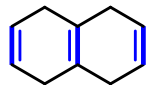
¹H NMR (600 MHz, CDCl₃): δ 5.73-5.69 (m, 2H), 5.57-5.52 (m, 1H), 3.70 (t, J = 6.3 Hz, 2H), 2.76-2.68 (m, 2H), 2.67-2.57 (m, 2H), 2.35-2.21 (m, 2H).

¹³C NMR (151 MHz, CDCl₃): δ 130.5, 123.3, 123.2, 120.7, 59.1, 39.7, 27.9, 25.9.

HRMS (ESI-TOF): calc'd for C₈H₁₂O [M+H]⁺: 125.0966, found 125.0901.

TLC: R_f = 0.7 (3:1 hexanes:EtOAc).

Compound SI-6



1,4,5,8-tetrahydronaphthalene (SI-6).(36-38)

Following **General Procedure A** or **B** on 0.1 mmol scale (9 F/mol) with naphthalene. Purification by flash column chromatography (silica, 1:1 hexanes:EtOAc) afforded 9.9 mg (75%, Faradic yield: 22%) of the title compound **SI-6**.

Physical State: white solid.

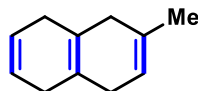
¹H NMR (400 MHz, CDCl₃): δ 5.73 (s, 4H), 2.54 (s, 8H).

¹³C NMR (151 MHz, CDCl₃): δ 124.6, 123.5, 31.0

GCMS: calc'd for C₁₀H₁₂ [M]⁺: 132.1, found 132.1, 117.0.

TLC: R_f = 0.89 (20:1 hexanes: EtOAc, KMnO₄).

Compound SI-7



2-methyl-1,4,5,8-tetrahydronaphthalene (SI-7).(36)

Following **General Procedure A** on 0.1 mmol scale (8 F/mol) with 2-methylnaphthalene. Purification by flash column chromatography (silica, 1:1 hexanes:EtOAc) afforded 9.9 mg (68%, Faradic yield: 25%) of the title compound **SI-7**.

Physical State: colorless oil.

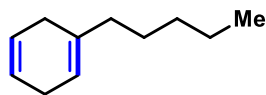
¹H NMR (500 MHz, CDCl₃): δ 5.73 (m, 2H), 5.43 (d, *J* = 1.6, Hz, 1H), 2.55-2.54 (m, 6H), 2.47-2.43 (m, 2 H), 1.69 (s, 3H).

¹³C NMR (151 MHz, CDCl₃): δ 131.6, 124.7, 124.6, 124.6, 123.3, 118.8, 35.9, 32.1, 30.9, 30.7, 23.2.

HRMS (ESI-TOF): calc'd for C₁₁H₁₄ [M+H]⁺: 147.1174, found 147.1169.

TLC: R_f = 0.88 (40:1 hexanes: EtOAc, I₂).

Compound SI-8



1-pentylcyclohexa-1,4-diene (SI-8).(39)

Following **General Procedure B** on 0.1 mmol scale (6 F/mol) with pentylbenzene. Purification by prep-TLC (100% Hexane) afforded 10.8 mg (72%, Faradic yield: 33%) of the title compound **SI-8**.

Physical State: colorless oil.

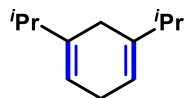
¹H NMR (600 MHz, CDCl₃): δ 5.72-5.66 (m, 2H), 5.42-5.37 (m, 1H), 2.73-2.48 (m, 4H), 1.99-1.87 (m, 2H), 1.44-1.37 (m, 2H), 1.35-1.22 (m, 4H), 0.89 (t, *J* = 7.2 Hz, 3H).

¹³C NMR (151 MHz, CDCl₃): δ 134.4, 123.6, 123.5, 117.2, 36.6, 30.8, 28.1, 26.2, 25.9, 21.7, 13.2.

GCMS: calc'd for C₁₁H₁₈ [M]⁺: 150.1, found 150, 91, 79.

TLC: R_f = 0.7 (100% hexane).

Compound SI-9



1,5-diisopropylcyclohexa-1,4-diene (SI-9).(40)

Following **General Procedure B** on 0.1 mmol scale (5 F/mol) with 1,3-diisopropylbenzene. Purification by prep-TLC (100% hexane) afforded 13.9 mg (85%, Faradic yield: 40%) of the title compound **SI-9**.

Physical State: colorless oil

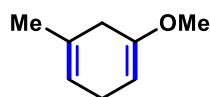
¹H NMR (600 MHz, CDCl₃): δ 5.43 (s, 2H), 2.72-2.68 (m, 2H), 2.57-2.53 (m, 2H), 2.24-2.17 (m, 2H), 1.04 (d, *J* = 6.9 Hz, 12H).

¹³C NMR (151 MHz, CDCl₃): δ 140.1, 115.0, 33.9, 27.0, 26.7, 20.4.

GCMS: calc'd for C₁₂H₂₀ [M+H]⁺: 164.2, found 121.1 [M-C₃H₇].

TLC: R_f = 0.8 (100% hexane).

Compound SI-10



1-methoxy-5-methylcyclohexa-1,4-diene (SI-10).(41-43)

Following **General Procedure A** or **B** on 0.1 mmol scale (6 F/mol) with 3-methylanisole. Extraction with *n*-pentanes/H₂O afforded 11.1 mg (89%, Faradic yield: 33%) of the title compound **SI-10**.

Physical State: colorless oil.

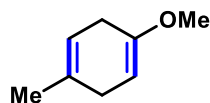
¹H NMR (400 MHz, C₆D₆): δ 5.38-5.36 (m, 1H), 4.48 (dd, *J* = 2.8, 2.4 Hz, 1H), 3.28 (s, 3H), 2.80-2.74 (m, 2H), 2.73-2.68 (m, 2H), 1.54 (m, 3H).

¹³C NMR (151 MHz, C₆D₆): δ 153.5, 130.7, 119.2, 90.4, 53.6, 33.7, 27.3, 22.9.

GCMS: calc'd for C₈H₁₂O [M]⁺: 124.1, found 124.1, 109.1, 91.0.

TLC: R_f = 0.63 (20:1 hexanes: EtOAc, I₂).

Compound SI-11



1-methoxy-4-methylcyclohexa-1,4-diene (SI-11).(40, 44)

Following **General Procedure B** on 0.1 mmol scale (6 F/mol) with 4-methylanisole. Extraction with *n*-pentanes/H₂O and concentration under reduced pressure afforded 7.9 mg (64%, Faradic

yield: 33%) of the title compound **SI-11**.

Physical State: colorless oil.

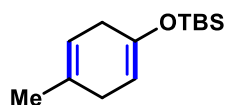
¹H NMR (400 MHz, C₆D₆): δ 5.28-5.25 (m, 1H), 4.45 (m, 1H), 3.27 (s, 3H), 2.83 (m, 2H), 2.61 (m, 2H), 1.59 (s, 3H).

¹³C NMR (151 MHz, C₆D₆): δ 153.7, 131.6, 118.4, 90.5, 53.6, 31.5, 29.8, 22.8.

GCMS: calc'd for C₈H₁₂O [M]⁺: 124.1, found 124.1, 109.1, 91.0.

TLC: R_f = 0.65 (20:1 hexanes: EtOAc, I₂).

Compound SI-12



tert-butyldimethyl((4-methylcyclohexa-1,4-dien-1-yl)oxy)silane (**SI-12**).*(45)*

Following **General Procedure A** or **B** on 0.1 mmol scale (9 F/mol) with *tert*-butyldimethyl(*p*-tolxyloxy)silane (**SI-48**). Purification using basic Alumina (5:1 hexane/EtOAc) afforded 20.3 mg (72%, Faradic yield: 22%) of the title compound **SI-12**.

Physical State: colorless oil.

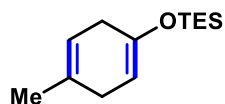
¹H NMR (400 MHz, C₆D₆): δ 5.27 (m, 1H), 4.91 (m, 1H), 2.75-2.69 (m, 2H), 2.62-2.57 (m, 2H), 1.57 (s, 3H), 0.99 (s, 9H), 0.14 (s, 6H).

¹³C NMR (151 MHz, C₆D₆): δ 148.8, 131.4, 118.7, 101.1, 31.9, 31.8, 25.9, 22.9, 18.3, -4.2.

HRMS (ESI-TOF): calc'd for C₁₃H₂₄OSi [M+H]⁺: 225.1675, found 225.1674.

TLC: R_f = 0.71 (20:1 hexane/EtOAc, I₂).

Compound SI-13



triethyl((4-methylcyclohexa-1,4-dien-1-yl)oxy)silane (**SI-13**).*(45)*

Following **General Procedure B** on 0.1 mmol scale (9 F/mol) with triethyl(*p*-tolxyloxy)silane (**SI-49**). Purification using basic Alumina (5:1 hexane/EtOAc) afforded 19.6 mg (70%, Faradic yield: 22%) of the title compound **SI-13**.

Physical State: colorless oil.

¹H NMR (400 MHz, C₆D₆): δ 5.29-5.27 (m, 1H), 4.95-4.92 (m, 1H), 2.80-2.74 (m, 2H), 2.63-

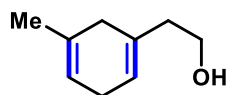
2.57 (m, 2H), 1.56 (s, 3H), 1.01 (t, $J = 7.6$ Hz, 9H), 0.67 (q, $J = 7.6$ Hz, 6H).

^{13}C NMR (151 MHz, C_6D_6): δ 148.9, 131.4, 118.8, 100.4, 31.9, 31.9, 22.9, 7.0, 5.5.

HRMS (ESI-TOF): calc'd for $\text{C}_{13}\text{H}_{24}\text{OSi}$ $[\text{M}+\text{H}]^+$: 225.1675, found 225.1676.

TLC: $R_f = 0.77$ (20:1 hexane/EtOAc, I_2).

Compound SI-14



2-(5-methylcyclohexa-1,4-dien-1-yl)ethan-1-ol (SI-14). (46)

Following **General Procedure A** or **B** on 0.1 mmol scale (6-7 F/mol) with 2-(*m*-tolyl)ethan-1-ol.

Purification by prep-TLC (3:1 hexanes:EtOAc) afforded 10.4 mg (76%, Faradic yield: 33%) of the title compound **SI-14**.

Physical State: colorless oil.

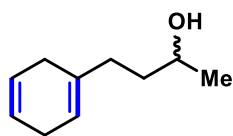
^1H NMR (600 MHz, CDCl_3): δ 5.55 (s, 1H), 5.42 (s, 1H), 3.71 (t, $J = 6.3$ Hz, 2H), 2.70 (s, 2H), 2.51 (t, $J = 8.2$ Hz, 2H), 2.27 (t, $J = 6.3$ Hz, 2H), 1.69 (s, 3H).

^{13}C NMR (151 MHz, CDCl_3): δ 130.4, 130.1, 120.6, 117.5, 59.1, 39.5, 32.8, 26.9, 22.3.

HRMS (ESI-TOF): calc'd for $\text{C}_9\text{C}_{14}\text{O}$ $[\text{M}+\text{H}]^+$: 139.1117, found 139.1115.

TLC: $R_f = 0.8$ (3:1 hexanes:EtOAc, I_2).

Compound SI-15



3-(4-methylcyclohexa-1,4-dien-1-yl)propan-2-ol (SI-15).

Following **General Procedure A** on 0.1 mmol scale (4-5 F/mol) with 4-phenylbutan-2-one.

Purification by prep-TLC (1:1, hexane:EtOAc) afforded 11.6 mg (70%, Faradic yield: 50%) of the title compound **SI-15**.

Physical State: white solid.

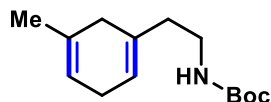
^1H NMR (600 MHz, CDCl_3): δ 5.72-5.70 (m, 2H), 5.47-5.46 (m, 1H), 3.83-3.79 (m, 1H), 2.70-2.59 (m, 4H), 2.14-1.95 (m, 2H), 1.68-1.47 (m, 2H), 1.20 (d, $J = 6.2$ Hz, 3H).

^{13}C NMR (151 MHz, CDCl_3): δ 134.9, 124.4, 124.4, 118.8, 68.2, 36.9, 34.0, 29.1, 26.9, 23.6.

HRMS (ESI-TOF): calc'd for C₁₀C₁₅NO [M+H]⁺: 153.1279, found 153.1279.

TLC: R_f = 0.7 (3:1, hexane:EtOAc, I₂).

Compound SI-16



N-(2-(5-methylcyclohexa-1,4-dien-1-yl)ethyl)acetamide (SI-16).

Following **General Procedure A** or **B** on 0.1 mmol scale (7 F/mol) with **SI-50**. Purification by flash column chromatography (silica, 3:1 hexanes:EtOAc) afforded 16.3 mg (69%, Faradic yield: 29%) of the title compound **SI-16**.

Physical State: opaque liquid.

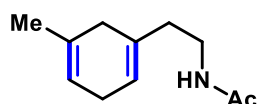
¹H NMR (600 MHz, CDCl₃): δ 5.49-5.47 (m, 1H), 5.42-5.39 (m, 1H), 4.51 (s, 1H), 3.27-2.30 (m, 2H), 2.71-2.65 (m, 2H), 2.48 (t, *J* = 8.1 Hz, 2H), 2.17 (t, *J* = 8.1 Hz, 2H), 1.67 (s, 3H), 1.44 (s, 9H).

¹³C NMR (151 MHz, CDCl₃): δ 156.1, 132.0, 131.2, 120.8, 118.5, 38.2, 37.4, 33.7, 29.9, 28.6, 27.8, 23.1.

HRMS (ESI-TOF): calc'd for C₁₄H₂₃NO₂ [M+Na]⁺: 260.1626, found 260.1631.

TLC: R_f = 0.55 (5:1 hexanes:EtOAc, I₂).

Compound SI-17



N-(2-(5-methylcyclohexa-1,4-dien-1-yl)ethyl)acetamide (SI-17).

Following **General Procedure A** or **B** on 0.1 mmol scale (6 F/mol) with **SI-51**. Purification by flash column chromatography (silica, 1:1 hexanes:EtOAc) afforded 7.7 mg (43%, Faradic yield: 33%) of the title compound **SI-17**.

Physical State: opaque liquid.

¹H NMR (600 MHz, CDCl₃): δ 5.52-5.50 (m, 1H), 5.45-5.42 (m, 1H), 3.38 (q, *J* = 6.8 Hz, 2H), 2.72-2.68 (m, 2H), 2.50 (t, *J* = 8.1 Hz, 2H), 2.21 (t, *J* = 8.1 Hz, 2H), 1.98 (s, 3H), 1.70 (m, 3H).

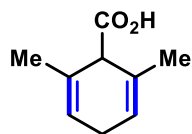
¹³C NMR (151 MHz, CDCl₃): δ 169.5, 131.3, 130.6, 120.3, 117.9, 36.4, 36.3, 33.0, 27.2, 22.9,

22.7.

HRMS (ESI-TOF): calc'd for C₁₁H₁₇NO [M+H]⁺: 180.1388, found 180.1385.

TLC: R_f = 0.20 (1:1 hexanes:EtOAc, I₂).

Compound SI-18



2,6-dimethylcyclohexa-2,5-diene-1-carboxylic acid (SI-18).(46, 47)

Following **General Procedure A** or **B** on 0.1 mmol scale (10-11 F/mol) with 2,6-dimethylbenzoic acid. Purification by prep-TLC (1:1 hexanes:EtOAc and 1% AcOH) afforded 8.4 mg (55%, Faradic yield: 20%) of the title compound **SI-18**.

Physical State: white solid.

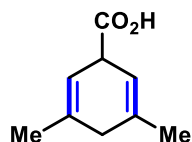
¹H NMR (400 MHz, CDCl₃): δ 5.68 (s, 2H), 3.48 (t, *J* = 6.35 Hz, 1H), 2.82-2.64 (m, 2H), 1.77 (s, 6H).

¹³C NMR (151 MHz, CDCl₃): δ 175.8, 127.5, 121.5, 51.2, 26.6, 20.9.

HRMS (ESI-TOF): calc'd for C₉H₁₂O₂ [M+H]⁺: 153.0916, found 153.0912.

TLC: R_f = 0.4 (1:1 hexanes:EtOAc and 1% AcOH, I₂).

Compound SI-19



3,5-dimethylcyclohexa-2,5-diene-1-carboxylic acid (SI-19).(47, 48)

Following **General Procedure A** or **B** on 0.1 mmol scale (10-11 F/mol) with 3,5-dimethylbenzoic acid. Purification by prep-TLC (1:1 hexanes:EtOAc and 1% AcOH) afforded 7.7 mg (50%, Faradic yield: 20%) of the title compound **SI-19**.

Physical State: white solid.

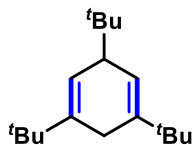
¹H NMR (600 MHz, CDCl₃): δ 5.53-5.52 (m, 2H), 3.78-3.75 (m, 1H), 2.50 (qd, *J* = 22.0, 7.7 Hz, 2H), 1.75 (s, 6H).

¹³C NMR (125 MHz, CDCl₃): δ 178.54, 134.60, 115.79, 43.96, 35.79, 23.16.

HRMS (ESI-TOF): calc'd for C₉H₁₂O₂ [M+H]⁺: 153.0916, found 153.0911.

TLC: R_f = 0.4 (1:1 hexanes:EtOAc and 1% AcOH, I₂).

Compound SI-20



1,3,5-tri-*tert*-butylcyclohexa-1,4-diene (SI-20).

Prepared following **General Procedure B** on a 0.1 mmol scale (7 F/mol) with 1,3-di-*tert*-butylbenzene. Purification by flash column chromatography (silica, hexanes) afforded 16.2 mg (65%, Faradic yield: 29%) of the title compound **SI-20**.

Physical State: colorless oil.

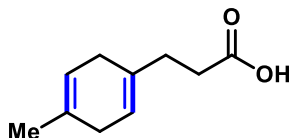
¹H NMR (500 MHz, CDCl₃): δ 5.58 (dd, *J* = 2.0, 0.9 Hz, 1H), 2.75-2.70 (m, 1H), 2.49-2.45 (m, 2H), 1.09 (s, 18H), 0.86 (s, 9H).

¹³C NMR (151 MHz, CDCl₃): δ 145.3, 118.2, 48.1, 37.0, 35.5, 29.4, 27.4, 25.2.

GCMS: calc'd for C₁₈H₃₂[M]⁺: 248.2, found 248.1, 58.1, 57.1.

TLC: R_f = 0.9 (hexanes, I₂).

Compound SI-21



3-(4-methylcyclohexa-1,4-dien-1-yl)propanoic acid (SI-21).(49)

Following **General Procedure B** on 0.1 mmol scale (8-9 F/mol) with 3-(*p*-tolyl)propanoic acid. Purification by prep-TLC (1:1 hexanes:EtOAc and 1% AcOH) afforded 8.3 mg (50%, Faradic yield: 25%) of the title compound **SI-21**.

Physical State: white solid.

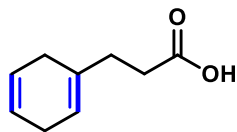
¹H NMR (400 MHz, CDCl₃): δ 5.50-5.42 (m, 1H), 5.43-5.40 (m, 1H), 2.62-2.53 (m, 4H), 2.51-2.48 (m, 2H), 2.36-2.28 (m, 2H), 1.67 (s, 3H).

¹³C NMR (151 MHz, CDCl₃): δ 179.1, 133.1, 131.4, 119.3, 118.4, 32.3, 31.8, 31.7, 30.1, 23.11.

HRMS (ESI-TOF): calc'd for C₁₀H₁₄O₂ [M+H]⁺: 167.1072, found 167.1073.

TLC: $R_f = 0.5$ (1:1 hexanes:EtOAc and 1% AcOH, I_2).

Compound SI-22



3-(cyclohexa-1,4-dien-1-yl)propanoic acid (SI-22). (50, 51)

Following **General Procedure A** or **B** on 0.1 mmol scale (8-9 F/mol) with 3-phenylpropanoic acid. Purification by prep-TLC (1:1 hexanes:EtOAc and 1% AcOH) afforded 10.3 (68%, Faradic yield: 25%) of the title compound **SI-22**.

Physical State: white solid.

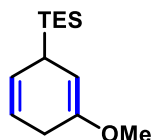
^1H NMR (600 MHz, CDCl_3): δ 5.73-5.65 (m, 2H), 5.50-5.43 (m, 1H), 2.73-2.56 (m, 4H), 2.50 (d, $J = 6.7$ Hz, 2H), 2.30 (t, $J = 7.8$ Hz, 2H).

^{13}C NMR (151 MHz, CDCl_3): δ 179.0, 133.2, 124.4, 124.1, 119.3, 32.2, 32.1, 29.1, 26.8.

HRMS (ESI-TOF): calc'd for $\text{C}_9\text{H}_{12}\text{O}_2$ $[\text{M}+\text{H}]^+$: 153.0916, found 153.0912.

TLC: $R_f = 0.5$ (1:1 hexanes:EtOAc and 1% AcOH, I_2).

Compound SI-23



triethyl(3-methoxycyclohexa-2,5-dien-1-yl)silane (SI-23).

Prepared following **General Procedure A** or **B** on a 0.1 mmol scale (6 F/mol) with triethyl(3-methoxyphenyl)silane. Purification by flash column chromatography (silica, 20:1 hexanes: CH_2Cl_2) afforded 6.4 mg (54%, Faradic yield: 33%) of the title compound **SI-23**.

Physical State: colorless oil.

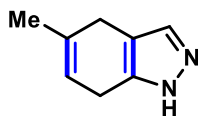
^1H NMR (500 MHz, CDCl_3): δ 8.42 (d, $J = 6.0$ Hz, 1H), 7.42 (d, $J = 7.7$ Hz, 1H), 7.09 (dd, $J = 7.7, 6.0$ Hz, 1H), 4.87 (t, $J = 3.7$ Hz, 1H), 3.66-3.63 (m, 2H), 3.62 (s, 3H), 3.48-3.46 (m, 2H).

^{13}C NMR (151 MHz, CDCl_3): δ 154.9, 152.1, 147.5, 136.3, 128.6, 121.3, 91.0, 54.5, 32.5, 32.0.

GCMS: calc'd for $\text{C}_{13}\text{H}_{24}\text{OSi}$ $[\text{M}]^+$: 224.19, found 224.20.

TLC: $R_f = 0.47$ (1:1 hexane:EtOAc).

Compound SI-24



5-methyl-4,7-dihydro-1H-indazole (SI-24).

Following **General Procedure A** on 0.1 mmol scale (3.5 F/mol) with **SI-52**. Purification by prep-TLC (3:1, hexane:EtOAc) afforded 5.2 mg (39%, Faradic yield: 57%) of the title compound **SI-24**.

Physical State: white solid.

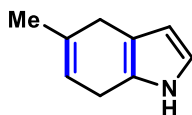
¹H NMR (600 MHz, CDCl₃): δ 7.36 (s, 1H), 5.59-5.57 (m, 1H), 3.33-3.29 (m, 2H), 3.13 (t, J = 5.7 Hz, 2H), 1.84-1.83 (m, 3H).

¹³C NMR (151 MHz, CDCl₃): δ 132.4, 131.5, 117.6, 113.9, 113.5, 27.2, 23.7, 23.5.

HRMS (ESI-TOF): calc'd for C₈H₁₀N₂ [M+H]⁺: 153.0916, found 153.0912.

TLC: R_f = 0.6 (3:1, hexane:EtOAc, I₂).

Compound SI-25



5-methyl-4,7-dihydro-1H-indole (SI-25).(52)

Prepared following **General Procedure A** on a 0.1 mmol scale (8 F/mol) with 5-methyl-1H-indole. Purification by flash column chromatography (silica, 1:1 hexanes:EtOAc) afforded 10.0 mg (76%, Faradic yield: 25%) of the title compound **SI-25**.

Physical State: colorless oil.

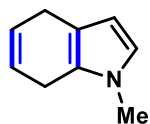
¹H NMR (600 MHz, CDCl₃): δ 7.77 (s, 1H), 6.69 (t, J = 2.3 Hz, 1H), 6.02 (t, J = 2.3 Hz, 1H), 5.54 (m, 1H), 3.25-3.23 (m, 2H), 3.15-3.11 (m, 2H), 1.82 (m, 3H).

¹³C NMR (151 MHz, CDCl₃): δ 133.3, 124.4, 117.3, 116.5, 114.7, 106.6, 29.9, 24.5, 23.8.

HRMS (ESI-TOF): calc'd for C₉H₁₁N [M+H]⁺: 134.0970, found 134.0965.

TLC: R_f = 0.7 (10:1 hexane:EtOAc, I₂).

Compound SI-26



1-methyl-4,7-dihydro-1H-indole (SI-26).(53-55)

Prepared following **General Procedure B** on a 0.1 mmol scale (6.5 F/mol) with 1-methyl-1H-indole. Purification by flash column chromatography (silica, 1:1 hexanes:EtOAc) afforded 7.0 mg (53%, Faradic yield: 31%) of the title compound **SI-26**.

Physical State: pale yellow oil.

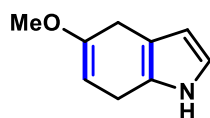
¹H NMR (600 MHz, CDCl₃): δ 6.58 (d, *J* = 2.2 Hz, 1H), 5.97 (d, *J* = 2.2 Hz, 1H), 5.92 (d, *J* = 7.9 Hz, 1H), 5.86 (d, *J* = 7.9 Hz, 1H), 3.54 (s, 3H), 3.27-3.25 (m, 4H).

¹³C NMR (151 MHz, CDCl₃): δ 126.1, 125.5, 122.4, 120.3, 114.2, 105.6, 33.1, 25.5, 23.3.

HRMS (ESI-TOF): calc'd for C₈H₉N [M+H]⁺: 134.0964, found 134.0966.

TLC: R_f = 0.45 (10:1 hexane:EtOAc, I₂).

Compound SI-27



5-methoxy-4,7-dihydro-1H-indole (SI-27).(56)

Prepared following **General Procedure A** or **B** on a 0.1 mmol scale (3-4 F/mol) with 5-methoxy-1H-indole. Purification using neutral Alumina (100% hexane) afforded 11.6 mg (78%, Faradic yield: 66%) of the title compound **SI-27**.

Physical State: colorless oil.

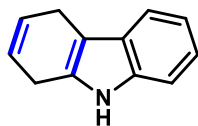
¹H NMR (400 MHz, C₆D₆): δ 6.38 (t, *J* = 2.7 Hz, 1H), 6.09 (t, *J* = 2.6 Hz, 1H), 4.62-4.61(m, 1H), 3.54 (td, *J* = 6.2, 1.3 Hz, 2H), 3.32 (s, 3H), 3.05 (td, *J* = 6.2, 3.6 Hz, 2H).

¹³C NMR (151 MHz, C₆D₆): δ 156.0, 123.7, 116.9, 114.0, 106.9, 90.0, 54.1, 28.2, 23.2.

HRMS (ESI-TOF): calc'd for C₉H₁₁NO [M+H]⁺: 150.0913, found 150.0916.

TLC: R_f = 0.7 (5:1, hexane:EtOAc, I₂).

Compound SI-28



4,9-dihydro-1H-carbazole (SI-28).(57)

Prepared following **General Procedure A** or **B** on a 0.1 mmol scale (10 F/mol) with 9H-carbazole. Purification using neutral Alumina (4:1 hexanes:EtOAc) afforded 6.6 mg (39%, Faradic yield: 20%) of the title compound **SI-28** as an inseparable mixture with 9H-carbazole.

Physical State: white solid.

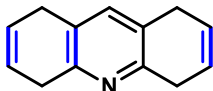
¹H NMR (600 MHz, CDCl₃): δ 7.49 (d, *J* = 7.7 Hz, 1H), 7.32 (d, *J* = 8.0 Hz, 1H), 7.17-7.07 (m, 2H), 6.09-6.02 (m, 1H), 5.95-5.89 (m, 1H), 3.44 (s, 4H).

¹³C NMR (151 MHz, CDCl₃): δ 134.9, 130.2, 126.3, 124.8, 121.6, 120.5, 118.4, 117.1, 109.6, 106.6, 23.6, 22.4.

HRMS (ESI-TOF): calc'd for C₁₂H₁₁N [M+H]⁺: 170.0970, found 170.0967.

TLC: R_f = 0.5 (4:1 hexanes:EtOAc, I₂).

Compound SI-29



1,4,5,8-tetrahydroacridine (SI-29).(38)

Following **General Procedure A** or **B** on 0.2 mmol scale (15 F/mol) with acridine. Purification by flash column chromatography (silica, 5:1 hexanes:EtOAc) afforded 14.1 mg (39%, Faradic yield: 13%) of the title compound **SI-29**.

Physical State: white solid.

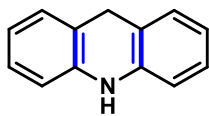
¹H NMR (600 MHz, CDCl₃): δ 7.13 (s, 1H), 5.98-5.93 (m, 2H), 5.88-5.83 (m, 2H), 3.48-3.47 (m, 4H), 3.39-3.38 (m, 4H).

¹³C NMR (151 MHz, CDCl₃): δ 151.9, 136.2, 126.9, 125.3, 123.8, 32.7, 29.4.

HRMS (ESI-TOF): calc'd for C₁₃H₁₃N [M+H]⁺: 184.1126, found 184.1133.

TLC: R_f = 0.29 (5:1, hexanes:EtOAc, I₂).

Compound SI-30



9,10-dihydroacridine (SI-30).(53)

Following **General Procedure A** or **B** on 0.2 mmol scale (4 F/mol) with acridine. Purification by flash column chromatography (silica, 5:1 hexanes:EtOAc) afforded 16.3 mg (45%, Faradic yield: 50%) of the title compound **SI-30**.

Physical State: yellow solid.

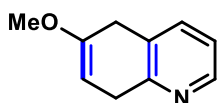
¹H NMR (400 MHz, CDCl₃): δ 7.12-7.06 (m, 4H), 6.86 (td, $J = 7.2, 1.2$ Hz, 2H), 6.67 (dd, $J = 7.6, 1.2$ Hz, 2H), 5.95 (s, 1H), 4.06 (s, 2H).

¹³C NMR (151 MHz, CDCl₃): δ 140.3, 128.7, 127.1, 120.8, 120.2, 113.6, 31.5.

HRMS (ESI-TOF): calc'd for C₁₃H₁₁N [M+H]⁺: 182.0970, found 182.0972.

TLC: R_f = 0.54 (5:1 hexanes:EtOAc, I₂).

Compound SI-31



6-methoxy-5,8-dihydroquinoline (SI-31).

Prepared following **General Procedure A** or **B** on a 0.1 mmol scale (8 F/mol) with 6-methoxyquinoline. Purification by flash column chromatography (silica, 1:1 hexanes:EtOAc) afforded 6.4 mg (40%, Faradic yield: 25%) of the title compound **SI-31**.

Physical State: colorless oil.

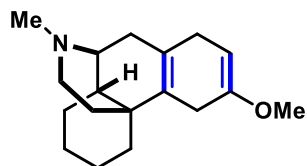
¹H NMR (500 MHz, CDCl₃): δ 8.42 (d, $J = 6.0$ Hz, 1H), 7.42 (d, $J = 7.7$ Hz, 1H), 7.09 (dd, $J = 7.7, 6.0$ Hz, 1H), 4.87 (t, $J = 3.7$ Hz, 1H), 3.66-3.63 (m, 2H), 3.62 (s, 3H), 3.48-3.46 (m, 2H).

¹³C NMR (151 MHz, CDCl₃): δ 154.9, 152.1, 147.5, 136.3, 128.6, 121.3, 91.0, 54.5, 32.5, 32.0.

HRMS (ESI-TOF): calc'd for C₁₀H₁₂NO [M+H]⁺: 162.0919, found 162.0918.

TLC: R_f = 0.47 (1:1 hexane:EtOAc).

Compound SI-32



(4b*S*,8a*S*,9*S*)-3-methoxy-11-methyl-4,5,6,7,8,8a,9,10-octahydro-1H-9,4b-(epiminoethano)phenanthrene (SI-32).

Prepared following **General Procedure A** or **B** on a 0.1 mmol scale (7 F/mol) with dextromethorphan hydrobromide. Purification by flash column chromatography (silica, 12.5:1 CH₂Cl₂:MeOH) afforded 6.4 mg (54%, Faradic yield: 29%) of the title compound **SI-32**.

Physical State: white solid.

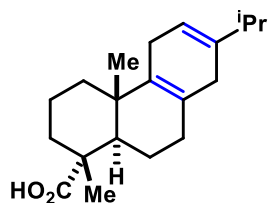
¹H NMR (500 MHz, CDCl₃): δ 4.67 (t, *J* = 3.3 Hz, 1H), 3.59 (s, 3H), 2.78-2.75 (m, 2H), 2.70-2.65 (m, 2H), 2.56-2.49 (m, 2H), 2.40-2.38 (m, 1H), 2.36 (s, 3H), 2.06 (d, *J* = 18.5 Hz, 1H), 1.87-1.84 (m, 2H), 1.71-1.65 (m, 2H), 1.58-1.55 (m, 2H), 1.45-1.38 (m, 6H), 1.01 (dd, *J* = 13.6, 3.5 Hz, 1H).

¹³C NMR (151 MHz, CDCl₃): δ 153.5, 128.6, 125.8, 90.3, 58.3, 54.0, 47.8, 42.6, 36.6, 36.5, 35.6, 31.6, 30.2, 27.5, 26.8, 26.3, 25.4, 23.6.

HRMS (ESI-TOF): calc'd for C₁₈H₂₈NO [M+H]⁺: 274.2171, found 274.2171.

TLC: R_f = 0.09 (12.5:1 CH₂Cl₂:MeOH).

Compound SI-33



(1*R*,4a*S*,10a*R*)-7-isopropyl-1,4a-dimethyl-1,2,3,4,4a,5,8,9,10,10a-decahydrophenanthrene-1-carboxylic acid (SI-33).

Prepared following **General Procedure B** on a 0.1 mmol scale (7 F/mol) with dehydrodiacetic acid. Purification by flash column chromatography (1:1 hexanes:EtOAc and 1% AcOH) afforded 24.9 mg (60%, Faradic yield: 29%) of the title compound **SI-33**.

Physical State: white solid.

¹H NMR (600 MHz, CDCl₃): δ 5.45 (s, 1H), 2.50 (dt, *J* = 20.9, 7.0 Hz, 1H), 2.38 (dt, *J* = 20.9,

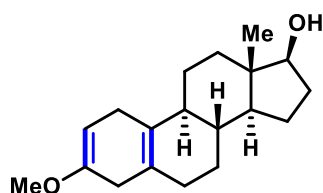
7.0 Hz, 1H), 2.17 (p, $J = 6.8$ Hz, 1H), 2.10-2.08 (m, 2H), 1.90 (dd, $J = 17.3, 6.6$ Hz, 1H), 1.79-1.74 (m, 2H), 1.67-1.61 (m, 4H), 1.39-1.36 (m, 1H), 1.22 (s, 3H), 1.02 (s, 3H), 1.01 (d, $J = 6.8$ Hz, 3H), 1.00 (d, $J = 6.8$ Hz, 3H).

^{13}C NMR (151 MHz, CDCl_3): δ 184.5, 140.2, 134.8, 124.4, 116.3, 47.6, 46.0, 36.8, 36.6, 36.0, 34.4, 33.2, 31.4, 25.4, 21.7, 21.4, 21.3, 19.8, 18.4, 16.4.

HRMS (ESI-TOF): calc'd for $\text{C}_{20}\text{H}_{31}\text{O}_2$ $[\text{M}+\text{H}]^+$: 303.2324, found 303.2321.

TLC: $R_f = 0.4$ (1:1 hexanes:EtOAc and 1% AcOH, I_2).

Compound SI-34



(8R,9S,13S,14S,17S)-3-methoxy-13-methyl-4,6,7,8,9,11,12,13,14,15,16,17-dodecahydro-1H-cyclopenta[a]phenanthren-17-ol (SI-34).

Following **General Procedure B** on 0.1 mmol scale (4-5 F/mol) with estradiol 3-methyl ether. Purification by prep-TLC (2:1 hexanes:EtOAc) afforded 18.7 (65%, Faradic yield: 50%) of the title compound **SI-34**.(58-60)

Physical State: white solid.

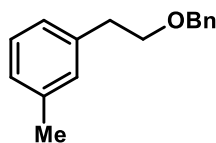
^1H NMR (400 MHz, CDCl_3): δ 4.69-4.58 (m, 1H), 3.68 (t, $J = 8.5$ Hz, 1H), 3.55 (s, 3H), 2.98-2.79 (m, 1H), 2.74-2.45 (m, 2H), 2.00-2.14 (m, 2H), 1.80-1.97 (m, 3H), 1.77-1.53 (m, 3H), 1.53-1.03 (m, 8H), 0.77 (s, 3H).

^{13}C NMR (100 MHz, CDCl_3): δ 152.8, 128.0, 125.1, 90.8, 82.1, 54.0, 50.0, 45.6, 43.5, 39.1, 37.16, 34.3, 30.8, 30.6, 28.5, 26.9, 25.5, 23.2, 11.4.

GCMS: calc'd for $\text{C}_{19}\text{H}_{28}\text{O}_2$ $[\text{M}]^+$: 288.20, found 284.10, 199, 160.

TLC: $R_f = 0.3$ (2:1 hexanes:EtOAc, I_2).

Compound SI-35



1-(2-(benzyloxy)ethyl)-3-methylbenzene (SI-35).

To a stirring solution of 2-(*m*-tolyl)ethan-1-ol (136.0 mg, 1.0 mmol) in DMF (3.0 mL) at 0 °C was portion-wise added NaH (42 mg, 1.0 mmol). After stirring for 15 min, BnBr (171 mg, 1.0 mmol) was added to the reaction mixture and allowed to stir for 1 h. The reaction mixture was quenched by the addition of NH₄Cl (15 mL), followed by extraction with hexanes (3 x 10 mL), dried over MgSO₄, and concentrated by reduced pressure. The crude reaction mixture was purified by flash column chromatography eluting with 100% hexanes to provide 253 mg (90%) of the title compound **SI-35**.

Physical State: colorless oil.

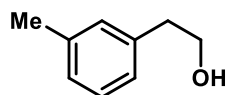
¹H NMR (400 MHz, CDCl₃): δ 7.37-7.27 (m, 5H), 7.18 (t, *J* = 8.0 Hz, 1H), 7.04 (s, 1H), 7.03 (d, *J* = 8.0 Hz, 1H), 4.53 (s, 2H), 3.69 (t, *J* = 7.2 Hz, 2H), 2.91 (t, *J* = 7.2 Hz, 2H), 2.33 (s, 3H).

¹³C NMR (151 MHz, CDCl₃): δ 139.0, 138.6, 138.0, 130.0, 128.5, 128.4, 127.8, 127.7, 127.1, 126.1, 73.1, 71.5, 36.4, 21.5.

HRMS (ESI-TOF): calc'd for C₁₆H₁₈O [M+H]⁺: 227.1436, found 227.1436

TLC: R_f = 0.4 (9:1 hexane/EtOAc, UV/Vis).

Compound SI-36



1-(2-(benzyloxy)ethyl)-3-methylbenzene (SI-36).

Prepared following **General Procedure B** on a 0.2 mmol scale (8 F/mol) with **SI-35**. Purification by prep-TLC (silica, 1:5 hexanes:EtOAc) afforded 13 mg (48%, Faradic yield: 25%) of the title compound **SI-36**.

Physical State: colorless oil.

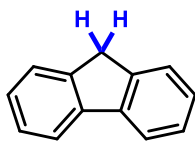
¹H NMR (500 MHz, CDCl₃): δ 7.23-7.19 (m, 1H), 7.06-7.02 (m, 2H), 3.86 (t, *J* = 6.8 Hz, 2H), 2.84 (t, *J* = 6.8 Hz, 2H), 2.34 (s, 3H).

¹³C NMR (151 MHz, CDCl₃): δ 138.5, 138.4, 130.0, 128.7, 127.4, 126.2, 63.9, 39.3, 21.5.

GCMS: calc'd for C₉H₁₂O [M]⁺: 136.1, found 136.0, 105.0.

TLC: R_f = 0.21 (1:5 hexanes:EtOAc, UV/Vis).

Compound SI-38



9H-fluorene (SI-38).

Following **General Procedure B** on 0.1 mmol scale (8 F/mol) with fluorenone **36**. Purification by flash column chromatography (silica, 20:1 hexanes:EtOAc) afforded 10.3 mg (62%, Faradic yield: 25%) of the title compound **SI-38**.

Physical State: orange solid.

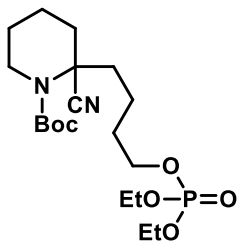
¹H NMR (600 MHz, CDCl₃): δ 7.80 (d, *J* = 7.5 Hz, 2H), 7.56 (dt, *J* = 7.0, 1.0 Hz, 2H), 7.39 (td, *J* = 6.5, 1.0 Hz, 2H), 7.31 (td, *J* = 7.0, 1.0 Hz, 2H), 3.91 (s, 2H).

¹³C NMR (151 MHz, CDCl₃): δ 143.4, 141.9, 126.9, 126.8, 125.2, 120.0, 37.1.

GCMS: calc'd for C₁₃H₁₀ [M]⁺: 166.07825, found 166.1, 167.0.

TLC: R_f = 0.88 (20:1 hexanes:EtOAc, UV/Vis).

Compound SI-39



tert-butyl 2-cyano-2-(4-((diethoxyphosphoryl)oxy)butyl)piperidine-1-carboxylate (SI-39).

Prepared according to literature procedure. (**61**, **62**)

Physical State: colorless oil.

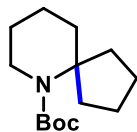
¹H NMR (400 MHz, CDCl₃): δ 4.14 (pd, *J* = 7.1, 0.8 Hz, 4H), 4.04 (q, *J* = 6.6 Hz, 2H), 3.81 (ddd, *J* = 13.0, 4.0, 4.0 Hz, 1H), 3.04 (m, 1H), 2.11-1.95 (m, 4H), 1.79-1.59 (m, 7H), 1.50 (s, 9H), 1.33 (td, 7.1, 1.0 Hz, 6H).

¹³C NMR (151 MHz, CDCl₃): δ 154.8, 121.1, 82.0, 67.1 (*J* = 5.9 Hz), 63.9 (*J* = 5.9 Hz), 56.1, 40.6, 35.1, 33.6, 30.2 (*J* = 7.0 Hz), 28.4, 25.7, 22.8, 20.5, 17.9, 16.3 (*J* = 6.6 Hz).

HRMS (ESI-TOF): calc'd for C₁₉C₃₅N₂O₆P [M+Na]⁺: 441.2130, found 418.2129.

TLC: R_f = 0.7 (1:1, hexane:EtOAc, anisaldehyde stain).

Compound SI-40



tert-butyl 6-azaspiro[4.5]decane-6-carboxylate (SI-40).(6I)

Following **General Procedure A** on 0.1 mmol scale (4 F/mol) with **SI-40**. Purification by prep-TLC (1:5, hexane:EtOAc) afforded 12.9 mg (54%, Faradic yield: 50%) of the title compound **SI-40**.

Physical State: colorless oil.

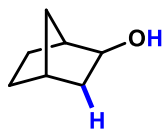
¹H NMR (600 MHz, CDCl₃): δ 3.50-3.41 (m, 2H), 2.09-1.96 (m, 2H), 1.93-1.82 (m, 2H), 1.82-1.68 (m, 2H), 1.68-1.58 (m, 2H), 1.58-1.47 (m, 8H), 1.45 (s, 9H).

¹³C NMR (151 MHz, CDCl₃): δ 156.1, 79.2, 66.2, 44.4, 37.5, 34.5, 28.8, 24.7, 23.9, 20.3.

GCMS (EI): calc'd for C₁₄H₂₅NO₂ [M]⁺: 239.2, found 239.10, 141.10, 110.0.

TLC: R_f = 0.4 (1:5, hexane:EtOAc, anisaldehyde stain).

Compound SI-42



(±1,4)-bicyclo[2.2.1]heptan-2-ol (SI-42).

Following **General Procedure A** or **B** on 0.1 mmol scale (3 F/mol) with *exo*-2,3-epoxynorbornane **41**. Purification by prep-TLC (1:5, hexane:EtOAc) afforded 10.3 mg (92%, Faradic yield: 66%) of the title compound **SI-42**.

Physical State: colorless oil.

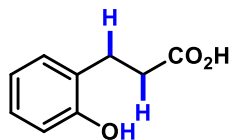
¹H NMR (600 MHz, CDCl₃): δ 3.76 (d, *J* = 6.9 Hz, 1H), 2.25 (s, 1H), 2.14 (d, *J* = 4.7 Hz, 1H), 1.66 (ddd, *J* = 13.2, 6.9, 2.5 Hz, 1H), 1.49-1.35 (m, 3H), 1.30 (s, 1H), 1.12 (dd, *J* = 9.8, 1.2 Hz, 1H), 1.02 (dd, *J* = 7.4, 2.3 Hz, 2H).

¹³C NMR (151 MHz, CDCl₃): δ 74.1, 43.5, 41.5, 34.6, 27.2, 23.5.

GCMS (EI): calc'd for C₇H₁₂O [M]⁺: 112.1, found 110, 94, 79.

TLC: R_f = 0.5 (5:1 hexane:EtOAc, anisaldehyde stain).

Compound SI-44



3-(2-hydroxyphenyl)propanoic acid (SI-44).(63)

Following **General Procedure A** or **B** on 0.2 mmol scale (8 F/mol) with benzofuran-2-carboxylic acid **43**. Purification by flash column chromatography (silica, 9:1 CH₂Cl₂:MeOH) afforded 17.5 mg (53%, Faradic yield: 38%) of the title compound **SI-44**.

Physical State: beige solid.

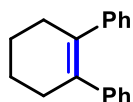
¹H NMR (600 MHz, CDCl₃): δ 7.12-7.09 (m, 2H), 6.89-6.81 (m, 2H), 6.40 (br s, 1H), 2.90 (t, *J* = 6.8 Hz, 2H), 2.74 (t, *J* = 6.8 Hz, 2H).

¹³C NMR (151 MHz, CDCl₃): δ 179.9, 154.0, 130.6, 128.2, 127.0, 121.1, 116.7, 34.8, 24.8.

HRMS (ESI-TOF): calc'd for C₉H₁₀O₃ [M-H]⁺: 165.0552, found 165.0547.

TLC: R_f = 0.36 (9:1 CH₂Cl₂:MeOH, UV/Vis).

Compound SI-46



3',4',5',6'-tetrahydro-1,1':2',1''-terphenyl (SI-46).

Prepared following **General Procedure B** on a 0.1 mmol scale (8 F/mol) with 1,6-diphenylhexane-1,6-dione **45** and a slow addition of TiCl₄ (1.0 M in CH₂Cl₂, 5.0 eq.) over 1 h, followed by an additional stirring at rt for 10 h. Et₂O (2 mL) was added followed by Na₂CO₃ (1 mL) and the layers separated. The organics were washed with water (2 mL), brine (2 mL), dried (Na₂SO₄), and concentrated under reduced pressure. Purification by flash column chromatography (silica, 9:1 hexanes:EtOAc) afforded 7.5 mg (32%, Faradic yield: 25%) of the title compound **SI-46**.

Physical State: colorless oil.

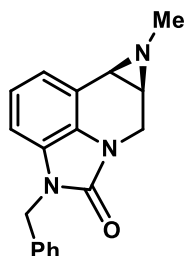
¹H NMR (600 MHz, CDCl₃): δ 7.10-7.08 (m, 4H), 7.05-7.02 (m, 2H), 6.99-6.97 (m, 4H), 2.47-2.44 (m, 4H), 1.85-1.83 (m, 4H).

¹³C NMR (151 MHz, CDCl₃): δ 144.0, 135.1, 129.2, 127.7, 125.8, 32.1, 23.4.

GCMS: calc'd for C₁₈H₁₈ [M]⁺: 234.1, found 234.1, 205.0, 191.0.

TLC: R_f = 0.9 (100% hexane, UV, Vis).

Compound SI-1



(7aS,8aR)-4-benzyl-8-methyl-7,7a,8,8a-tetrahydroazirino[2,3-c]imidazo[4,5,1-ij]quinolin-5(4H)-one (SI-1).

Generously provided by Pfizer.

Physical State: white solid.

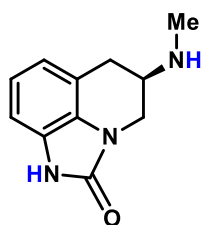
¹H NMR (600 MHz, CDCl₃): δ 7.32-7.22 (m, 5H), 7.11 (dd, *J* = 7.7, 0.8 Hz, 1H), 6.90 (t, *J* = 7.8 Hz, 1H), 6.70 (dd, *J* = 7.9, 0.9 Hz, 1H), 5.06 (d, *J* = 15.7 Hz, 1H), 4.95 (d, *J* = 15.6 Hz, 1H), 4.33 (d, *J* = 13.1 Hz, 1H), 3.91 (dd, *J* = 13.1, 3.6 Hz, 1H), 2.58 (s, 3H), 2.52 (d, *J* = 6.1 Hz, 1H), 2.32 (dd, *J* = 6.1, 3.5 Hz, 1H).

¹³C NMR (151 MHz, CDCl₃): δ 153.3, 135.4, 127.8, 127.1, 126.8, 123.5, 119.9, 118.9, 116.3, 106.6, 45.9, 44.1, 39.9, 37.3, 36.7.

HRMS (ESI-TOF): calc'd for C₁₈H₁₇N₃O [M+H]⁺: 292.1450, found 292.1456.

TLC: R_f = 0.2 (100% EtOAc, UV/Vis).

Compound PNU-95666E (Sumanirole, 2)



PNU-95666E.(64, 65)

Following **General Procedure B** on 0.1 mmol scale (7 F/mol) and **SI-40**. Purification by prep-TLC (9:1:0.1, CH₂Cl₂:MeOH:TEA) afforded 13.6 (67%, Faradic yield: 43%) of the title

compound **PNU-95666E**.

Physical State: colorless oil.

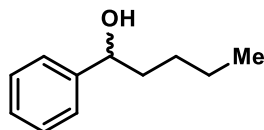
¹H NMR (600 MHz, CDCl₃): δ 6.99-6.95 (m, 1H), 6.91-6.86 (m, 2H), 4.01 (dd, *J* = 12.5, 3.9 Hz, 1H), 3.70 (dd, *J* = 12.4, 6.7 Hz, 1H), 3.30-3.28 (m, 1H), 3.14 (dd, *J* = 16.3, 4.2 Hz, 1H), 2.83 (dd, *J* = 16.3, 7.9 Hz, 1H), 2.52 (s, 3H).

¹³C NMR (151 MHz, CDCl₃): δ 156.3, 128.4, 127.8, 122.9, 121.0, 118.3, 108.4, 54.4, 42.8, 33.6, 30.5.

HRMS (ESI-TOF): calc'd for C₁₁H₁₃N₃O [M+H]⁺: 204.1137, found 204.1136.

TLC: R_f = 0.7 (9:1:0.1, CH₂Cl₂:MeOH:TEA, UV/Vis and I₂).

Compound SI-47



1-phenylpentan-1-ol (SI-47).(66)

Benzaldehyde (1 mmol) was added to a flask containing 50 mL of dry THF. The contents were then cooled to -78 °C. Then *n*-BuLi (0.1 mmol) was added dropwise (under argon). The reaction was allowed to warm slowly overnight. The reaction was quenched by adding saturated aqueous NH₄Cl, and the THF was removed on a rotavap. Et₂O was added and the layers separated. The Et₂O layer was dried over anhydrous MgSO₄. The crude material was purified using flash column chromatography (4:1, hexane:EtOAc), to afford the pure alcohol (**SI-47**) in 82% yield.

Physical State: colorless oil.

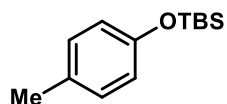
¹H NMR (600 MHz, CDCl₃): δ 7.44-7.12 (m, 5H), 4.63 (dd, *J* = 7.5, 5.9 Hz, 1H), 2.02 (d, *J* = 2.0 Hz, 1H), 1.83-1.74 (m, 1H), 1.74-1.64 (m, 1H), 1.42-1.28 (m, 3H), 1.28-1.19 (m, 1H), 0.88 (t, *J* = 7.2 Hz, 3H).

¹³C NMR (151 MHz, CDCl₃): δ 144.1, 127.5, 126.6, 125.0, 73.8, 37.9, 27.1, 21.7, 13.1.

GCMS (EI): calc'd for C₁₁H₁₆O [M]⁺: 164.10, 107.0 [M-C₄H₉].

TLC: R_f = 0.7 (100% hexane, UV/Vis).

Compound SI-48



tert-butyldimethyl(*p*-tolylloxy)silane (SI-48).

Prepared according to known procedure, see spectra.(45)

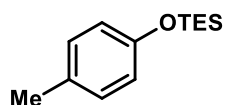
Physical State: colorless oil.

¹H NMR (600 MHz, CDCl₃): δ 7.04 (d, *J* = 6.0 Hz, 2H), 6.74 (d, *J* = 6.0 Hz, 2H), 2.29 (s, 3H), 1.00 (s, 9H), 0.20 (s, 6H).

¹³C NMR (151 MHz, CDCl₃): δ 153.5, 130.6, 130.0, 120.0, 25.9, 20.7, -4.30.

TLC: *R_f* = 0.85 (100% hexane, UV/Vis).

Compound SI-49



triethyl(*p*-tolylloxy)silane (SI-49).

Prepared according to known procedure, see spectra.(45)

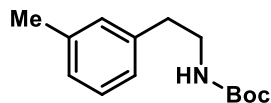
Physical State: colorless oil.

¹H NMR (600 MHz, CDCl₃): δ 7.03 (d, *J* = 6.0 Hz, 2H), 6.76 (d, *J* = 6.0 Hz, 2H), 2.29 (s, 3H), 1.01 (t, *J* = 6.0 Hz, 9H), 0.72 (q, *J* = 6.0 Hz, 6H).

¹³C NMR (151 MHz, CDCl₃): δ 153.4, 130.6, 130.0, 119.8, 20.7, 6.8, 5.1.

TLC: *R_f* = 0.87 (100% hexane, UV/Vis).

Compound SI-50



tert-butyl (3-methylphenethyl)carbamate (SI-50).

To a stirring solution of 2-(*m*-tolyl)ethan-1-amine (270 mg, 2.0 mmol) and Et₃N (202 mg, 2.0 mmol) in CH₂Cl₂ (6 mL) at rt was added Boc₂O (437 mg, 2.0 mmol, in 1 mL CH₂Cl₂). The reaction stirred for 2 h after which the mixture was filtered through a short pad of silica and concentrated under reduced pressure. The crude oil was purified by flash chromatography eluting

with hexanes/EtOAc (5:1) to afford 420 mg (89%) of **SI-50** as a colorless oil.

Physical State: colorless oil.

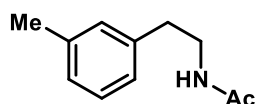
¹H NMR (400 MHz, CDCl₃): δ 7.21, (t, *J* = 7.5 Hz, 1H), 7.06 (d, *J* = 7.6 Hz, 1H), 7.04-7.00 (m, 2H), 4.56 (s, 1H), 3.40-3.39 (m, 2 H), 2.79 (t, *J* = 7.1 Hz, 2H), 2.36 (s, 3H), 1.46 (s, 9H).

¹³C NMR (151 MHz, CDCl₃): δ 156.0, 139.0, 138.3, 129.7, 128.6, 127.3, 125.9, 79.3, 41.9, 36.2, 28.6, 21.5.

HRMS (ESI-TOF): calc'd for C₁₄H₂₁NO₂ [M+Na]⁺: 258.1470, found 258.1475.

TLC: R_f = 0.28 (9:1, hexane/EtOAc, UV/Vis).

Compound SI-51



N-(3-methylphenethyl)acetamide (**SI-51**).

To a stirring solution of 2-(*m*-tolyl)ethan-1-amine (270 mg, 2.0 mmol) and Et₃N (263 mg, 2.6 mmol) in CH₂Cl₂ (10 mL) at 0 °C was dropwise added acetyl chloride (162 mg, 2.2 mmol, in 3 mL CH₂Cl₂). The reaction mixture stirred for 3 h after which saturated NaHCO₃ (5 mL) was added. The layers were separated, and the organic phase washed with water (5 mL), brine (5 mL), dried (Na₂SO₄) and concentrated under reduced pressure. The crude oil was purified by flash chromatography eluting with hexanes/EtOAc (1:1) to afford 265 mg (75%) of **SI-51** as a colorless oil.

Physical State: colorless oil.

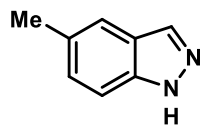
¹H NMR (400 MHz, CDCl₃): δ 7.20, (t, *J* = 7.5 Hz, 1H), 7.04 (d, *J* = 7.6 Hz, 1H), 7.01-6.97 (m, 2H), 5.59 (s, 1H), 3.49 (q, *J* = 7.0 Hz, 2H), 2.77 (t, *J* = 7.0 Hz, 2H), 2.33 (s, 3H), 1.93 (s, 3H).

¹³C NMR (151 MHz, CDCl₃): δ 170.2, 138.9, 138.4, 129.6, 128.6, 127.4, 125.8, 40.8, 35.6, 23.4, 21.5.

HRMS (ESI-TOF): calc'd for C₁₁H₁₅NO [M+H]⁺: 178.1232, found 178.1232.

TLC: R_f = 0.24 (1:1, hexane/EtOAc, UV/Vis).

Compound SI-52



5-methyl-1H-indazole (SI-52).

Generously donated by Pfizer

Physical State: tan solid.

¹H NMR (400 MHz, CDCl₃): δ 8.10 (d, J = 1.0 Hz, 1H), 7.53 (dd, J = 1.2, 1.0 Hz, 1H), 7.40 (d, J = 6.8 Hz, 1H), 7.23 (dd, J = 6.8, 1.2 Hz, 1H), 2.47 (s, 3H).

¹³C NMR (151 MHz, CDCl₃): δ 138.9, 134.5, 130.6, 129.1, 123.8, 120.0, 109.5, 21.5.

TLC: R_f = 0.72 (1:1 hexane/EtOAc).

References

1. A. B. Pangborn, M. A. Giardello, R. H. Grubbs, R. K. Rosen, F. J. Timmers, Safe and Convenient Procedure for Solvent Purification. *Organometallics* **15**, 1518-1520 (1996).
2. G. R. Fulmer *et al.*, NMR Chemical Shifts of Trace Impurities: Common Laboratory Solvents, Organics, and Gases in Deuterated Solvents Relevant to the Organometallic Chemist. *Organometallics* **29**, 2176-2179 (2010).
3. Wagner, C. D.; Naumkin, A. V.; Kraut-Vass, A.; Allison, J. W.; Powell, C. J.; Jr., J. R. R., NIST X-ray Photoelectron Spectroscopy Database. NIST Standard Reference Database 20, Version 3.2 (Web Version) 2000.
4. Gaussian 09, Revision A.02, J. Frisch, G. W. Trucks, H. B. Schlegel, G. E. Scuseria, M. A. Robb, J. R. Cheeseman, G. Scalmani, V. Barone, B. Mennucci, G. A. Petersson, H. Nakatsuji, M. Caricato, X. Li, H. P. Hratchian, A. F. Izmaylov, J. Bloino, G. Zheng, J. L. Sonnenberg, M. Hada, M. Ehara, K. Toyota, R. Fukuda, J. Hasegawa, M. Ishida, T. Nakajima, Y. Honda, O. Kitao, H. Nakai, T. Vreven, J. A. Montgomery, Jr., J. E. Peralta, F. Ogliaro, M. Bearpark, J. J. Heyd, E. Brothers, K. N. Kudin, V. N. Staroverov, R. Kobayashi, J. Normand, K. Raghavachari, A. Rendell, J. C. Burant, S. S. Iyengar, J. Tomasi, M. Cossi, N. Rega, J. M. Millam, M. Klene, J. E. Knox, J. B. Cross, V. Bakken, C. Adamo, J. Jaramillo, R. Gomperts, R. E. Stratmann, O. Yazyev, A. J. Austin, R.

- Cammi, C. Pomelli, J. W. Ochterski, R. L. Martin, K. Morokuma, V.G. Zakrzewski, G. A. Voth, P. Salvador, J. J. Dannenberg, S. Dapprich, A. D. Daniels, Ö. Farkas, J. B.Foresman, J. V. Ortiz, J. Cioslowski, and D. J. Fox, Gaussian, Inc., Wallingford CT, 2009
5. A. D. Becke, A new mixing of Hartree-Fock and local-density-functional theories. *J. Chem. Phys.* **98**, 1372-1377 (1993).
 6. A. D. Becke, Density-functional thermochemistry. III. The role of exact exchange. *J. Chem. Phys.* **98**, 5648-5652 (1993).
 7. C. Lee, W. Yang, R. G. Parr, Development of the Colle-Salvetti correlation-energy formula into a functional of the electron density. *Phys. Rev. B: Condens. Matter* **37**, 785-789 (1988).
 8. R. Ditchfield, W. J. Hehre, J. A. Pople, Self-consistent molecular-orbital methods. IX. Extended Gaussian-type basis for molecular-orbital studies of organic molecules. *J. Chem. Phys.* **54**, 724-728 (1971).
 9. P. C. Hariharan, J. A. Pople, Accuracy of AHn equilibrium geometries by single determinant molecular orbital theory. *Mol. Phys.* **27**, 209-214 (1974).
 10. R. Krishnan, J. S. Binkley, R. Seeger, J. A. Pople, Self-consistent molecular orbital methods. XX. A basis set for correlated wave functions. *J. Chem. Phys.* **72**, 650-654 (1980).
 11. A.J. Bard, L. R. Faulkner, *Electrochemical methods: Fundamentals and Applications* (John Wiley and Sons, New York, ed. 2., 2001). Kinetics of Electrode Reactions (2001).
 12. V. V. Chaban, O. V. Prezhdo, Electron Solvation in Liquid Ammonia: Lithium, Sodium, Magnesium, and Calcium as Electron Sources. *J. Phys. Chem. B* **120**, 2500-2506 (2016).
 13. B. G. Janesko, G. Scalmani, M. J. Frisch, Quantifying solvated electrons' delocalization. *Phys. Chem. Chem. Phys.* **17**, 18305-18317 (2015).
 14. J. L. Atwood *et al.*, Neutral and anionic silylmethyl complexes of Group IIIb and lanthanoid metals; the x-ray crystal and molecular structure of [Li(thf)₄][Yb[CH(SiMe₃)₂]₃Cl] (thf = tetrahydrofuran). *J. Chem. Soc., Chem. Commun.*, 140-142 (1978).
 15. C. Eaborn, P. B. Hitchcock, J. D. Smith, A. C. Sullivan, Crystal structure of the tetrahydrofuran adduct of tris(trimethylsilyl)methyl lithium, [Li(THF)₄][Li[C(SiMe₃)₃]₂],

- an ate derivative of lithium. *J. Chem. Soc., Chem. Commun.*, 827-828 (1983).
16. C. Eaborn, P. B. Hitchcock, J. D. Smith, A. C. Sullivan, Preparation and crystal structure of the argentate complex $[\text{Li}(\text{tetrahydrofuran})_4][\text{Ag}[\text{C}(\text{SiMe}_3)_3]_2]$. *J. Chem. Soc., Chem. Commun.*, 870-871 (1984).
 17. P. G. Edwards, R. W. Gellert, M. W. Marks, R. Bau, Preparation and structure of the phenylcopper ($[\text{Cu}_5(\text{C}_6\text{H}_5)_6]^-$) anion. *J. Am. Chem. Soc.* **104**, 2072-2073 (1982).
 18. H. J. Reich, J. P. Borst, R. R. Dykstra, P. D. Green, A nuclear magnetic resonance spectroscopic technique for the characterization of lithium ion pair structures in THF and THF/HMPA solution. *J. Am. Chem. Soc.* **115**, 8728-8741 (1993).
 19. G. Kresse, J. Furthmuller, Efficient iterative schemes for ab initio total-energy calculations using a plane-wave basis set. *Phys. Rev. B: Condens. Matter* **54**, 11169-11186 (1996).
 20. G. Kresse, J. Hafner, Ab initio molecular-dynamics simulation of the liquid-metal-amorphous-semiconductor transition in germanium. *Phys. Rev. B: Condens. Matter* **49**, 14251-14269 (1994).
 21. E. G. Moroni, G. Kresse, J. Hafner, J. Furthmuller, Ultrasoft pseudopotentials applied to magnetic Fe, Co, and Ni: From atoms to solids. *Phys. Rev. B: Condens. Matter* **56**, 15629-15646 (1997).
 22. J. P. Perdew, M. Ernzerhof, K. Burke, Rationale for mixing exact exchange with density functional approximations. *J. Chem. Phys.* **105**, 9982-9985 (1996).
 23. P. E. Blochl, Projector augmented-wave method. *Phys. Rev. B: Condens. Matter* **50**, 17953-17979 (1994).
 24. G. Kresse, D. Joubert, From ultrasoft pseudopotentials to the projector augmented-wave method. *Phys. Rev. B: Condens. Matter Mater. Phys.* **59**, 1758-1775 (1999).
 25. S. Grimme, J. Antony, S. Ehrlich, H. Krieg, A consistent and accurate ab initio parametrization of density functional dispersion correction (DFT-D) for the 94 elements H-Pu. *J. Chem. Phys.* **132**, 154104/154101-154104/154119 (2010).
 26. G. Henkelman, H. Jonsson, A dimer method for finding saddle points on high dimensional potential surfaces using only first derivatives. *J. Chem. Phys.* **111**, 7010-7022 (1999).
 27. G. Henkelman, H. Jonsson, Improved tangent estimate in the nudged elastic band method

- for finding minimum energy paths and saddle points. *J. Chem. Phys.* **113**, 9978-9985 (2000).
28. G. Henkelman, B. P. Uberuaga, H. Jonsson, A climbing image nudged elastic band method for finding saddle points and minimum energy paths. *J. Chem. Phys.* **113**, 9901-9904 (2000).
29. J.-S. Filhol, M. Neurock, Elucidation of the electrochemical activation of water over Pd by first principles. *Angew. Chem., Int. Ed.* **45**, 402-406 (2006).
30. C. D. Taylor, S. A. Wasileski, J.-S. Filhol, M. Neurock, First principles reaction modeling of the electrochemical interface: Consideration and calculation of a tunable surface potential from atomic and electronic structure. *Phys. Rev. B: Condens. Matter Mater. Phys.* **73**, 165402/165401-165402/165416 (2006).
31. L. D. Chen, M. Urushihara, K. Chan, J. K. Noerskov, Electric Field Effects in Electrochemical CO₂ Reduction. *ACS Catal.* **6**, 7133-7139 (2016).
32. S.G. Winikoff, J.L. DiMeglio, J. Medina Ramos, J. Rosenthal, M. Neurock, *Nature Comm., submitted, (2018)*.
33. G. Henkelman, A. Arnaldsson, H. Jónsson, A fast and robust algorithm for Bader decomposition of charge density. *Comput. Mat. Sci.* **36**, 354-360 (2006).
34. A. Menzek, M. G. Karakaya, A. A. Kaya, Reductions of benzene derivatives whose benzylic positions bear oxygen atoms under mild conditions. *Helv. Chim. Acta* **91**, 2299-2307 (2008).
35. P. S. Engel, R. L. Allgren, W.-K. Chae, R. A. Leckonby, N. A. Marron, Thermolysis of allylic azoalkanes. *J. Org. Chem.* **44**, 4233-4239 (1979).
36. C. Petrier, K. Suslick, Ultrasound-enhanced reactivity of calcium in the reduction of aromatic hydrocarbons. *Ultrason. Sonochem.* **7**, 53-61 (2000).
37. M. J. Webber *et al.*, Towards the enantioselective synthesis of (-)-euonyminol - preparation of a fully functionalised lower-rim model. *Org. Biomol. Chem.* **11**, 2514-2533 (2013).
38. A. J. Birch, H. H. Mantsch, Reductions of acridine by metal-ammonia solutions. *Aust. J. Chem.* **22**, 1103-1104 (1969).
39. I. Matsuda, M. Shibata, S. Sato, Y. Izumi, Cyclo-codimerization of 1,3-butadiene derivatives with non-activated terminal acetylenes catalyzed by a cationic rhodium(I)

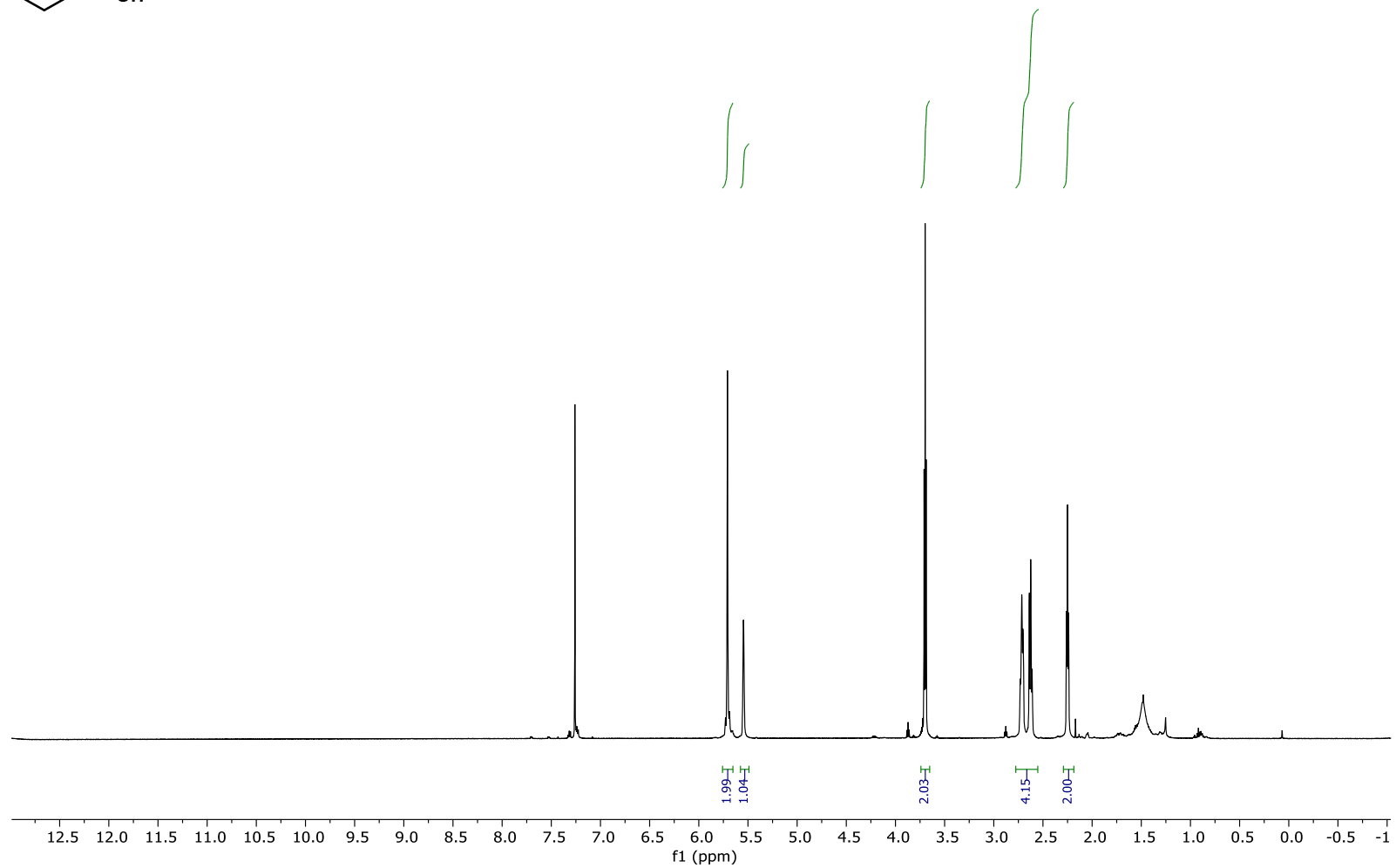
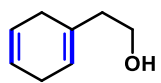
- complex. *Tetrahedron Lett.* **28**, 3361-3362 (1987).
40. A. Paptchikhine, K. Itto, P. G. Andersson, Sequential Birch reaction and asymmetric Ir-catalyzed hydrogenation as a route to chiral building blocks. *Chem. Commun. (Cambridge, U. K.)* **47**, 3989-3991 (2011).
 41. J. D. Burch *et al.*, Tetrahydroindazoles as Interleukin-2 Inducible T-Cell Kinase Inhibitors. Part II. Second-Generation Analogues with Enhanced Potency, Selectivity, and Pharmacodynamic Modulation in Vivo. *J. Med. Chem.* **58**, 3806-3816 (2015).
 42. F. J. Del Campo *et al.*, Low-temperature sonoelectrochemical processes. Part 2: Generation of solvated electrons and Birch reduction processes under high mass transport conditions in liquid ammonia. *J. Electroanal. Chem.* **507**, 144-151 (2001).
 43. S. A. Monti, S.-C. Chen, Y.-L. Yang, S.-S. Yuan, O. P. Bourgeois, Rearrangement approaches to polycyclic skeletons. 1. Bridgehead-substituted bicyclo[3.2.1]octene derivatives from bicyclo[2.2.2]octene precursors. *J. Org. Chem.* **43**, 4062-4069 (1978).
 44. S. V. Ley *et al.*, A highly convergent total synthesis of the spiroacetal macrolide (+)-milbemycin β 1. *Tetrahedron* **45**, 7161-7194 (1989).
 45. J. Liu *et al.*, Regioselective Iridium-Catalyzed Asymmetric Monohydrogenation of 1,4-Dienes. *J. Am. Chem. Soc.* **139**, 14470-14475 (2017).
 46. B. K. Peters *et al.*, Enantio- and Regioselective Ir-Catalyzed Hydrogenation of Di- and Trisubstituted Cycloalkenes. *J. Am. Chem. Soc.* **138**, 11930-11935 (2016).
 47. J. Iwasaki, H. Ito, M. Nakamura, K. Iguchi, A synthetic study of briarane-type marine diterpenoid, pachyclavulide B. *Tetrahedron Lett.* **47**, 1483-1486 (2006).
 48. K. D. Ashtekar, M. Vetticatt, R. Yousefi, J. E. Jackson, B. Borhan, Nucleophile-Assisted Alkene Activation: Olefins Alone Are Often Incompetent. *J. Am. Chem. Soc.* **138**, 8114-8119 (2016).
 49. F. K. Cheung, A. M. Hayes, J. Hannedouche, A. S. Y. Yim, M. Wills, "Tethered" Ru(II) Catalysts for Asymmetric Transfer Hydrogenation of Ketones. *J. Org. Chem.* **70**, 3188-3197 (2005).
 50. Y. J. Zhu *et al.*, Efficient construction of bioactive trans-5A5B6C spiro lactones via bicyclo[4.3.0] α -hydroxy ketones. *Org. Biomol. Chem.* **16**, 1163-1166 (2018).
 51. B. B. Snider, T. C. Kirk, A new route to functionalized trans-hydrindenones. *J. Am. Chem. Soc.* **105**, 2364-2368 (1983).

52. N. Takenaka, J. Chen, B. Captain, R. S. Sarangthem, A. Chandrakumar, Helical Chiral 2-Aminopyridinium Ions: A New Class of Hydrogen Bond Donor Catalysts. *J. Am. Chem. Soc.* **132**, 4536-4537 (2010).
53. P. Lei *et al.*, A Practical and Chemoselective Ammonia-Free Birch Reduction. *Org. Lett.* **20**, 3439-3442 (2018).
54. H. Shimogawa, H. Mori, A. Wakamiya, Y. Murata, Impacts of dibenzo- and dithienofused structures at the b,g bonds in the BODIPY skeleton. *Chem. Lett.* **42**, 986-988 (2013).
55. H. Cavdar, N. Saracoglu, A new approach for the synthesis of 2-substituted indole derivatives via Michael type adducts. *Tetrahedron* **61**, 2401-2405 (2005).
56. W. A. Remers, G. J. Gibs, C. Pidacks, M. J. Weiss, Ring selectivity in the reduction of certain indoles and quinolines by lithium and methanol in liquid ammonia. *J. Am. Chem. Soc.* **89**, 5513-5514 (1967).
57. J. W. Ashmore, G. K. Helmkamp, Improved procedure for the Birch reduction of indole and carbazole. *Org. Prep. Proced. Int.* **8**, 223-225 (1976).
58. E. Kariv-Miller, K. E. Swenson, G. K. Lehman, R. Andruzzi, Selective cathodic Birch reductions. *J. Org. Chem.* **50**, 556-560 (1985).
59. A. F. Fentiman, Jr., R. H. Poirier, Electrochemical Birch reduction of estrone. *Chem. Ind. (London, U. K.)*, 813-814 (1966).
60. H. L. Dryden, Jr., G. M. Webber, R. R. Burtner, J. A. Cella, Use of sodium metal in the Birch reduction of aromatic compounds. *J. Org. Chem.* **26**, 3237-3245 (1961).
61. S. A. Wolckenhauer, S. D. Rychnovsky, Generation and Utility of Tertiary α -Aminoorganolithium Reagents. *Org. Lett.* **6**, 2745-2748 (2004).
62. H. Wakita *et al.*, Synthesis of 5,6,7-trinor-4,8-inter-m-phenylene PGI₂ and Beraprost. *Tetrahedron* **55**, 2449-2474 (1999).
63. S. Shabbir *et al.*, Pd nanoparticles on reverse phase silica gel as recyclable catalyst for Suzuki-Miyaura cross coupling reaction and hydrogenation in water. *J. Organomet. Chem.* **846**, 296-304 (2017).
64. T. Nemoto, M. Hayashi, D. Xu, A. Hamajima, Y. Hamada, Enantioselective synthesis of (R)-Sumanirole using organocatalytic asymmetric aziridination of an α,β -unsaturated aldehyde. *Tetrahedron: Asymmetry* **25**, 1133-1137 (2014).

65. D. K. Joshi, J. W. Sutton, S. Carver, J. P. Blanchard, Experiences with Commercial Production Scale Operation of Dissolving Metal Reduction Using Lithium Metal and Liquid Ammonia. *Org. Proc. Res. & Dev.* **9**, 997-1002 (2005).
66. S. C. Berk, M. C. P. Yeh, N. Jeong, P. Knochel, Preparation and reactions of functionalized benzylic organometallics of zinc and copper. *Organometallics* **9**, 3053-3064 (1990).

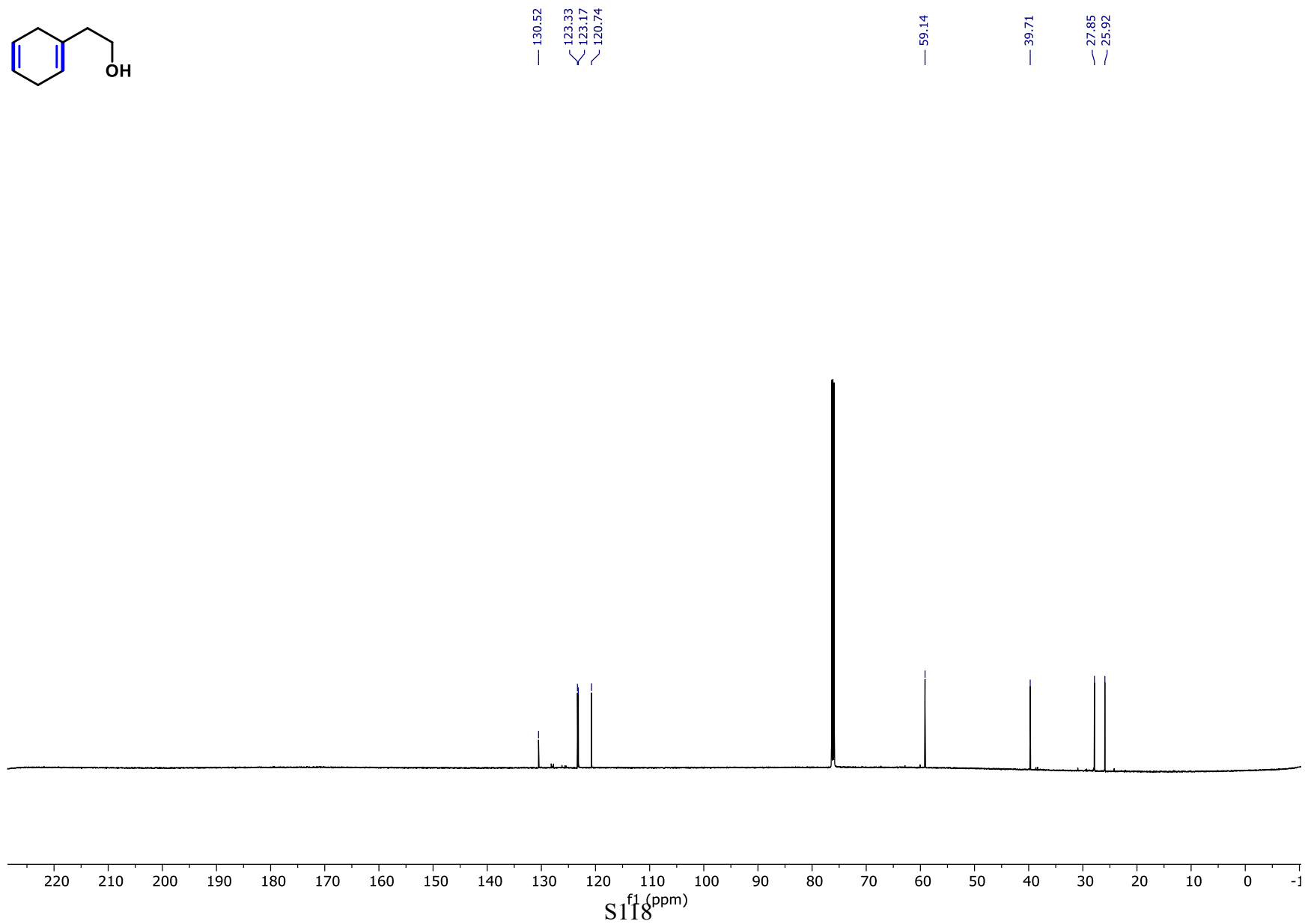
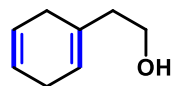
NMR Spectra

Compound SI-4 ¹H NMR

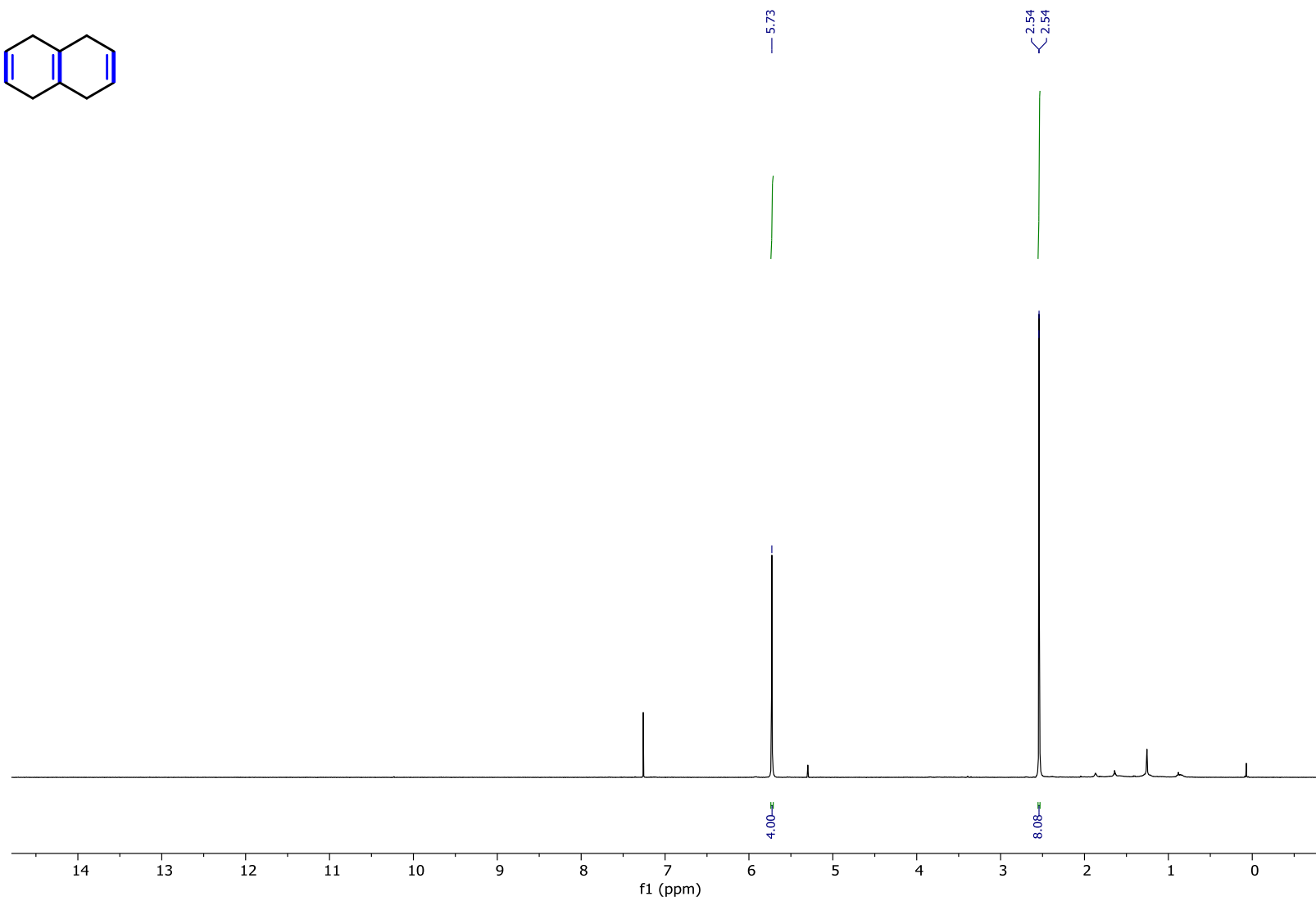
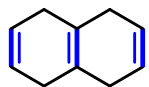


S117

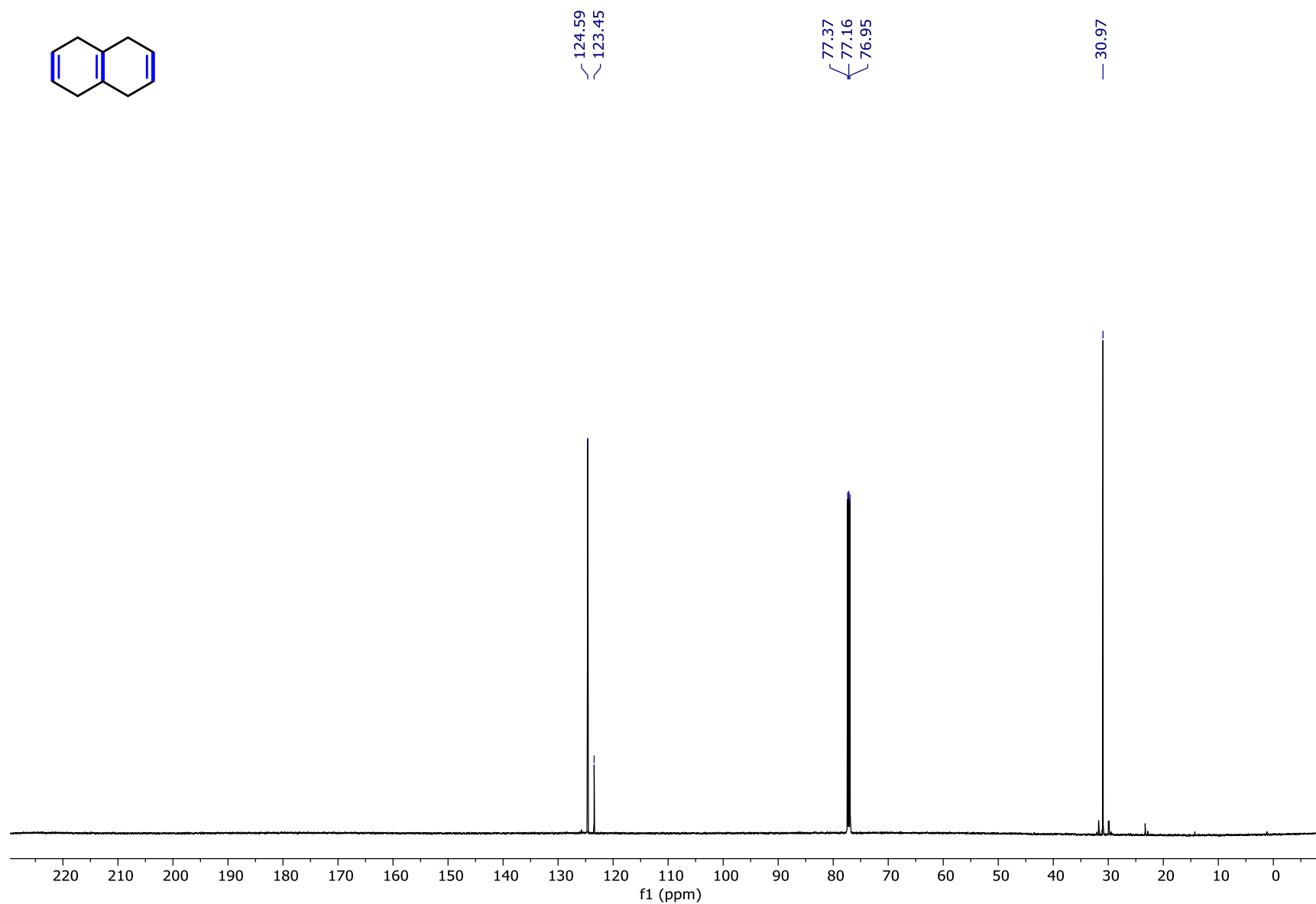
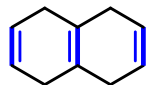
Compound SI-4 ¹³C NMR



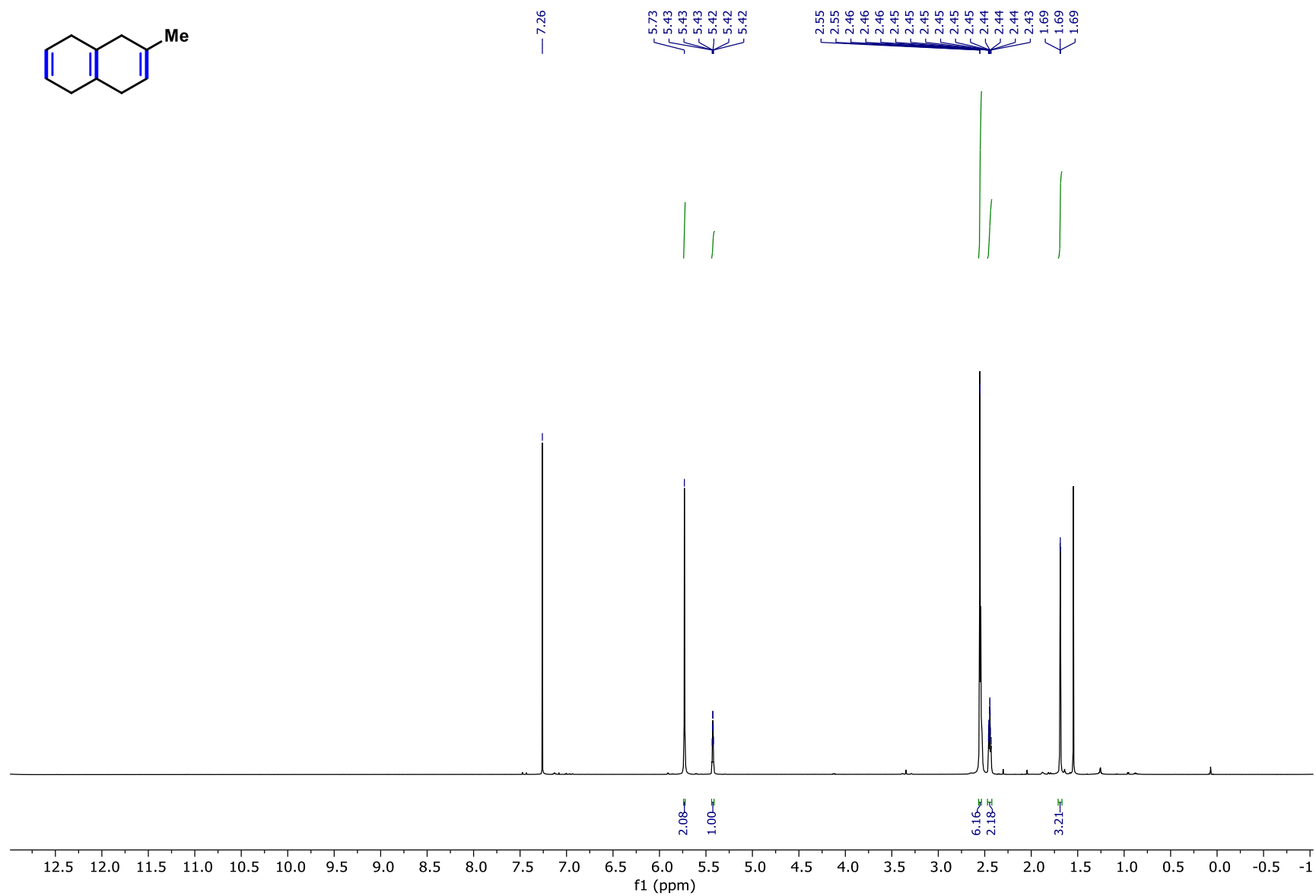
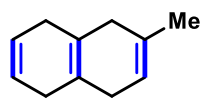
Compound SI-6 ¹H NMR



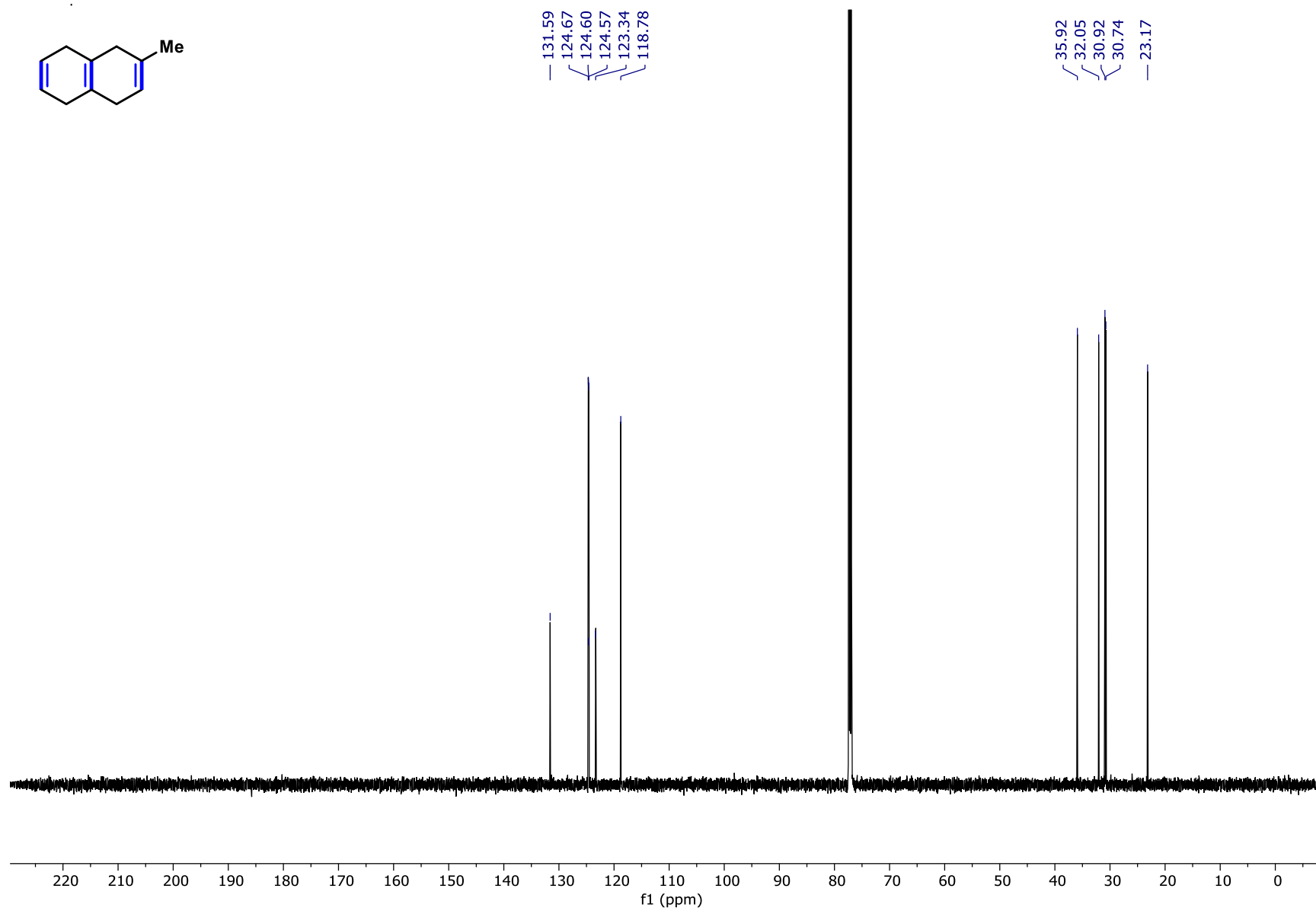
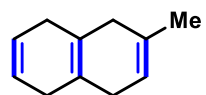
Compound SI-6 ¹³C NMR



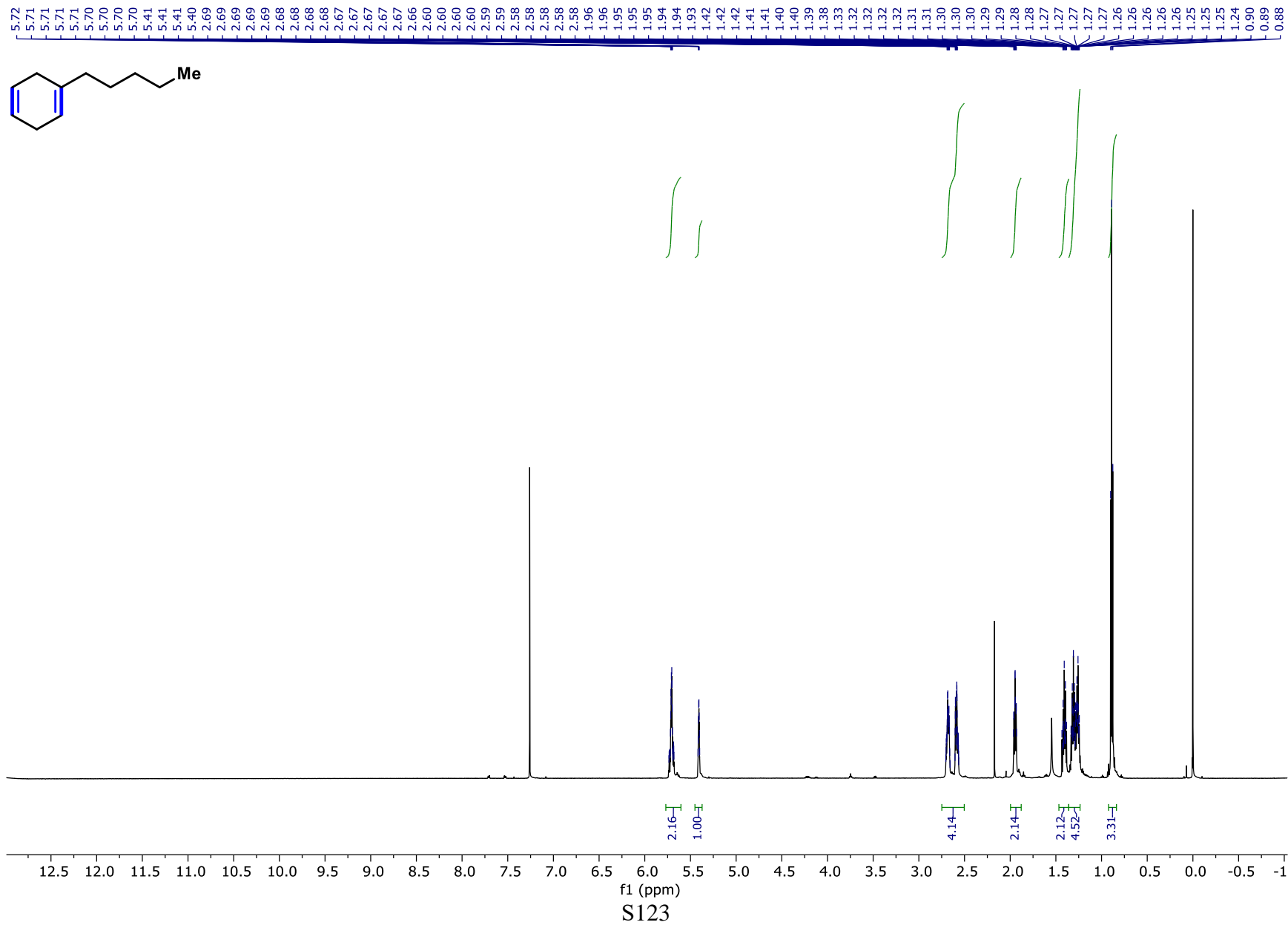
Compound SI-7 ¹H NMR



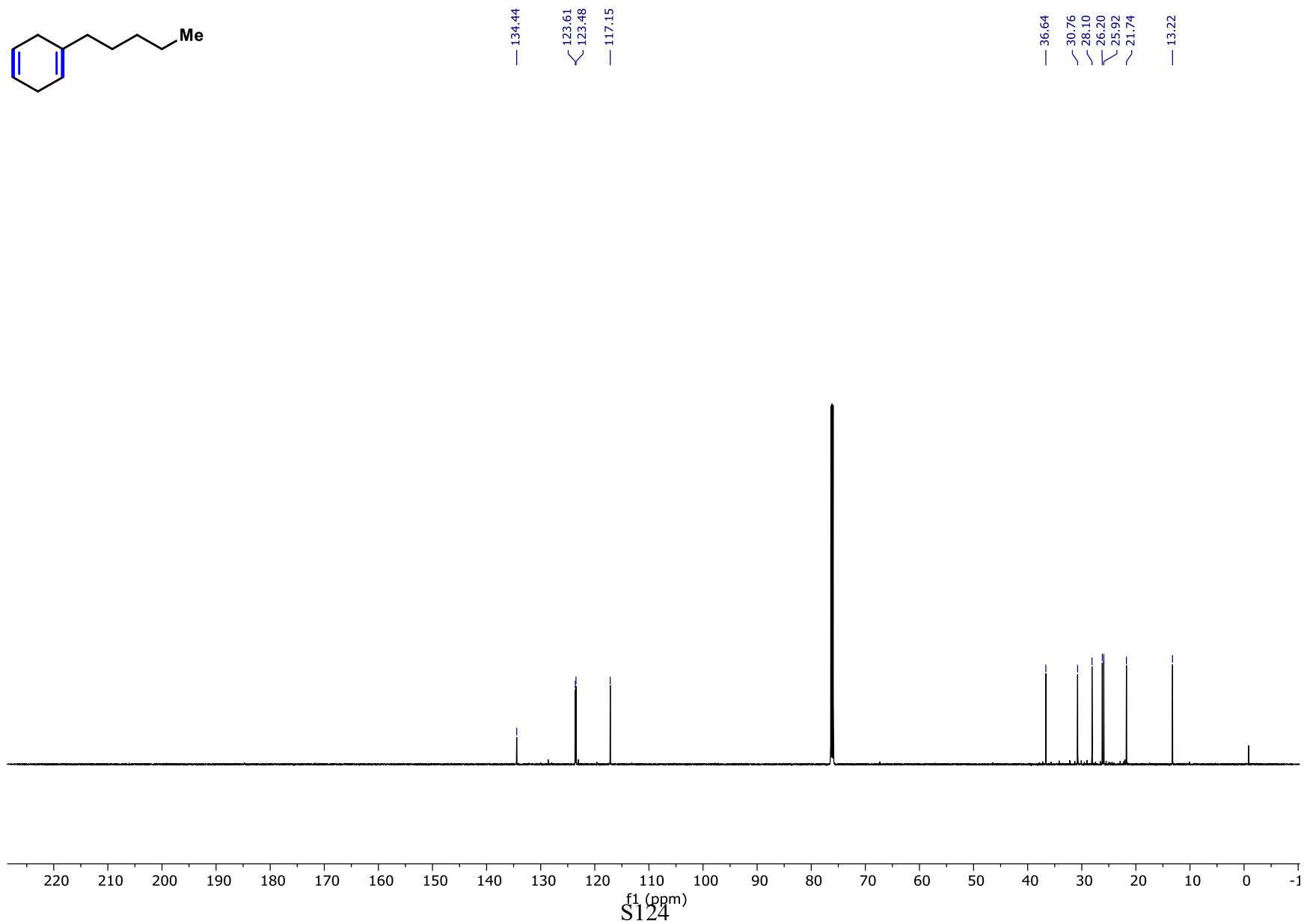
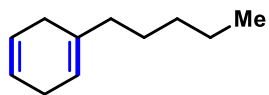
Compound SI-7 ¹³C NMR



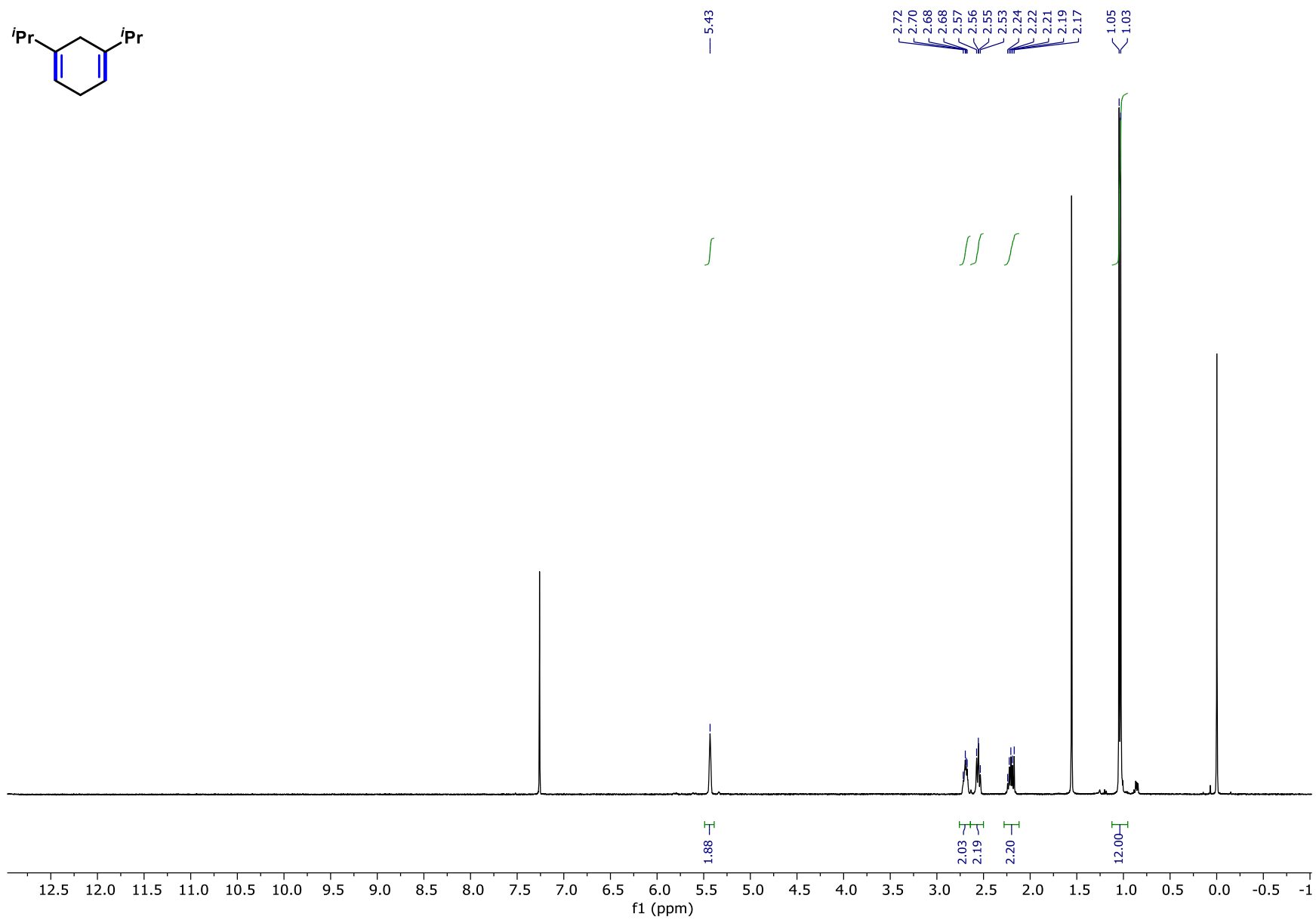
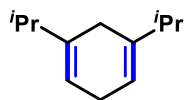
Compound SI-8 ¹H NMR



Compound SI-8 ¹³C NMR

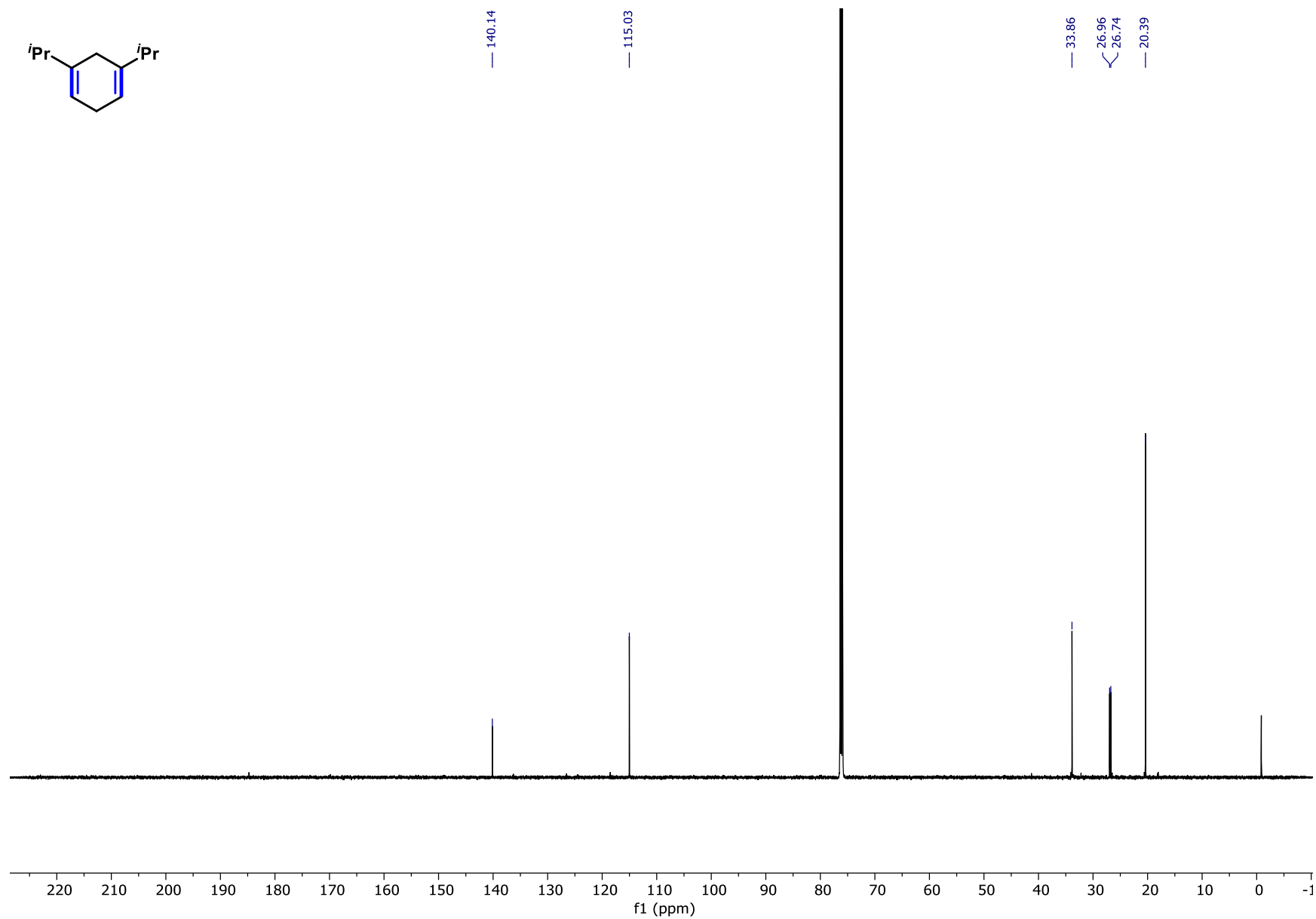
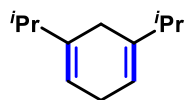


Compound SI-9 ¹H NMR



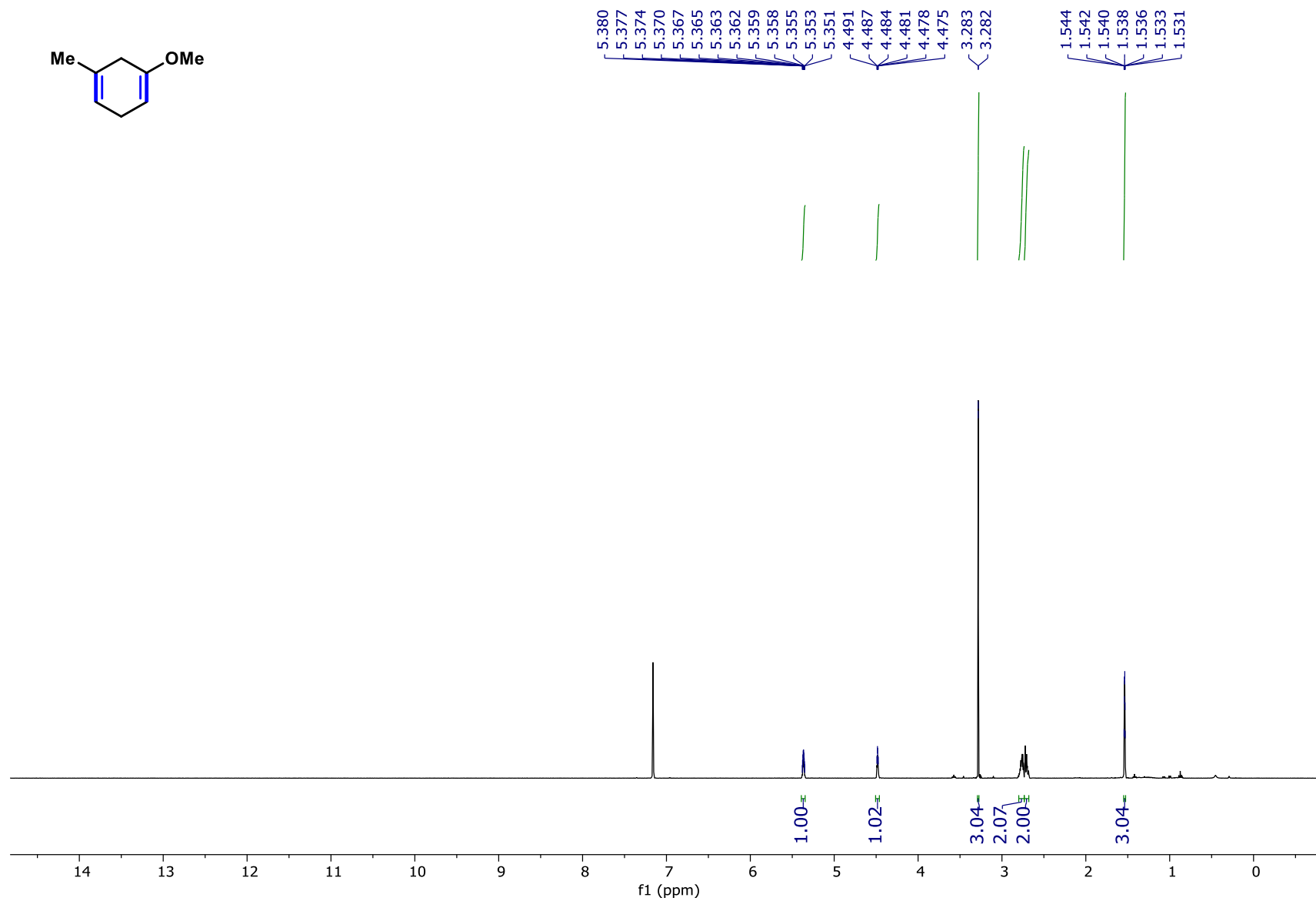
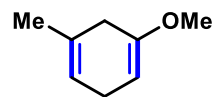
S125

Compound SI-9 ¹³C NMR

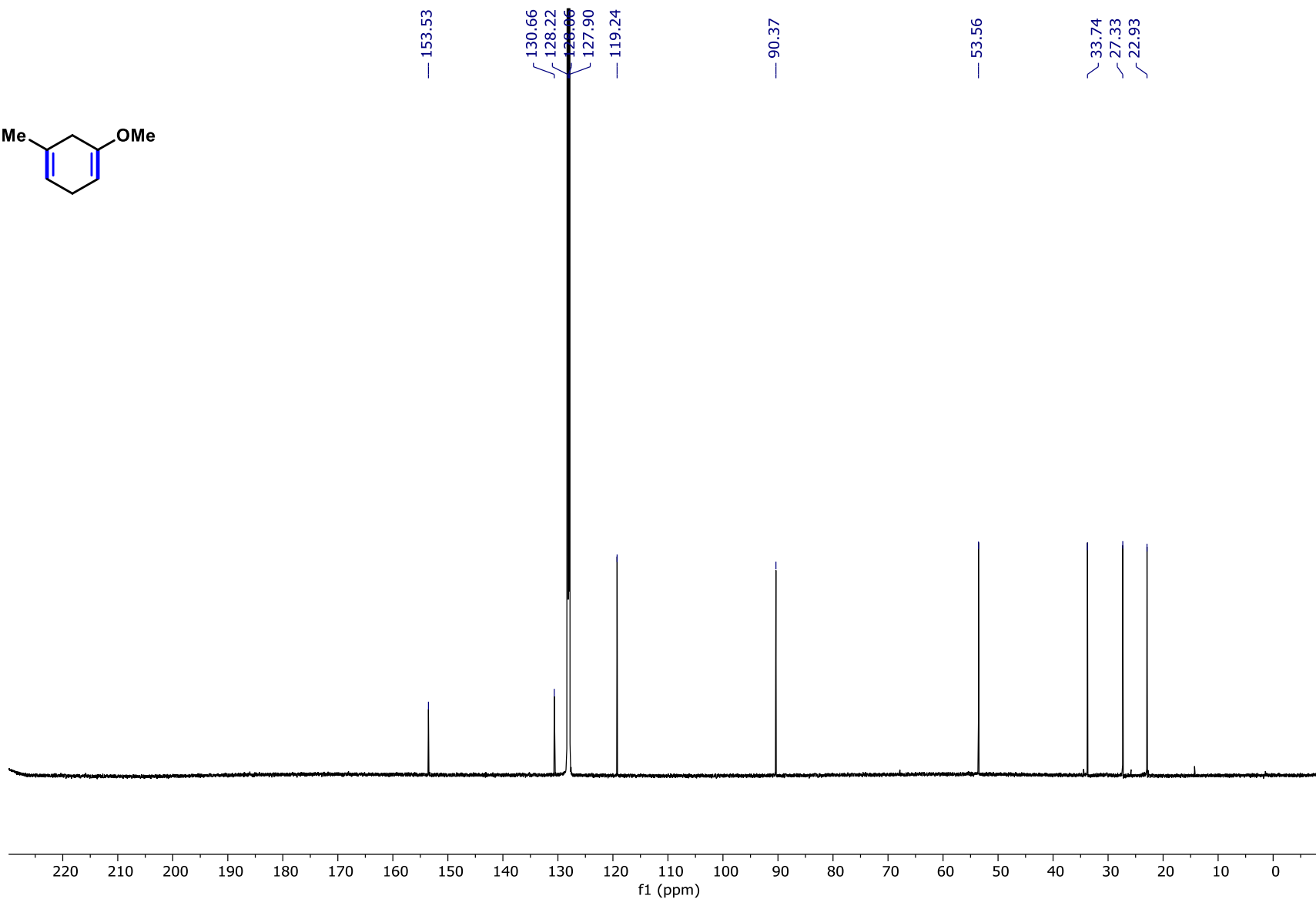
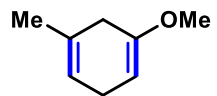


S126

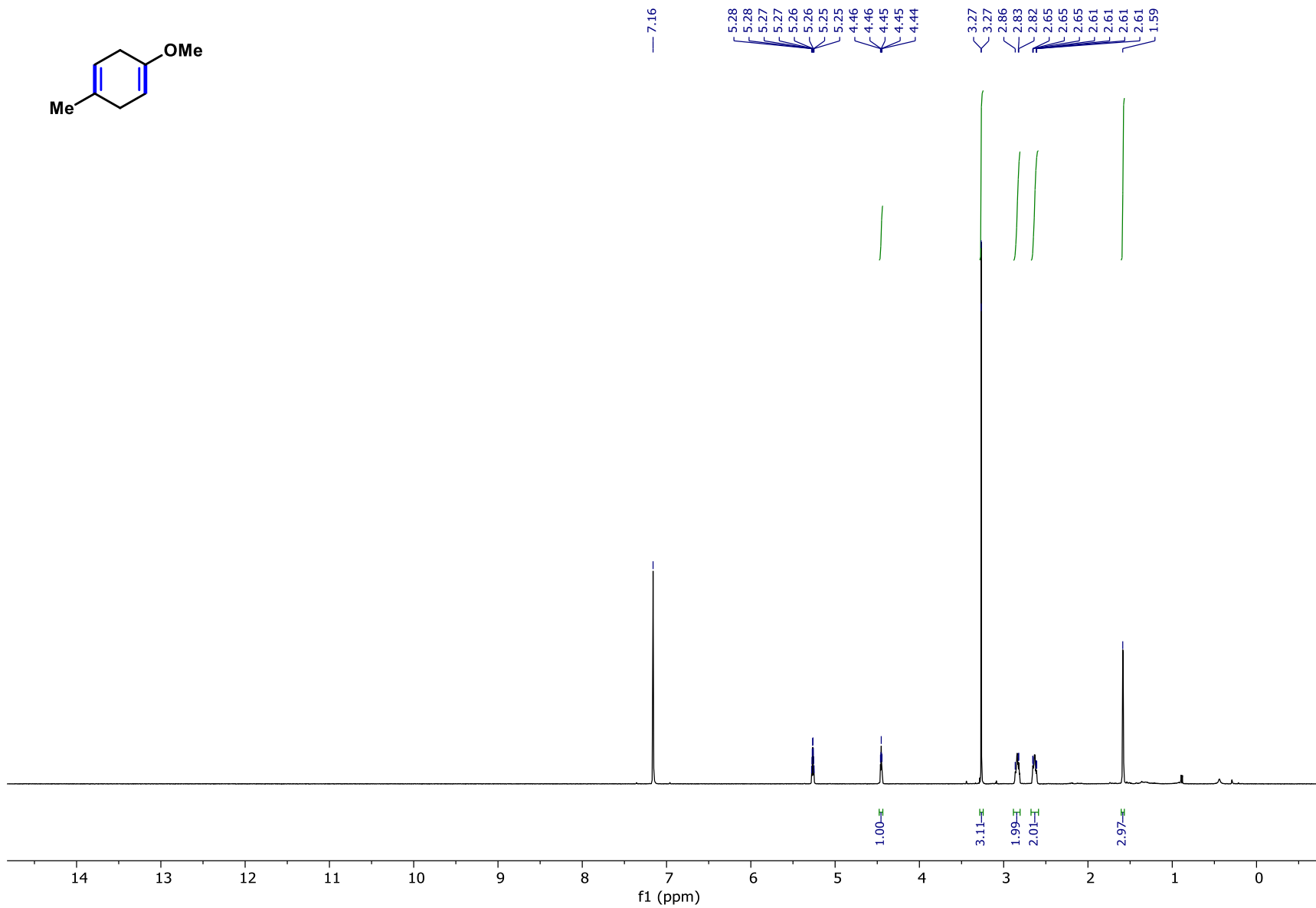
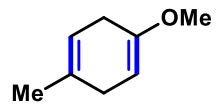
Compound SI-10 ¹H NMR



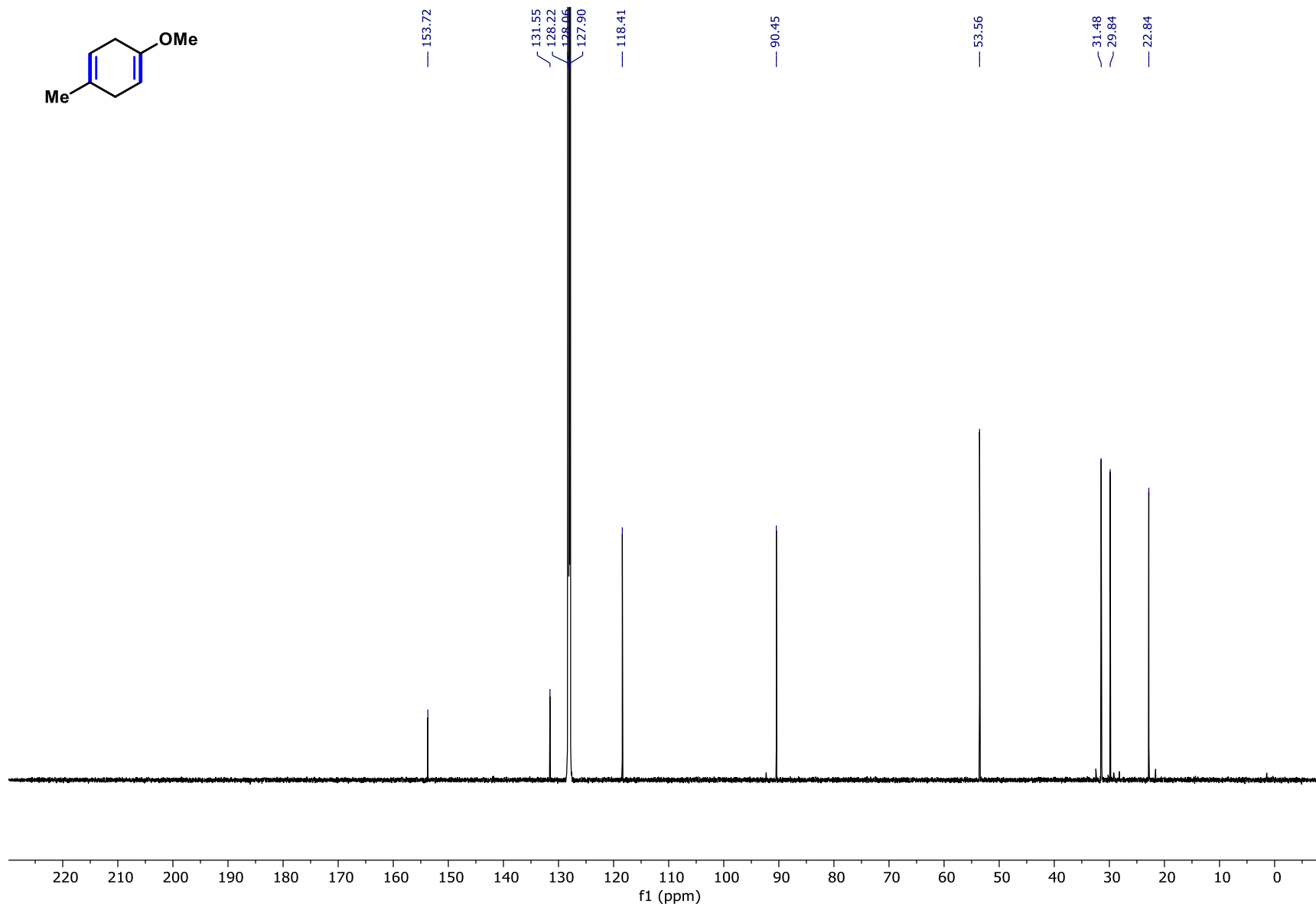
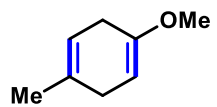
Compound SI-10 ¹³C NMR



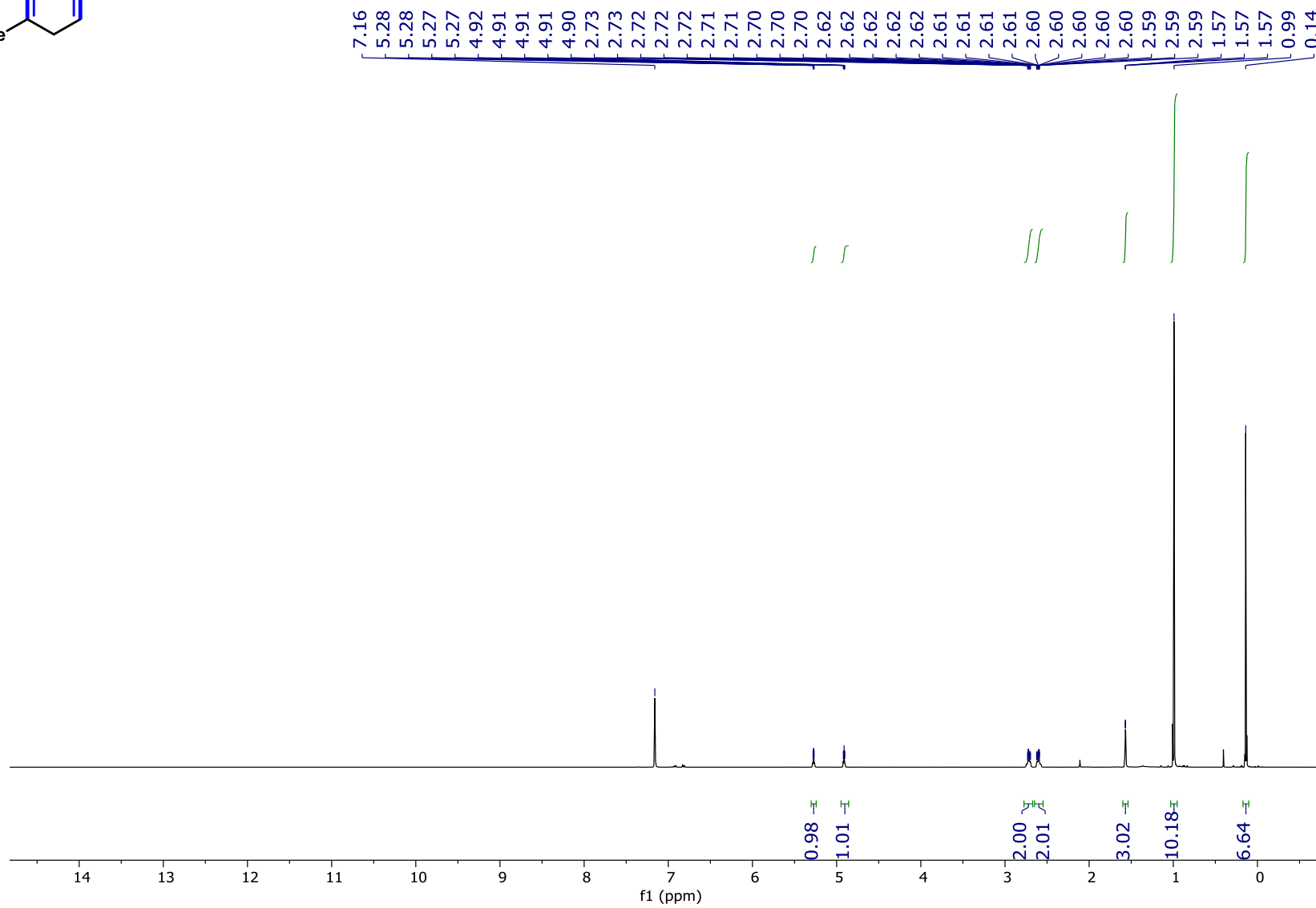
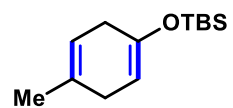
Compound SI-11 ¹H NMR



Compound SI-11 ¹³C NMR

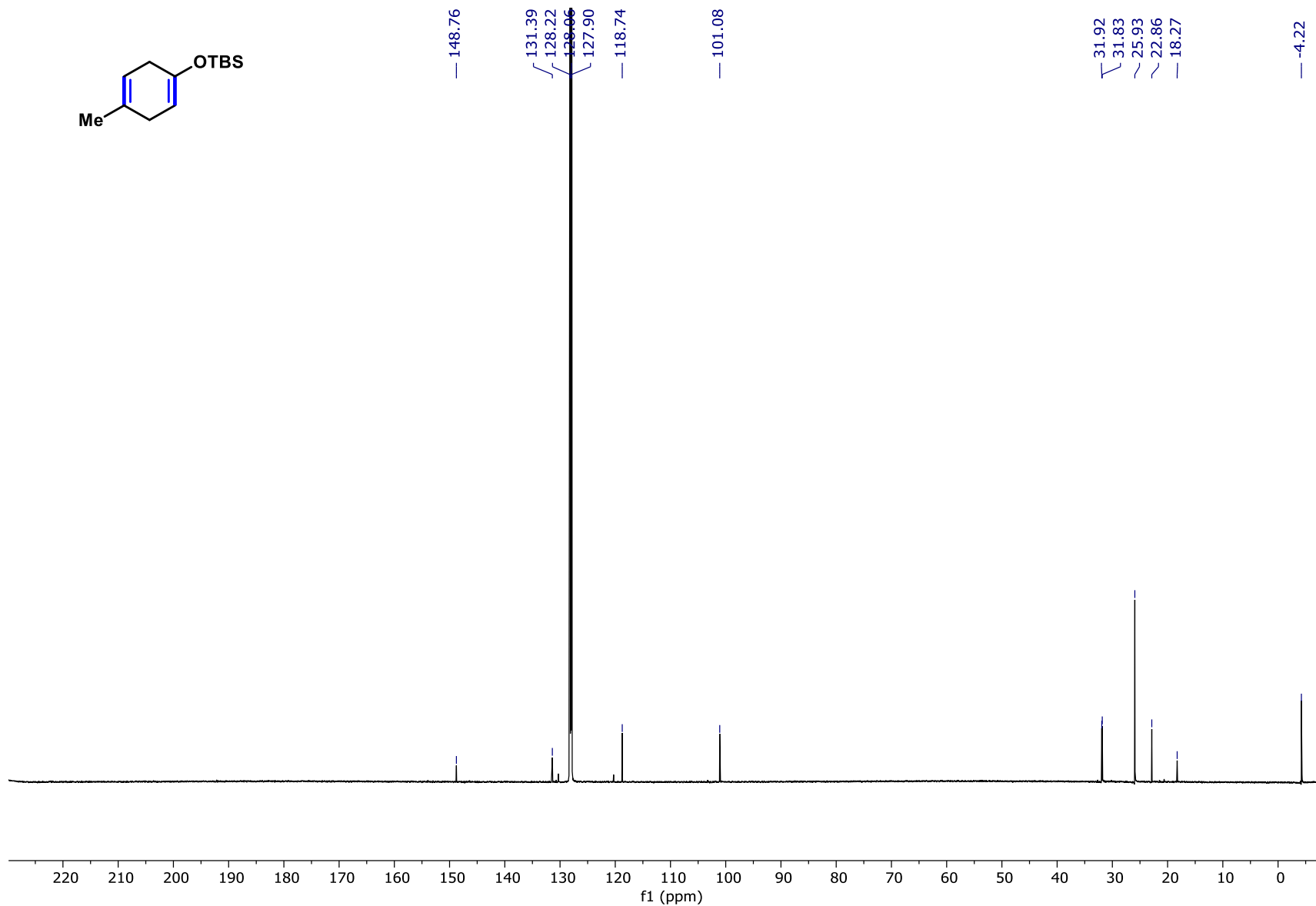
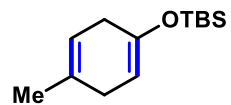


Compound SI-12 ¹H NMR

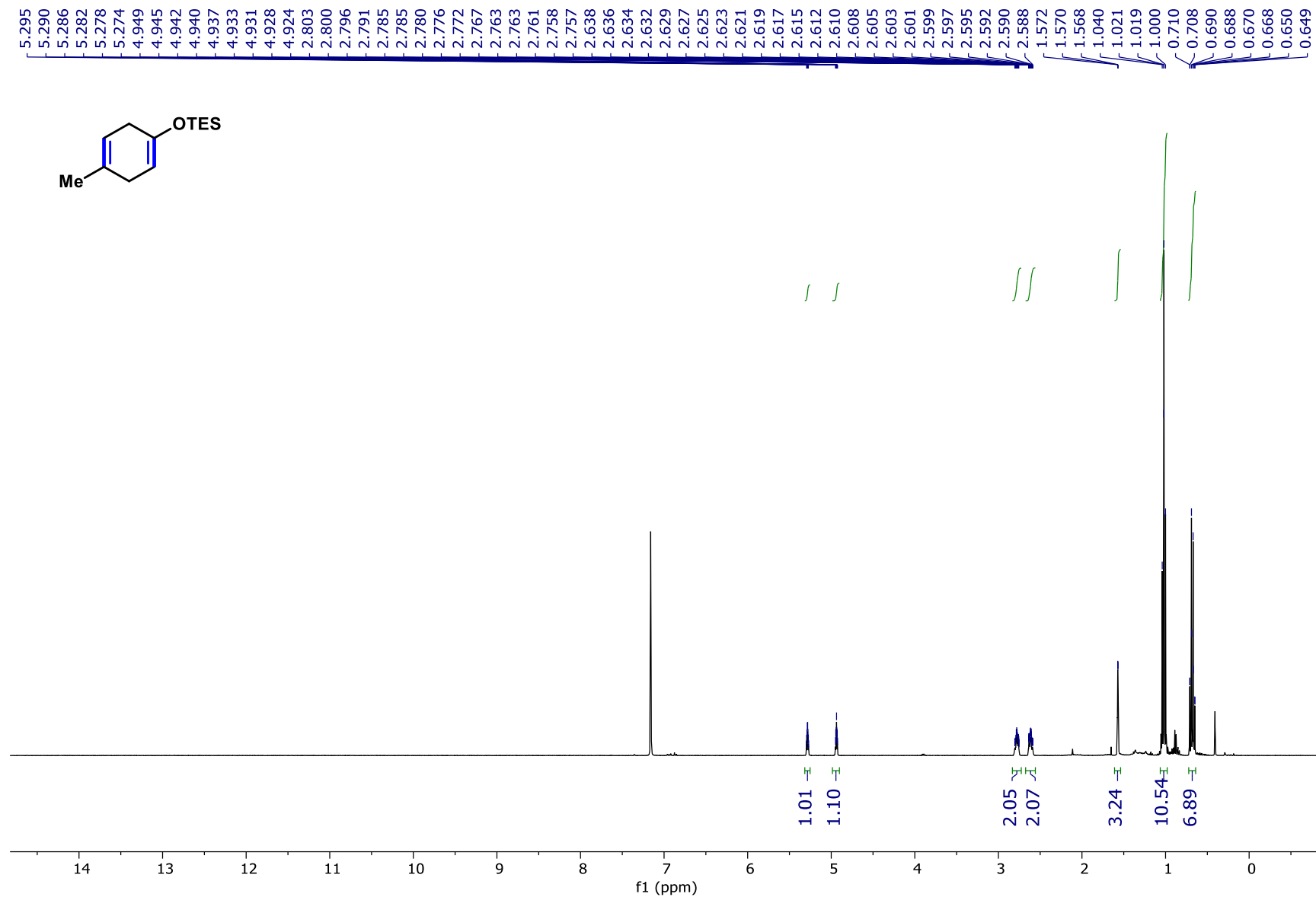


S131

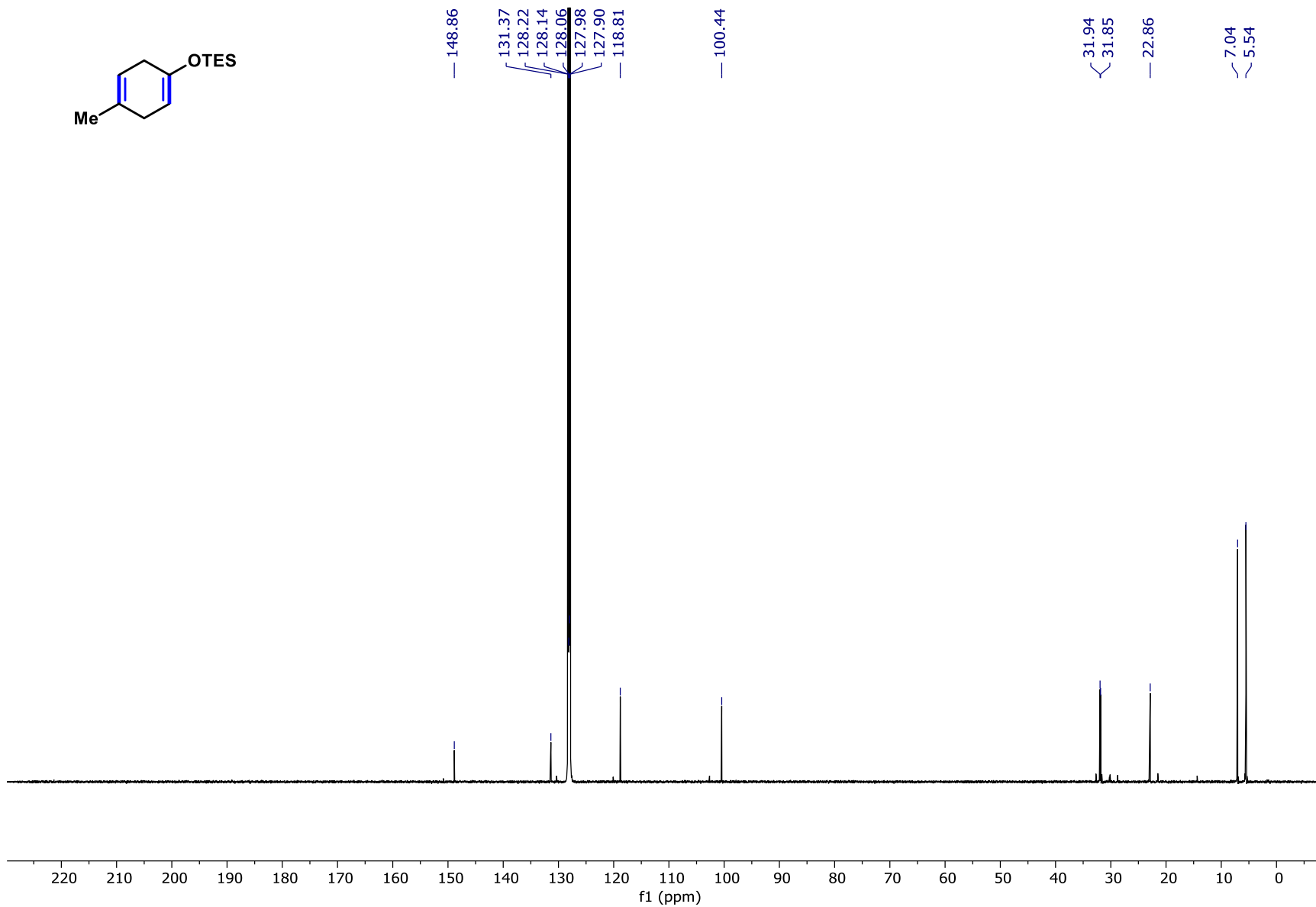
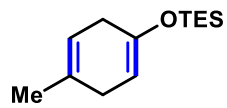
Compound SI-12 ¹³C NMR



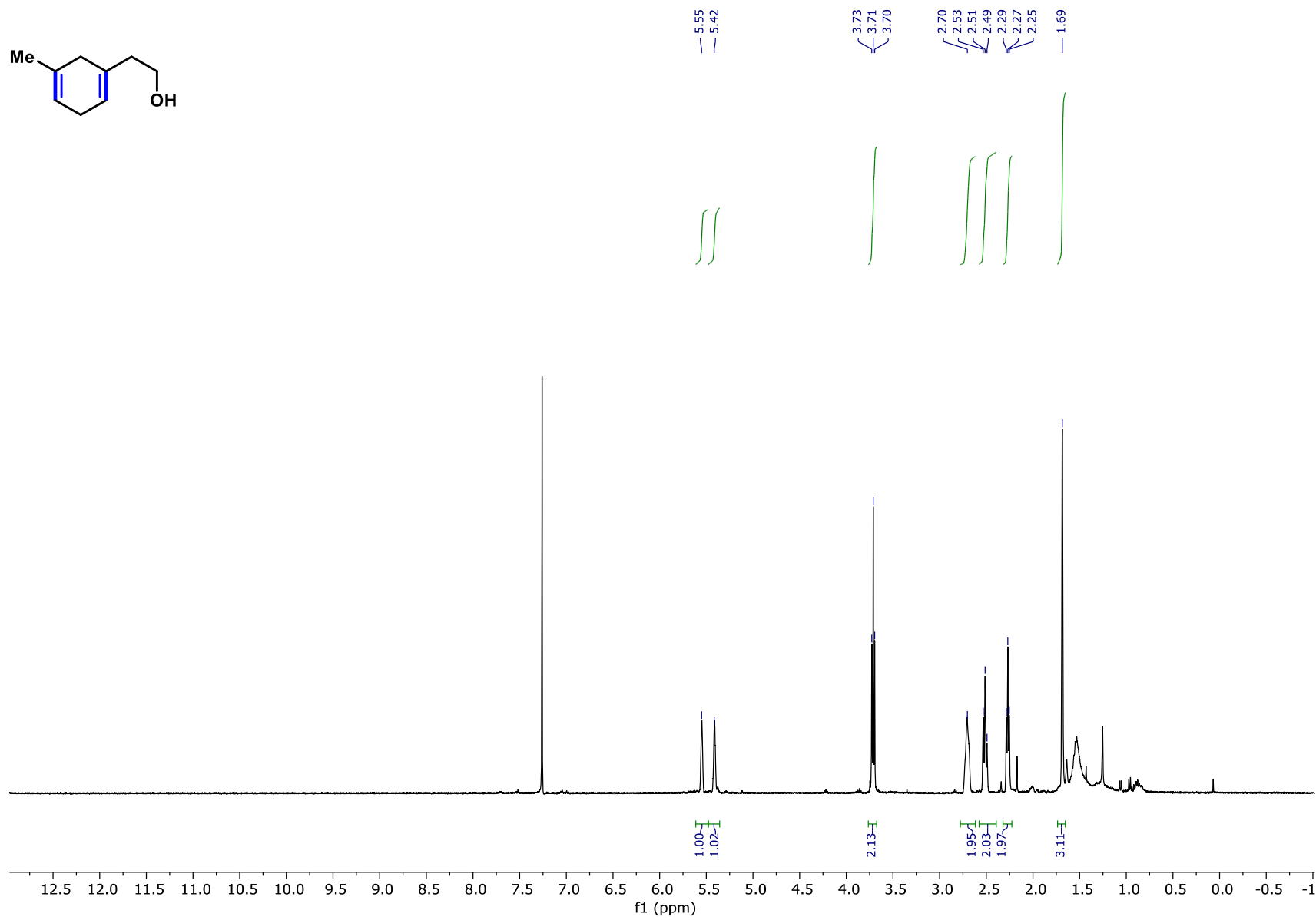
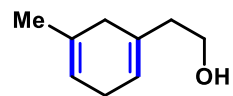
Compound SI-13 ¹H NMR



Compound SI-13 ¹³C NMR

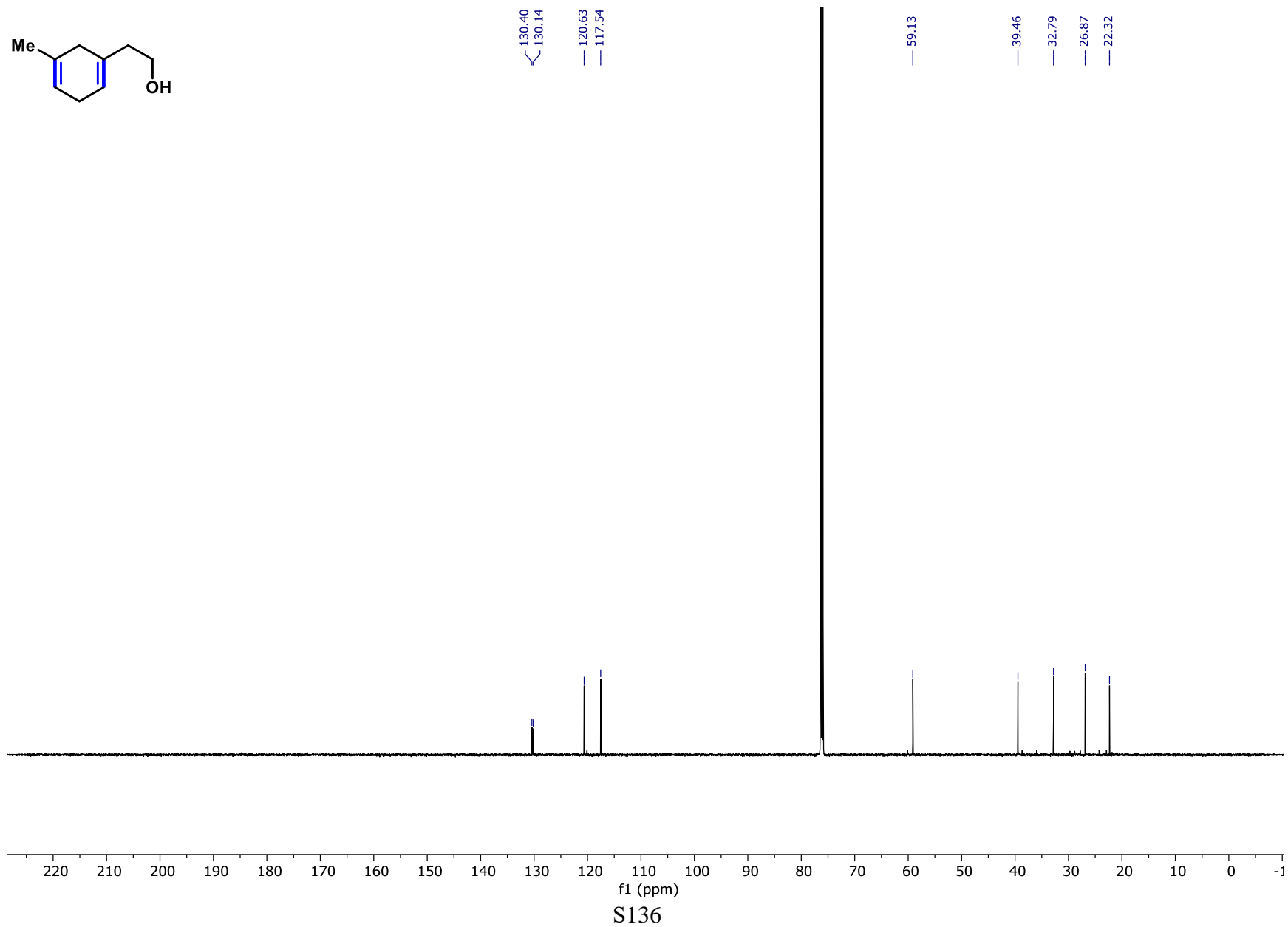
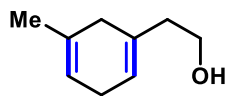


Compound SI-14 ¹H NMR

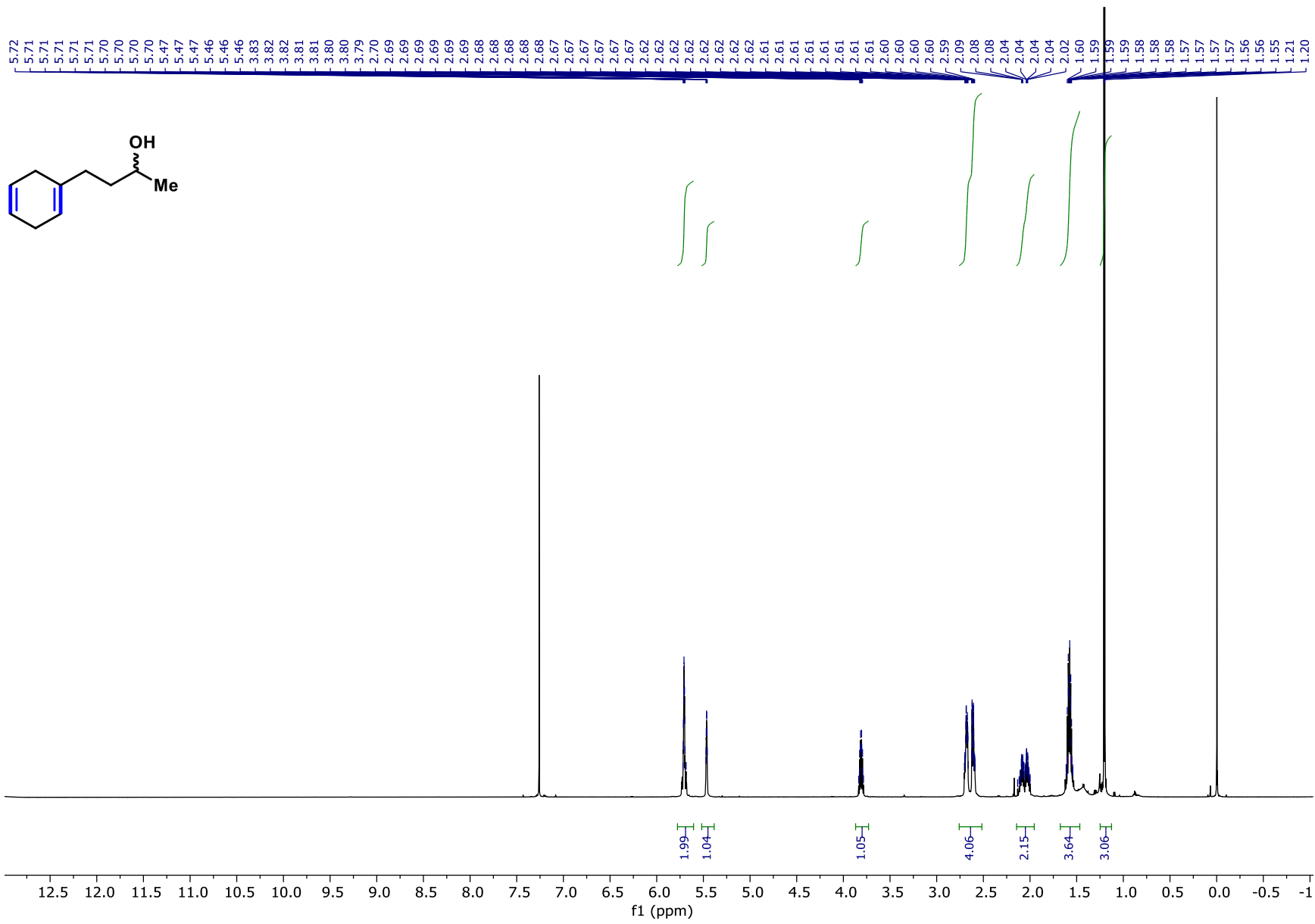


S135

Compound SI-14 ¹³C NMR

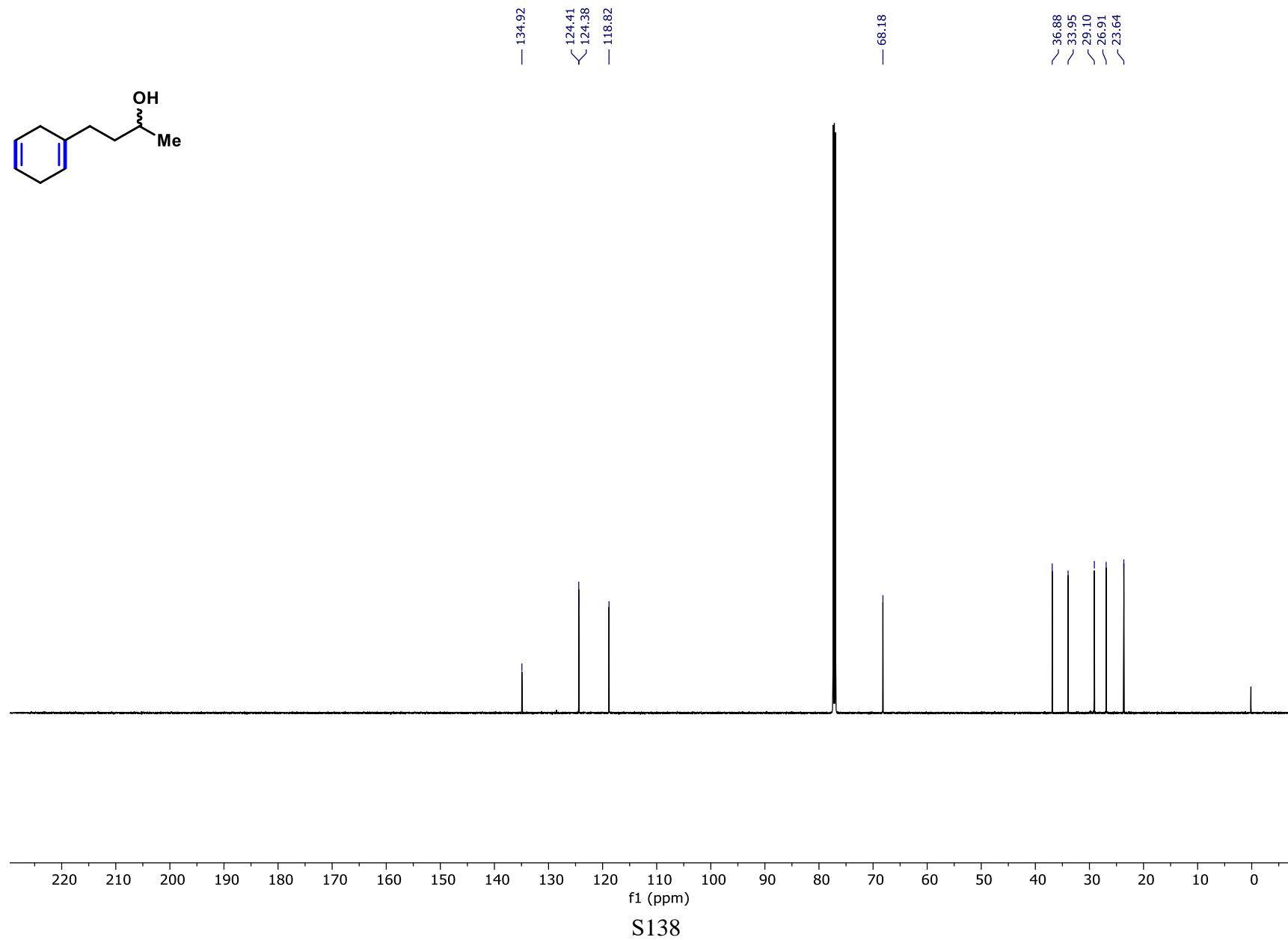
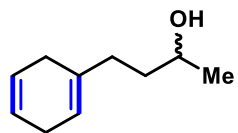


Compound SI-15 ¹H NMR

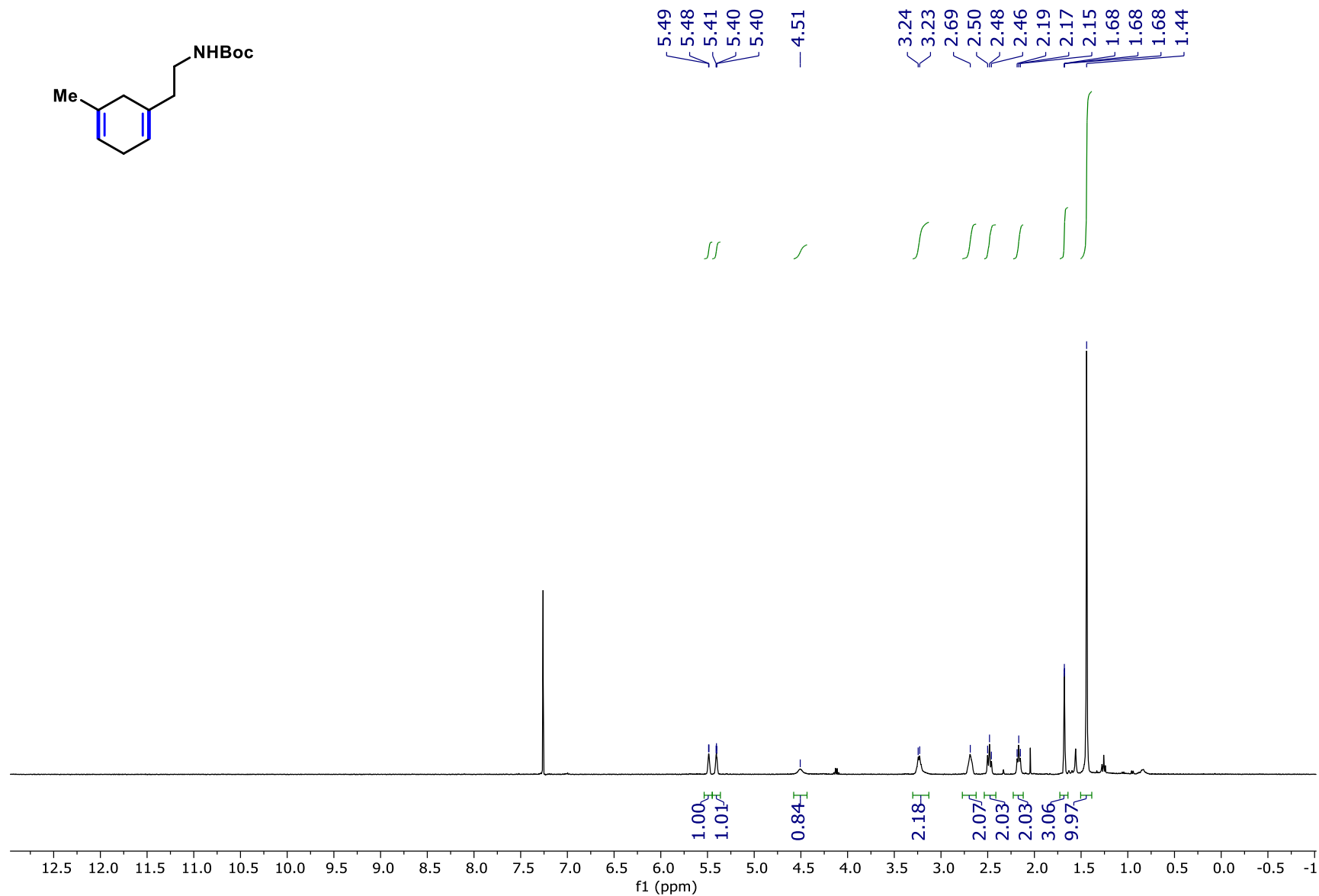
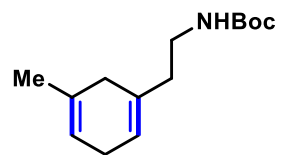


S137

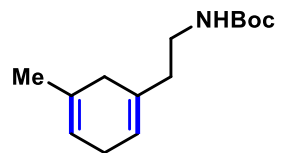
Compound SI-15 ¹³C NMR



Compound SI-16 ¹H NMR



Compound SI-16 ¹³C NMR

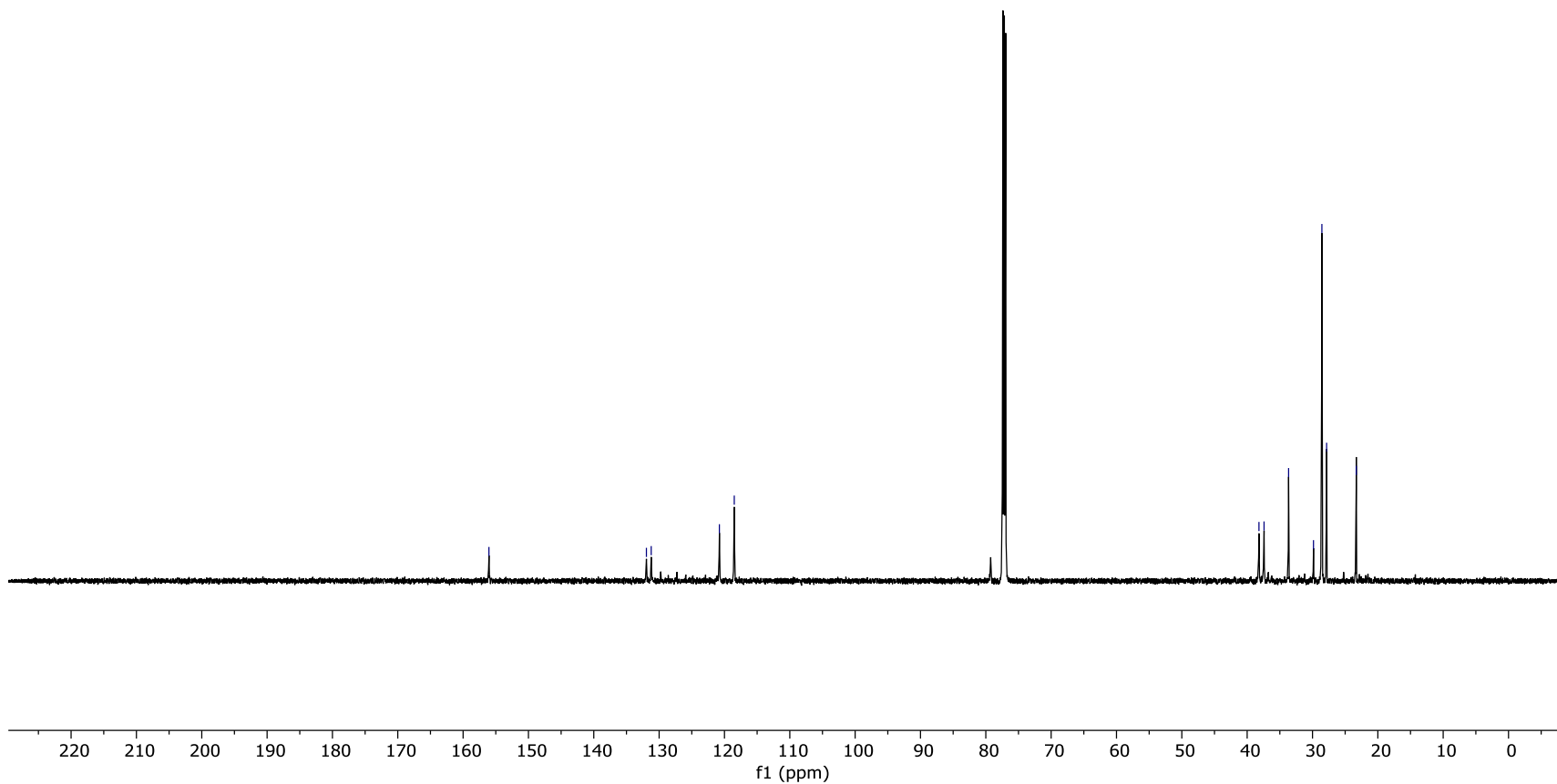


156.05

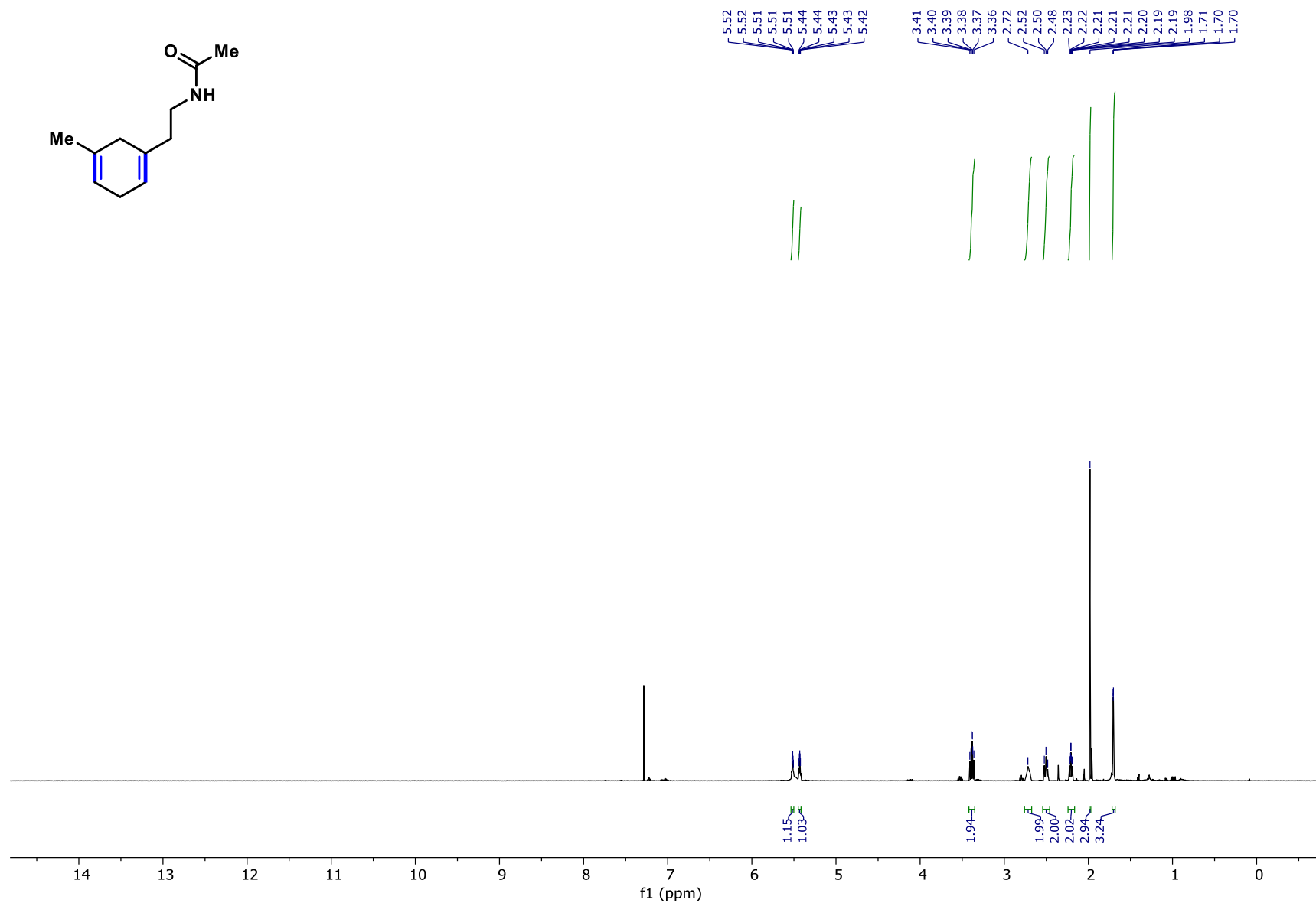
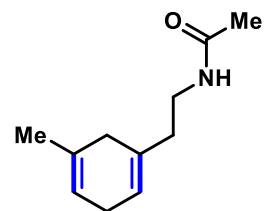
131.95
131.21

120.78
118.50

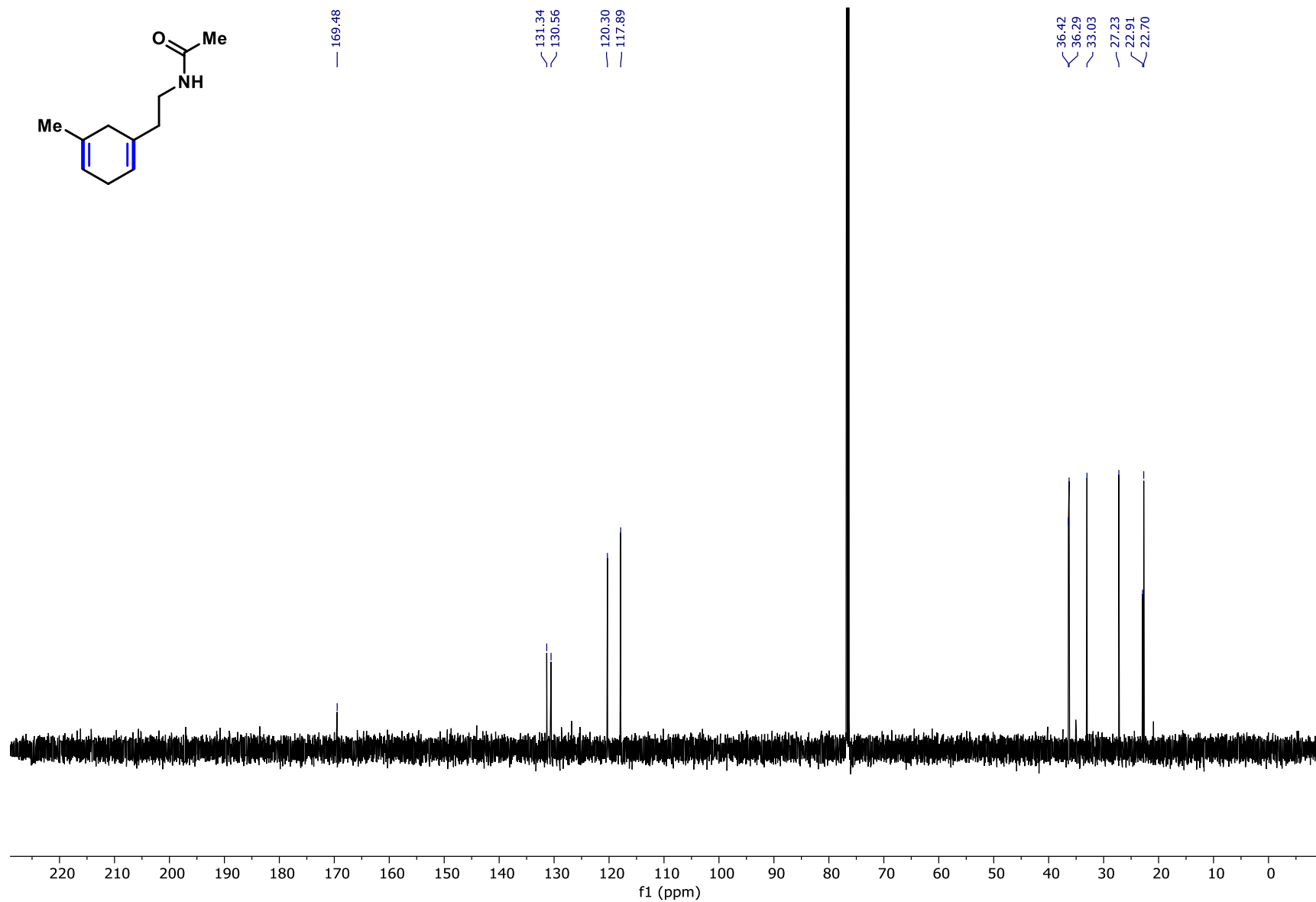
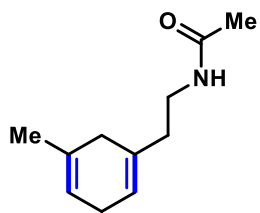
38.19
37.42
33.66
29.85
28.56
27.84
23.31



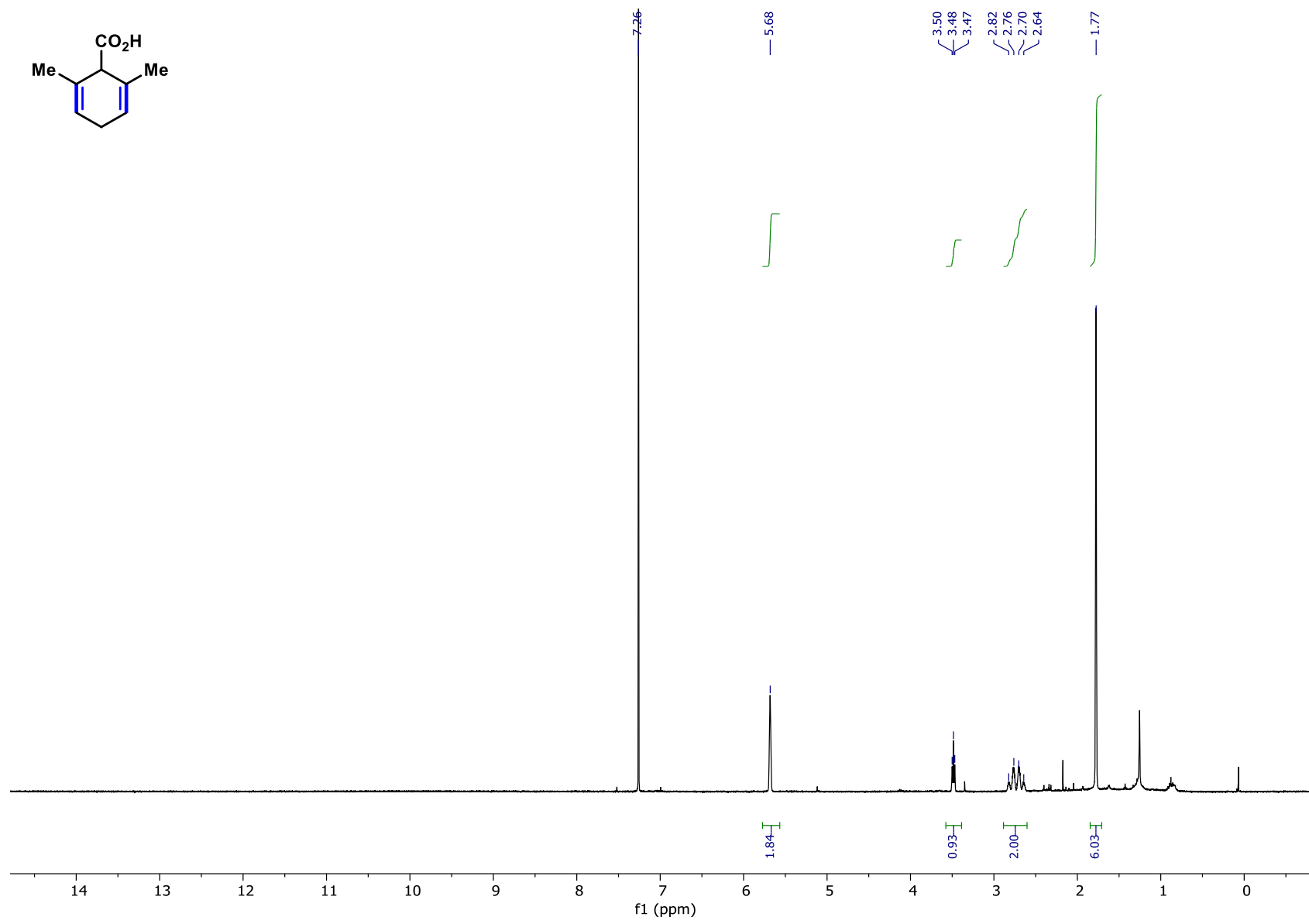
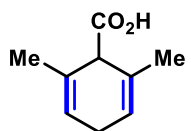
Compound SI-17 ¹H NMR



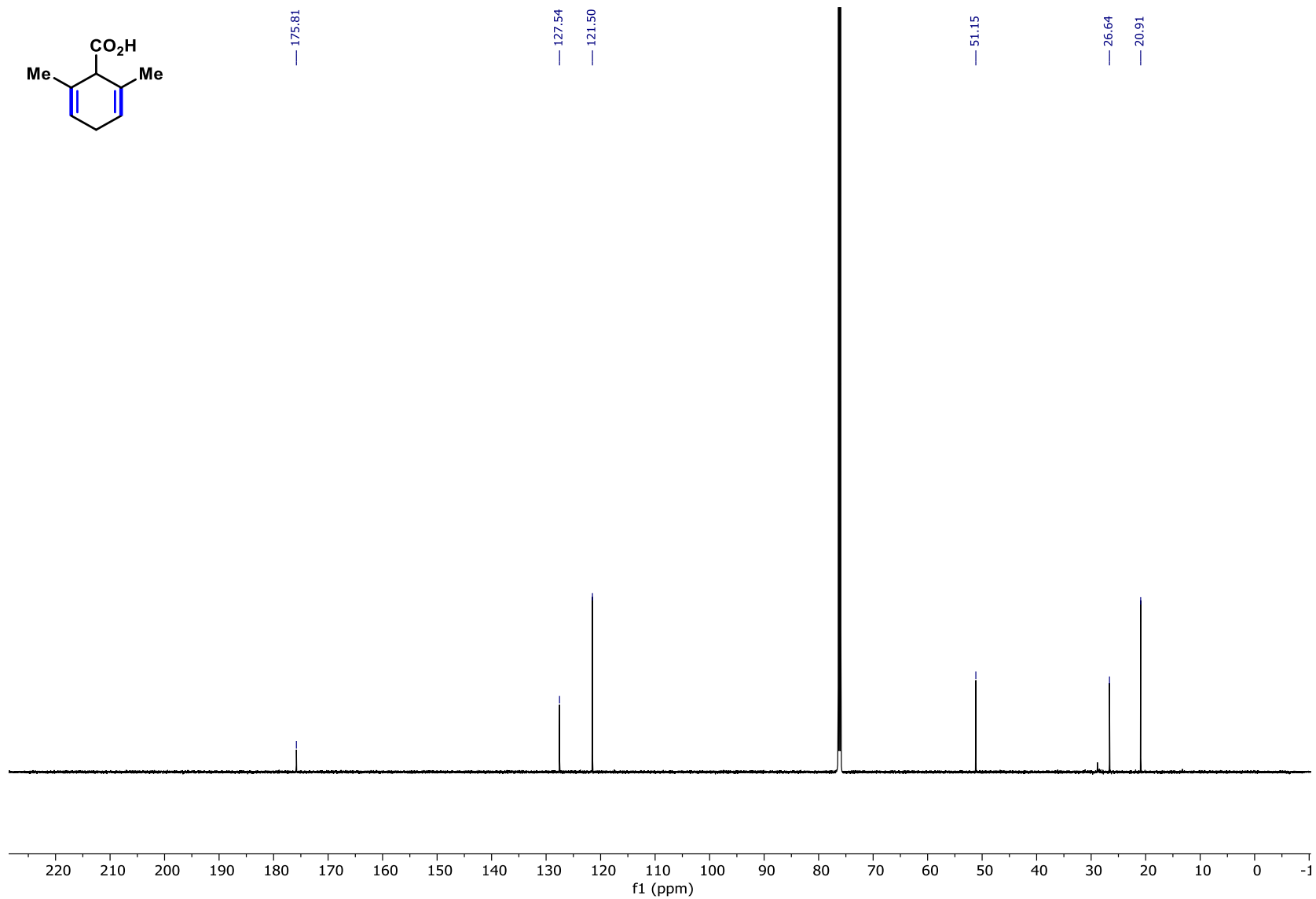
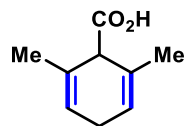
Compound SI-17 ¹³C NMR



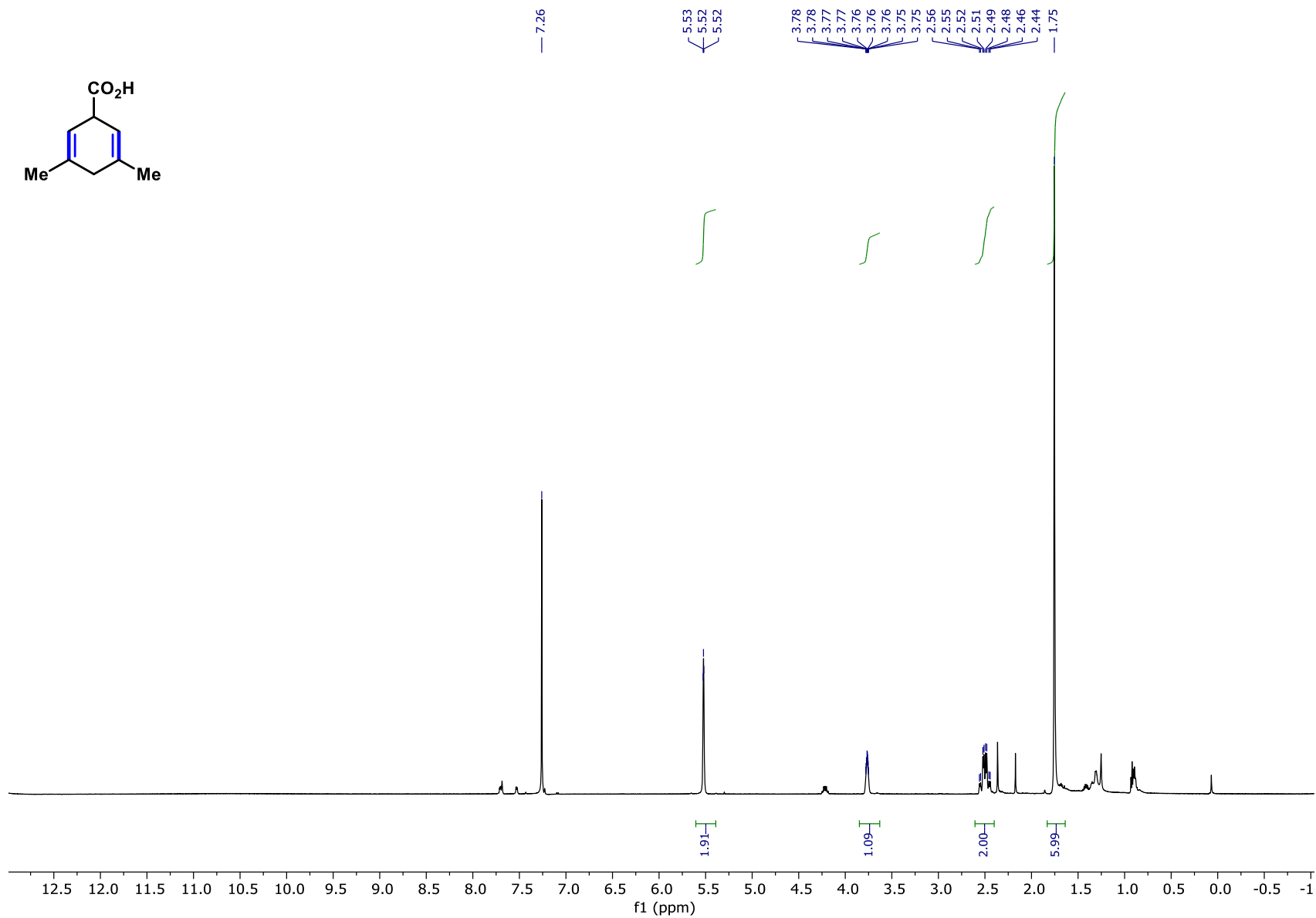
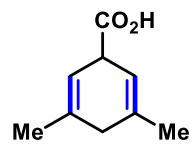
Compound SI-18 ¹H NMR



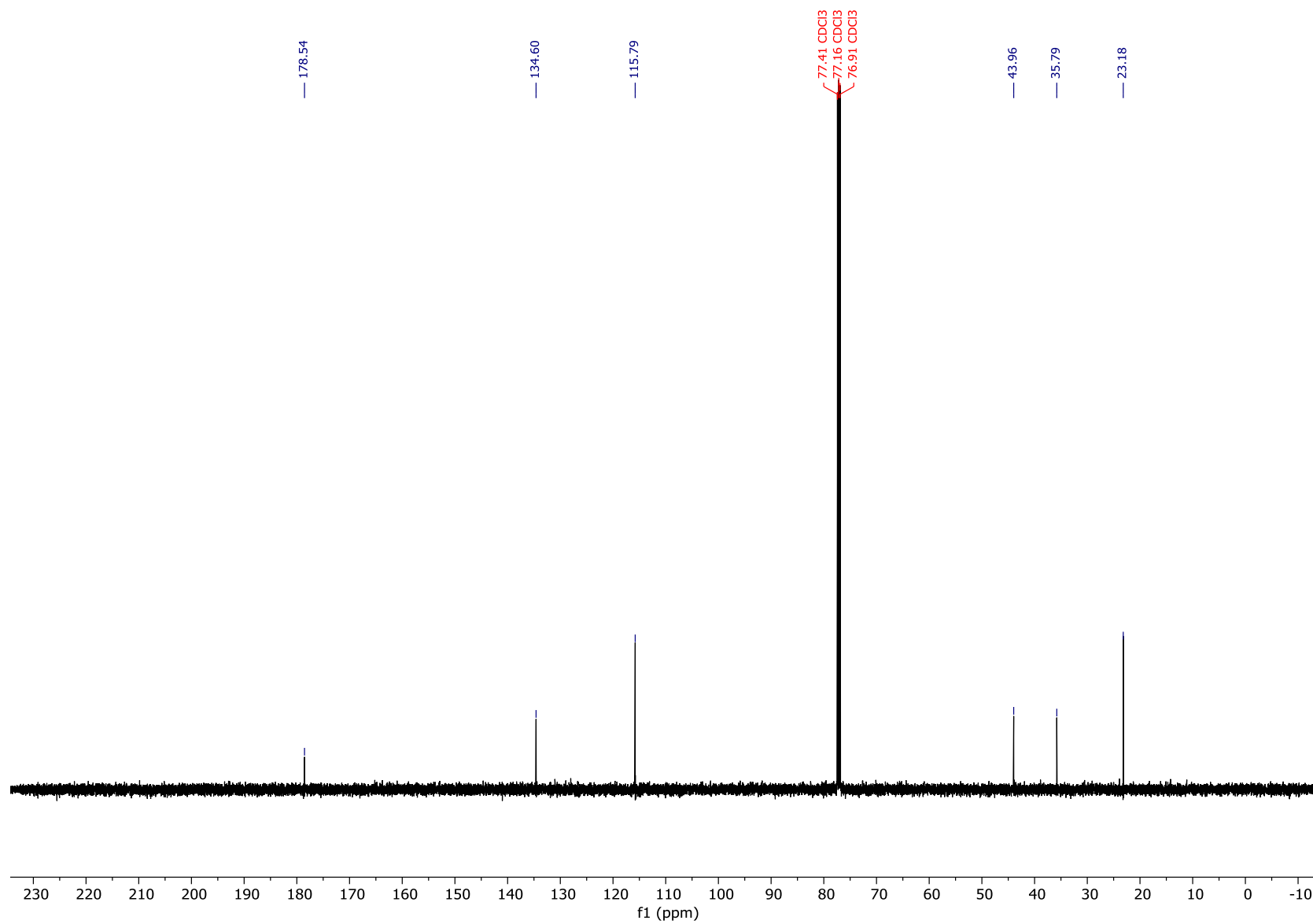
Compound SI-18 ¹³C NMR



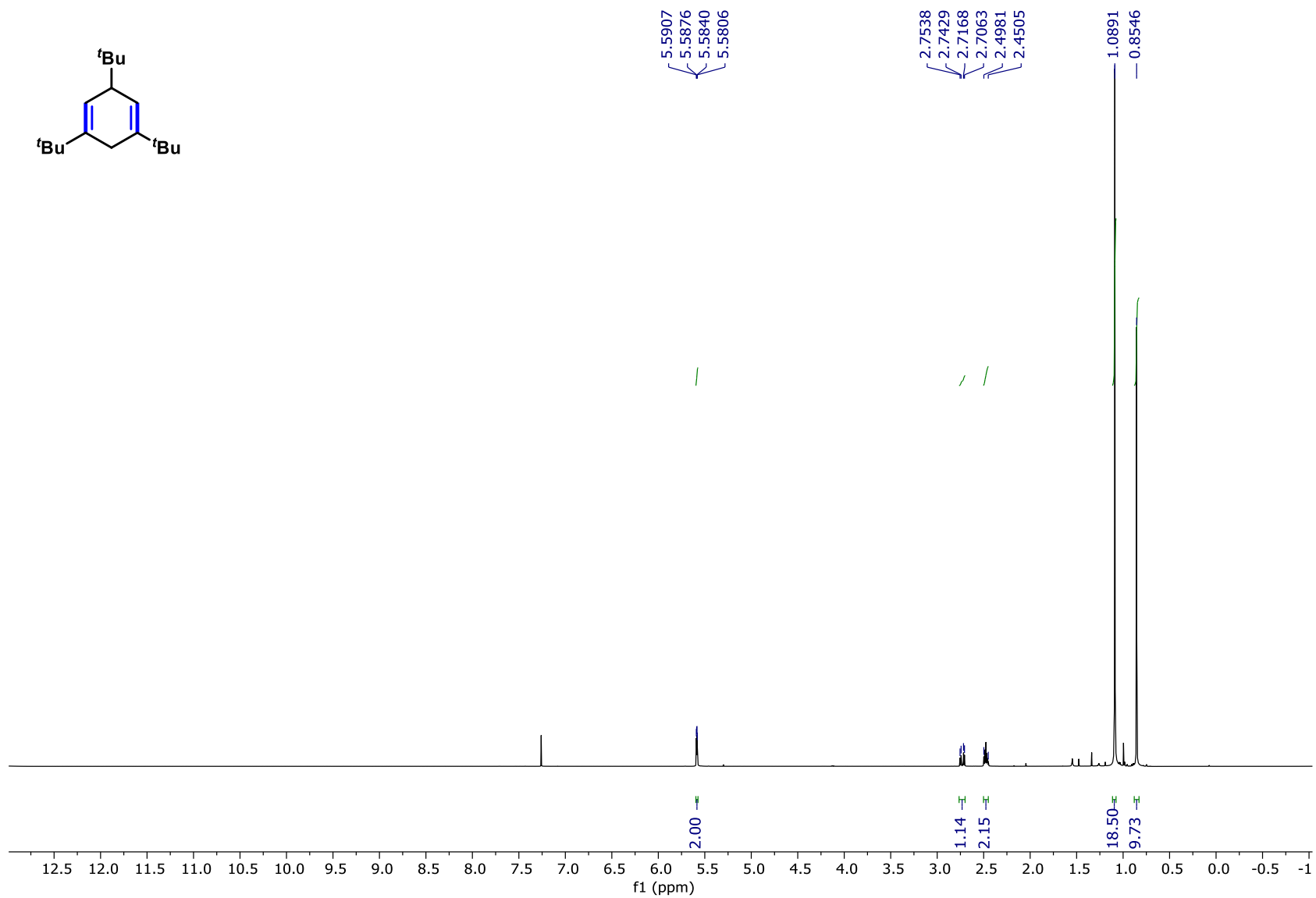
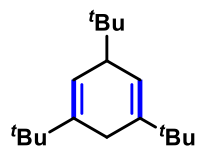
Compound SI-19 ¹H NMR



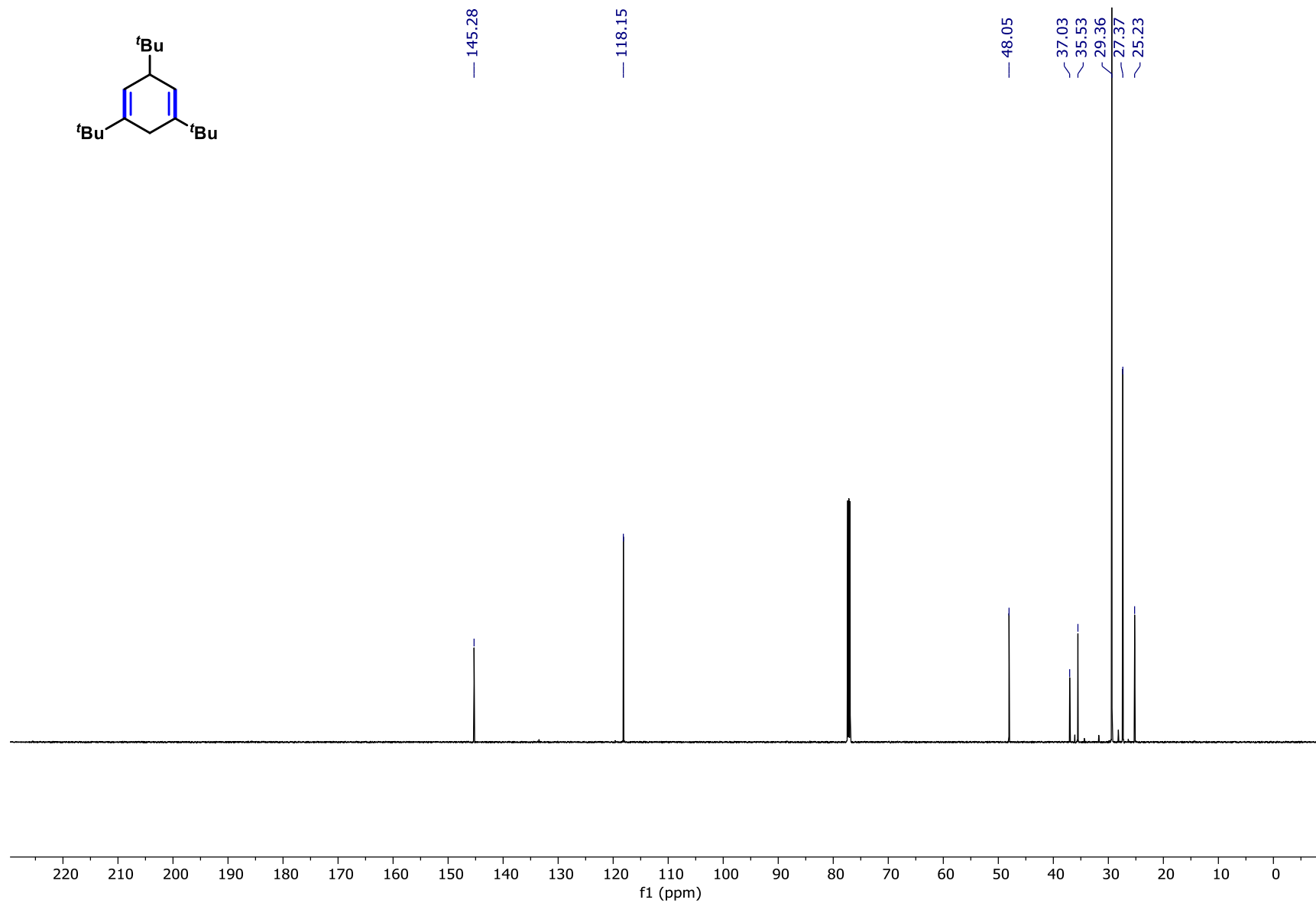
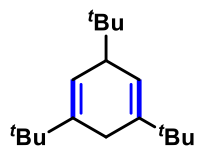
Compound SI-19 ¹³C NMR



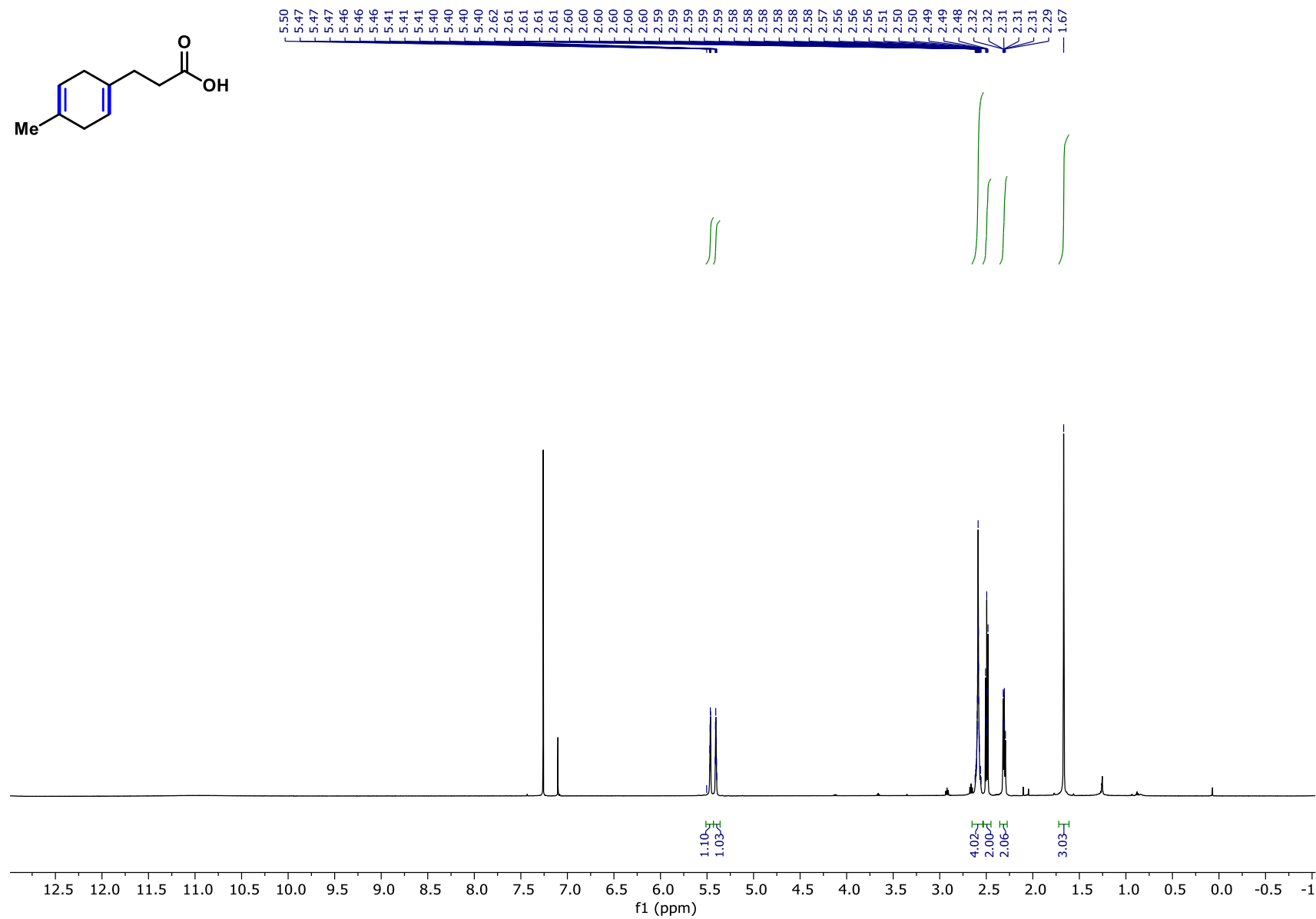
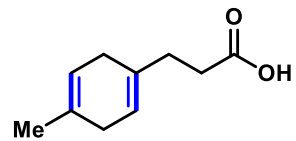
Compound SI-20 ¹H NMR



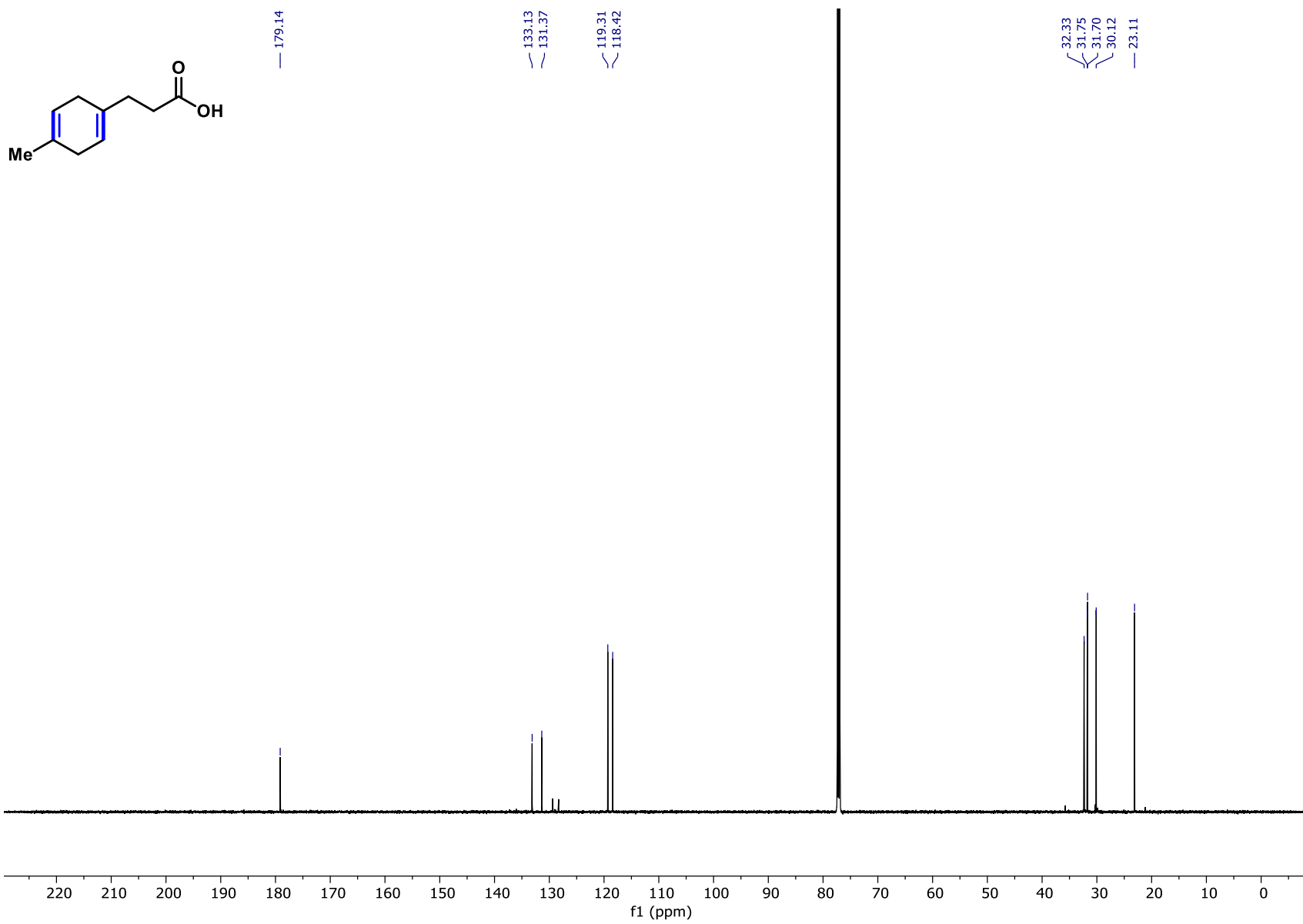
Compound SI-20 ¹³C NMR



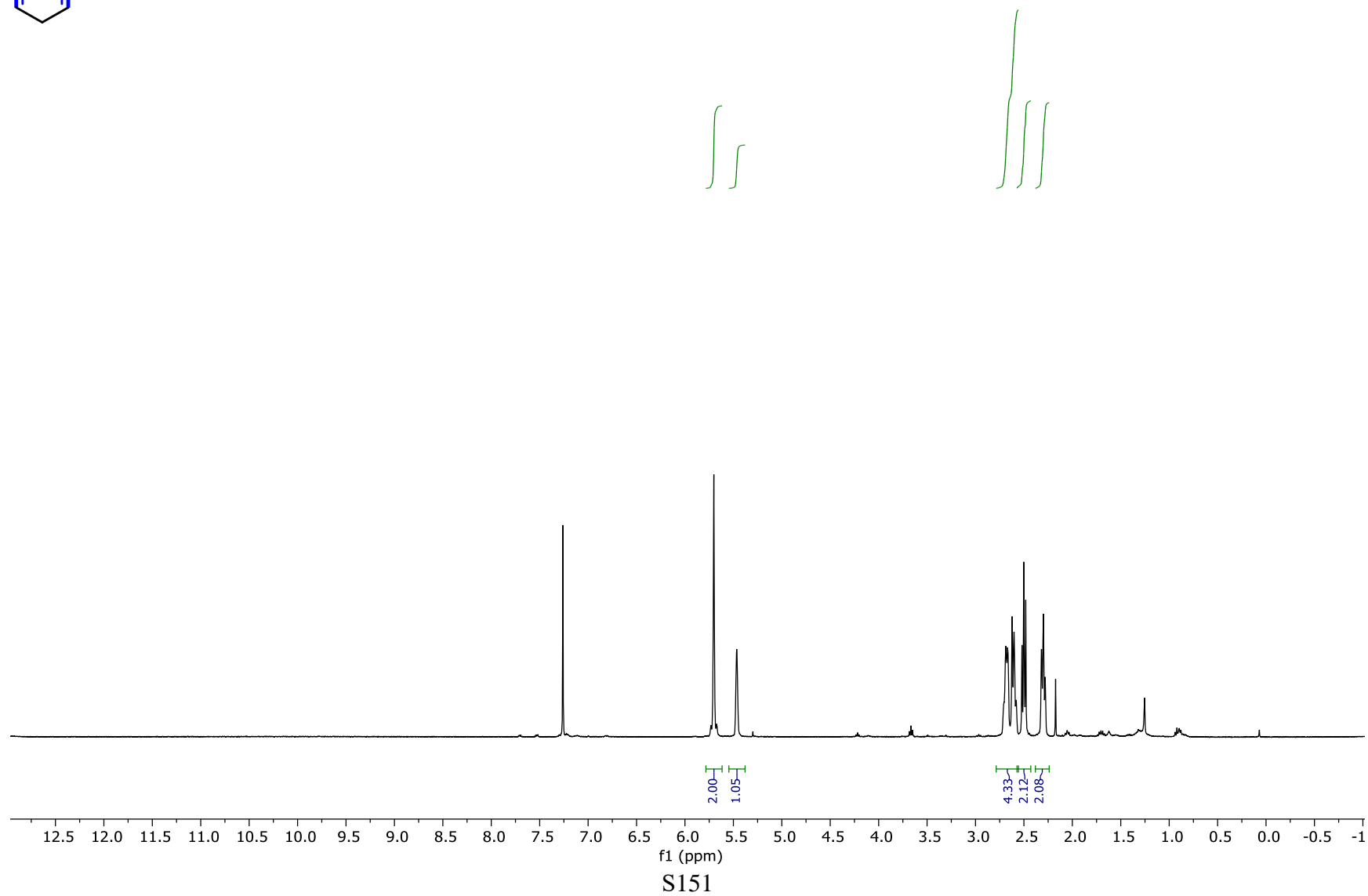
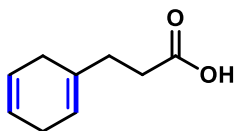
Compound SI-21 ¹H NMR



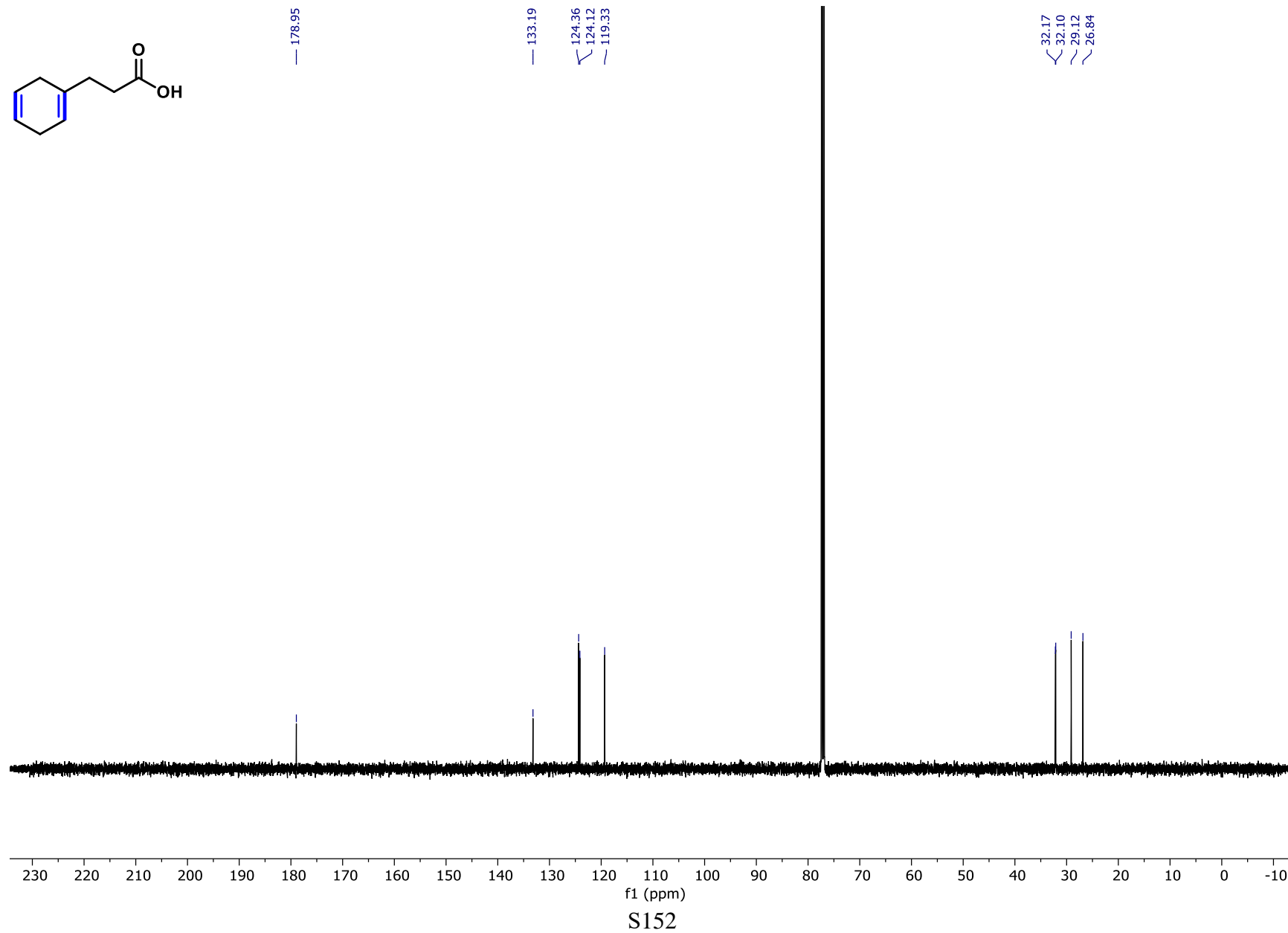
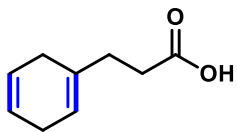
Compound SI-21 ¹³C NMR



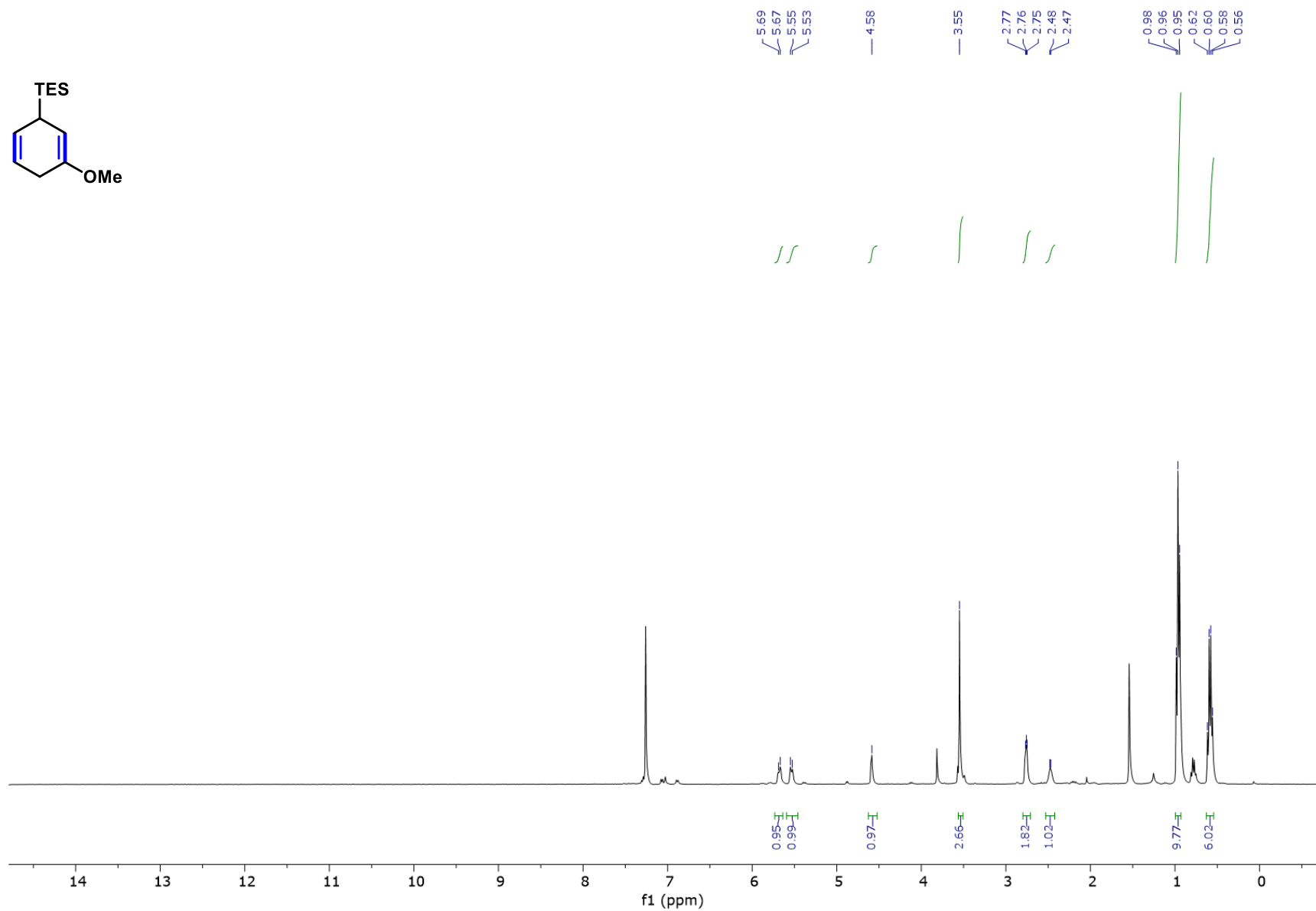
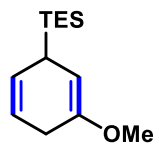
Compound SI-22 ¹H NMR



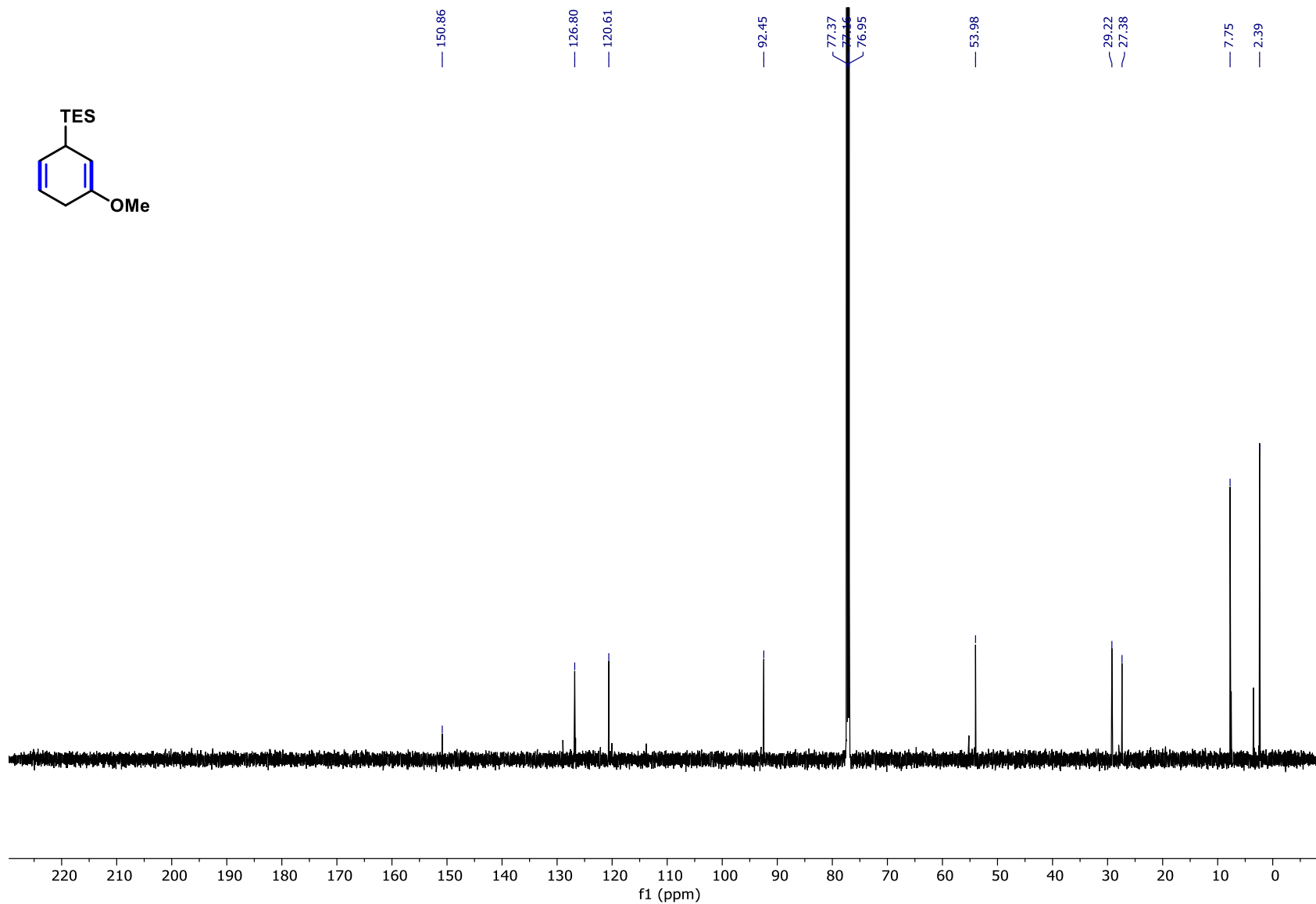
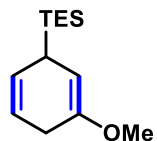
Compound SI-22 ¹³C NMR



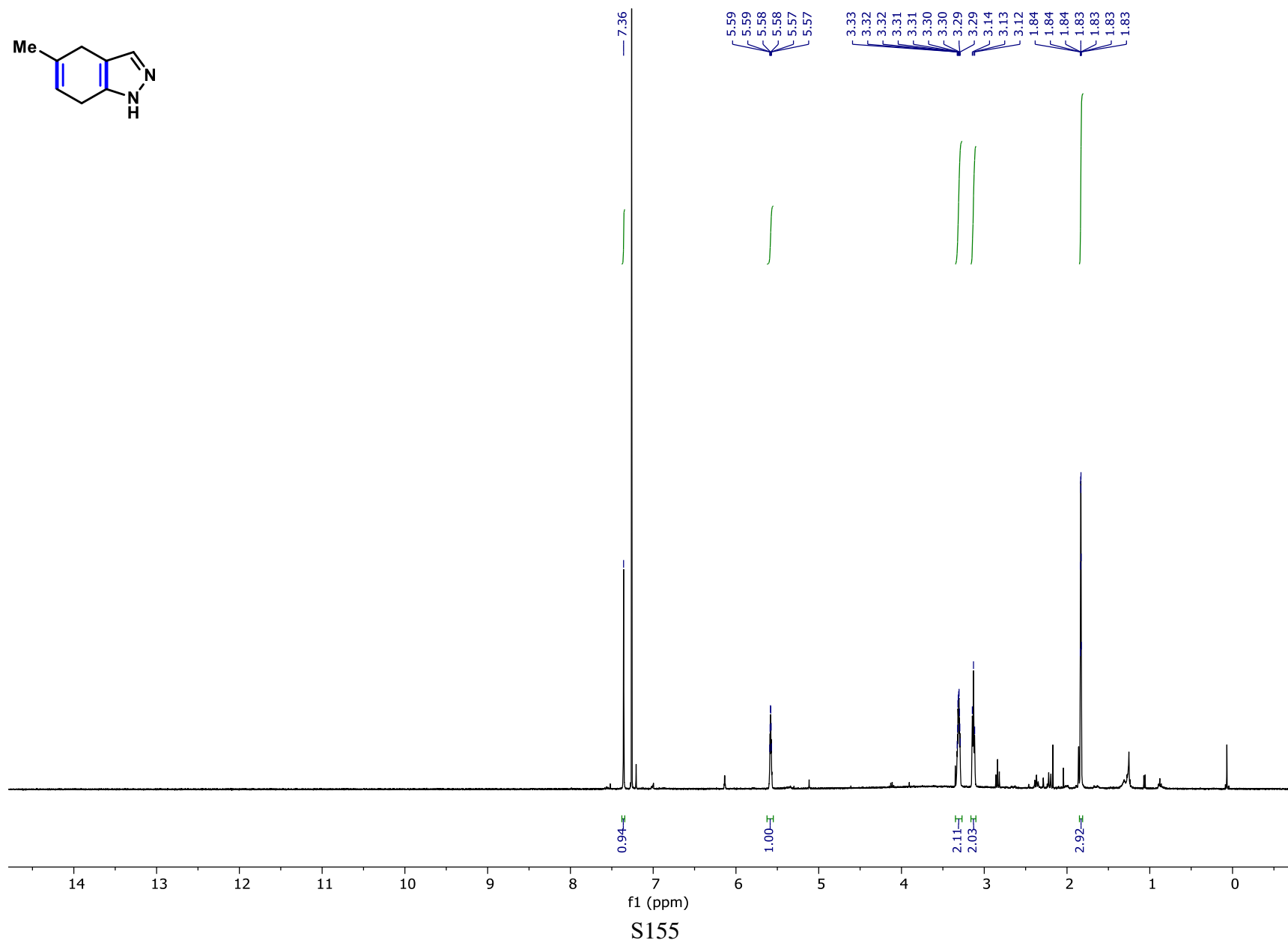
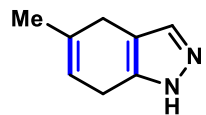
Compound SI-23 ¹H NMR



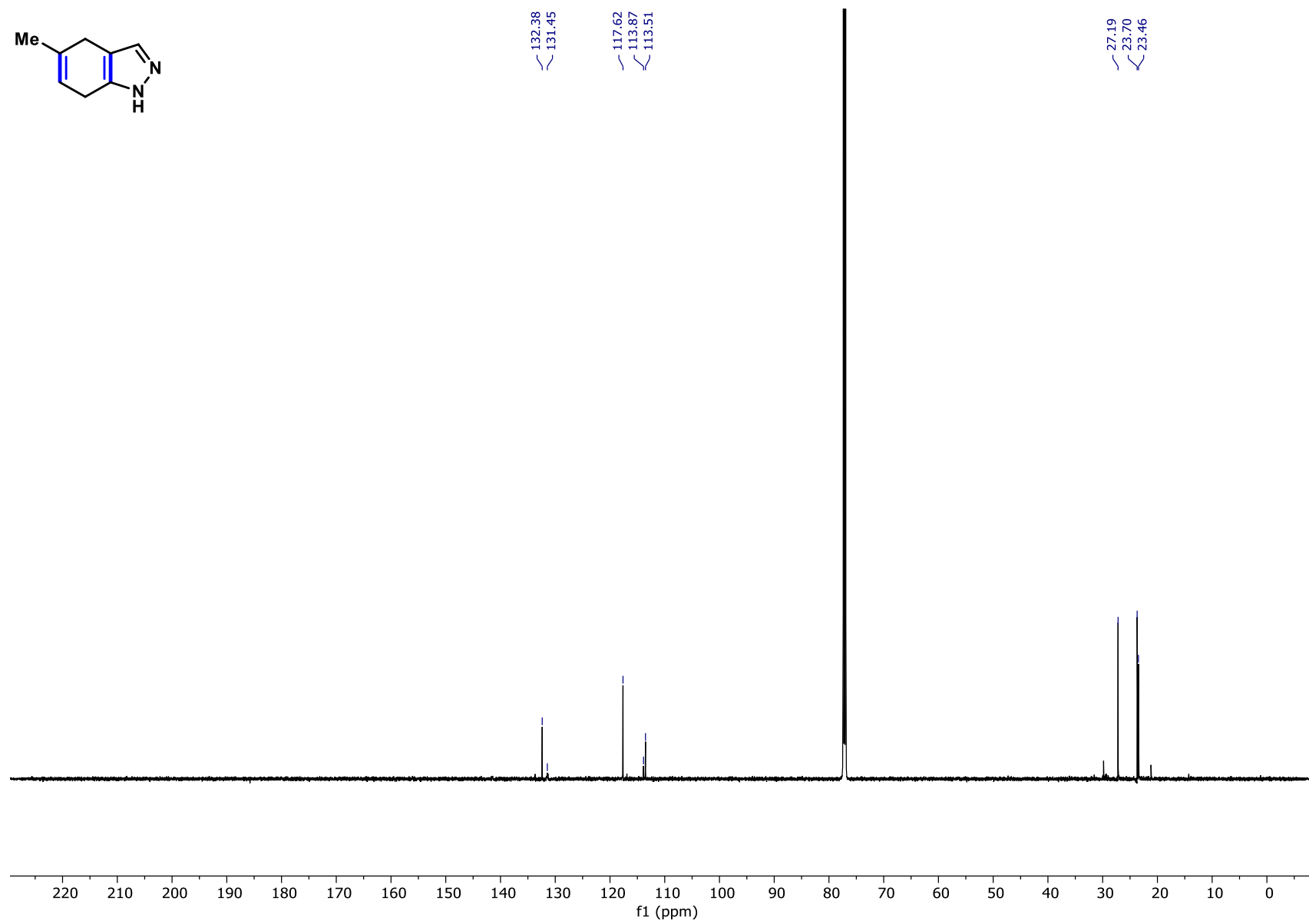
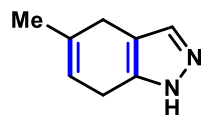
Compound SI-23 ¹³C NMR



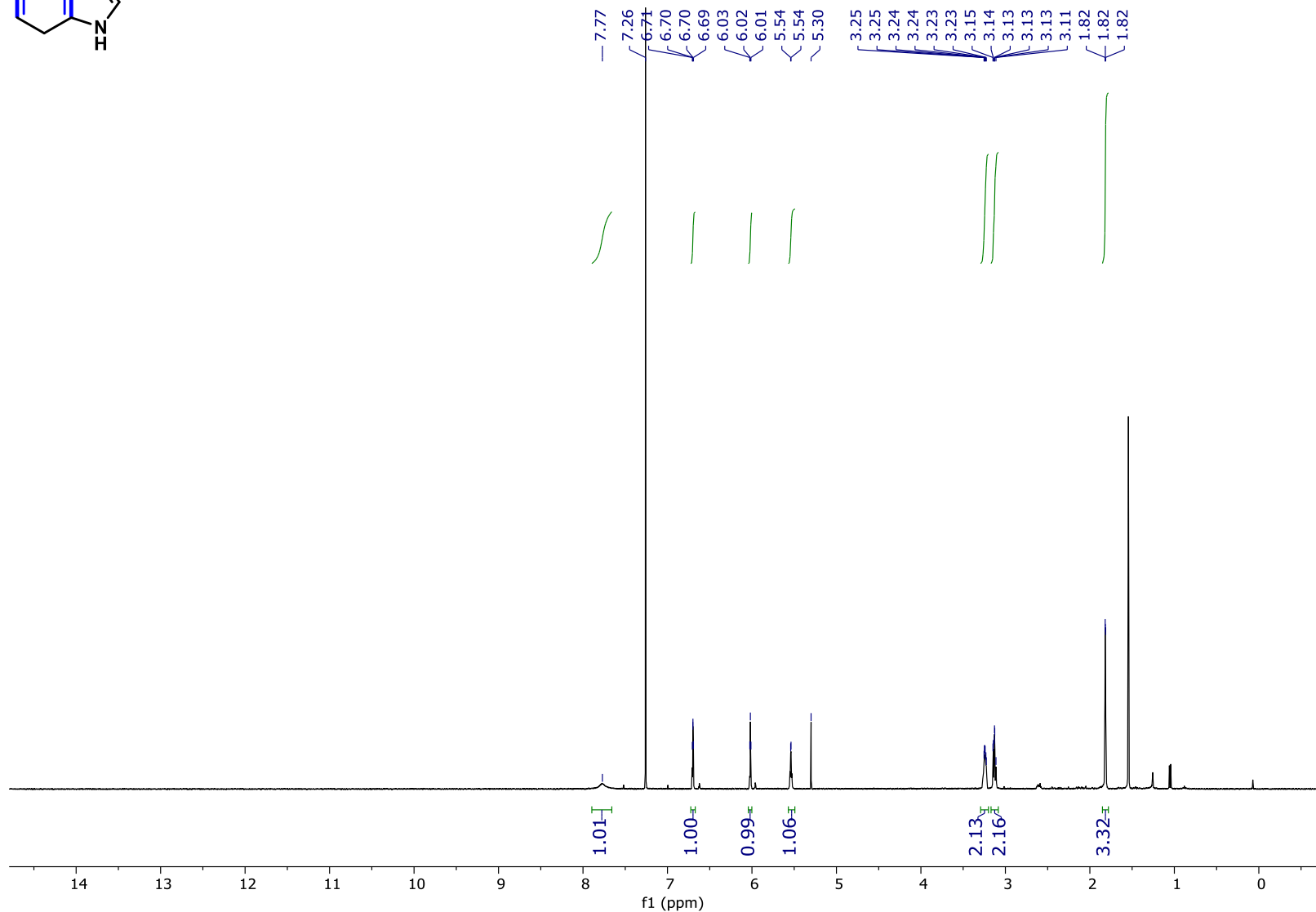
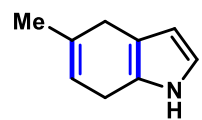
Compound SI-24 ¹H NMR



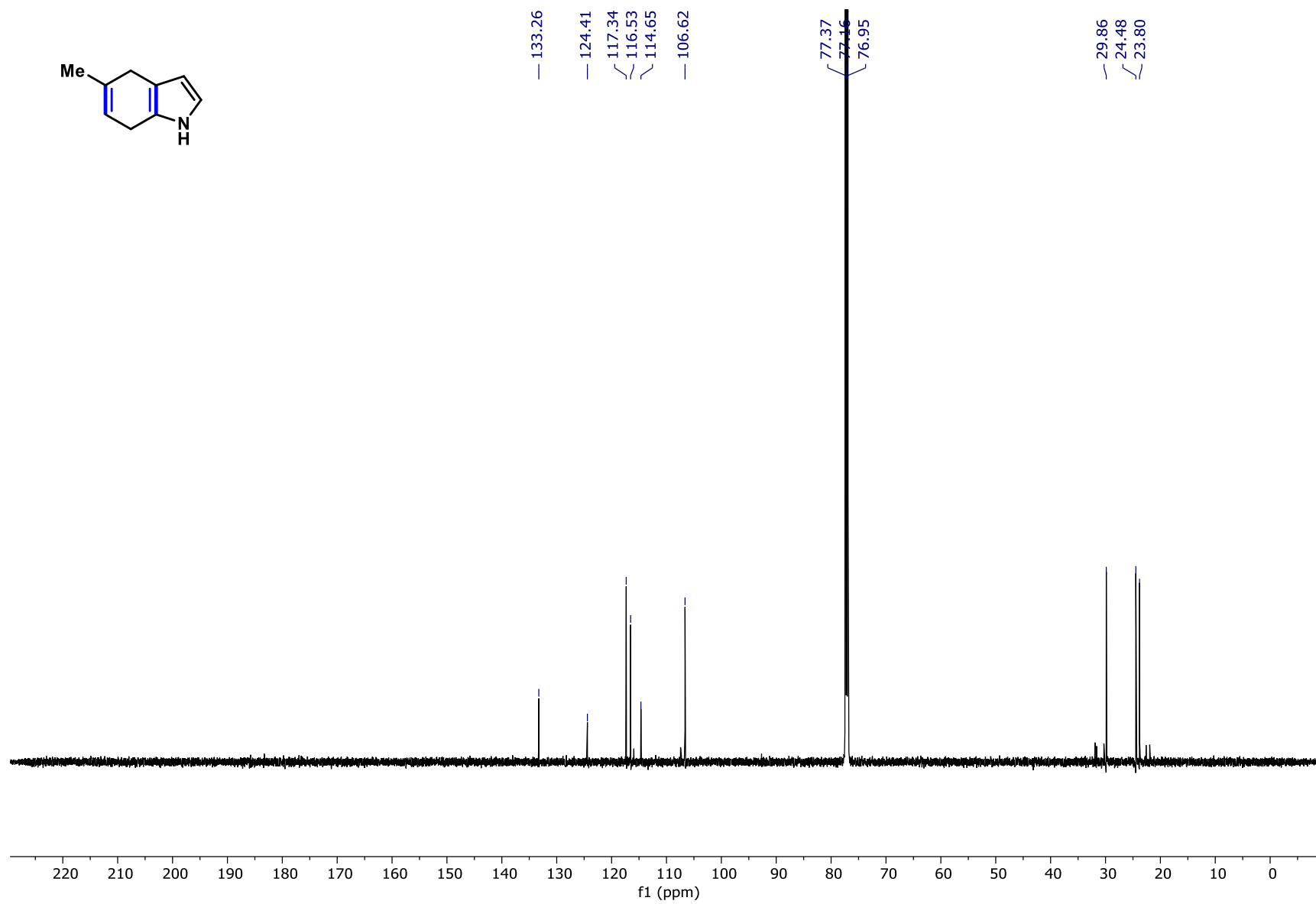
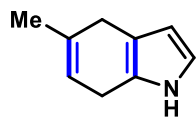
Compound SI-24 ¹³C NMR



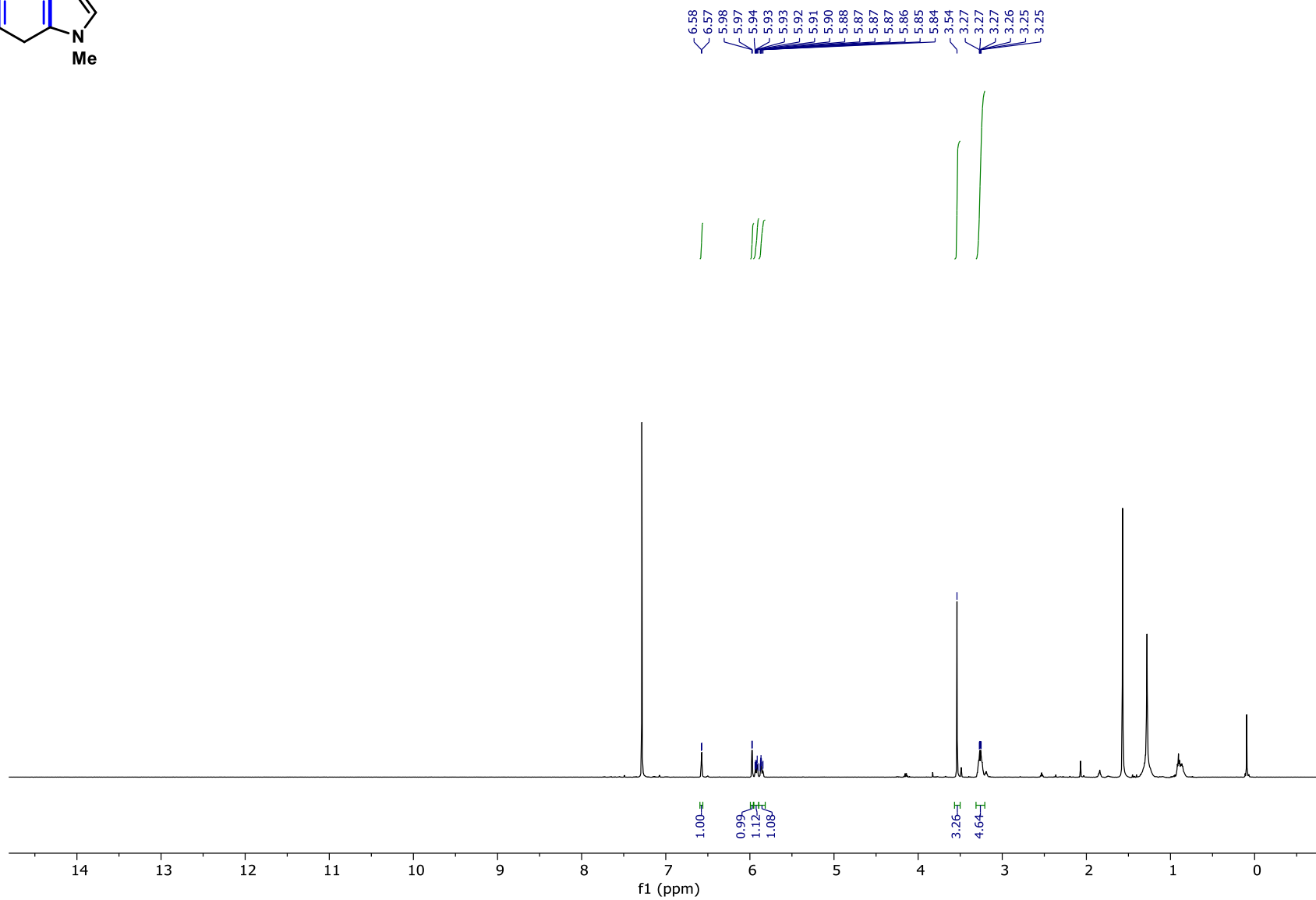
Compound SI-25 ¹H NMR



Compound SI-25 ¹³C NMR

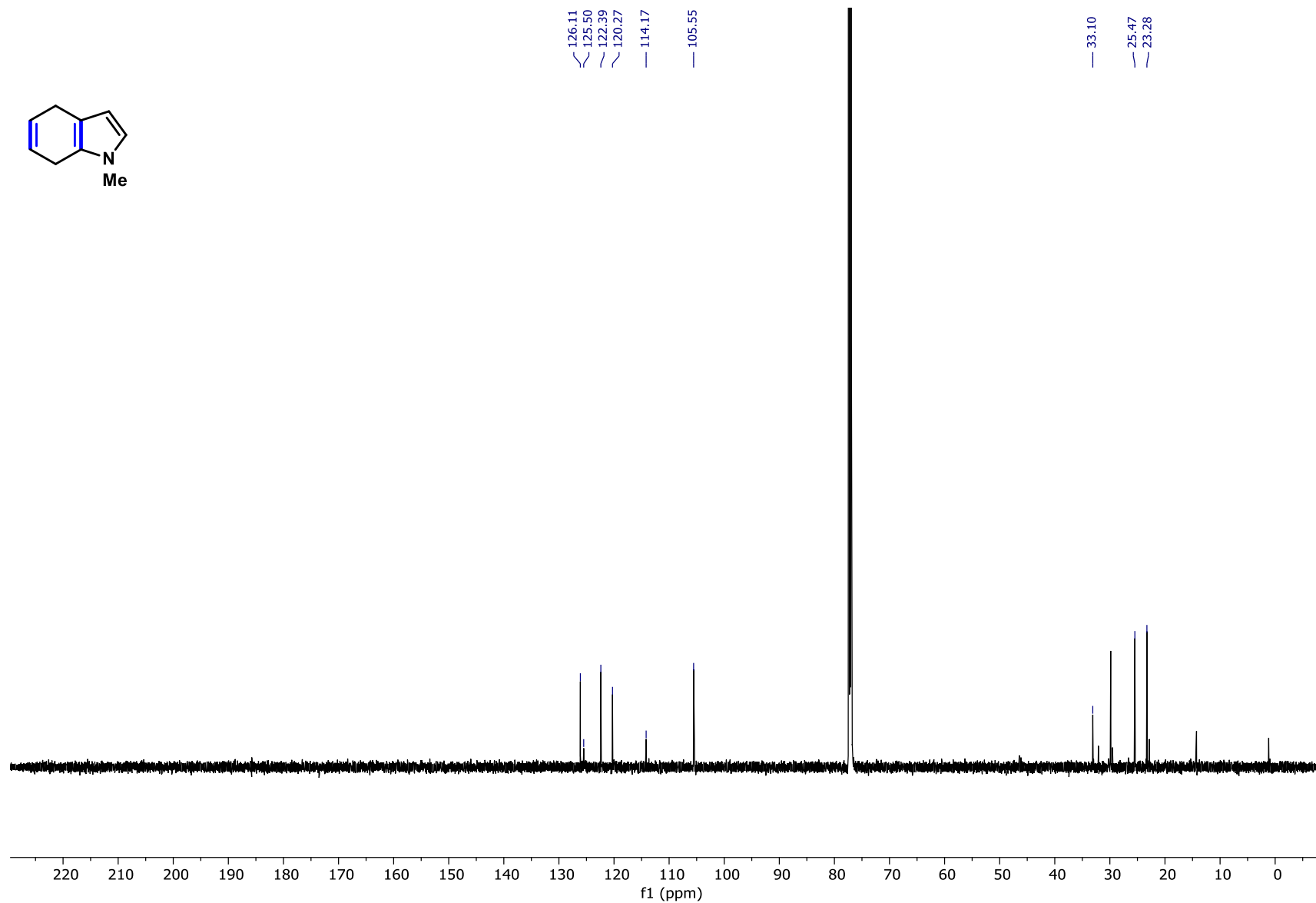
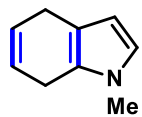


Compound SI-26 ¹H NMR

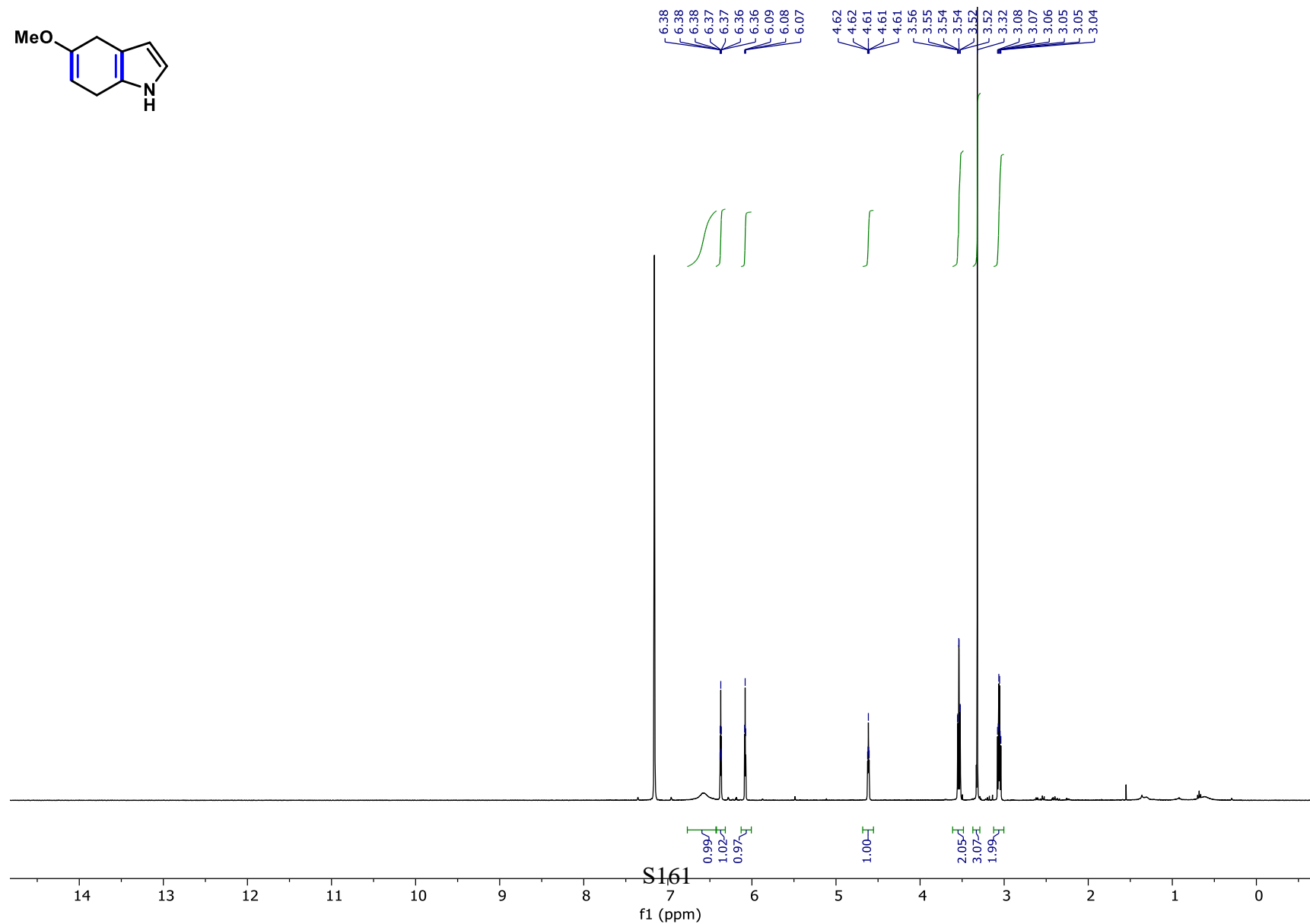
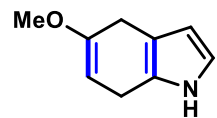


S159

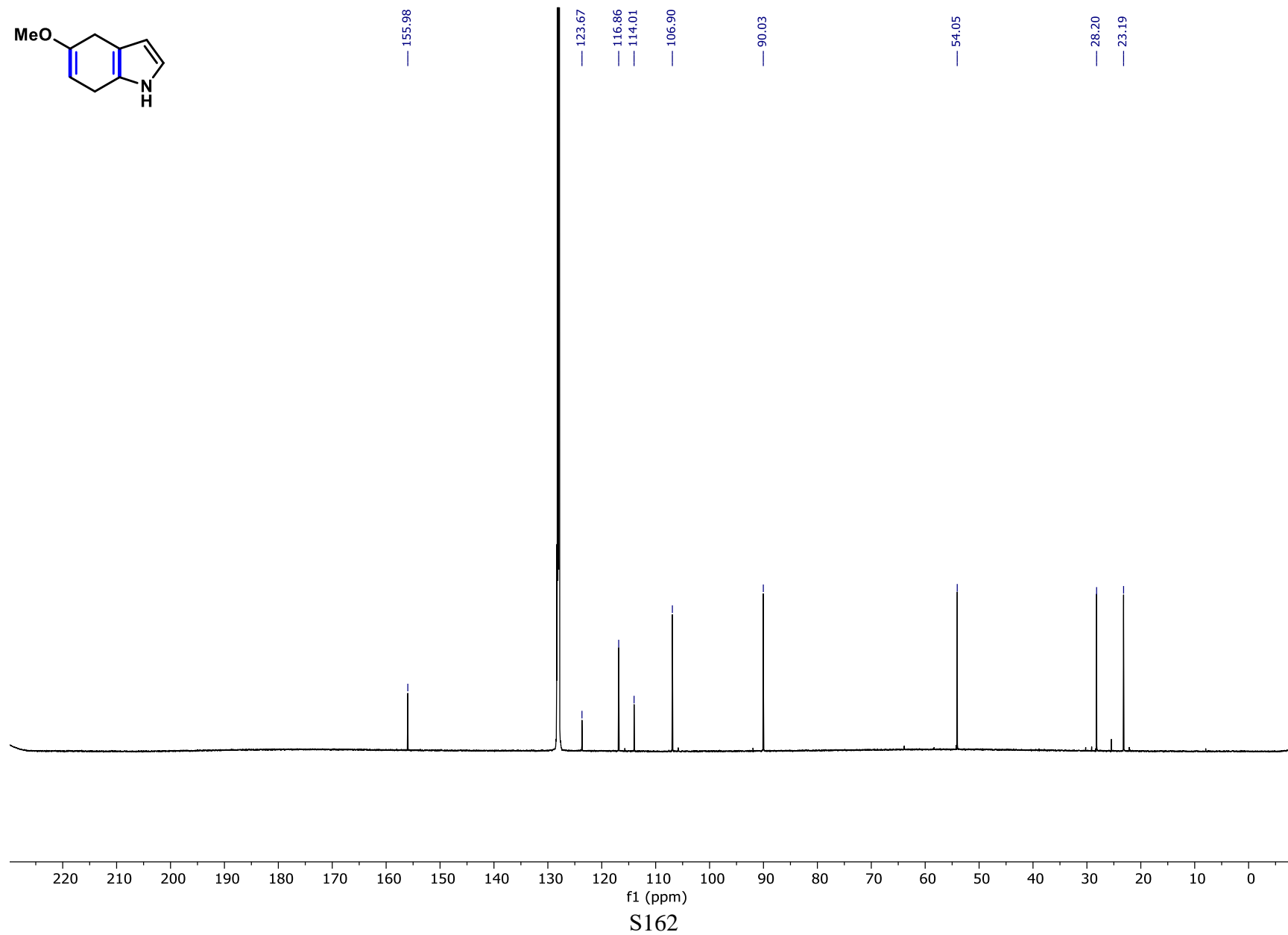
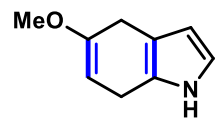
Compound SI-26 ¹³C NMR



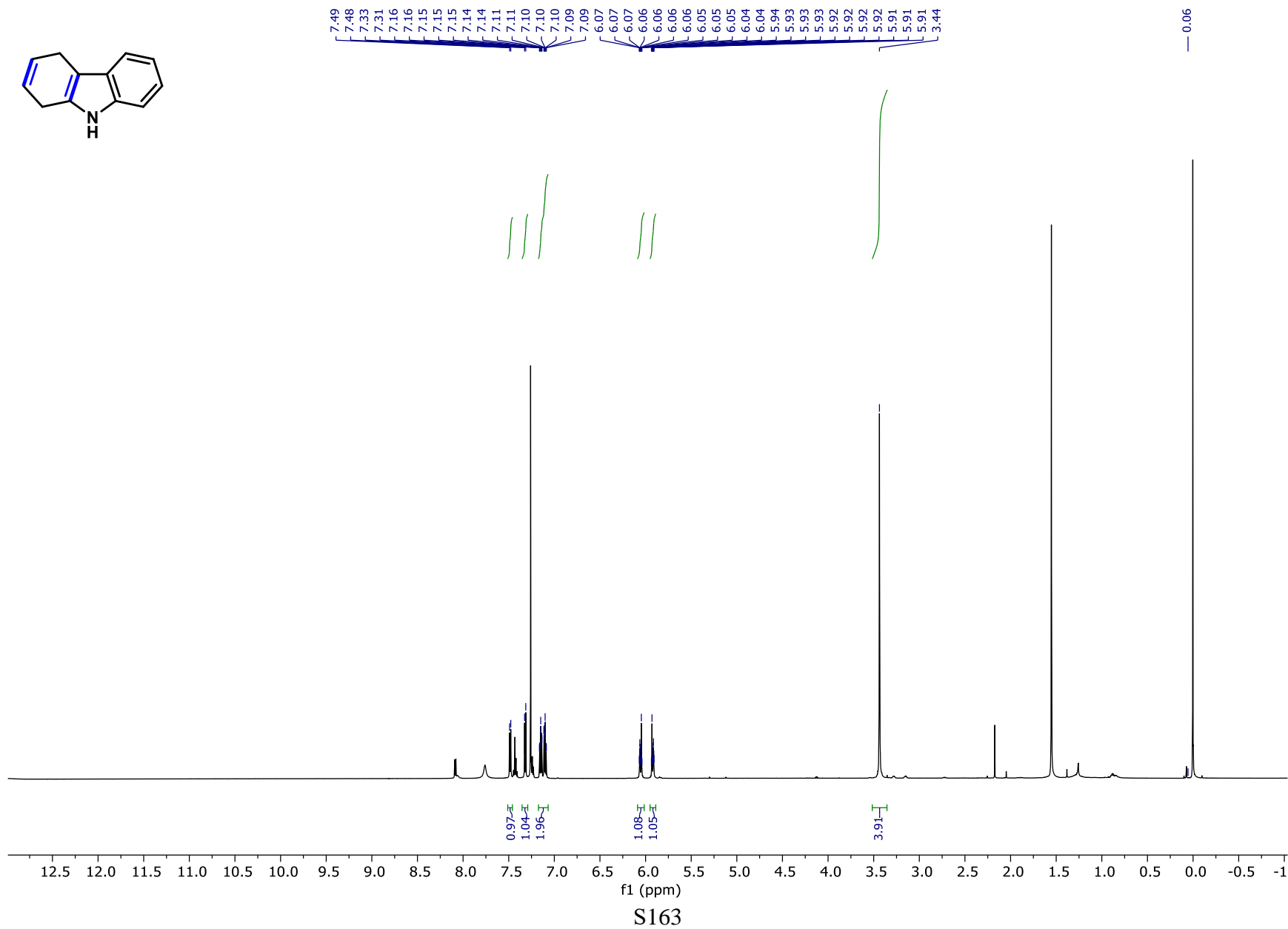
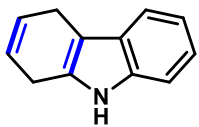
Compound SI-27 ¹H NMR



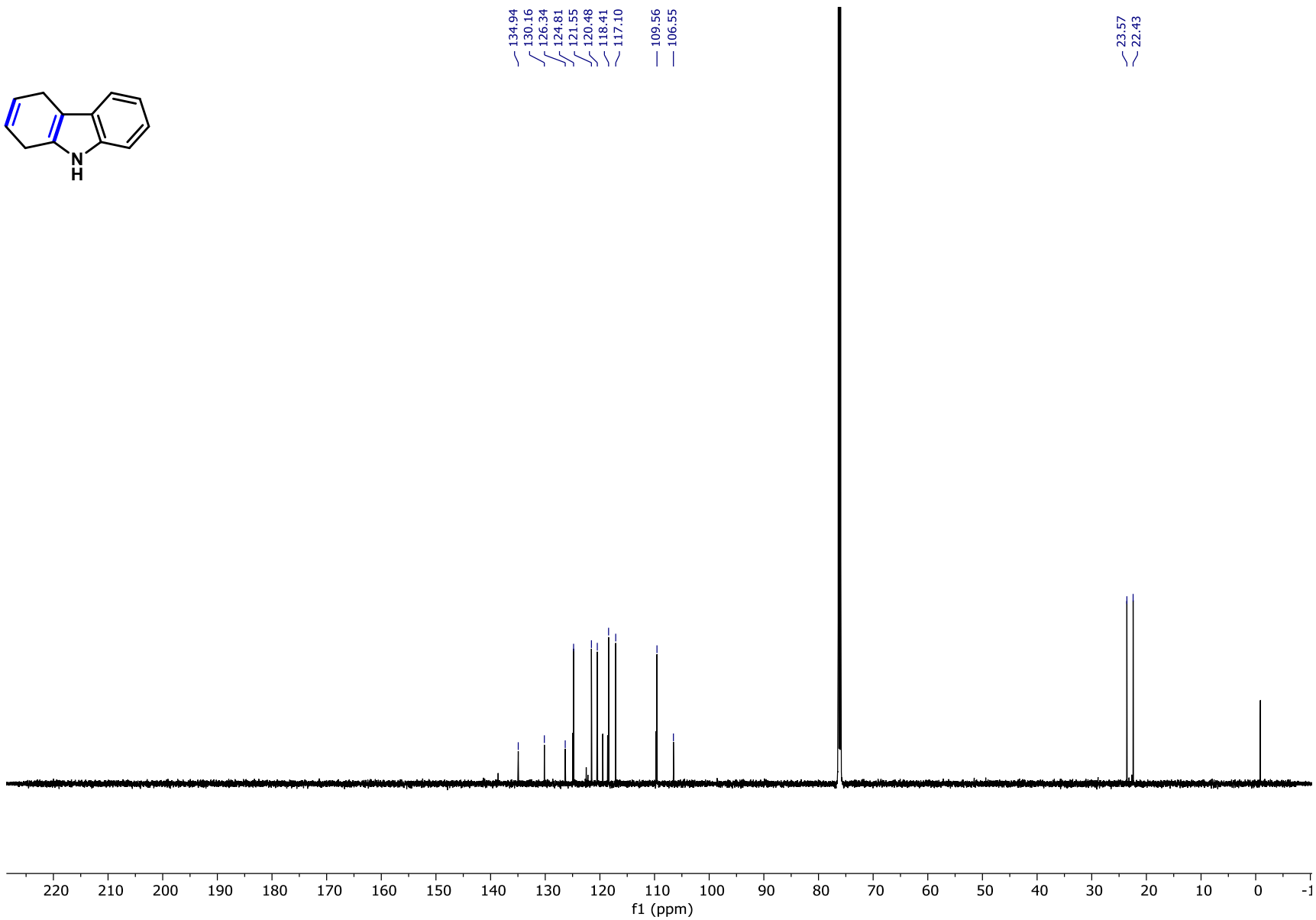
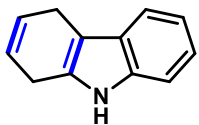
Compound SI-27 ¹³C NMR



Compound SI-28 ¹H NMR

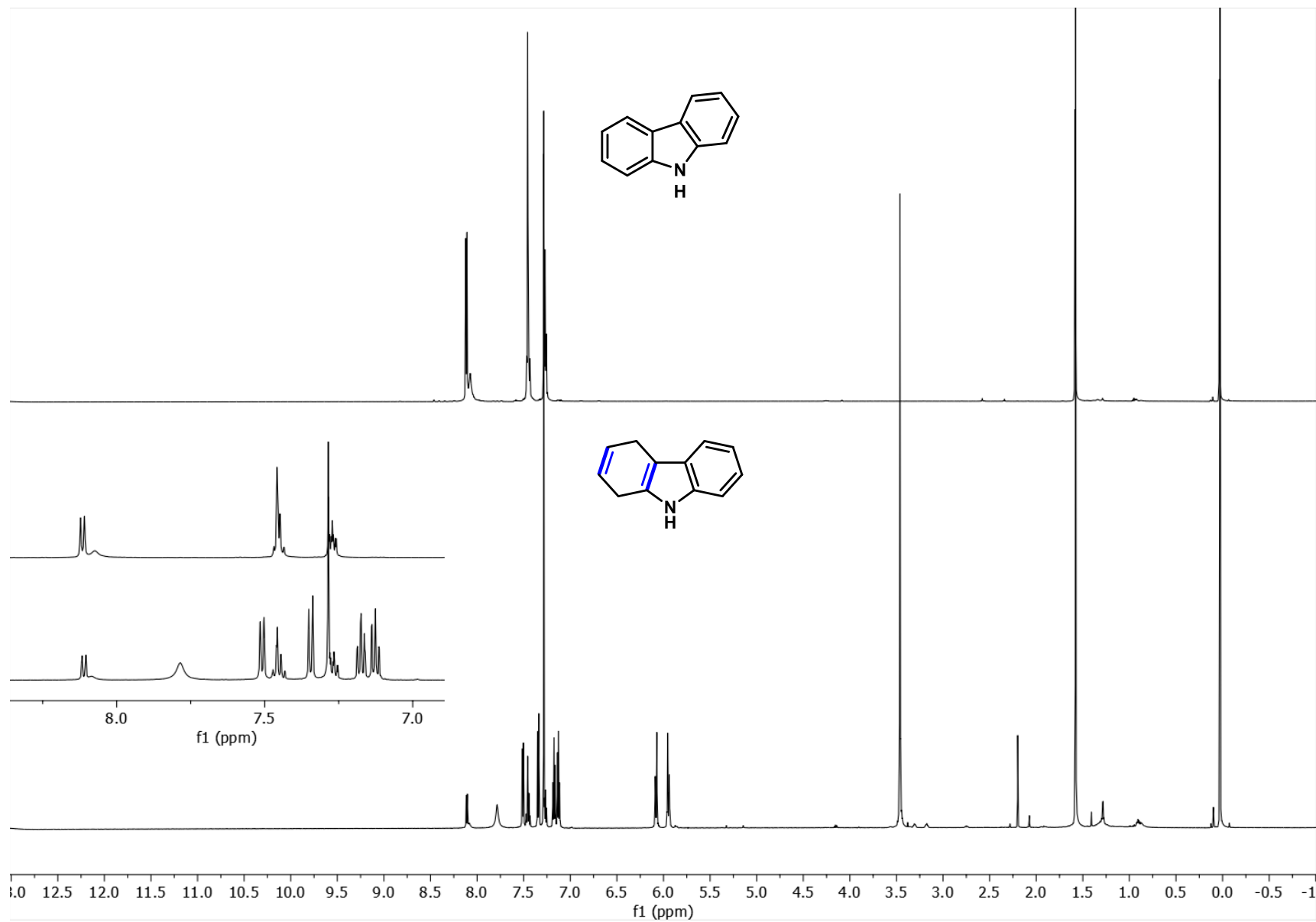


Compound SI-28 ¹³C NMR



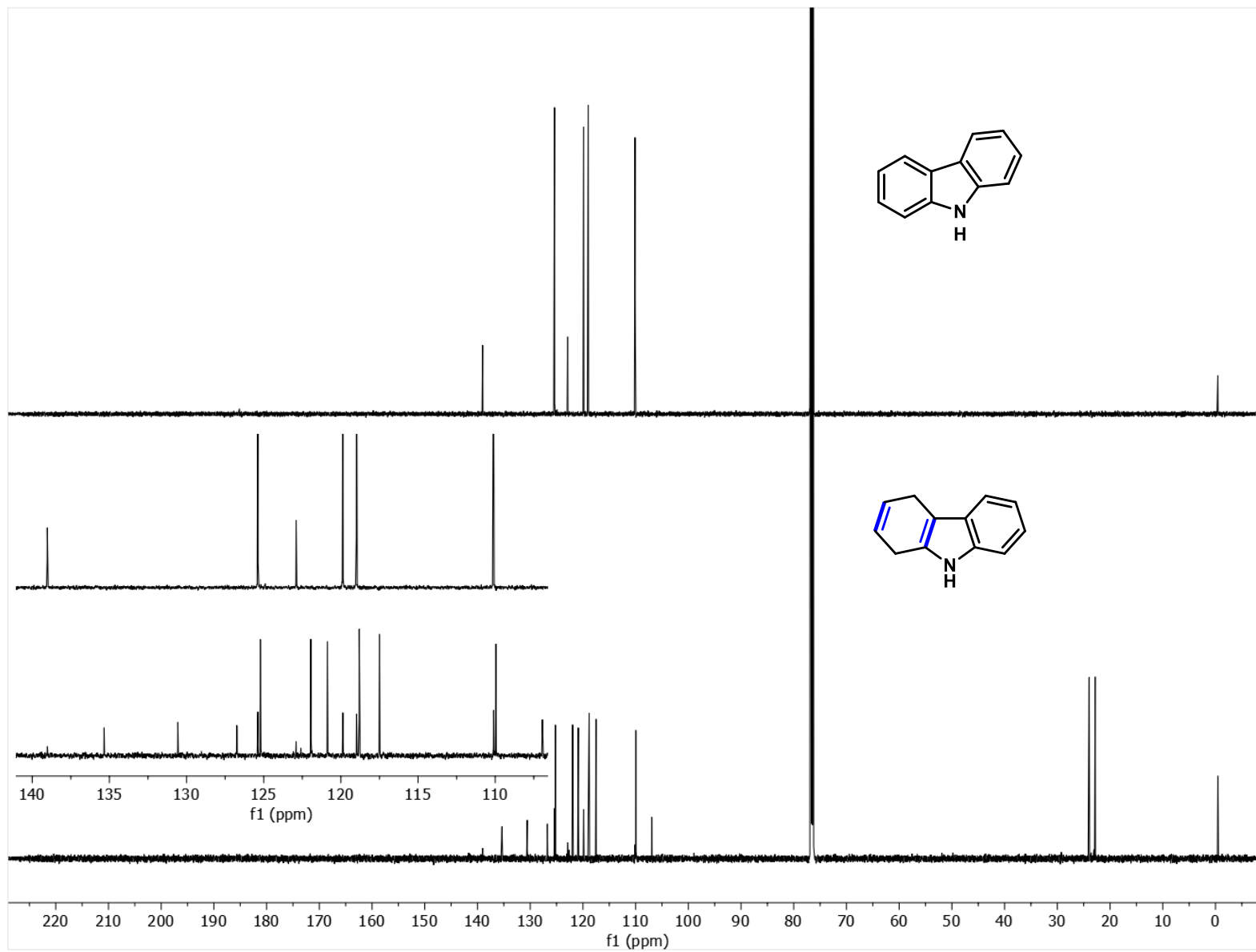
S164

Compound SI-28, carbazole overlay ¹H NMR

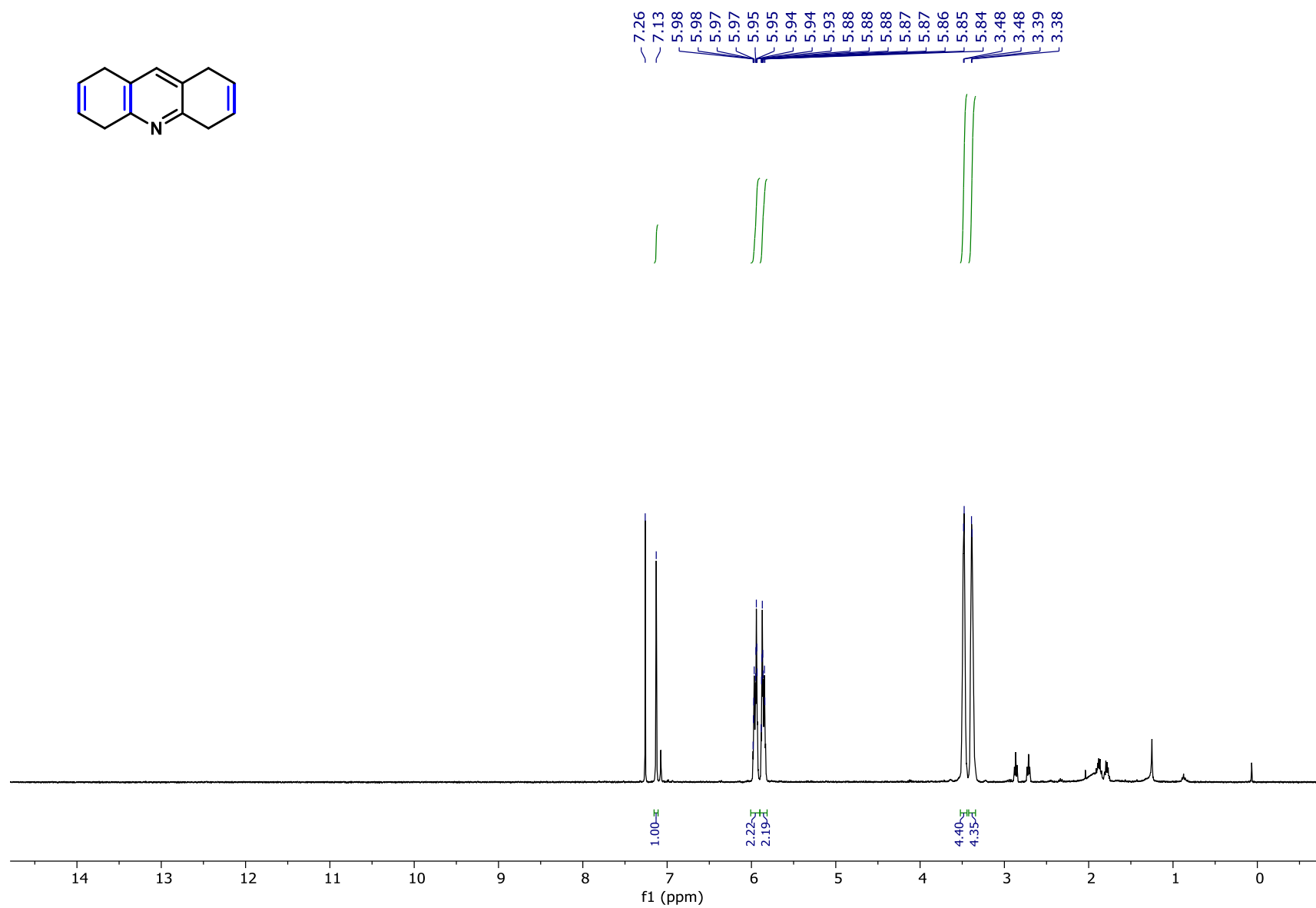
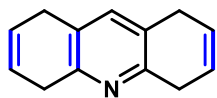


S165

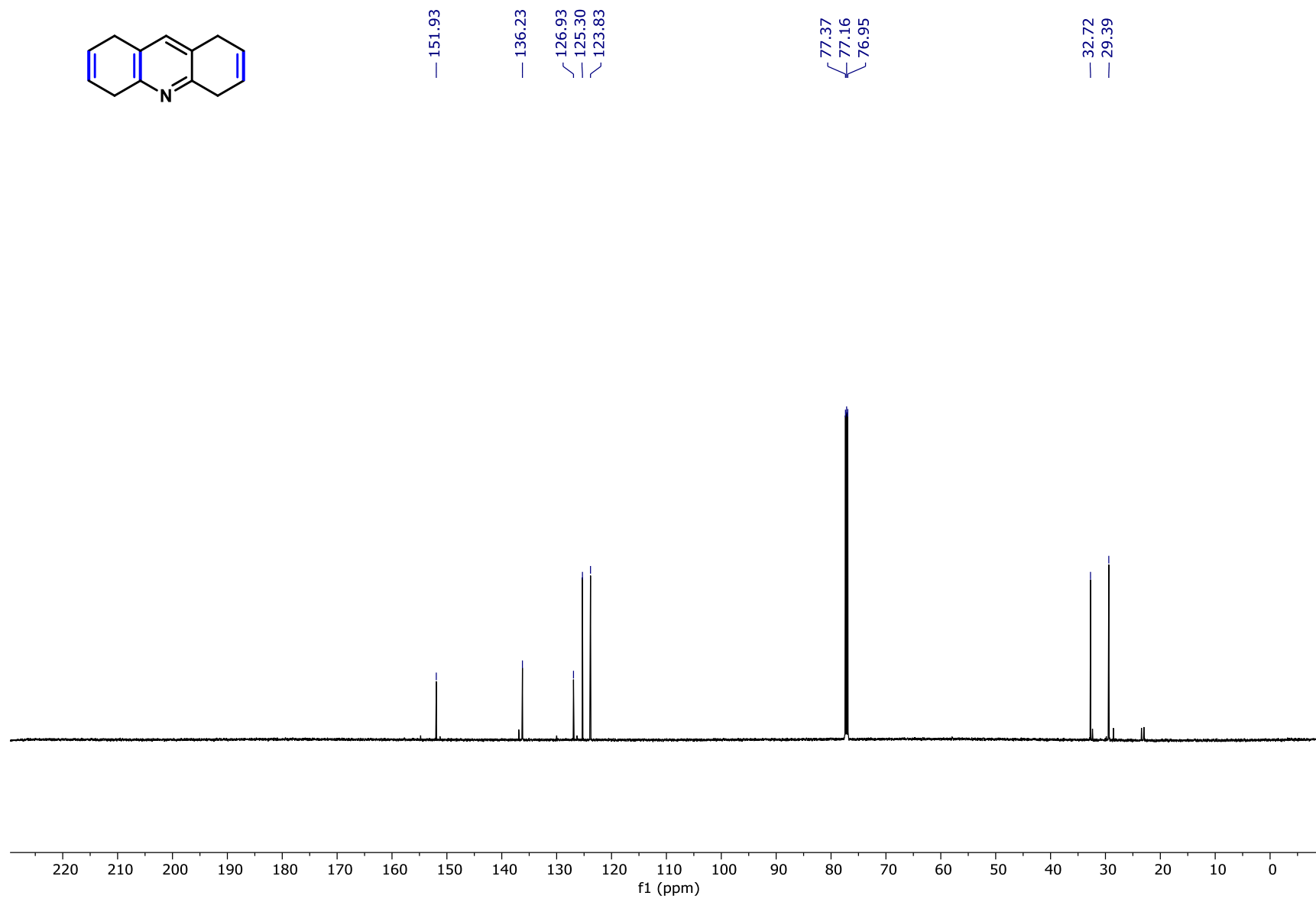
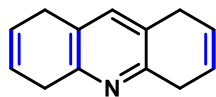
Compound SI-28, carbazole overlay ^{13}C NMR



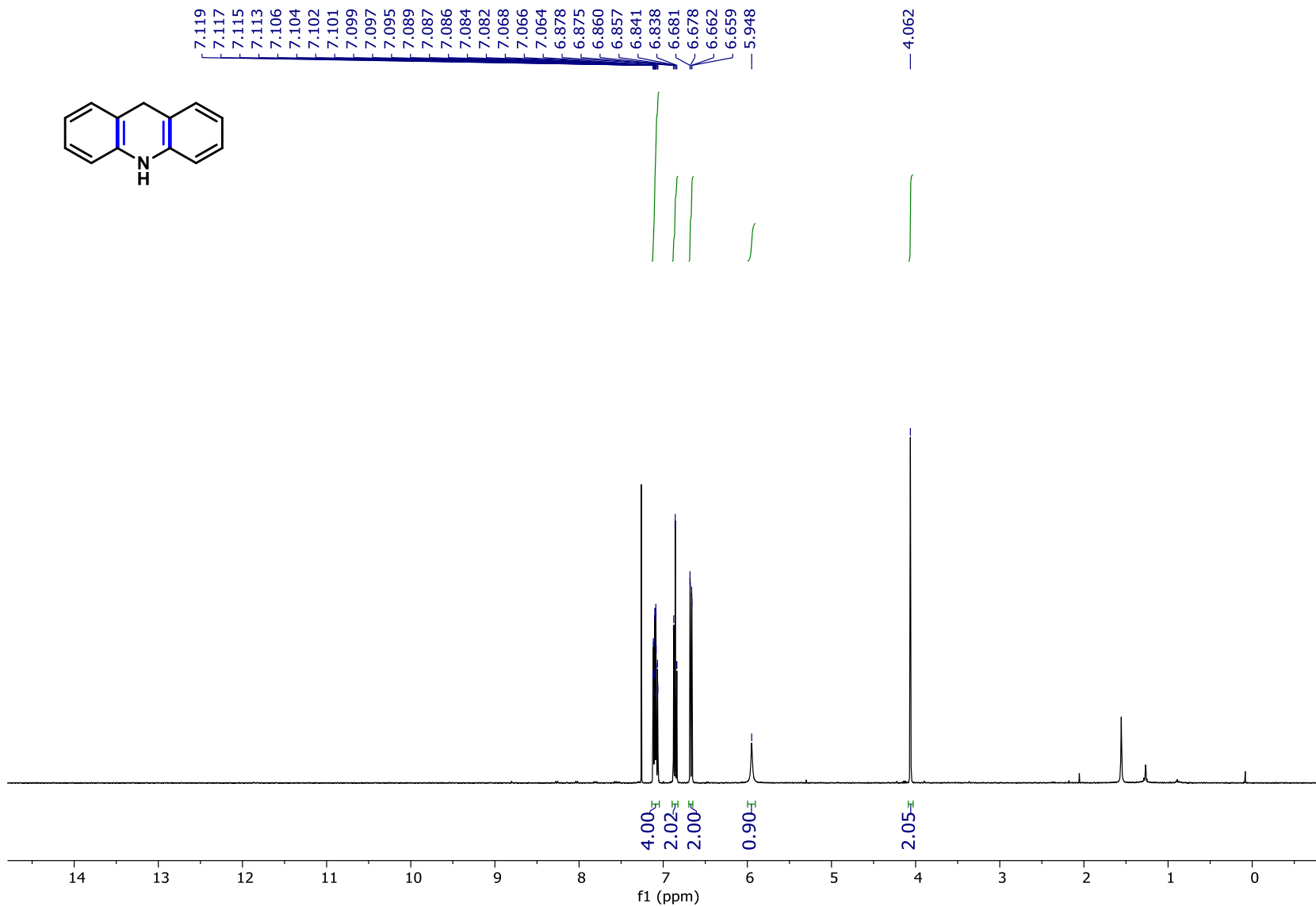
Compound SI-29 ¹H NMR



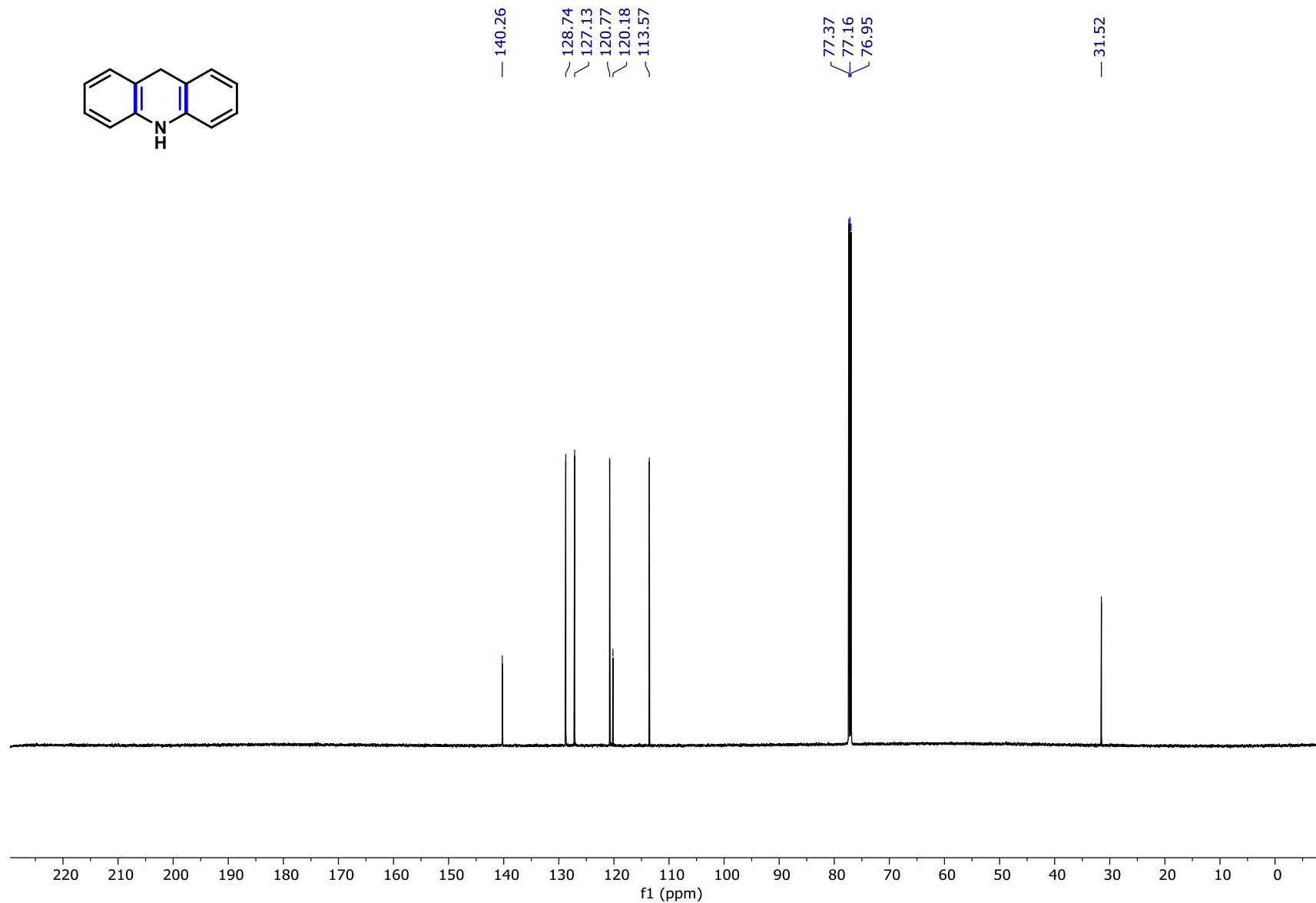
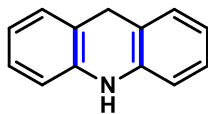
Compound SI-29 ¹³C NMR



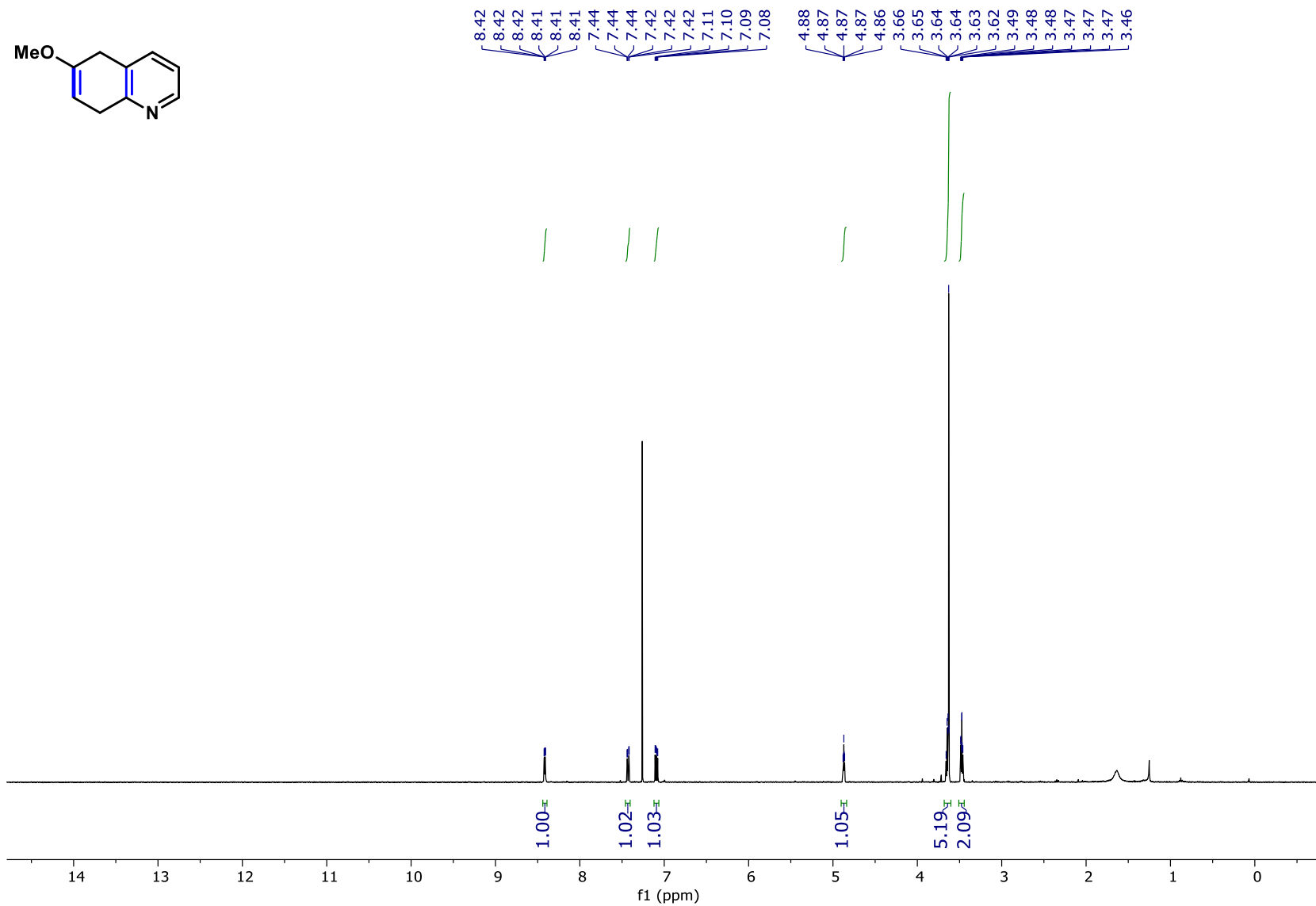
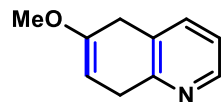
Compound SI-30 ¹H NMR



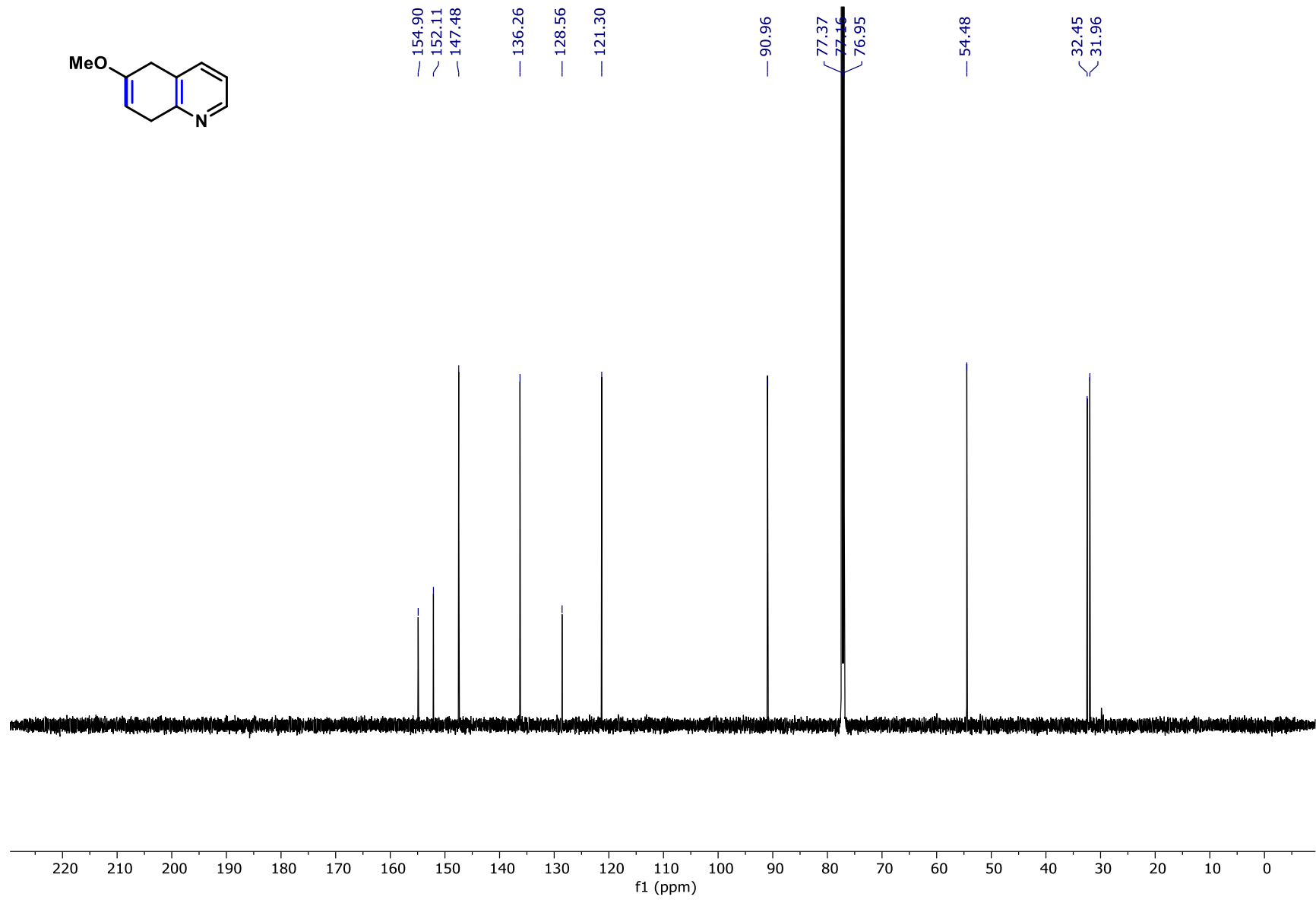
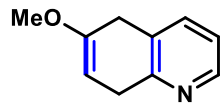
Compound SI-30 ¹³C NMR



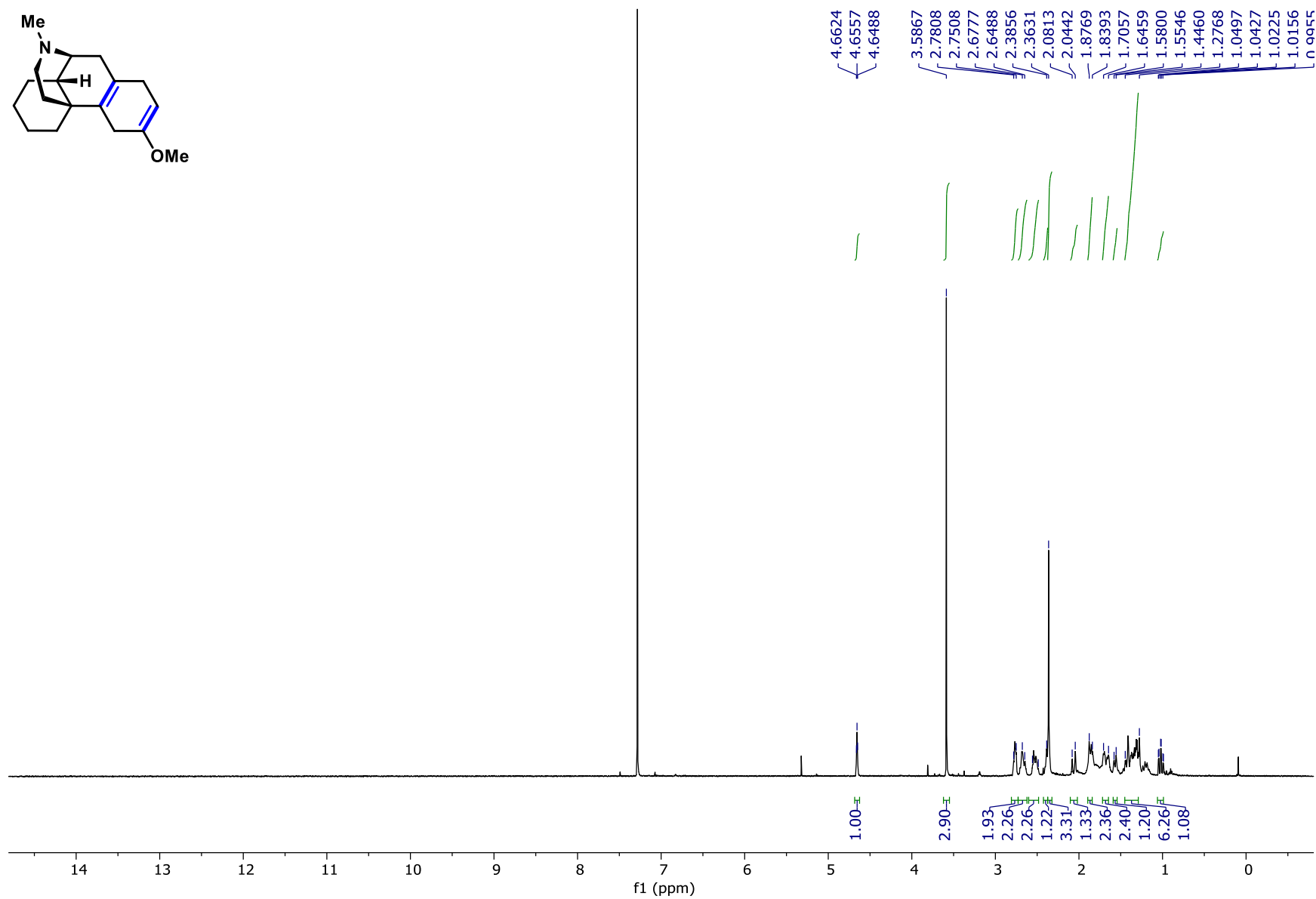
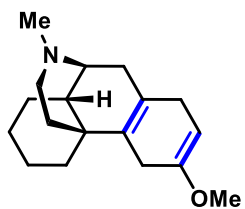
Compound SI-31 ¹H NMR



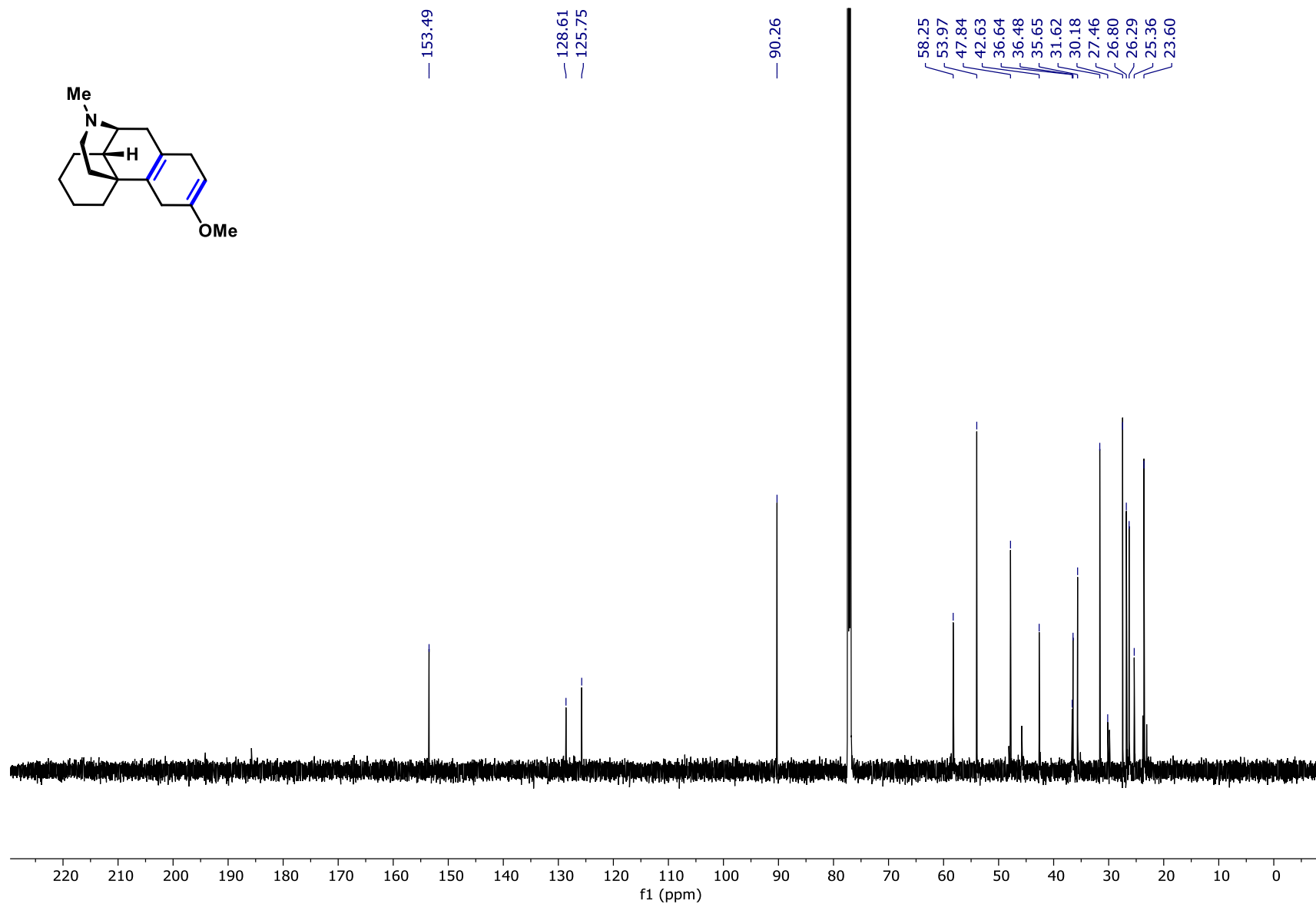
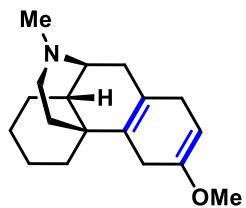
Compound SI-31 ¹³C NMR



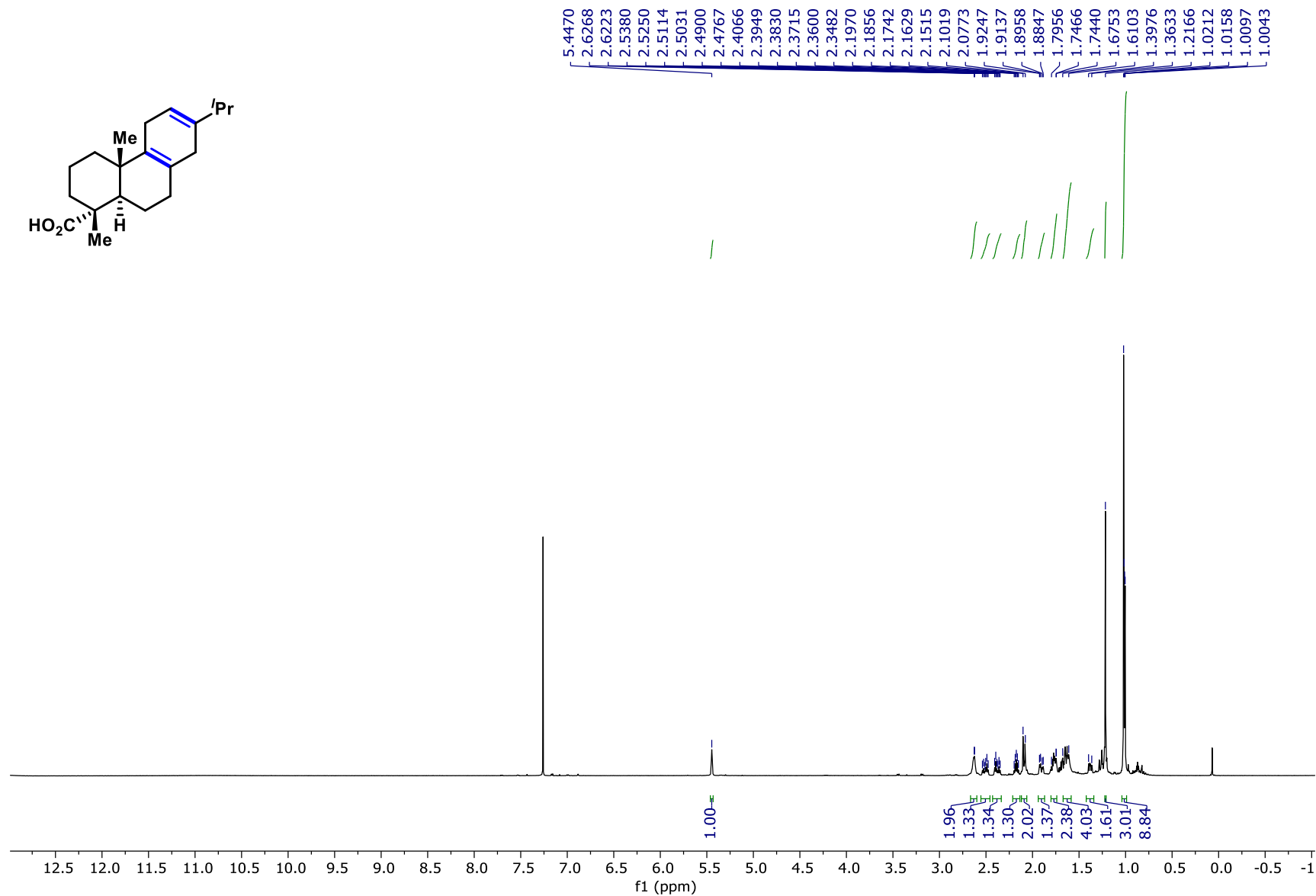
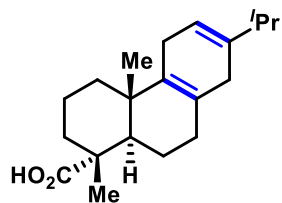
Compound SI-32 ¹H NMR



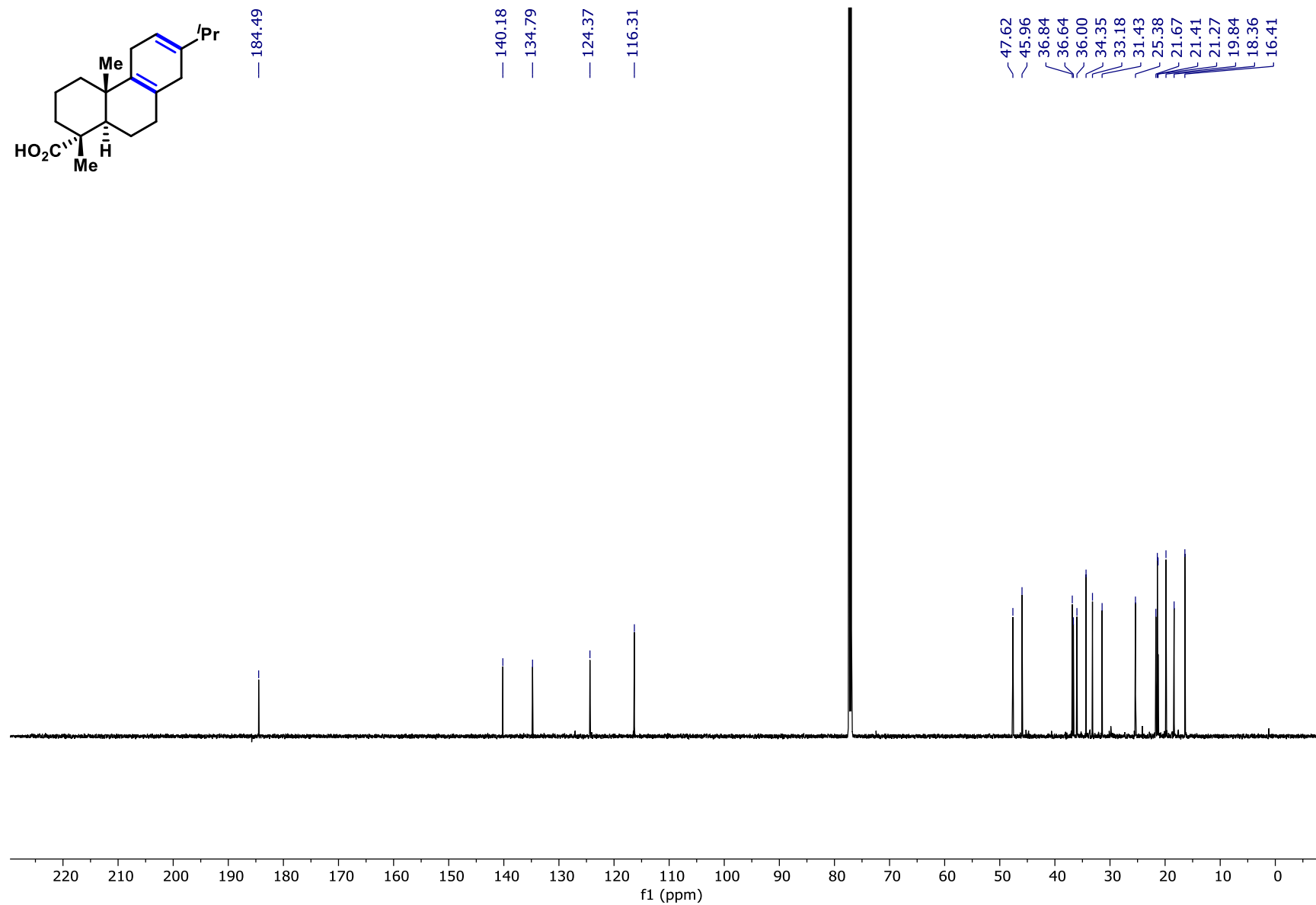
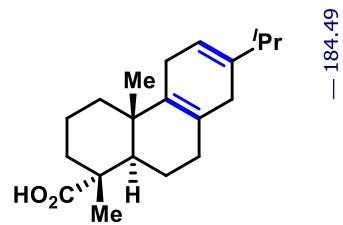
Compound SI-32 ¹³C NMR



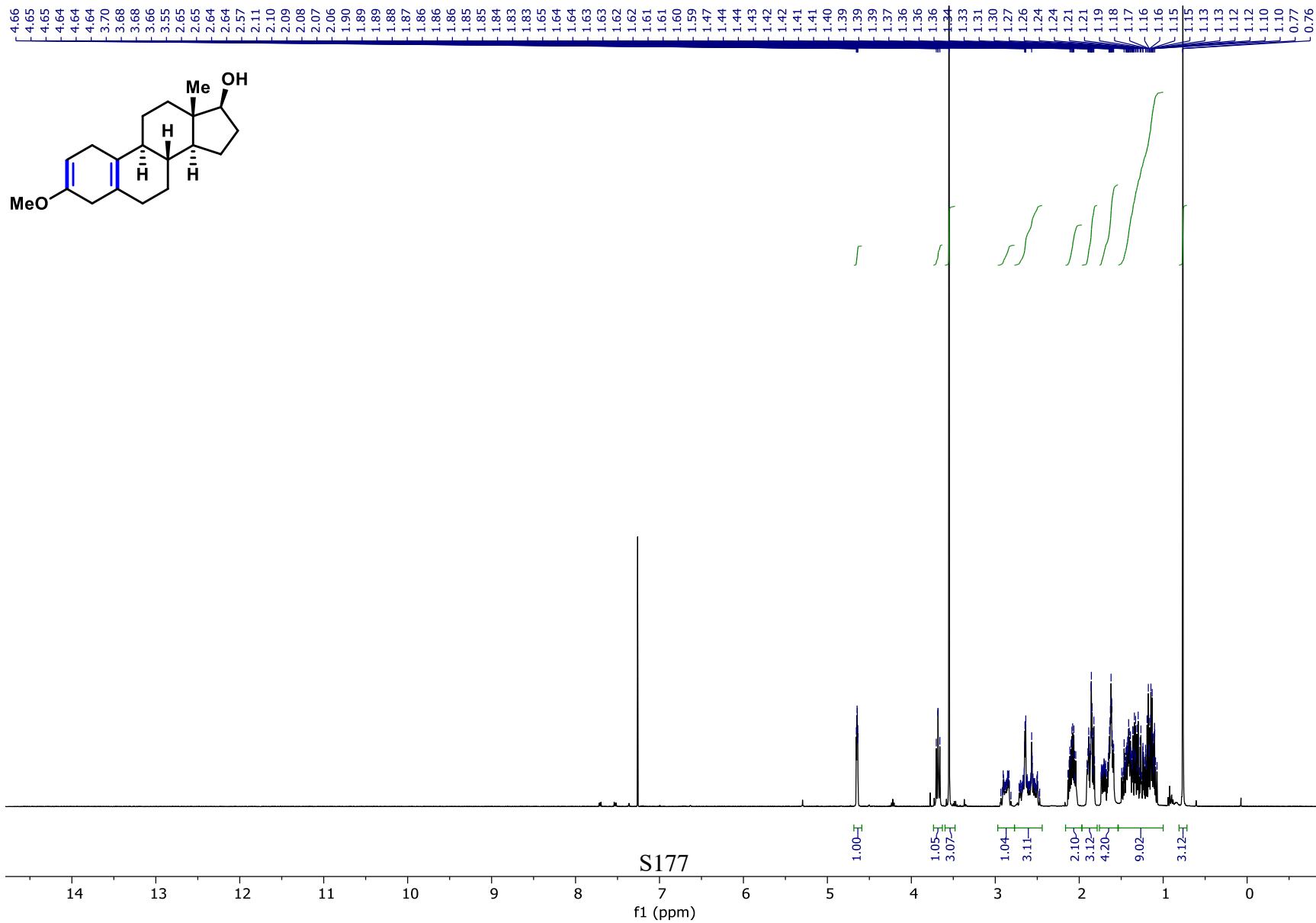
Compound SI-33 ¹H NMR



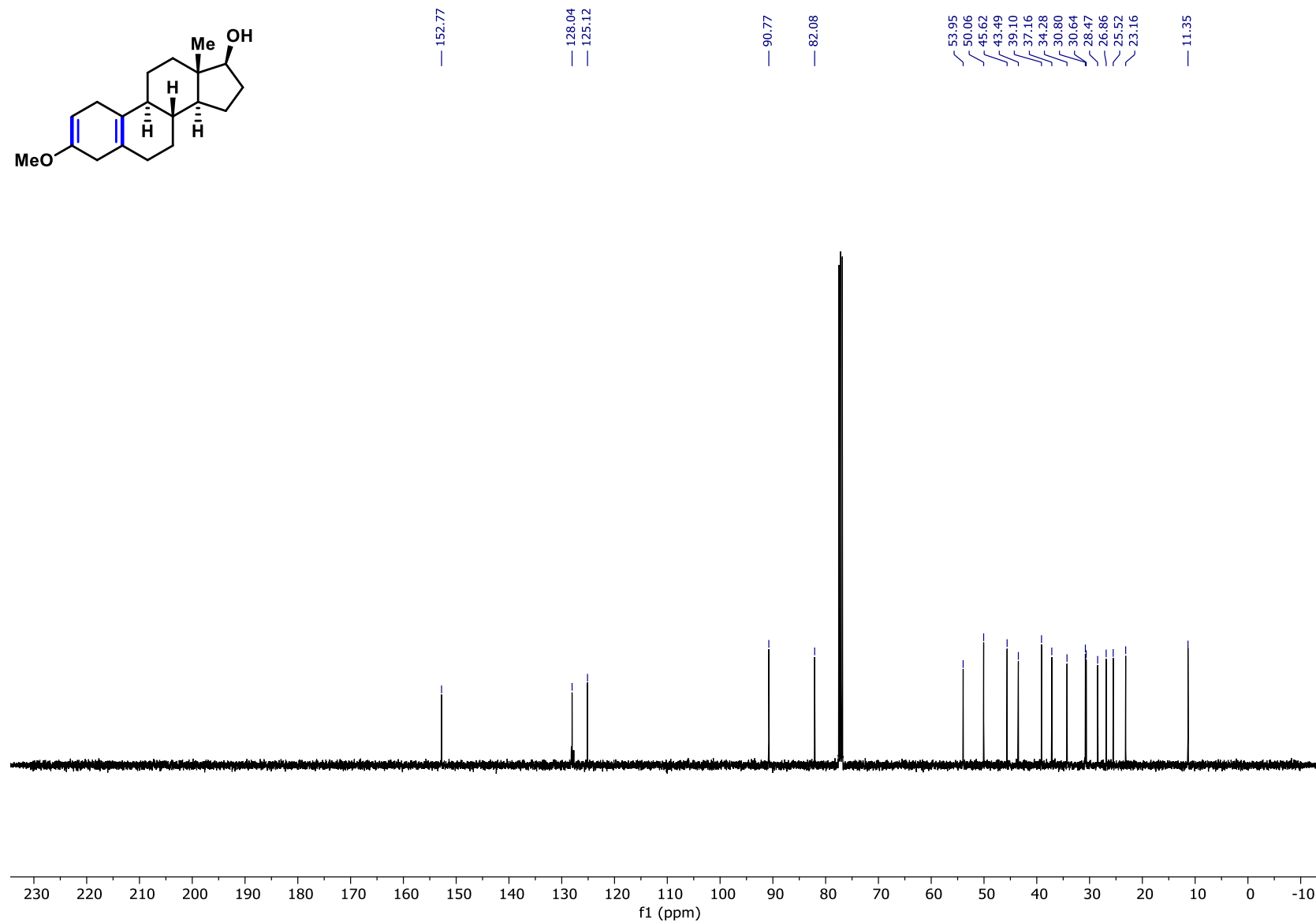
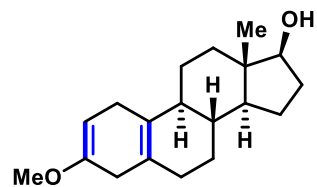
Compound SI-33 ¹³C NMR



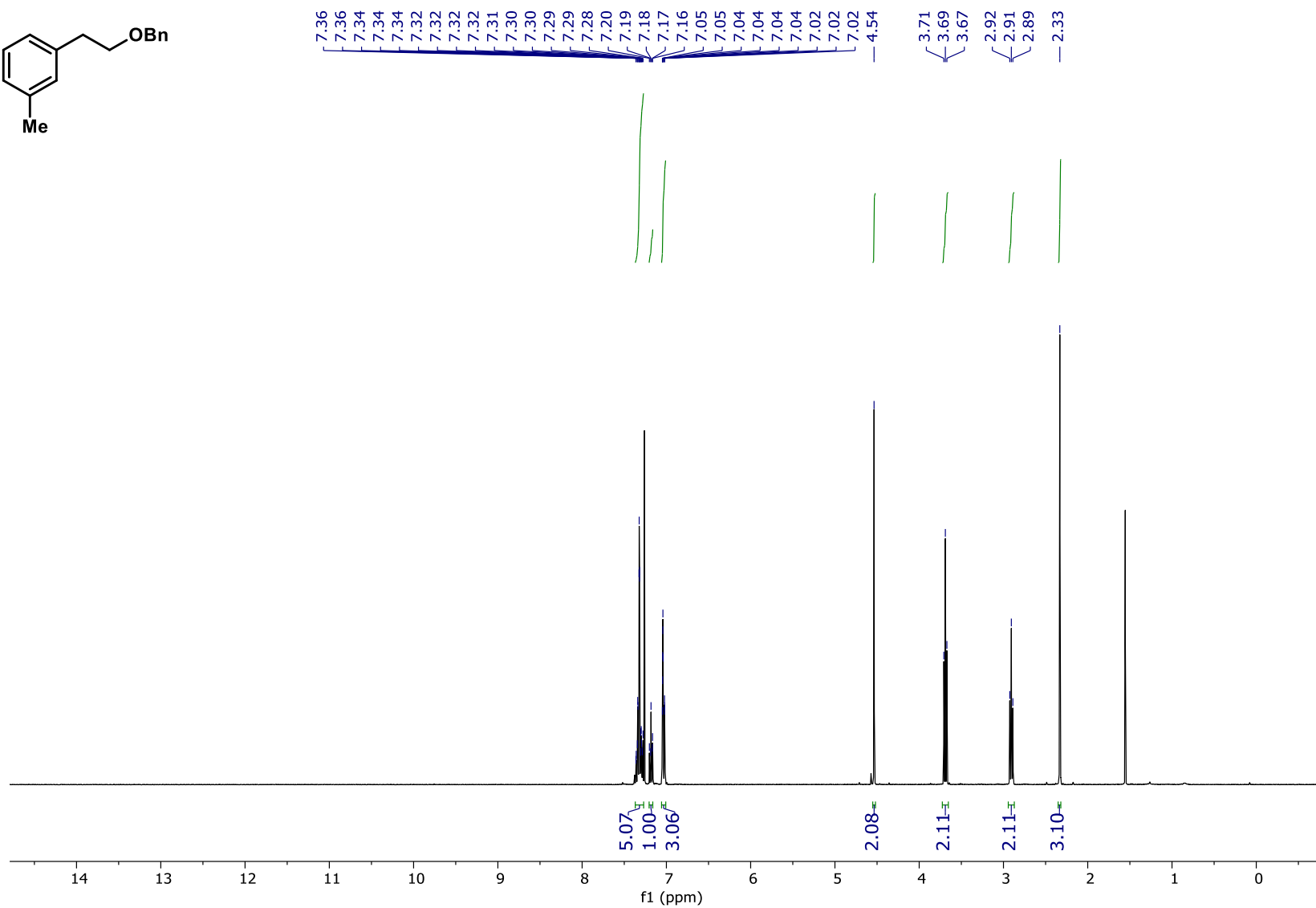
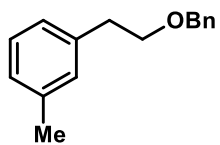
Compound SI-34 ¹H NMR



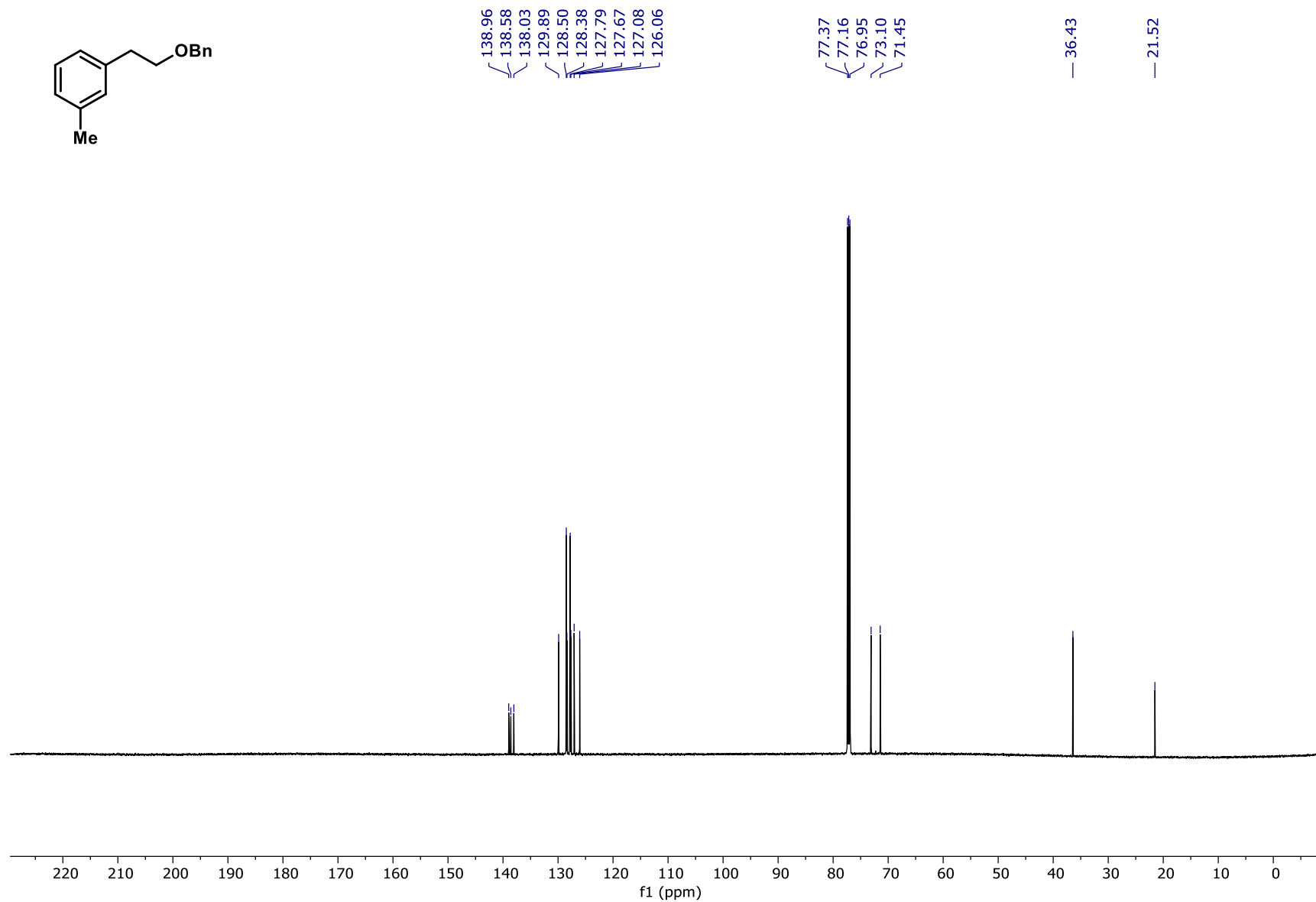
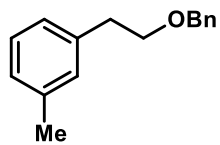
Compound SI-34 ¹³C NMR



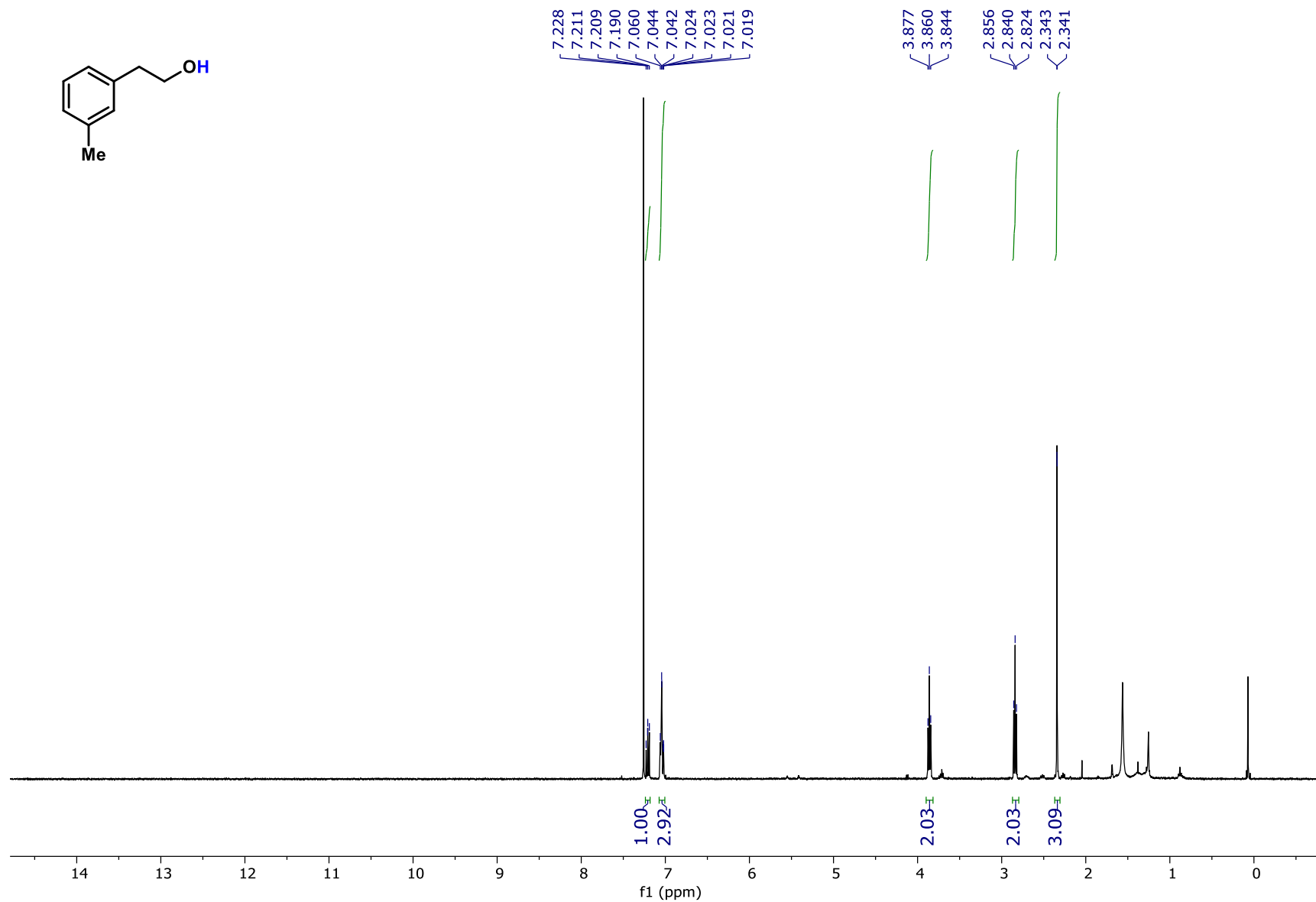
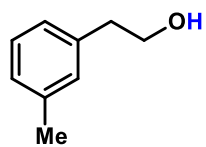
Compound SI-35 ¹H NMR



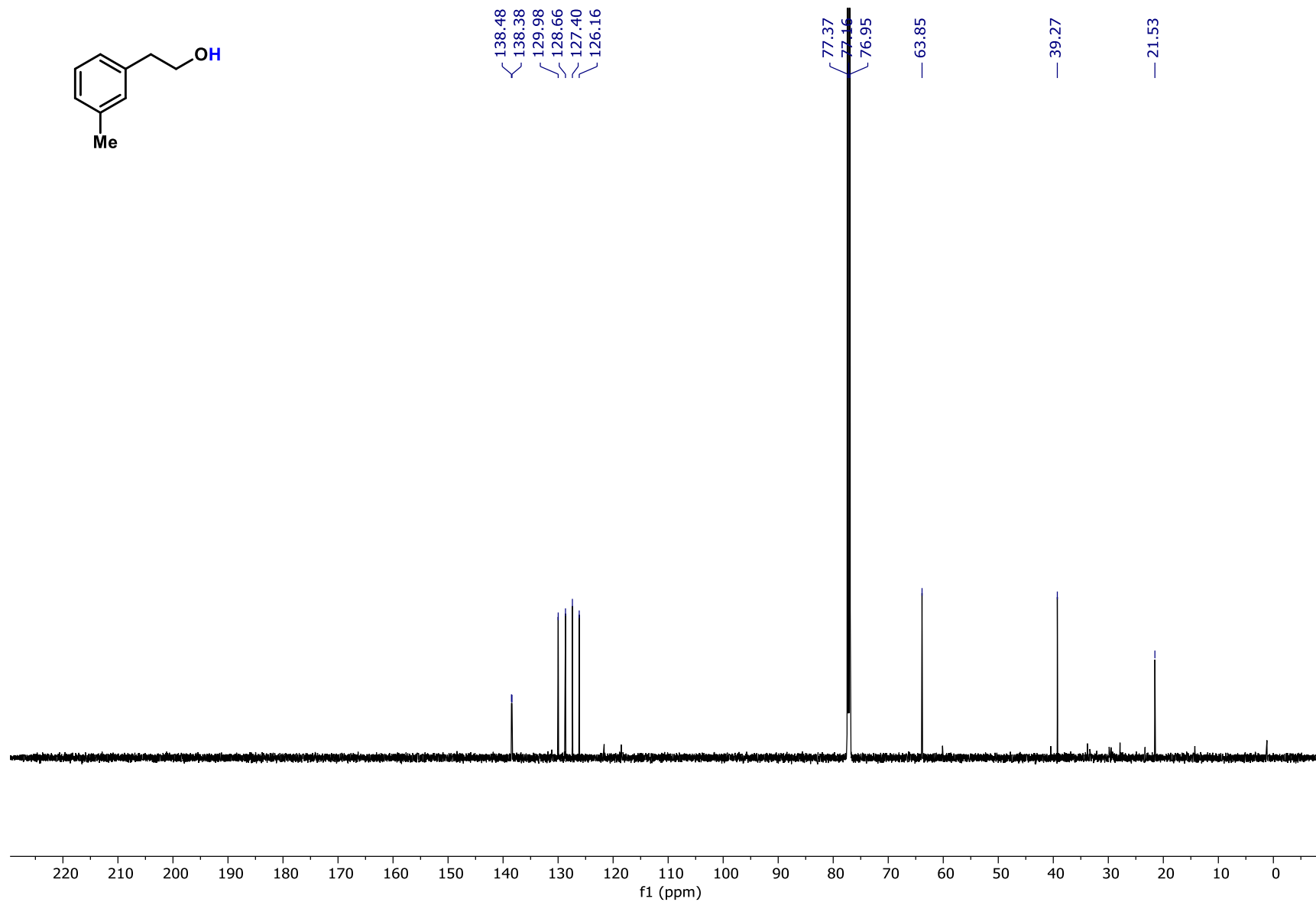
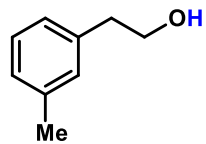
Compound SI-35 ¹³C NMR



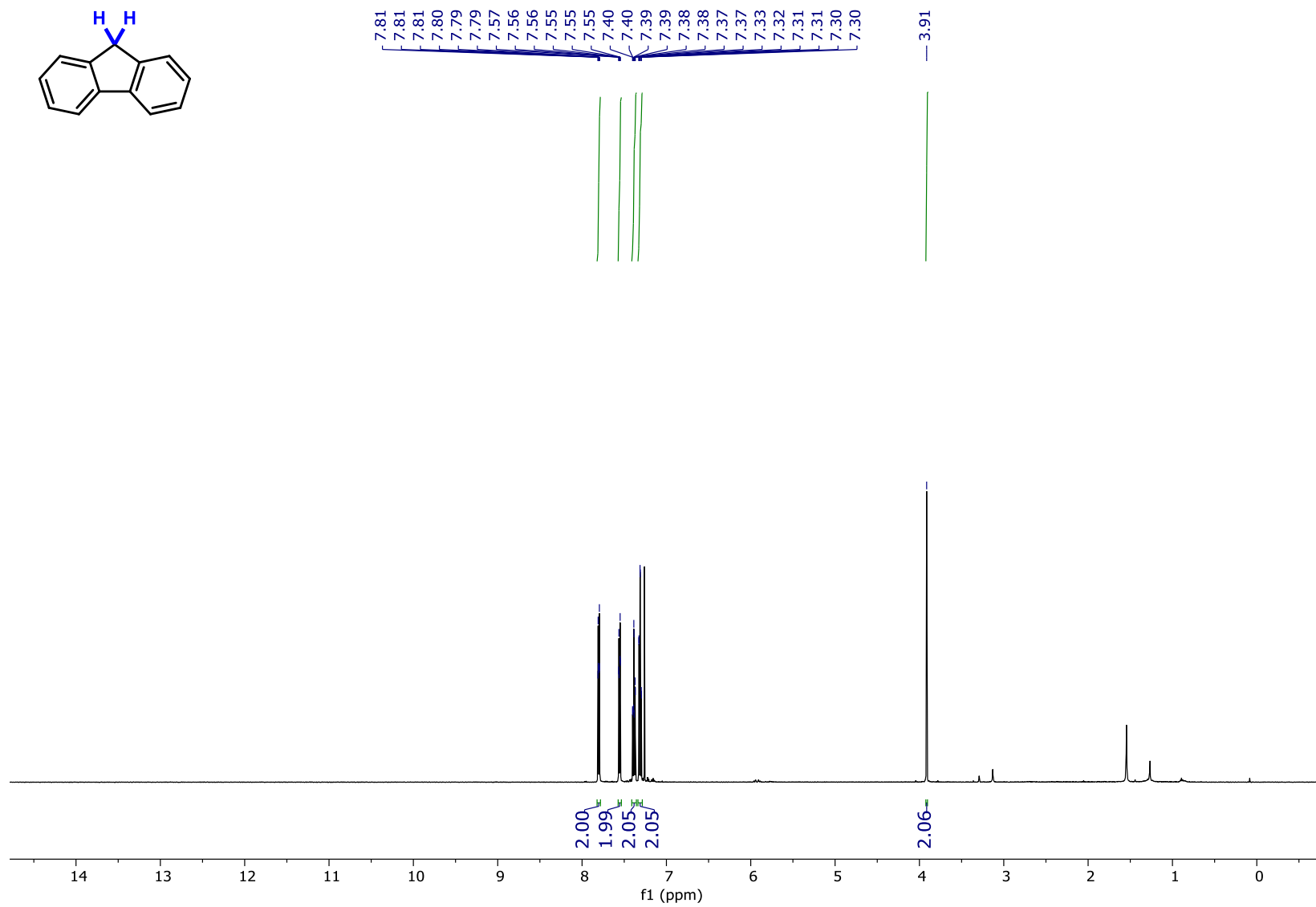
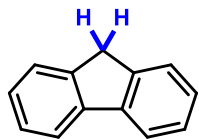
Compound SI-36 ¹H NMR



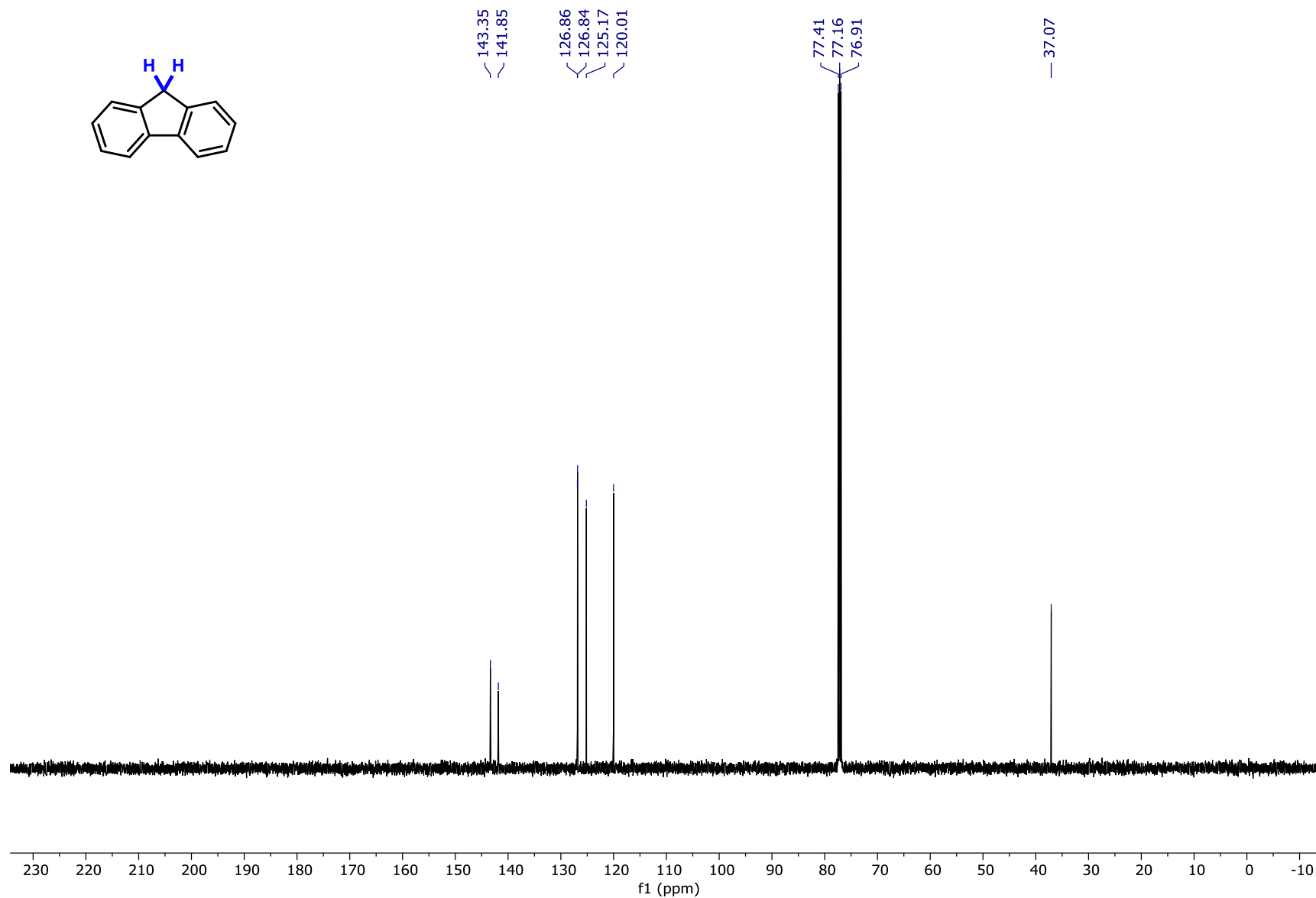
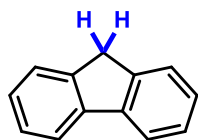
Compound SI-36 ¹³C NMR



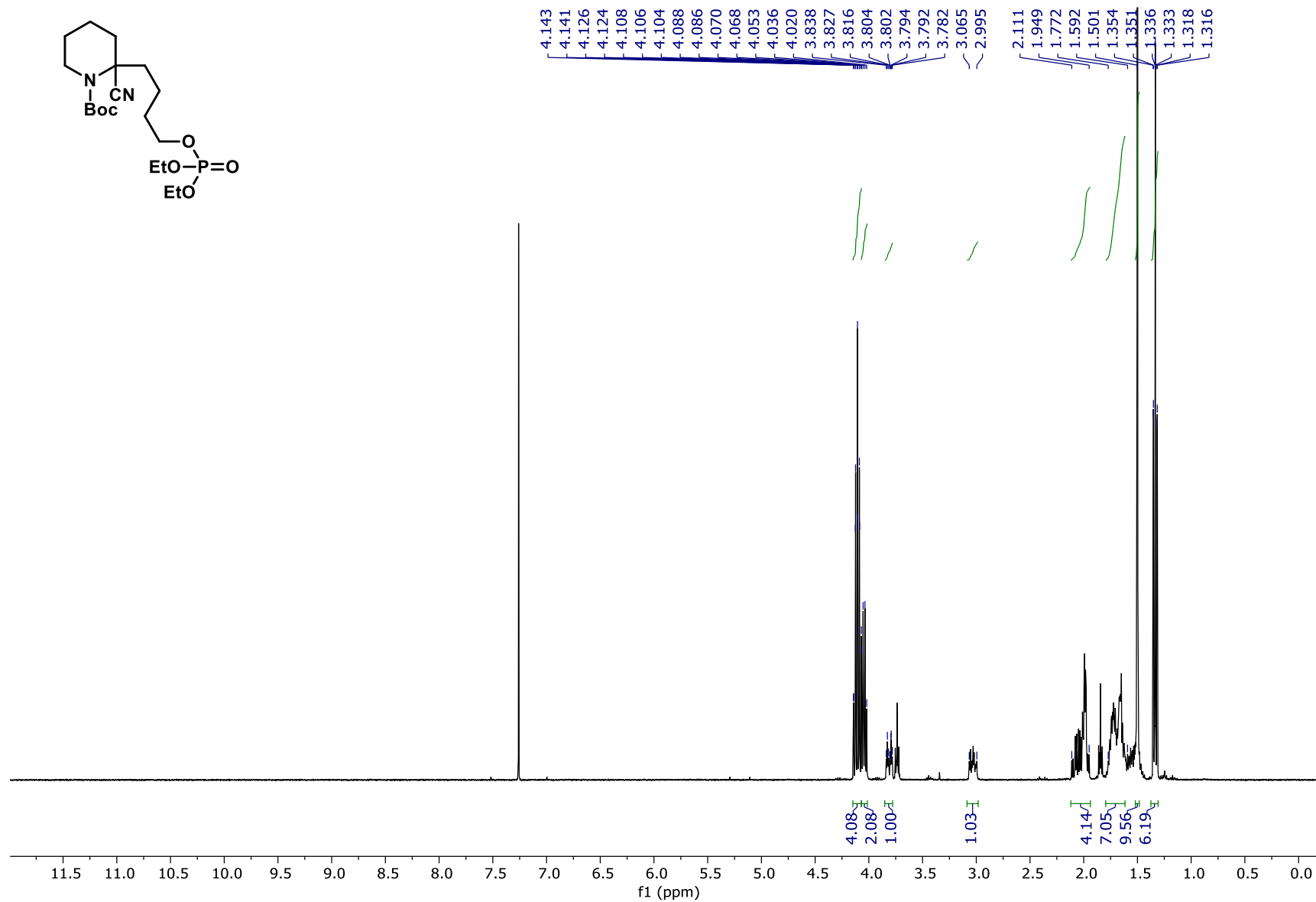
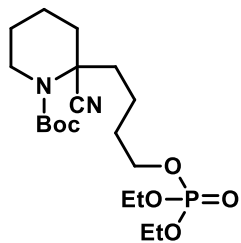
Compound SI-38 ¹H NMR



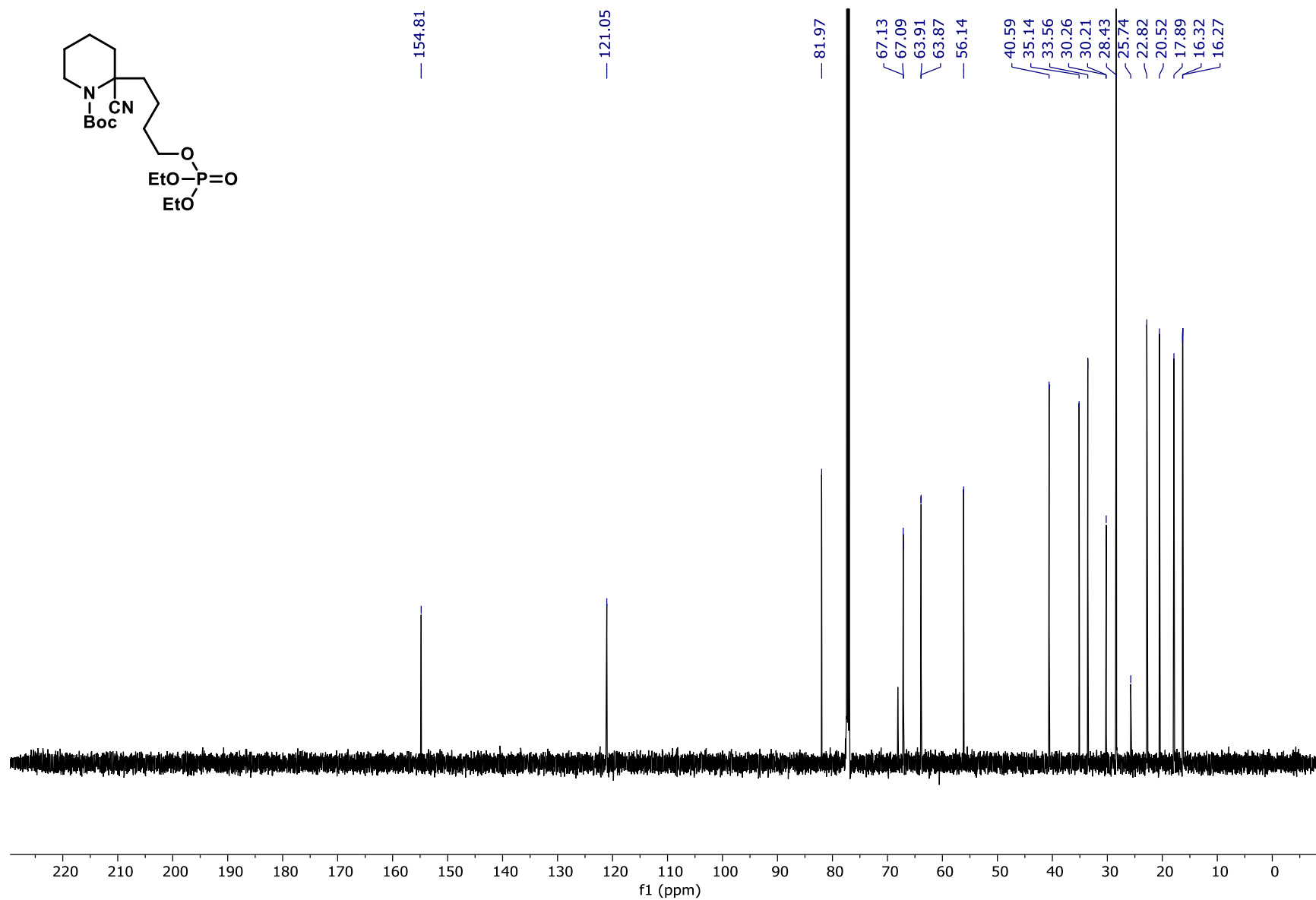
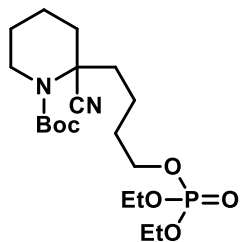
Compound SI-38 ¹³C NMR



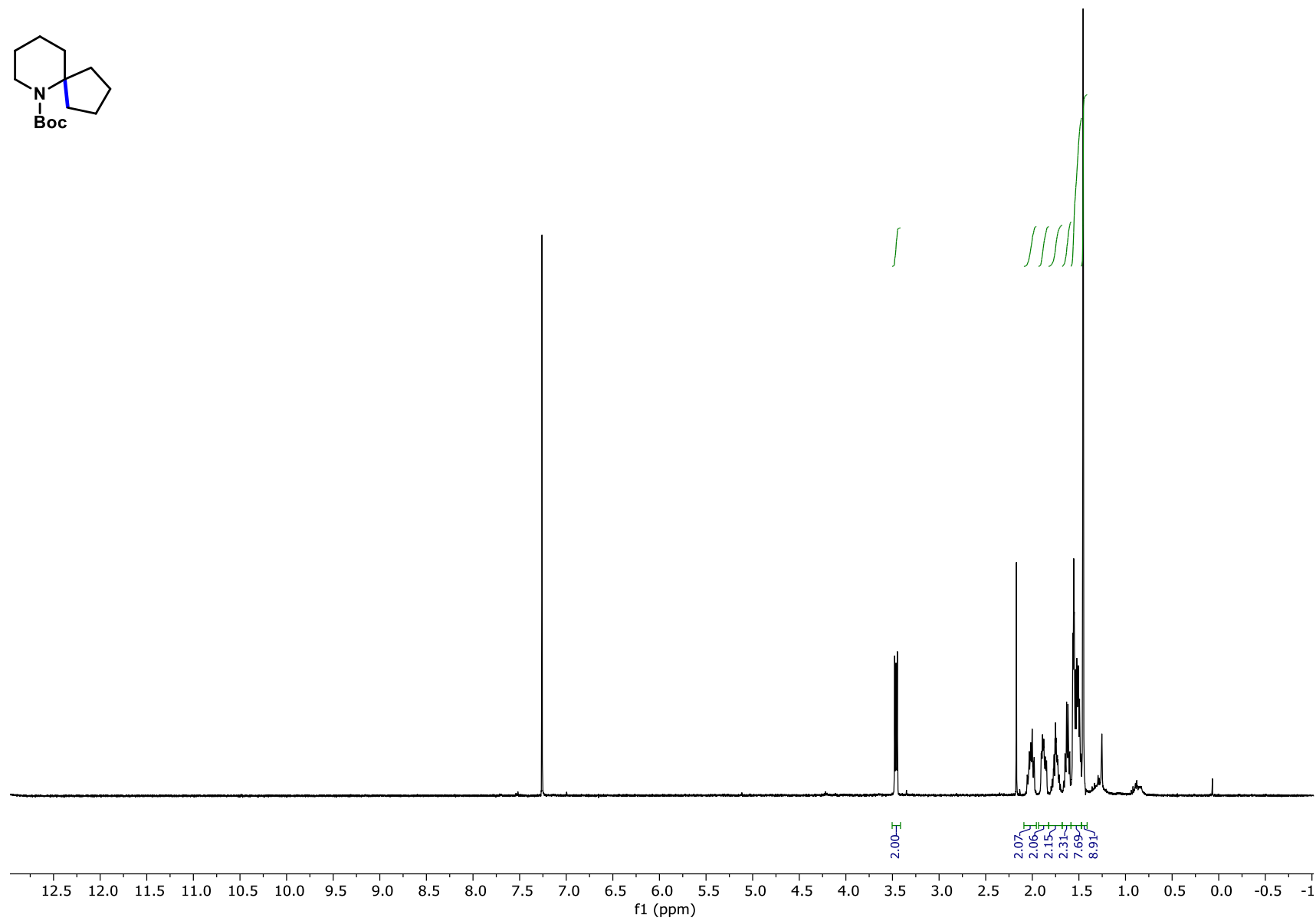
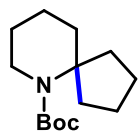
Compound SI-39 ¹H NMR



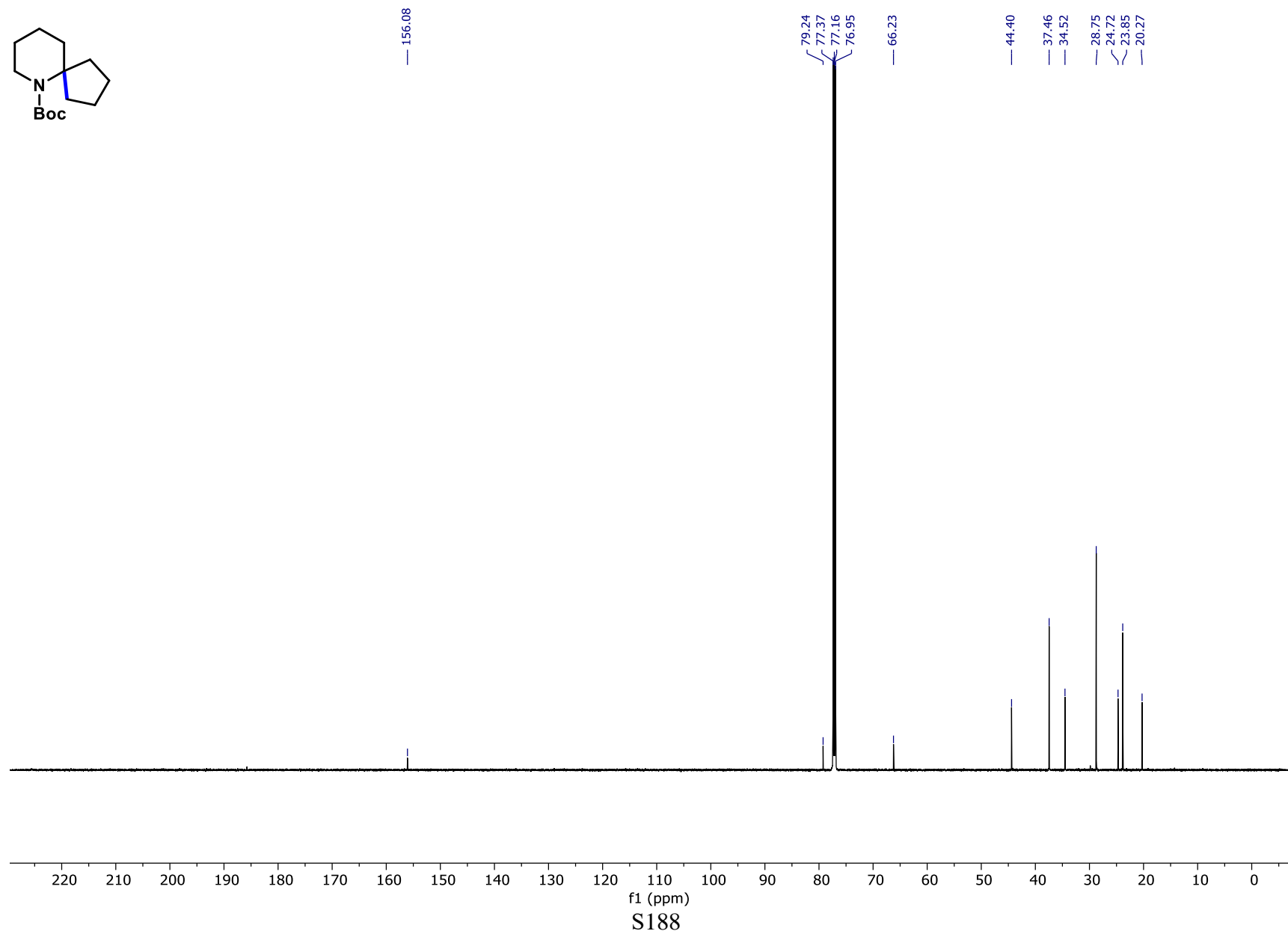
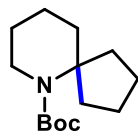
Compound SI-39 ¹³C NMR



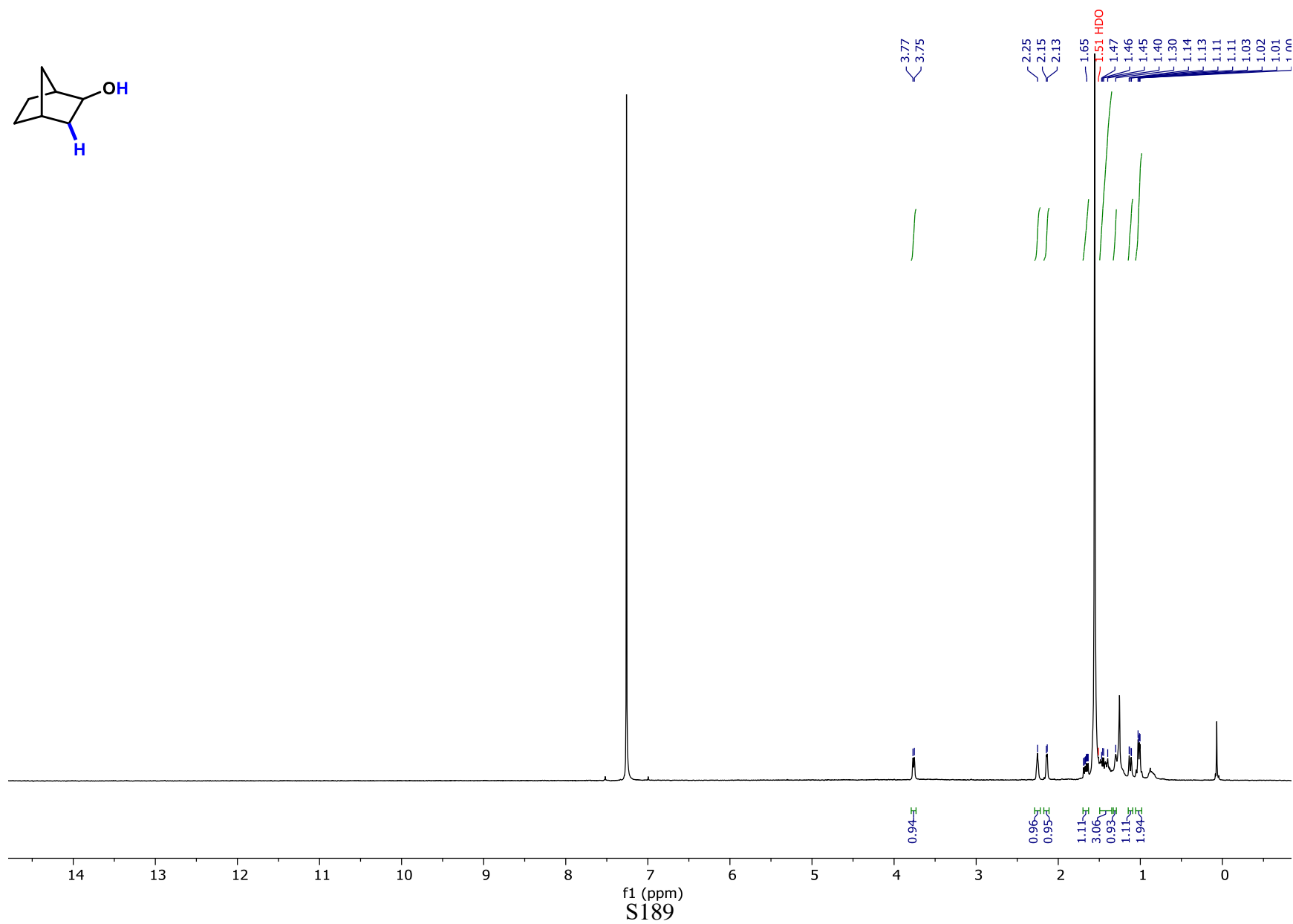
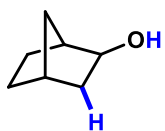
Compound SI-40 ¹H NMR



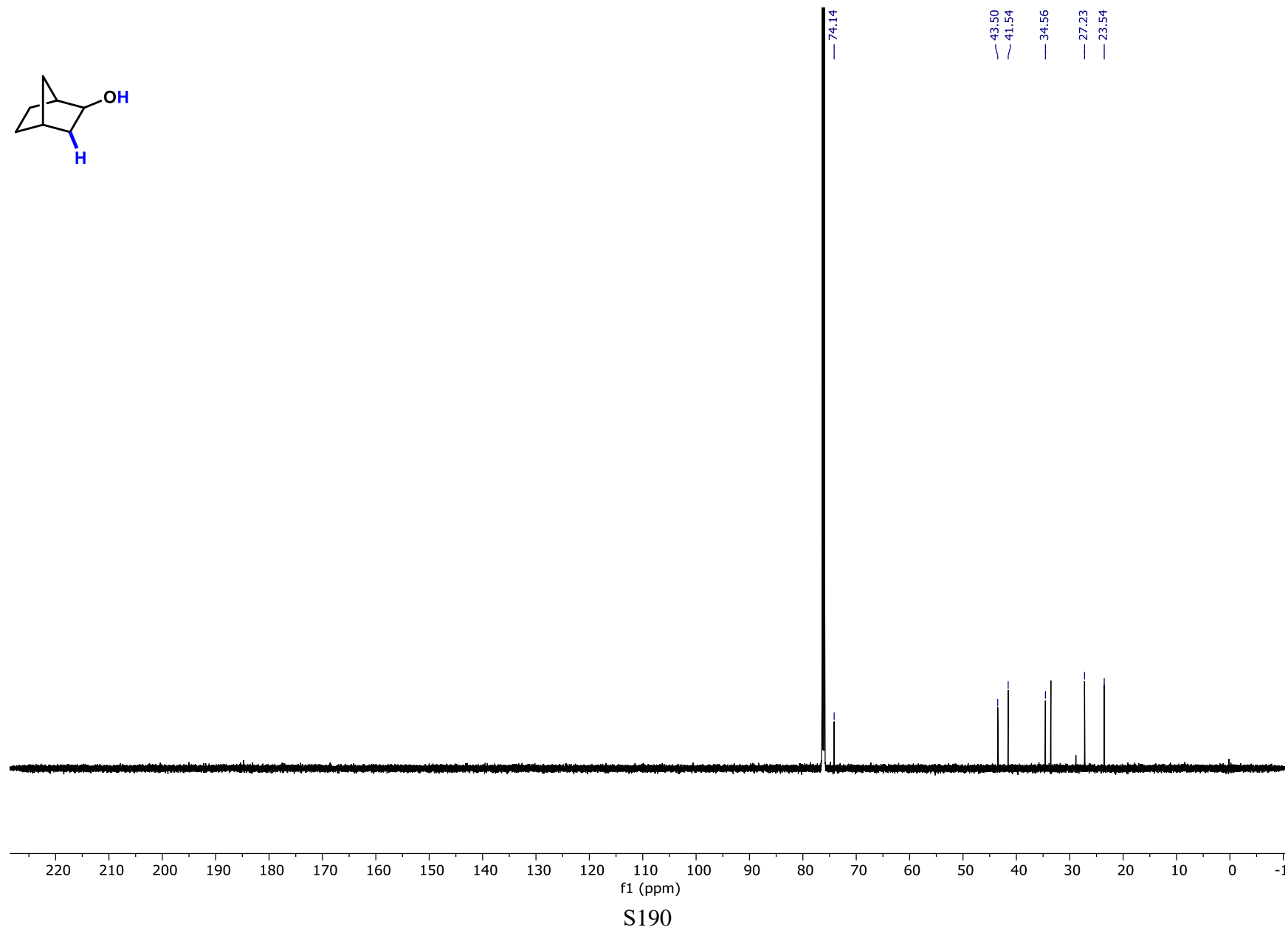
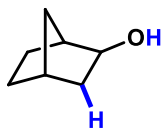
Compound SI-40 ¹³C NMR



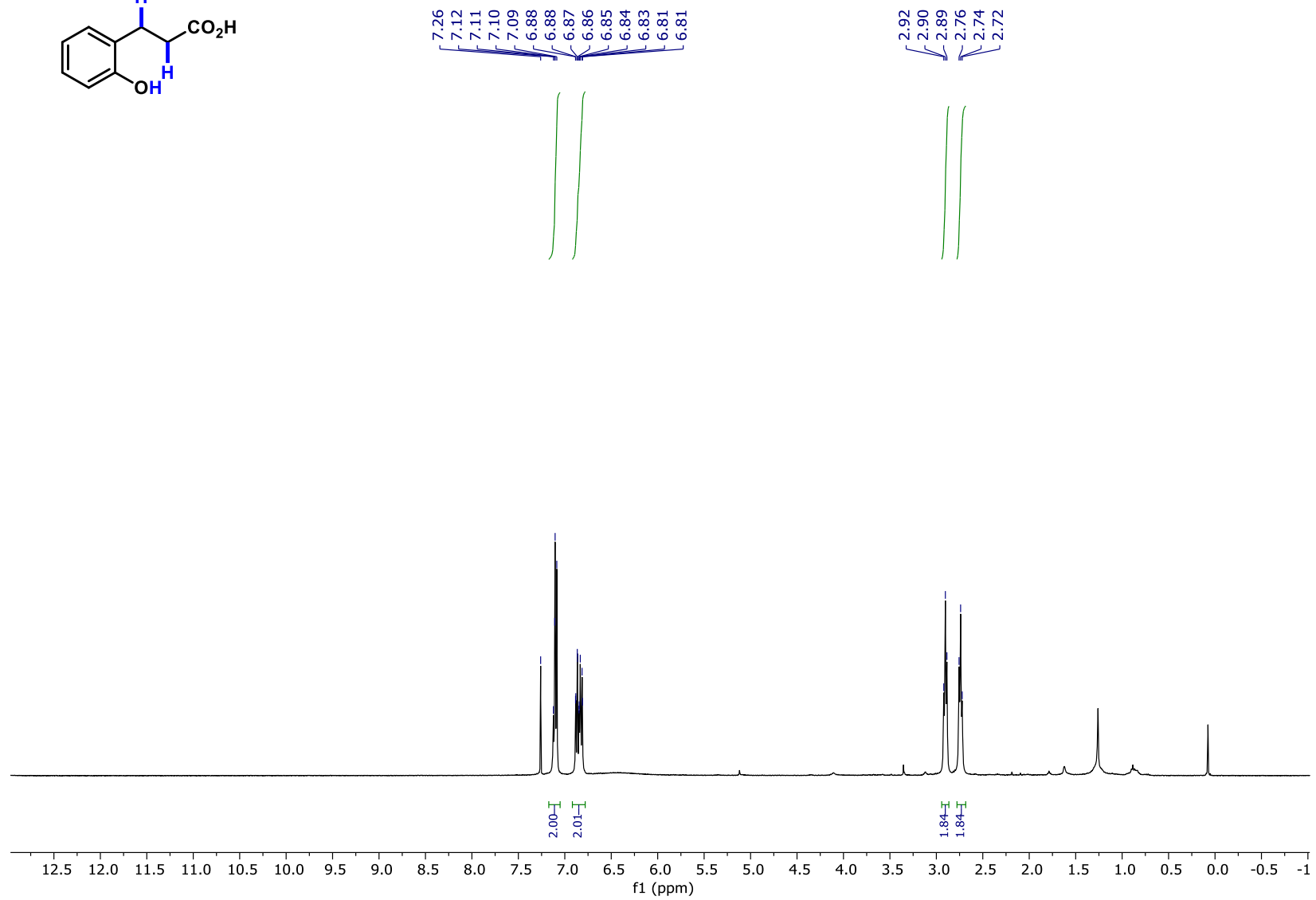
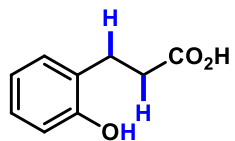
Compound SI-42 ¹H NMR



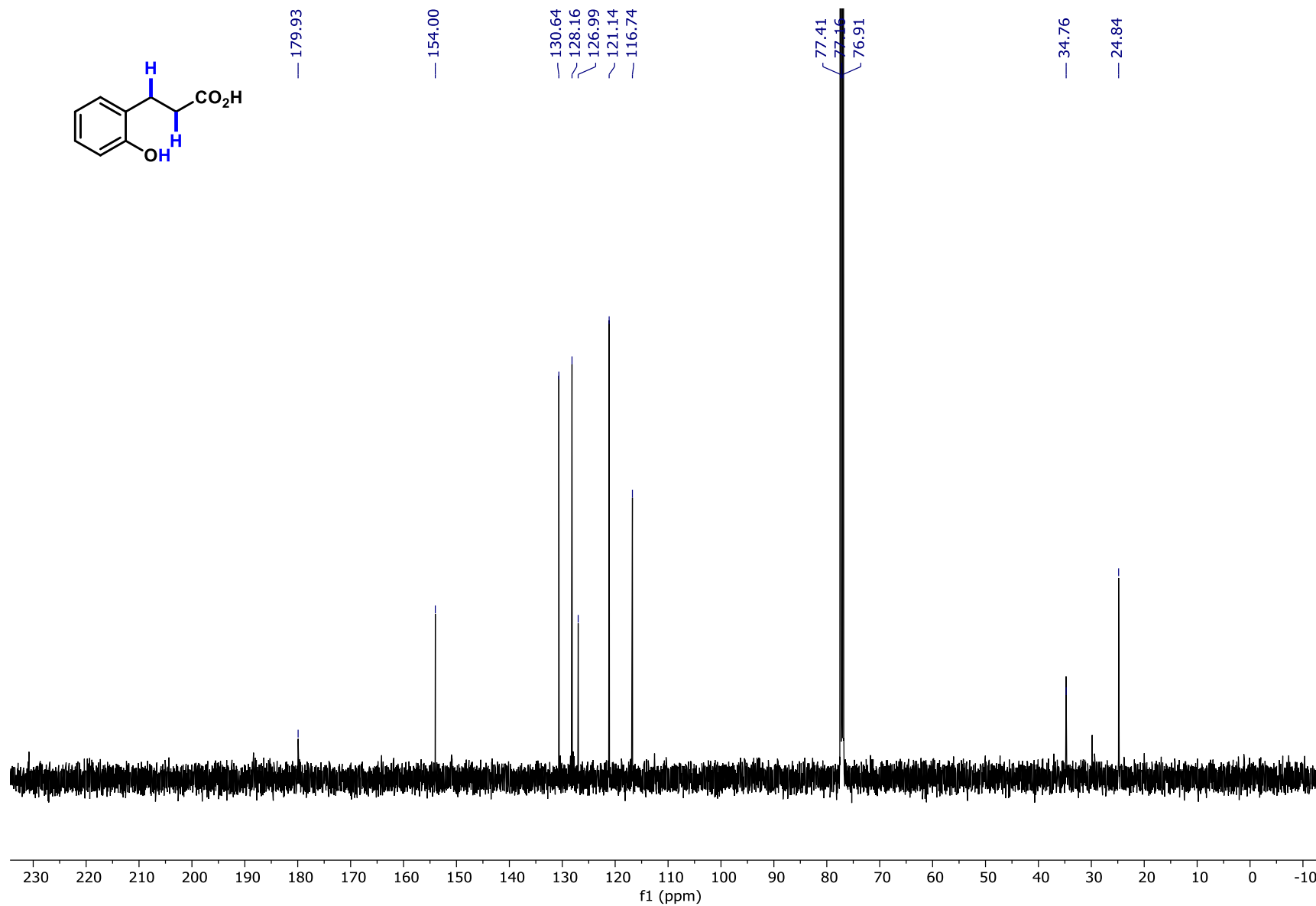
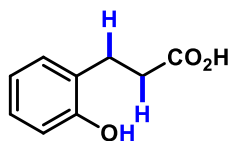
Compound SI-42 ¹³C NMR



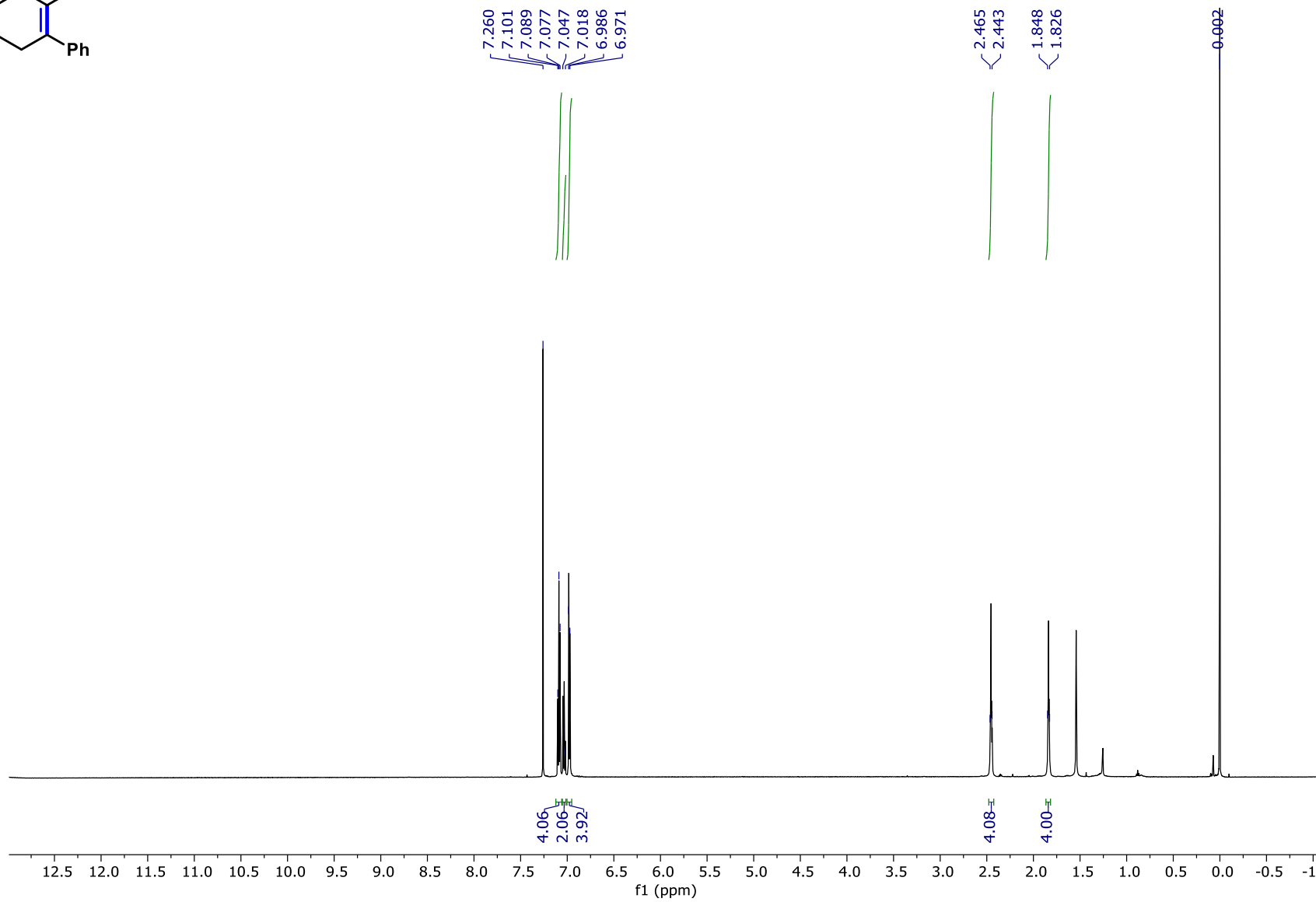
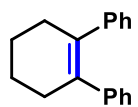
Compound SI-44 ¹H NMR



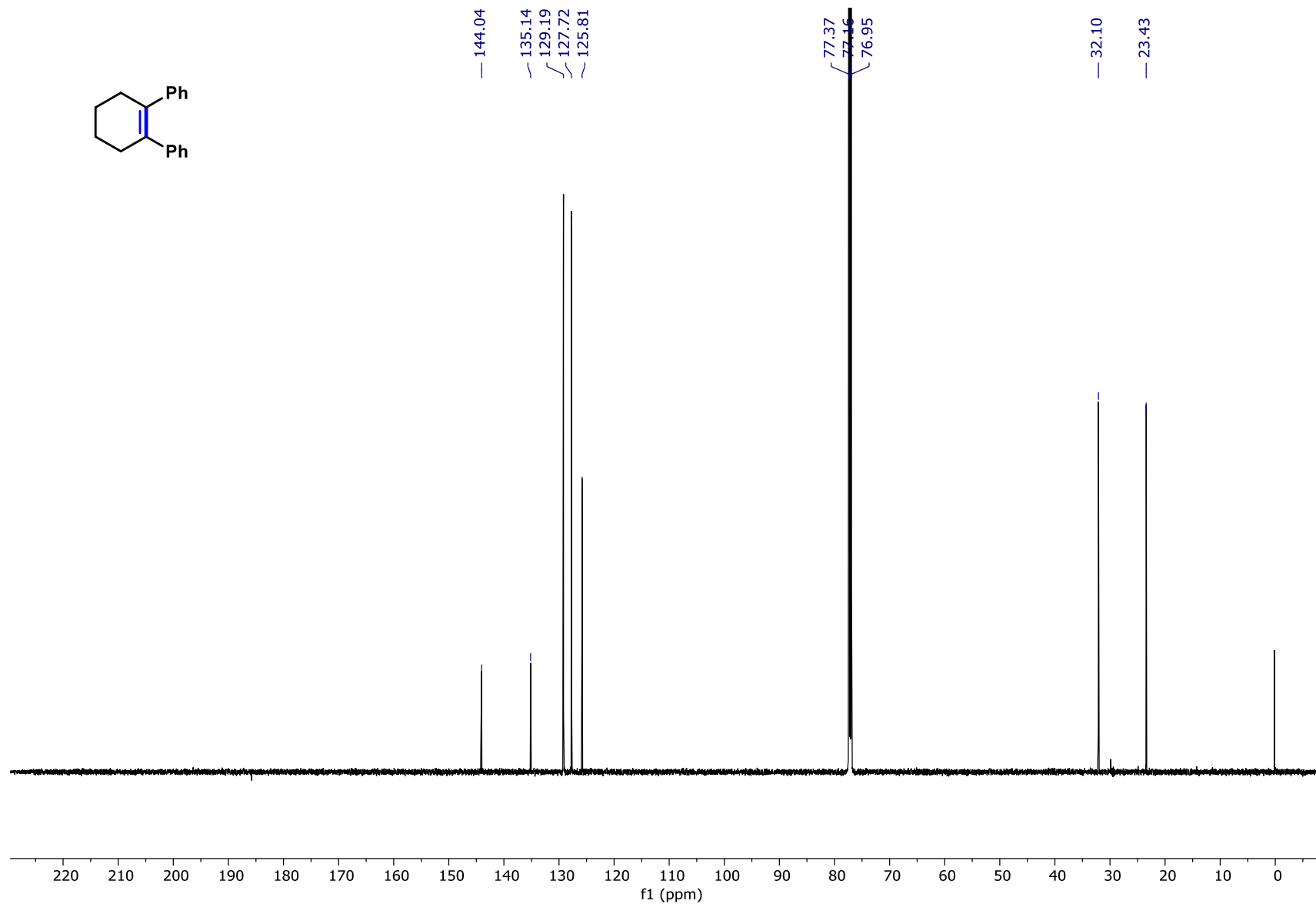
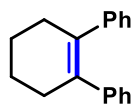
Compound SI-44 ¹³C NMR



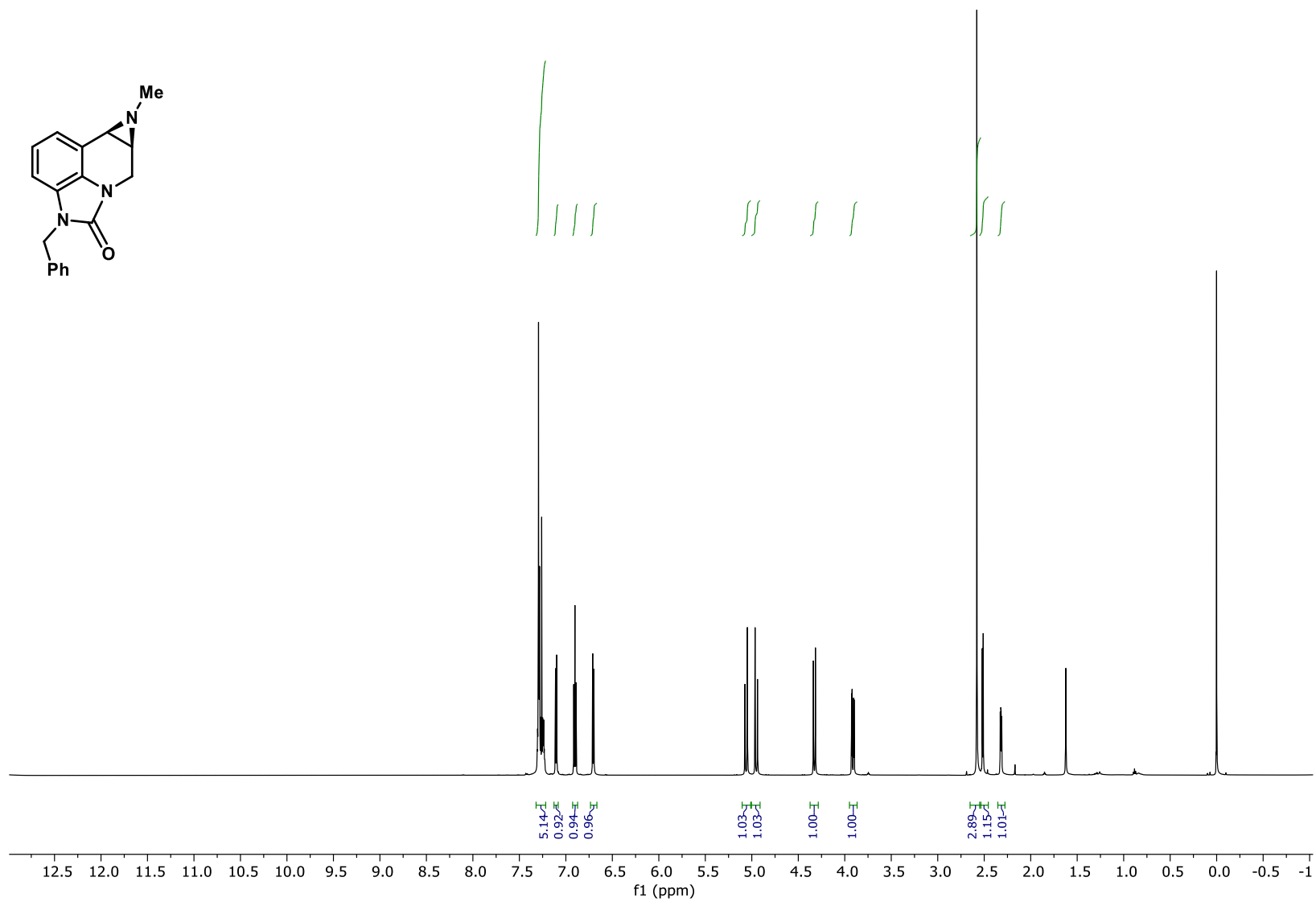
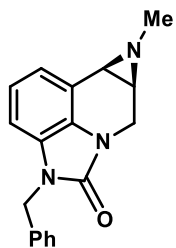
Compound SI-46 ¹H NMR



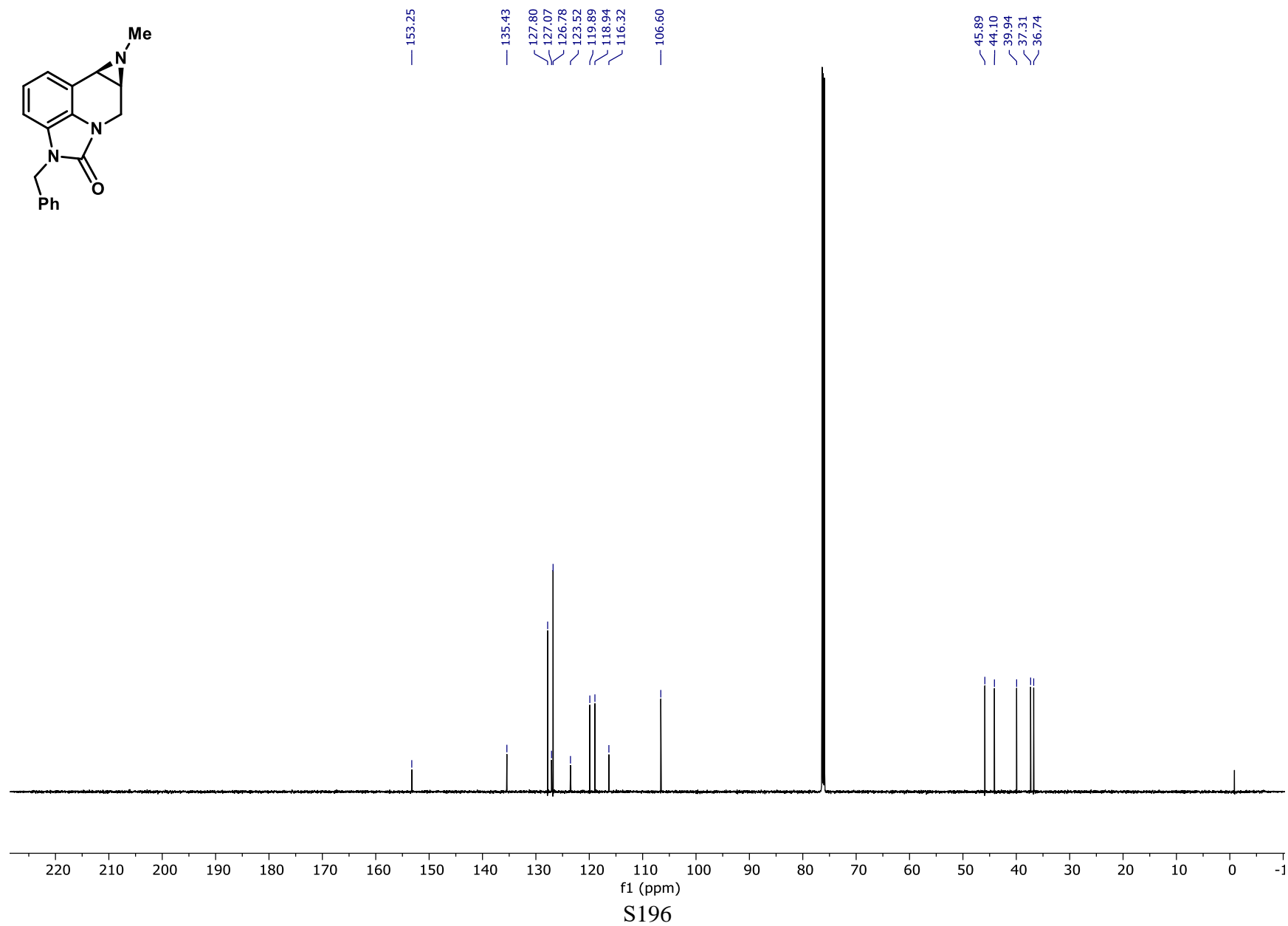
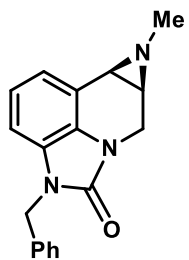
Compound SI-46 ¹³C NMR



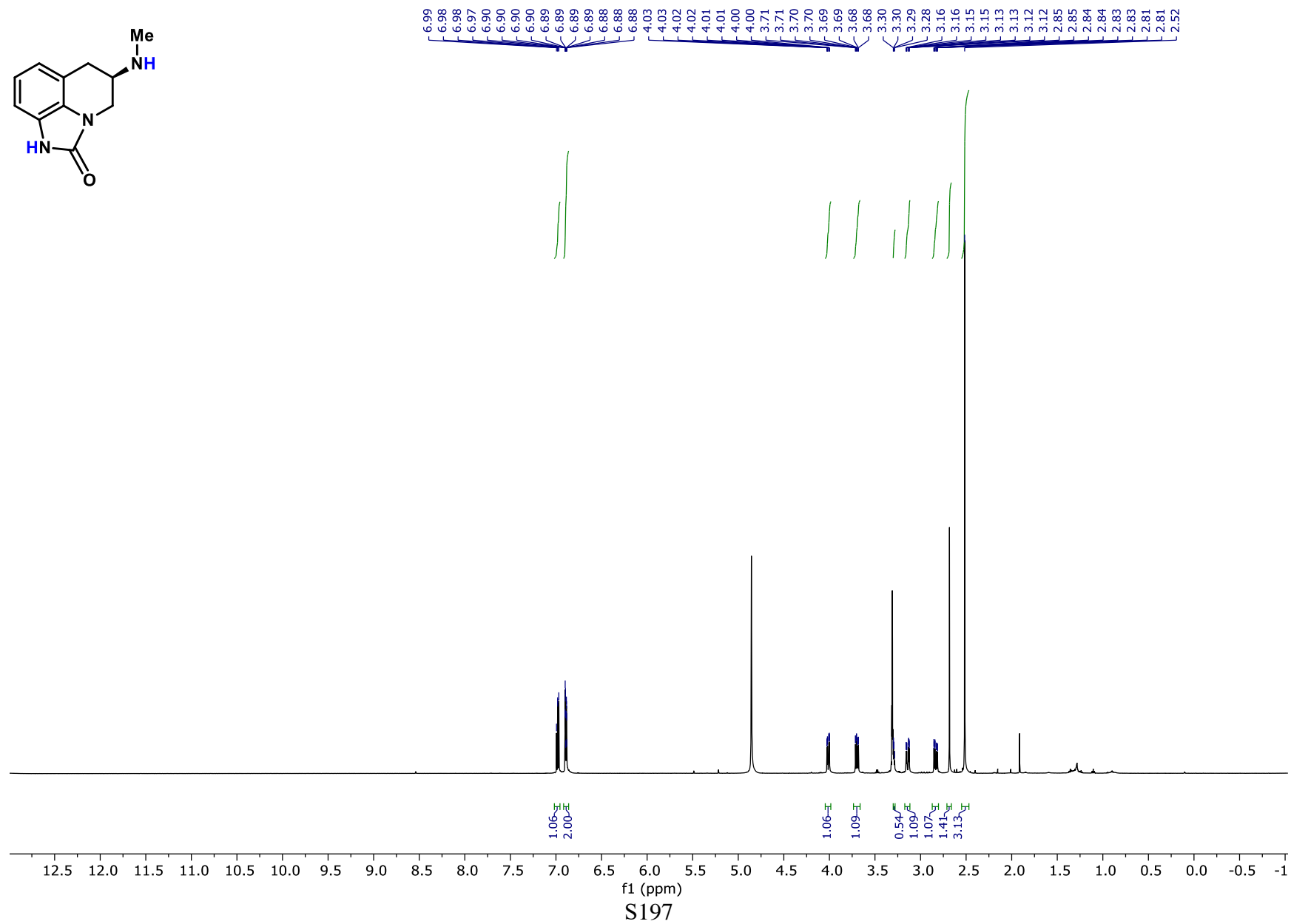
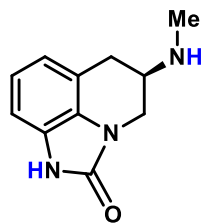
Compound SI-1 ¹H NMR



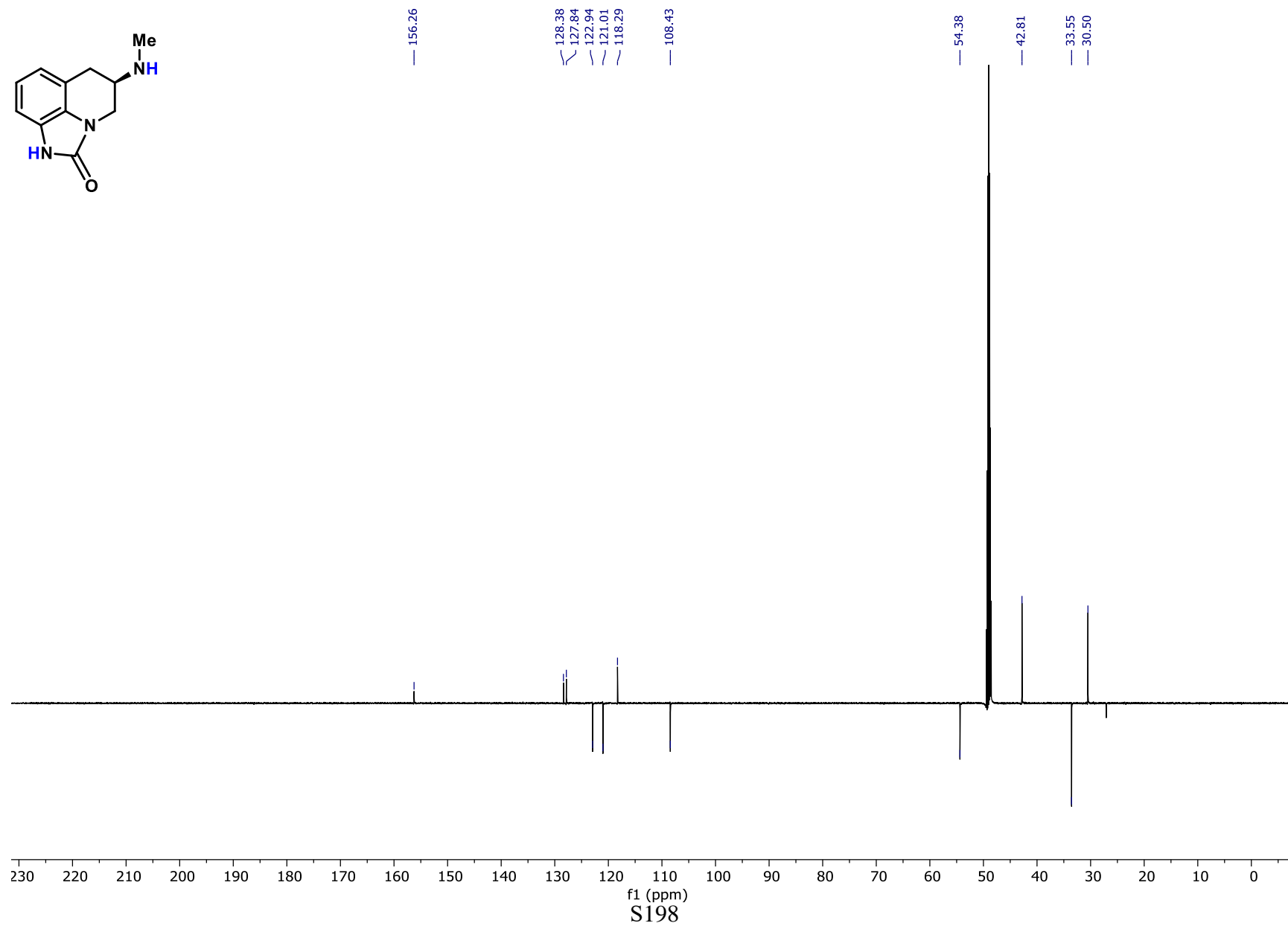
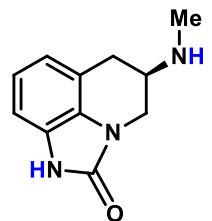
Compound SI-1 ¹³C NMR



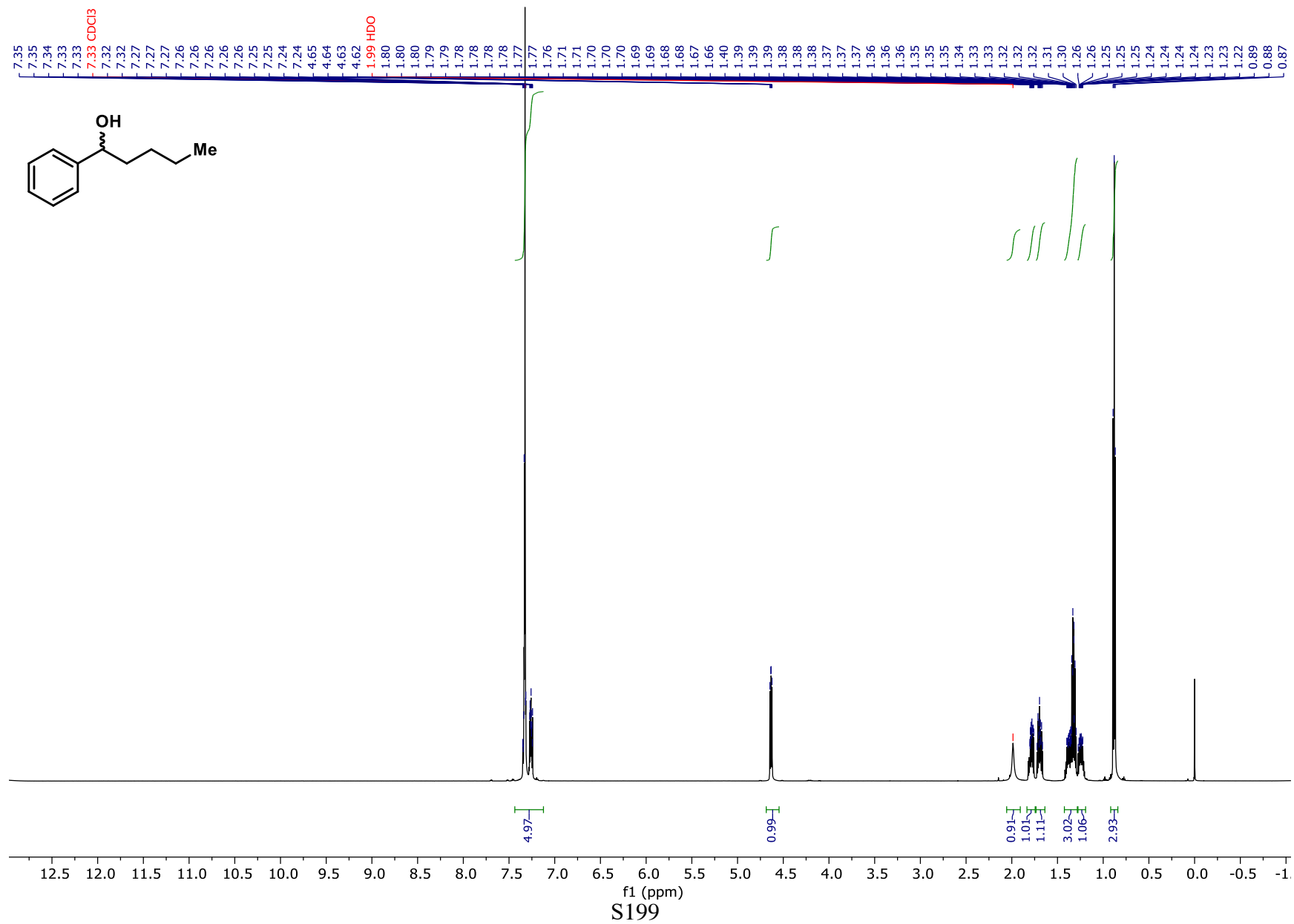
PNU95666E (2) ¹H NMR



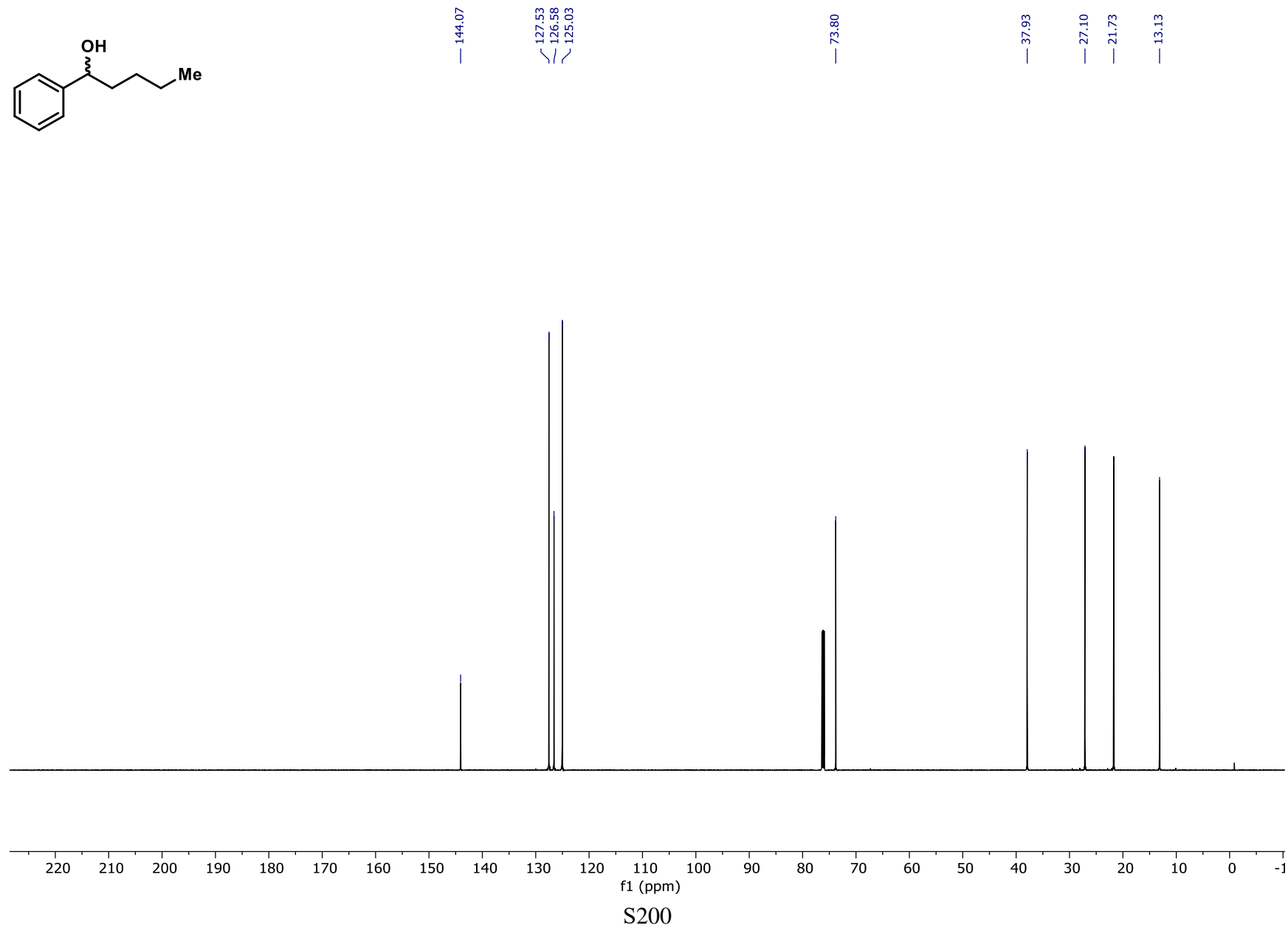
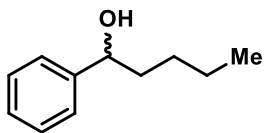
PNU95666E (2) ¹³C NMR



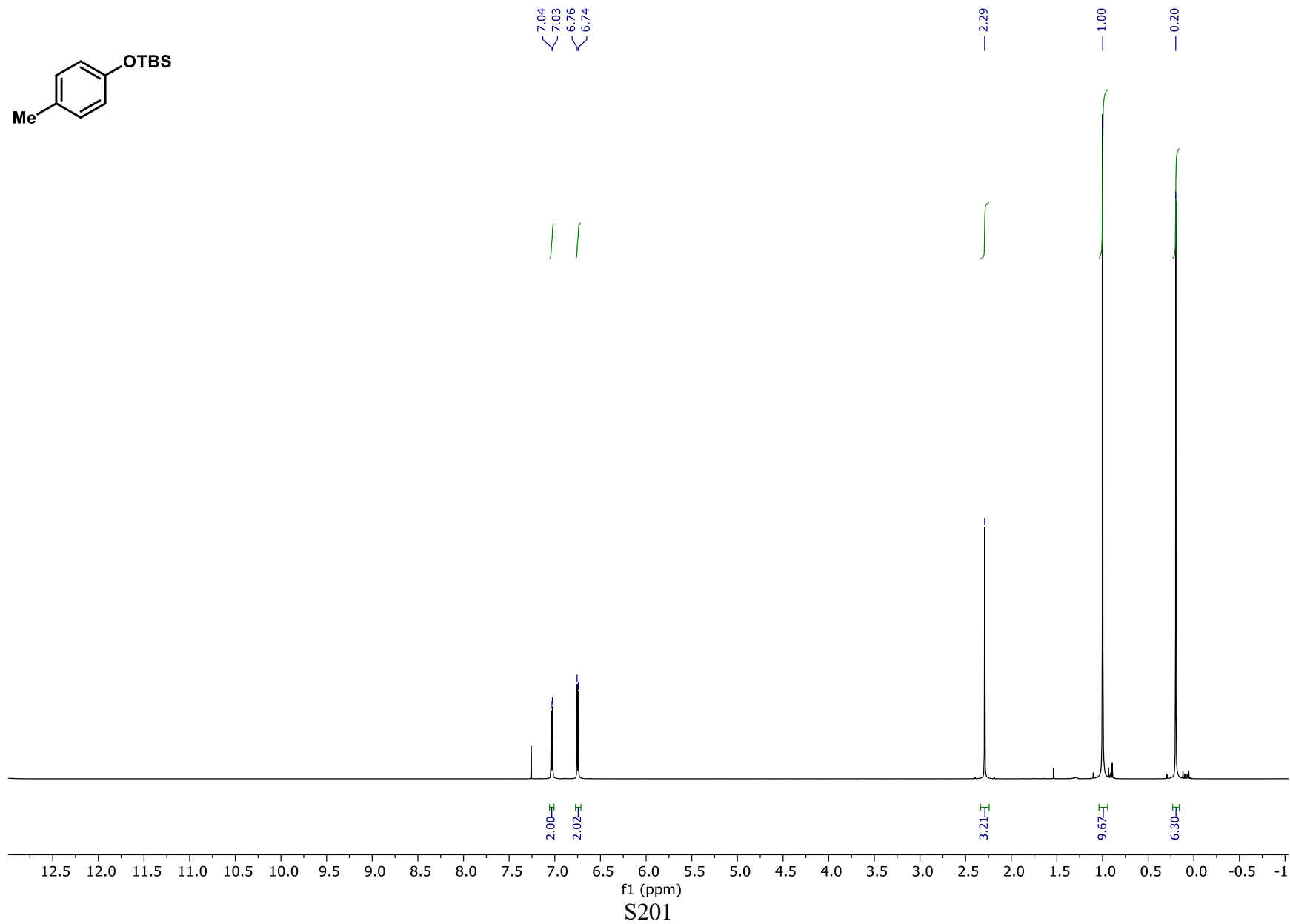
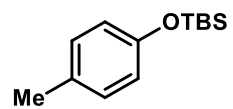
Compound SI-47 ¹H NMR



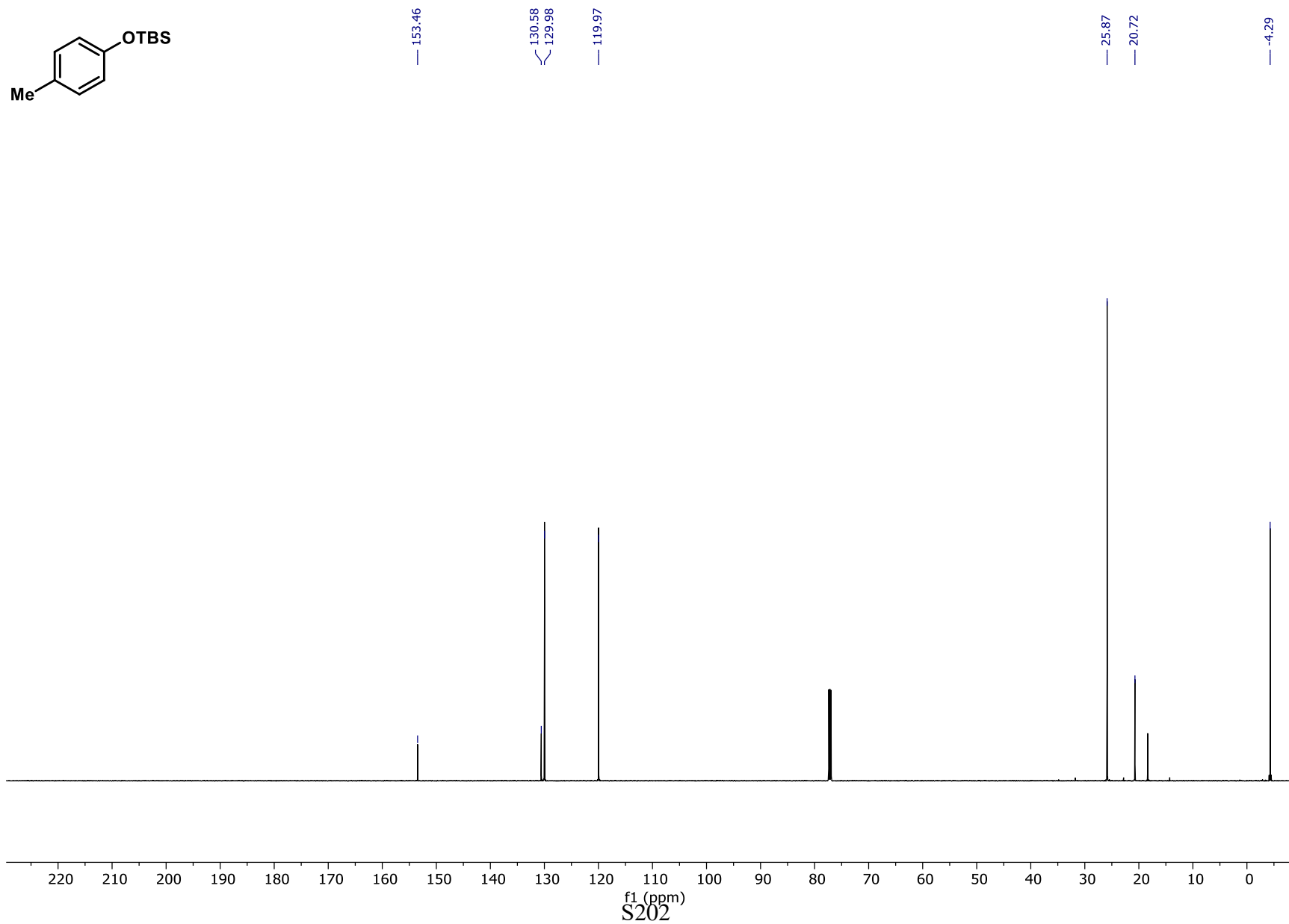
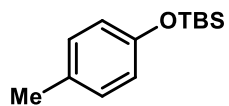
Compound SI-47 ¹³C NMR



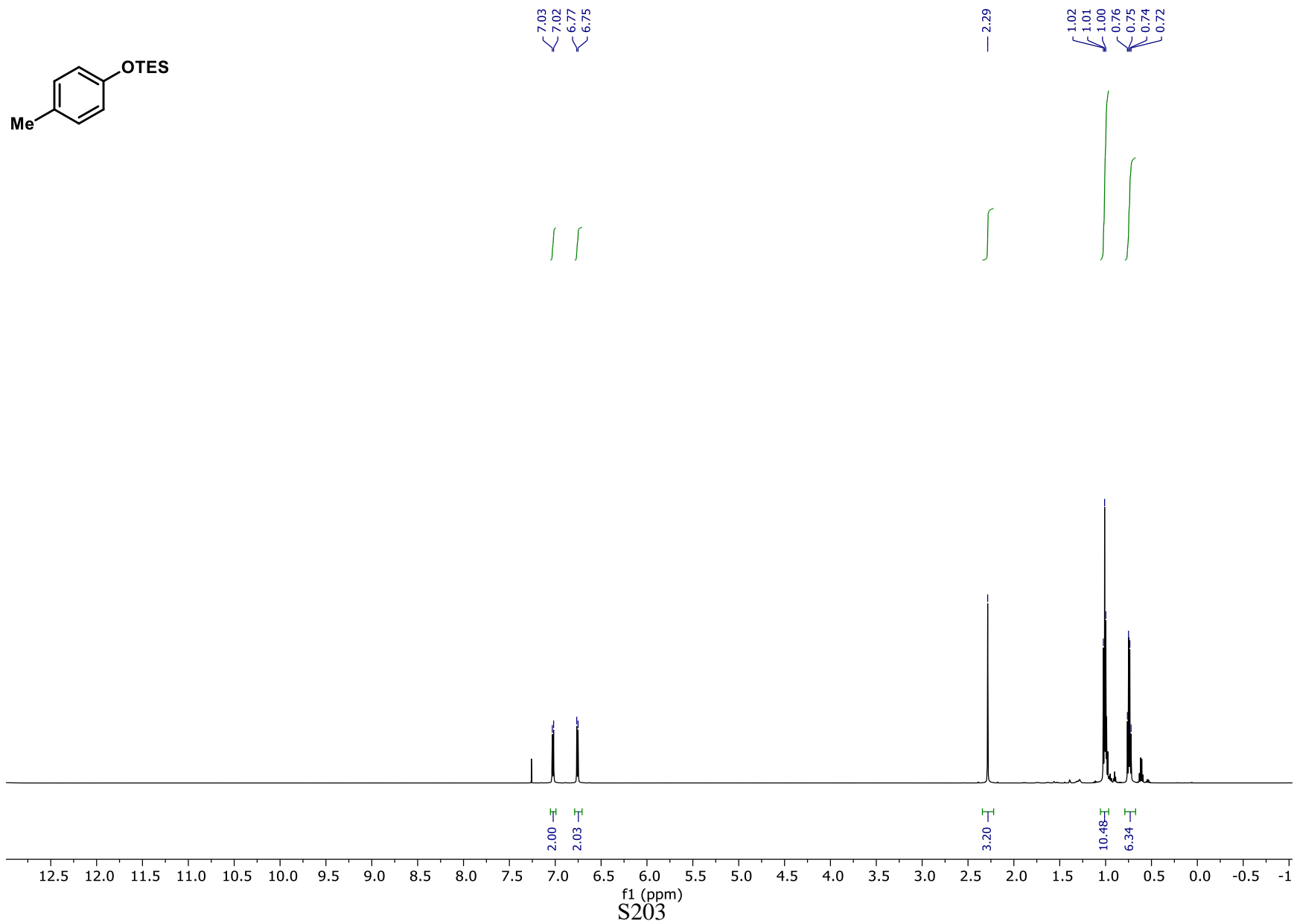
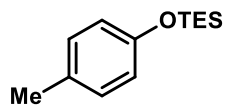
Compound SI-48 ¹H NMR



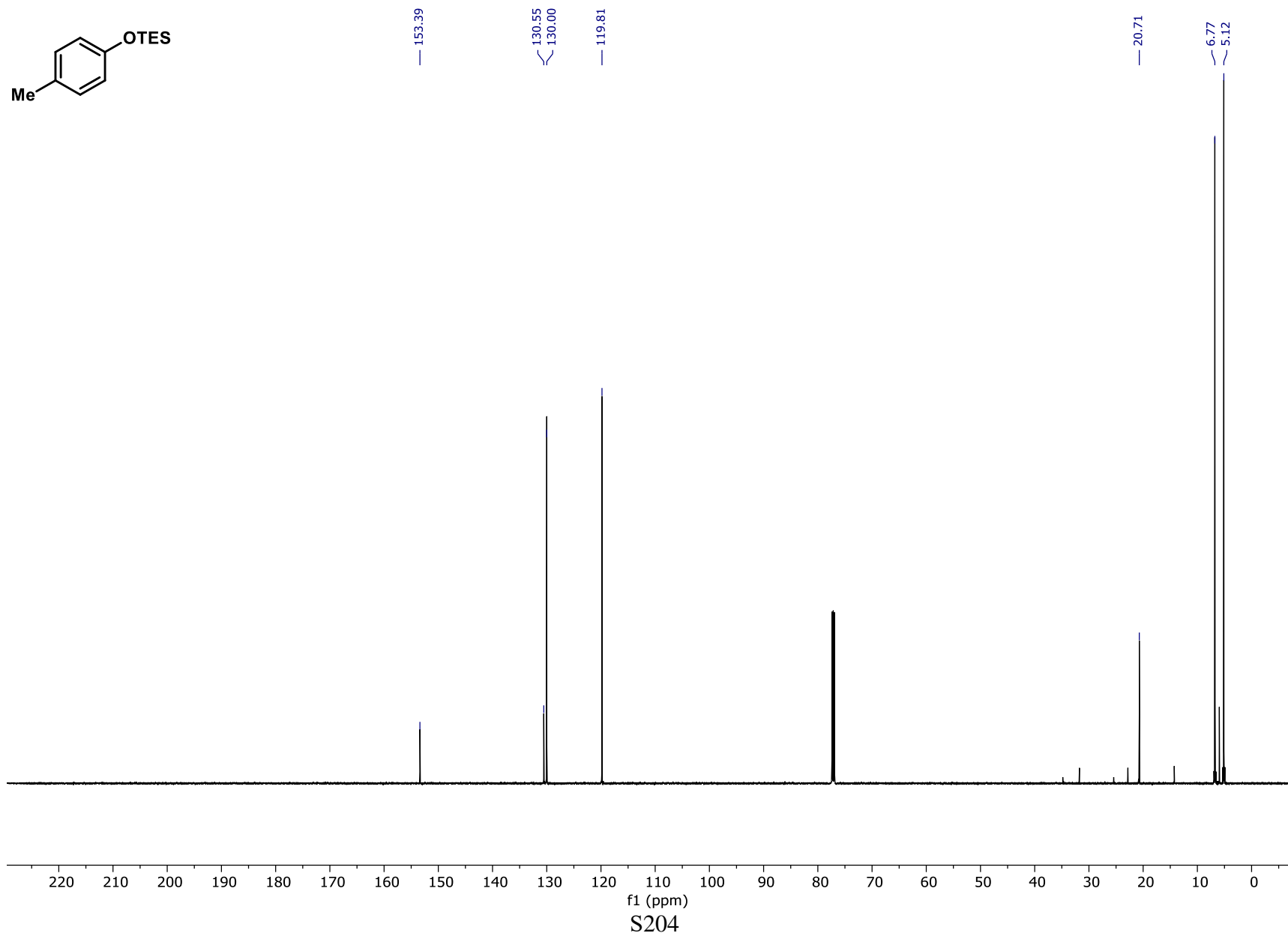
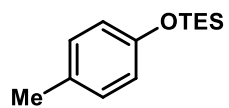
Compound SI-48 ¹³C NMR



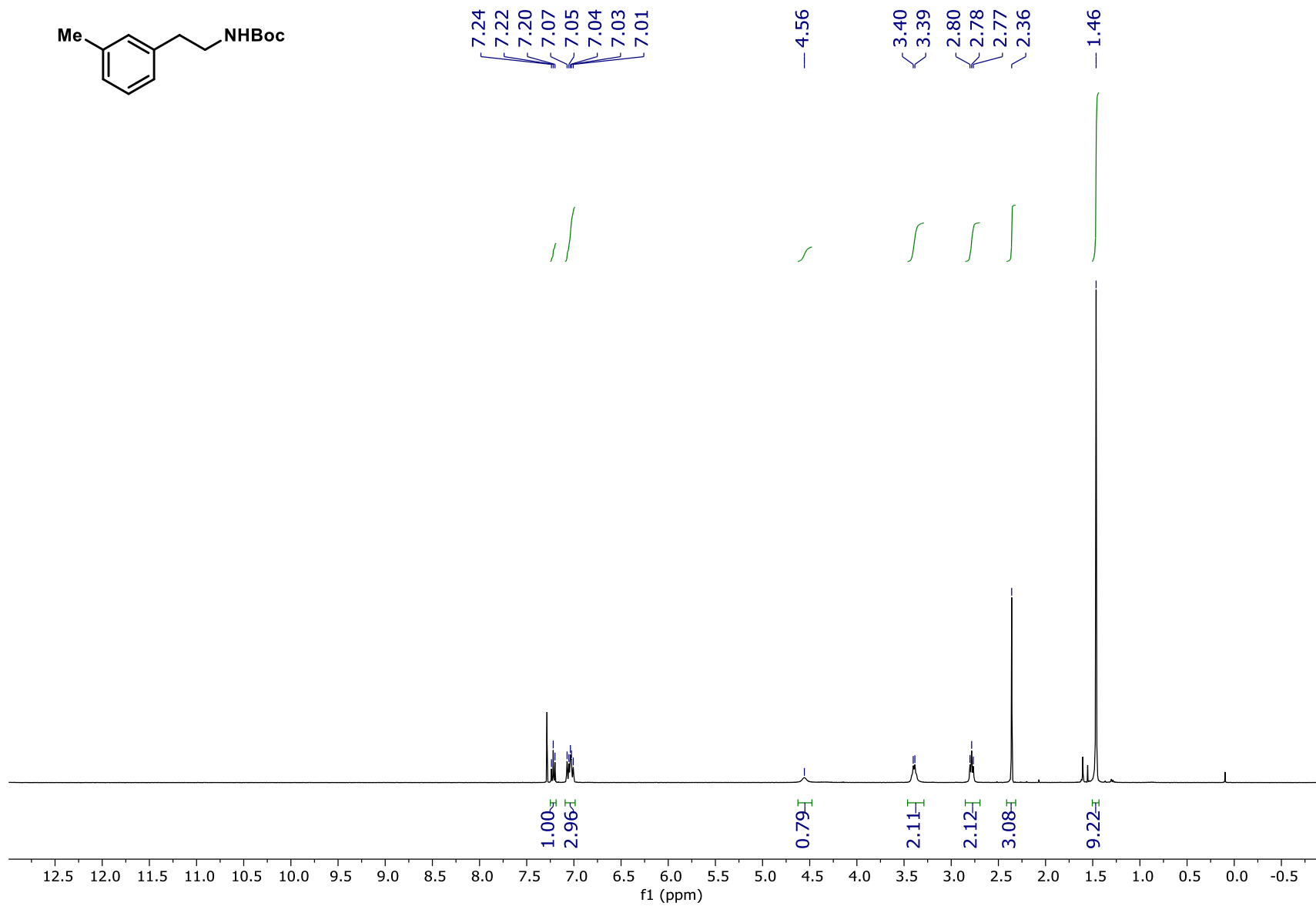
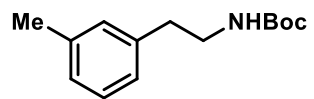
Compound SI-49 ¹H NMR



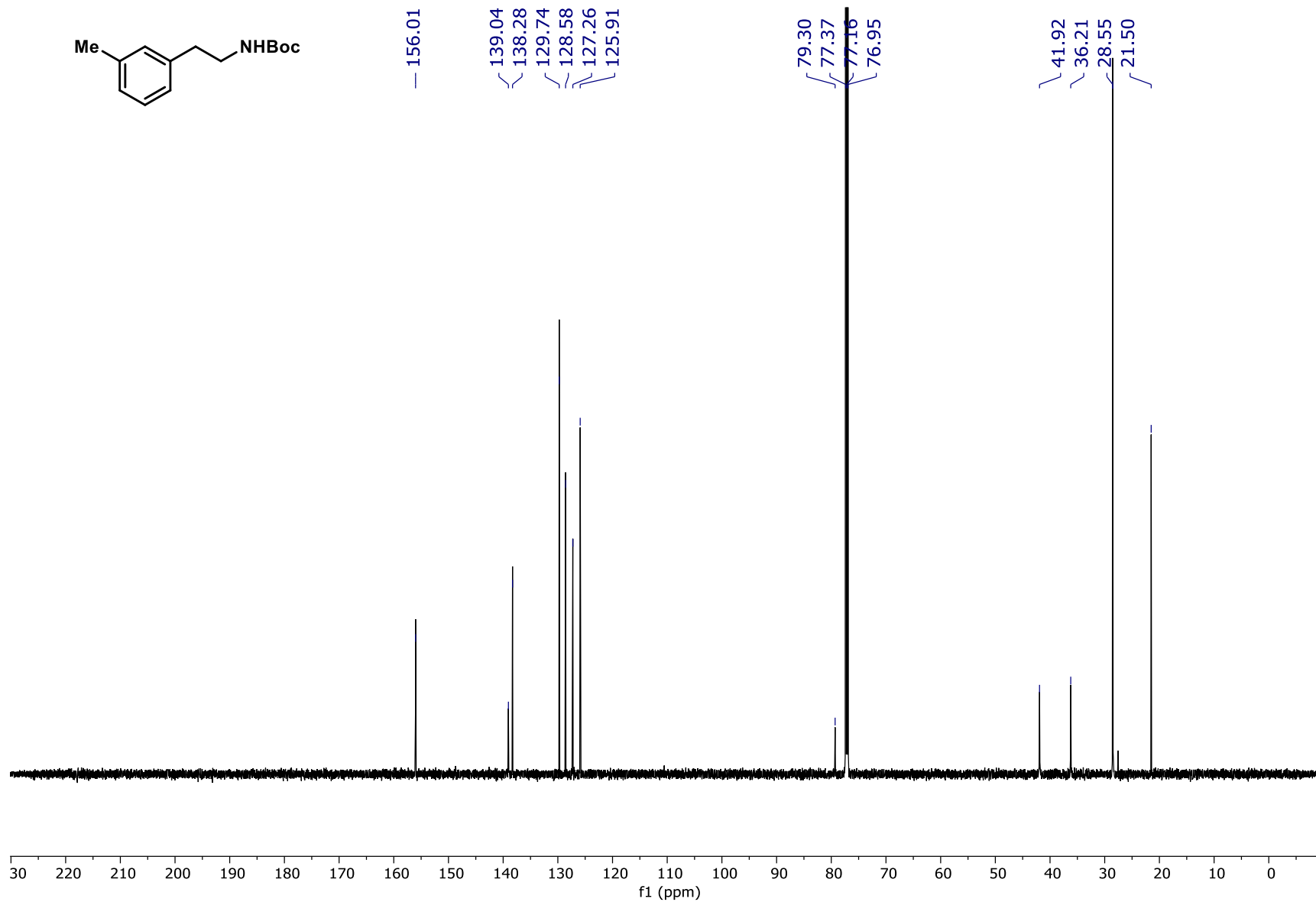
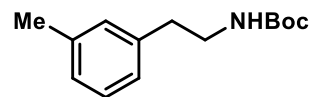
Compound SI-49 ¹³C NMR



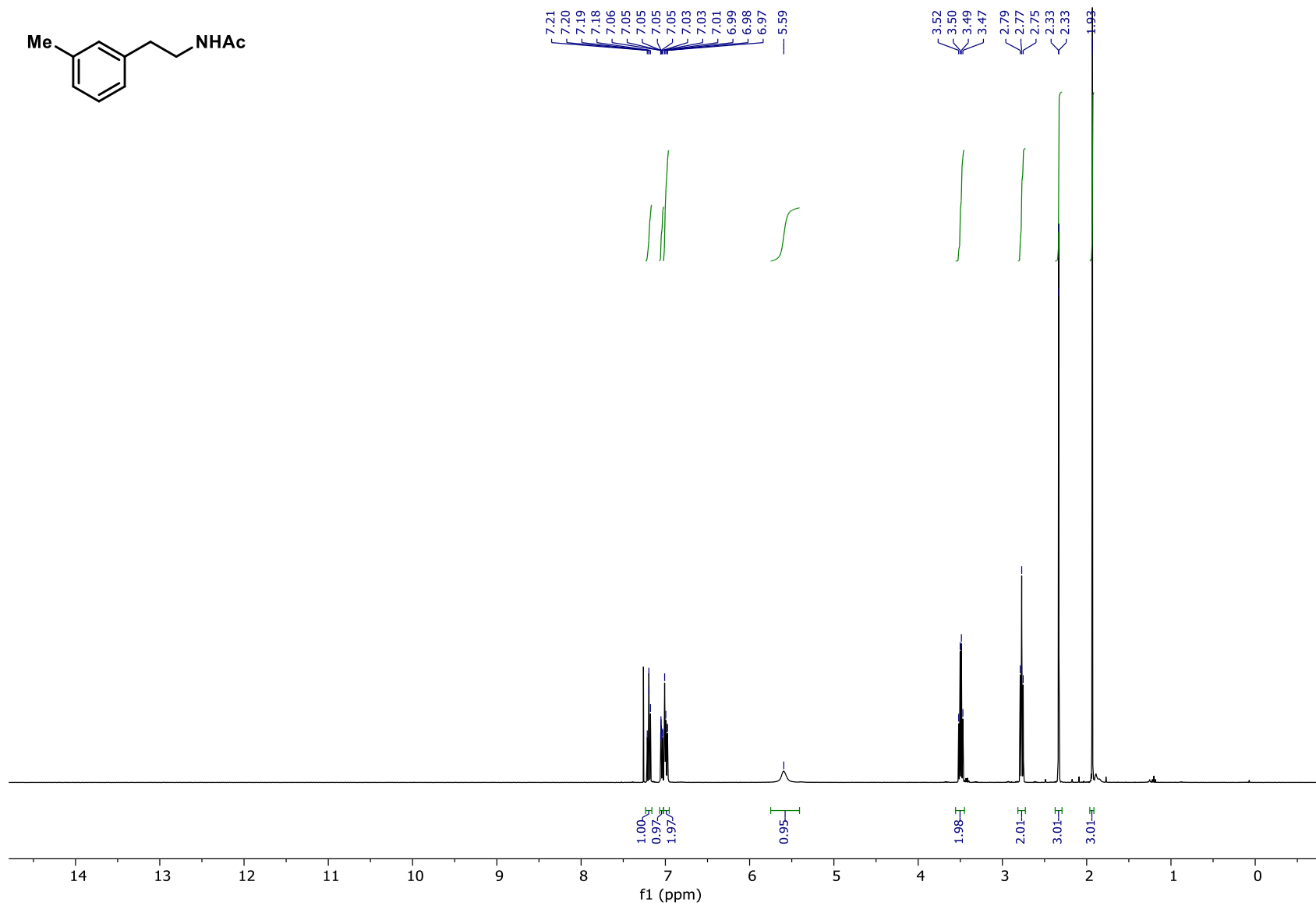
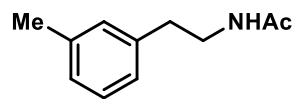
Compound SI-50 ¹H NMR



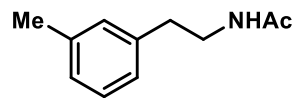
Compound SI-50 ¹³C NMR



Compound SI-51 ¹H NMR



Compound SI-51 ¹³C NMR

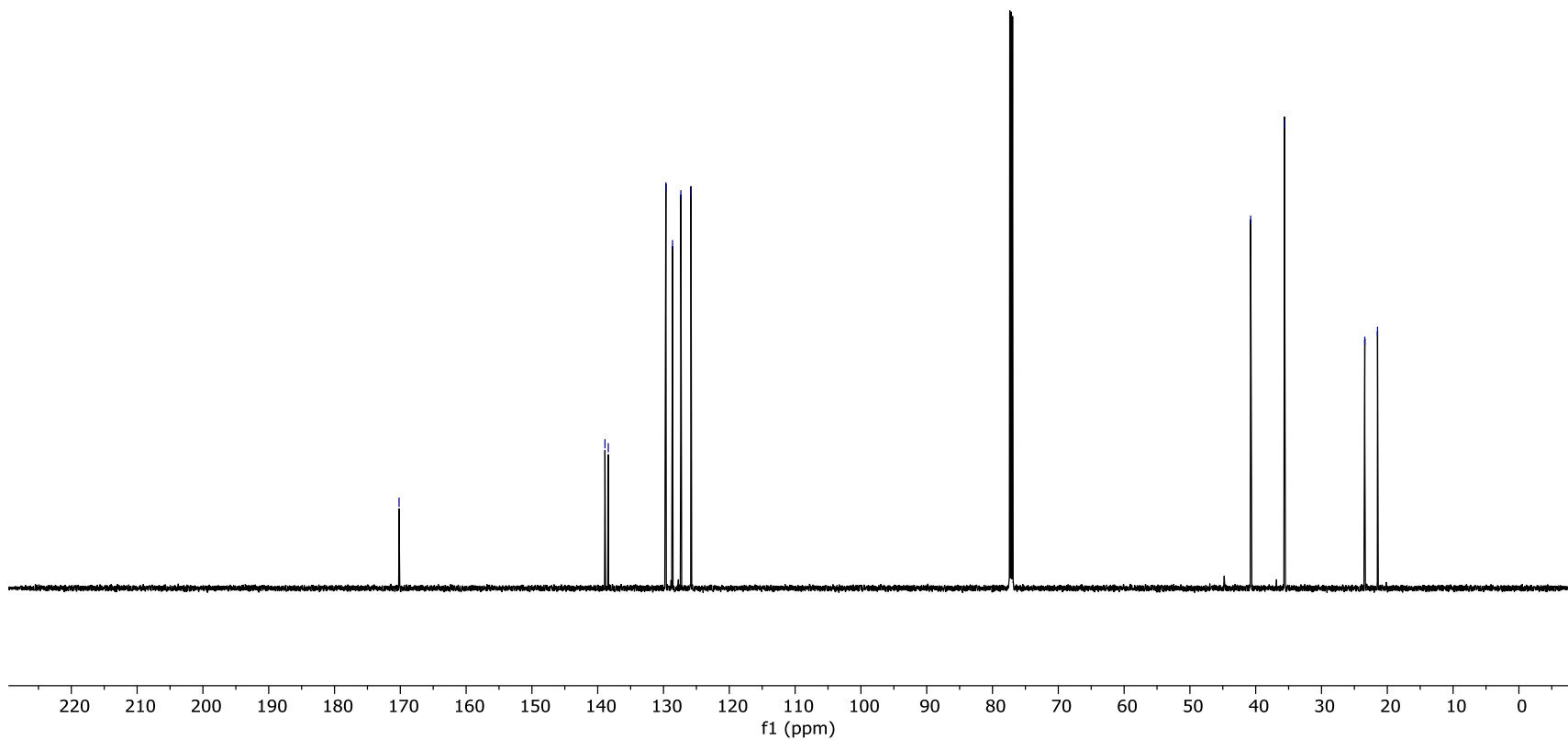


— 170.19

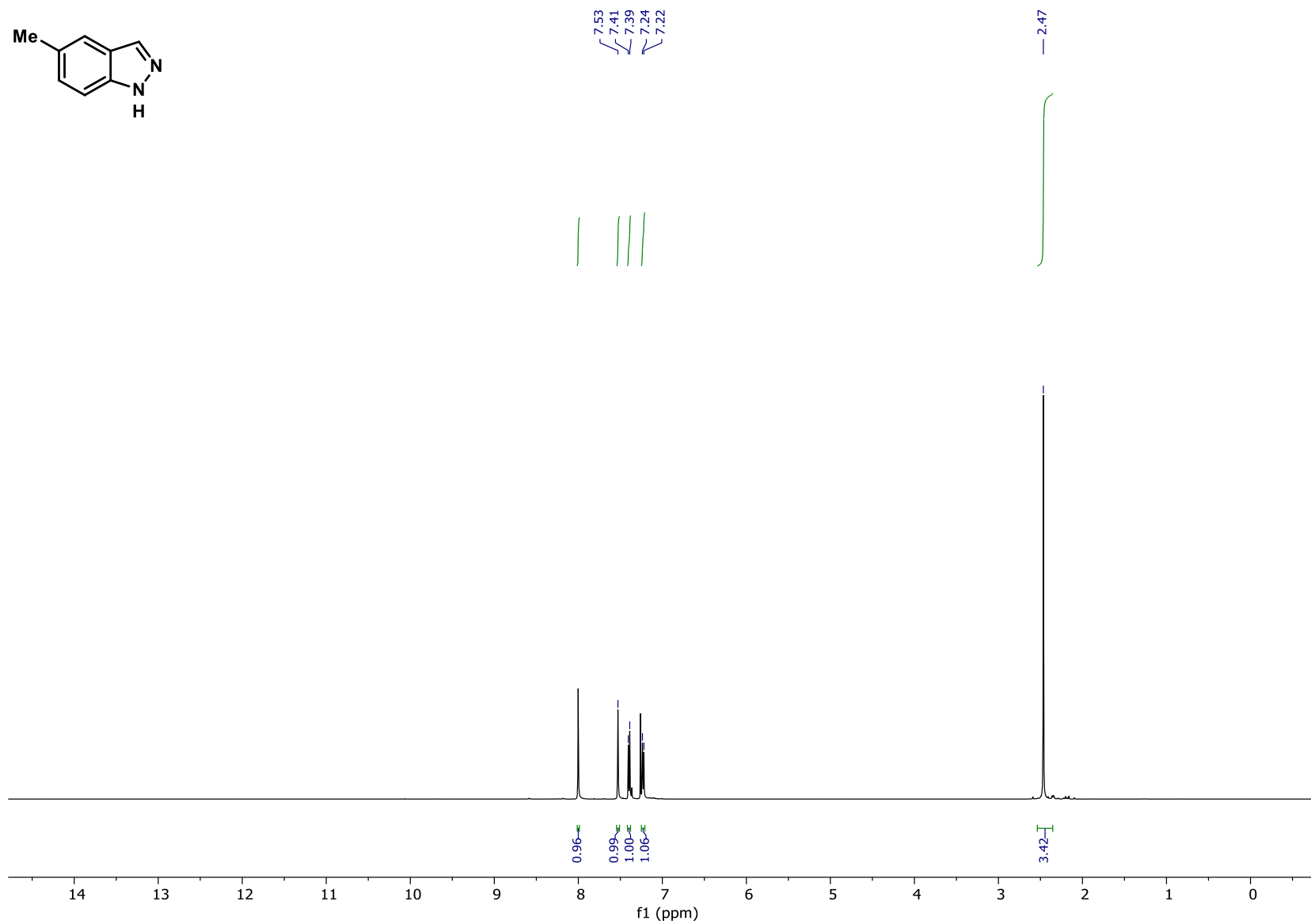
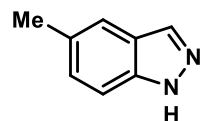
138.89
138.39
129.64
128.63
127.37
125.82

— 40.77
— 35.63

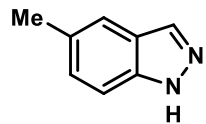
— 23.42
— 21.49



Compound SI-51 ¹H NMR



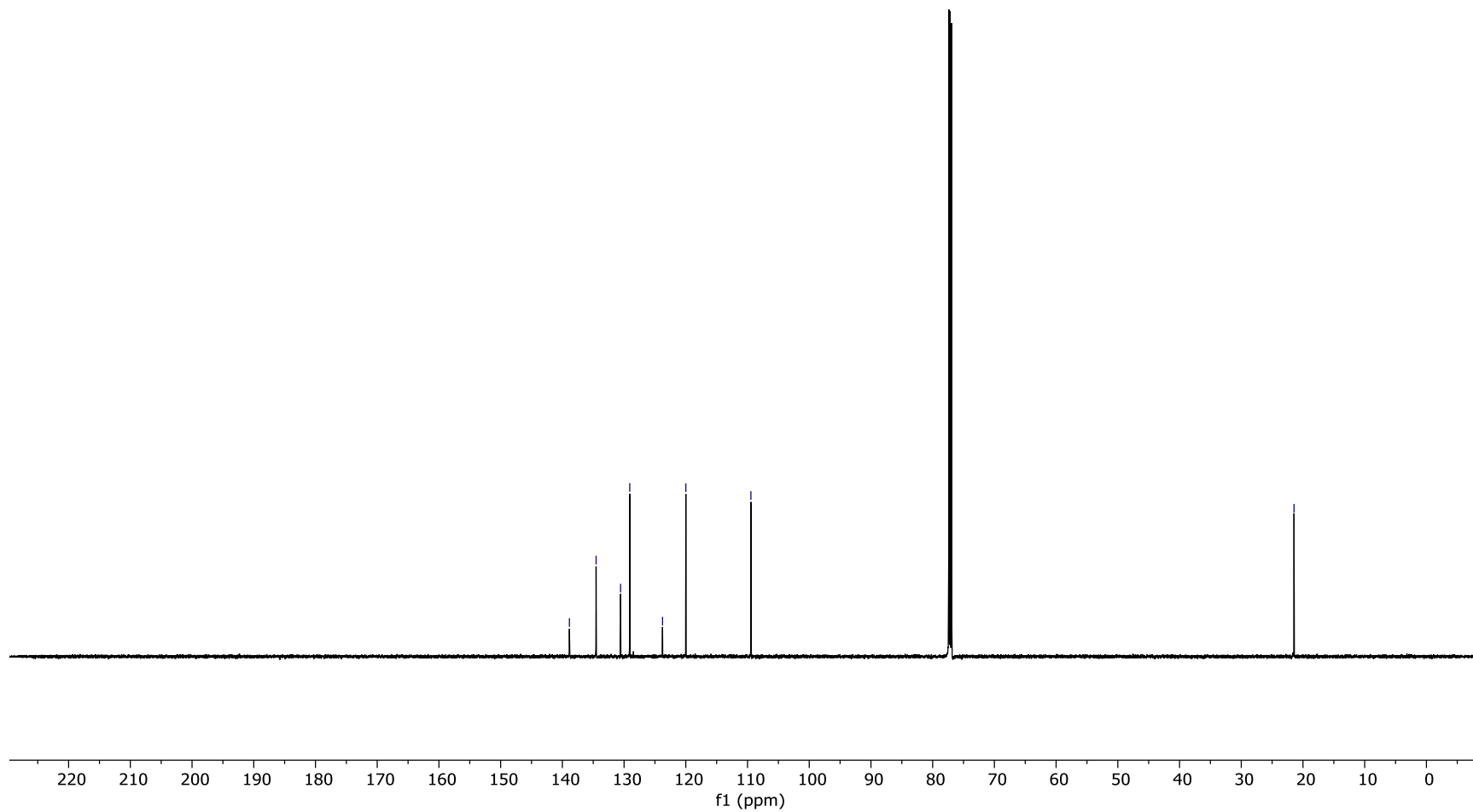
Compound SI-52 ¹³C NMR



138.86
134.53
130.56
129.08
123.77
119.99

109.45

21.45



S210